CENTRE d' ETUDES et de RECHERCHES
GEODYNAMIQUES et ASTRONOMIQUES

FIFTH INTERNATIONAL WORKSHOP ON LASER RANGING INSTRUMENTATION

VOLUME II

HERSTMONCEUX CASTLE
SEPTEMBER 10–14 / 1984

PROCEEDINGS
COMPILED AND EDITED BY
J. GAIGNEBET

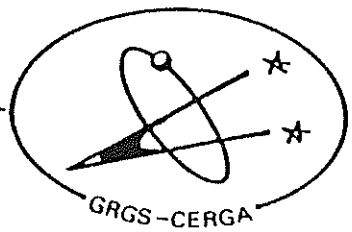

GROUPE de RECHERCHES de GEODESIE SPATIALE

produced by the Geodetic Institute,
University of Bonn, Nussallee 17,
D-5300 Bonn 1
1985

CONTENTS

USE OF THE GLOBAL POSITIONING SYSTEM FOR THE NASA TRANSPORTABLE LASER RANGING NETWORK

C. Wardrip*, P. Kushmeider
Goddard Space Flight Center
Greenbelt, MD 20771 USA

Telephone (301) 344 7000
TWX 710 828 9716

J. Buisson, J. Oaks, M. Lister
Naval Research Laboratory
4555 Overlook avenue S.W. Washington DC 20375

Telephone (202) 545 6700

P. Dachel, T. Stalder
*Bendix Field Engineering Coporation
One Bendix Road
Colombia, Maryland 21045

Telephone (301) 964 7000
Telex 197700

ABSTRACT

Present time synchronization techniques used in the NASA Goddard Space Flight Center (GSFC) Transportable Laser Rangin Network (TLRN) will be discussed. The operational aspects of the Naval Research Laboratory (NRL) developed Global Positioning System (GPS) receiver and the Stanford Telecommunications, Inc. (STI) GPS receiver, both of which are used in the GSFC-TLRN, will also be discussed. In addition, operational time data taken via GPS at TLRN sites located at Goldstone, California ; Santiago, Chile ; Cerra Tollola, Chile ; Otay Mountain, California ; Cabo San Lucas, Mexico and Arequipa, Peru during 1983 and 1984 will be presented.

Use of the Global Positioning System for the NASA Transportable Laser Ranging Network

Introduction

The NASA Goddard Spaceflight Center (GSFC) and the Naval Research Laboratory (NRL) initially transferred time by satellite in 1977 using the NRL Navigation Technology Satellite (NTS) [1,2]. This system provided accuracies of several hundred nanoseconds [3]. As an outgrowth of that program a joint effort was started in 1979 to develop Global Positioning System (GPS) timing receivers using signals radiated by the GPS satellites. These receivers were designed to provide precise time measurements between the time standard of the U.S. Naval Observatory and clocks at remote locations. NASA is currently using the GPS time transfer receivers in the GSFC Transportable Laser Ranging Network (TLRN) in support of the GSFC Crustal Dynamics Program.

Geophysical data suggest that the surface of the earth is composed of rigid plates 50 to 150 kilometers thick. These plates move slowly (1 to 10 centimeters per year) in response to driving forces resulting from motion in the earth's interior.

In 1978 the Crustal Dynamics Project was launched to study the movement of the earth's plates. One of the techniques being used to measure plate motion is Satellite Laser Ranging (SLR). SLR uses the measurement of the time of flight of very short laser pulses to a retroreflector on a satellite [4].

Ground-based lasers transmit intense light pulses to these retroreflectors and record the round-trip travel time for the pulse to return. If the orbit of the satellite is well-known, such ranging permits precise determination of the location of the laser station on the Earth's surface. When two stations range to the same satellite simultaneously, the distance between the stations can be accurately determined.

The GSFC Transportable Laser Ranging Network which supplies the SLR data, presently consists of eight Mobile Laser Systems (MOBLAS, Fig. 1) and four highly Transportable Laser Ranging Systems (TLRS). These systems have been deployed globally to measure regional deformation, plate motion, plate deformation, and polar motion. TLRS-1 and TLRS-2 have been using NRL built GPS receivers since the early part of 1984 and the middle of 1983 respectively. Since the installation of a GPS timing receiver, TLRS-1 (Fig. 2) has gathered data at the following sites: 1) Goldstone, California, USA; 2) Santiago, Chile; and 3) Cerra Tollola, Chile. TLRS-2 (Fig. 3) has obtained GPS time transfer data from: 1) Otay Mountain, California, USA; and 2) Cabo San Lucas, Mexico. Operational GPS time transfer data from these field sites as well as from a semi-permanent laser station in Arequipa, Peru will be presented in this paper.

The NAVSTAR Global Positioning System

NAVSTAR GPS is a tri-service Department of Defense (DOD) program. The first GPS satellite flown was the Navigation Technology Satellite (NTS-II) which was designed and built by NRL personnel [5,6]. GPS provides the capability of very precise instantaneous navigation and transfer of time from any point on the Earth. GPS comprises three segments: The Space Segment, the Control Segment and the User Segment. The phase III Space Segment will consist of a constallation of 18 to 24 satellites, six to eight in

each of three orbital planes (Fig. 4). The satellite orbits are nearly circular at an altitude of about 20,000 km and inclined 55° to the equator. The period is one half of a sideral day, resulting in a constant ground track, but with the satellite appearing 4 minutes earlier each day.

Each satellite transmits its own identification and orbital information continuously. The transmissions are spread spectrum signals, formed by adding the data to a direct sequence code, which is then biphase modulated onto a carrier.

The control segment consists of a master control station (MCS) and monitor stations (MS) placed at various locations around the world [7]. The current Phase I MCS is located at Vandenberg Air Force Base with the support monitor tracking stations at Alaska, Guam, Hawaii, and Vandenberg, California (Fig. 5). The monitor stations collect data from each satellite and transmit to the MCS. The data is processed to determine the orbital characteristics of each satellite and the trajectory information is then uploaded to each satellite, once every 24 hours as the spacecraft passes over the MCS.

The user segment consists of a variety of platforms containing GPS receivers, which track the satellite signals and process the data to determine position and/or time. Navigation is performed by simultaneous or sequential reception of at least four satellites, and time transfer is performed by reception of a single satellite. Coverage of the Phase III constellation is such that at least four satellites will always be in view from any point on the earth's surface.

Time Transfer Method

To transfer time via a GPS satellite, pseudo-range measurements are made consisting of the propagation delay of the received signal biased by the time difference between the satellite clock and the ground station reference clock (see Fig. 6 and references [8] and [9]). Data from the navigation message contain the satellite clock information and the satellite ephemeris, which allows one to compute the satellite position and clock offset. Since the position of the satellite and ground station are known, the propagation delay can be computed, subtracted from the pseudo-range and then corrected for the GPS time offset to determine the results of ground station time relative to GPS time. The navigation message also contains coefficients which allow GPS time to be referenced to the U.S. Naval Observatory (USNO) time standard, therefore, the final result of ground station time relative to USNO time can be calculated in real time. The final results obtained from a single frequency receiver will contain a small error

due to the atmospheric delay, which may be modeled and corrected. If two ground station clocks are synchronized to GPS time, the results can be subtracted to obtain the time difference between the ground station clocks. This can be done at any time, but the best results are obtained when data is taken simultaneously by each ground station from the same satellite (common view), since any error contributed by the satellite is reduced when the data is subtracted.

GPS Time Transfer Receiver (TTR)

The GPS TTR [8] is a microcomputer based system which operates at the single L-band frequency of 1575 MHz (Fig. 7). The receiver uses the C/A code only (1.023 MHz), tracking this code to within 3% of a chip (30 ns). The receiver has the capability to track satellites throughout their doppler range from horizon to horizon, and can track any GPS satellite by changing the receiver internal code. The block diagram in Fig. 8 shows the GPS receiver configuration. Operator interface with the receiver is provided by a keyboard and CRT display. The time data is stored on floppy disks and can also be outputted to an external printer or computer via a serial data interface. The input requirements to the receiver include the antenna position in WGS-72 coordinates, 1 pulse per second from the station time standard and 5 MHz from the station time standard.

Method of Measurement

The NRL built GPS time transfer receivers are currently being operated in MOBLAS 1 and 5, TLRS 1 and 2, and a semi-permanent laser site in Arequipa, Peru. The timing receiver interfaces with the laser system as shown in Fig. 9. Figure 10 contains a block diagram of the TLRS timing subsystem. The TLRS systems require a minimum of 200 minutes of useable laser measurements at a given site before relocation to a new installation. The one pulse per second and 5 MHz input signals required by the receiver are supplied by the station cesium beam clock. The receiver operates in a fully automatic schedule mode, tracking each GPS satellite once per day. The tracking schedule is determined by the operator. Each satellite track is usually scheduled to last ten minutes. Two minutes are required for signal search and acquisition, and one minute for locking and synchronizing to the satellite data. The time transfer results of (Station - USNO) and (Station - GPS) are then sent to the Precise Timing Section of Bendix Field Engineering Corporation (BFEC) in Columbia, Maryland, USA for further processing.

GPS Time Transfer Results

The first TLRS-1 site visited with a GPS timing receiver was Goldstone, California (GDS). Figure 11 shows the time transfer results of the GDS station clock relative to the United States Naval Observatory clock ensemble (denoted by NOB in all of the data plots). The time transfer in microseconds is plotted by days. The term "predicted" indicates that these results were obtained directly from the spacecraft. Figure 12 contains the same time transfer results, namely, (NOB-GDS), however these values are calculated by differencing the (GDS-GPS) data received using the NRL receiver and (NOB-GPS) data obtained via a similar receiver at USNO. The plots of this common view method of time transfer are labeled "observed". Both the predicted and observed plots have a statistical summary included. This summary contains a time transfer in microseconds, a frequency offset term in parts in 10^{13}, an aging term in parts in 10^{14} per day, the root mean square (RMS) fit in nanoseconds, the number of points used and the number of points filtered for each satellite. The satellites are identified by NAVSTAR numbers. There is also a composite line which incorporates the data from all satellites. The time transfer, frequency and aging terms are all calculated for the epoch day shown above the summary table. Because the TLRN sites all use cesium beam clocks a first degree curve is fit to the data, therefore there is no aging term. While the RMS values of the individual satellites are all within the TLRN system requirements of 100 ns, the observed data appears to be noisier then the predicted data. Generally, the common view technique of time transfer yields more accurate results than using the predicted USNO term from the space vehicle. However, common view assumes that two stations track the same GPS satellite at the same time, and this was not the case at the GDS station. The tracking schedule used at GDS differed from the USNO schedule by as much as 12 hours. Therefore, the results shown in the observed plot are less precise.

After the GDS site the TLRS-1 system was relocated to Santiago, Chile (denoted by AGO in the data plots). Figures 13 and 14 show the predicted and observed time transfer results of AGO relative to USNO, (NOB-AGO), for the entire period of time the station was in operation. Several discontinuities are obvious on these plots. The first discontinuity, occurring on day 78, was due to a discrete jump in the station cesium of approximately 10 microseconds. The second obvious discontinuity is the result of a new station cesium clock being installed. The original cesium failed on day 93 and the new cesium began operation on day 98. Two other less obvious discontinuities can be found on the predicted plot but do not show up in the observed data. These jumps, occurring on days 84 and 105, are the results

of accumulated error in the predicted USNO term. The USNO prediction is transmitted by each GPS satellite, as part of the navigation message, once every 12.5 minutes. The NRL receiver does not update the USNO prediction for each satellite track due to the length of time this would require. Rather, a special track is used by the receiver to update the entire navigation message, including the USNO term. This track, scheduled once a day and lasting 20 minutes, can be taken from a GPS satellite. If the predicted USNO term is not updated daily, the error will grow rapidly. Errors on the order of several hundred nanoseconds have been observed when the USNO prediction is a few days old. This error does not exist when the common view technique is used between a remote station and USNO. The observed plot of (NOB-AGO), (Fig. 14), therefore contains no discontinuities on days 84 and 105.

The Santiago station data has been subdivided into its three distinct phases and the predicted and observed data for each phase is shown plotted in Figs. 15 through 20. In each of these plots there is an obvious bias in the data from one satellite to another. This problem results when the coordinates of the receiver's antenna are inaccurate. The best time transfer results are obtained when the position of the antenna is known to within 3 meters. The observed plots reveal that these results are consistently superior to the predicted method. However, it should be noted that the predicted results are within the requirements of the TLRN system.

From Santiago the TLRS-1 system was moved to Cerra Tollola, Chile (TOL). The entire data set, both predicted and observed, can be found in Figs. 21 and 22. These graphs indicate that there was an antenna coordinate error upon system installation. On day 145 new coordinates were determined and input to the GPS receiver. The predicted and observed data after this coordinate change have been plotted and are shown in Fig. 23 and 24. Again, both the predicted and observed results are within TLRN system requirements, with the observed data having a slightly lower RMS.

In the later part of 1983 the TLRS-2 systems was deployed with a GPS receiver at Otay Mountain, California (OTY). TLRS-2 remained at this location for over 100 days and gathered much data (Figs. 25 and 26). All discontinuities on these graphs are the result of phase adjustments to the station cesium clock. Station personnel were required to keep the TLRS-2 clock synchronized with USNO time to within a few microseconds. Figures 27 and 28 show a representative sample of predicted and observed data from the Mt. Otay site. This sample covers the period from day

271 through day 284 in 1983. Again a lower RMS can be seen in the observed data, with the predicted data fulfilling system requirements.

The next site TLRS-2 visited was Cabo San Lucas, Mexico (CSL). The predicted and observed plots are shown in Figs. 29 and 30 respectively. Only NAVSTAR 4 appears in the statistical summary of the observed plot because the program that generates these plots requires five tracks of a particular satellite in order to calculate the summary information. The satellite tracking schedule used at CSL differed somewhat from that used at USNO, therefore the number of common view points on the observed plot is lower than the total number of points on the predicted plot.

The final laser site to be discussed is a semi-permanent station in Arequipa, Peru (ARP) which supports the NASA GSFC Crustal Dynamics Program. A GPS receiver was installed at this location in the first quarter of 1984 (Fig. 31). The predicted and observed graphs are shown in Figs. 32 and 33. The discontinuities on the predicted plot occurring on days 107 and 118 are due to accumulated error in the predicted USNO term due to lack of update. These discontinuites, therefore, do not appear on the observed plot. Other discontinuities are the results of phase adjustments to the station cesium clock. Figures 34 and 35 contain the predicted and observed graphs for the period between days 125 and 167. Again, because of the difference in satellite tracking schedules between ARP and USNO, an ideal common view situation does not exist. Therefore, the predicted and observed results show little difference.

Future TLRN Systems

NRL built GPS time transfer receivers were recently installed in MOBLAS-1 deployed at Huahine, French Polynesia and MOBLAS-5 at Yarragadie, Australia. GPS time transfer data from these stations was not available at this writing.

The TLRS 3 and 4 systems are currently under development and testing at the NASA Goddard Space Flight Center. These TLRS systems will be using GPS timing receivers manufactured by Stanford Telecommunications, Inc. (STI). The STI receivers have been procured and are currently being tested at GSFC. Experimental data obtained under laboratory conditions at the GSFC laser laboratory using the STI receivers is shown in Fig. 36. The receivers were operated using an internal rubidium oscillator included in the STI receivers as an option. Therefore, a second degree curve has been fit to this data which results in an aging term being calculated and included in the summaries of Fig. 36. The STI receiver outputs the station time difference relative to either USNO or GPS, but not

both simultaneously. In these experiments the receivers were operated with the time difference relative to USNO, therefore, only the predicted plot can be shown.

Conclusion

The results of the operational data, gathered by the NRL built GPS time transfer receivers at field sites, indicate that the overall accuracy of the synchronization via the Global Positioning System is consistently better than 100 nanoseconds, which meets the synchronization requirement of the NASA laser ranging network. The results of the experimental data gathered by the STI timing receivers under laboratory conditions indicate that these receivers will also meet the TLRN system synchronization requirements. Field tests on the STI receivers are scheduled for the near future.

References

1. L. Raymond, O. J. Oaks, J. Osbone, G. Whitworth, J. Buisson, P. Landis, C. Wardrip, and J. Perry, "Navigation Technology Satellite (NTS) Low Cost Timing Receiver," Goddard Space Flight Center Report X814-77-205, Aug. 1977.

2. O. J. Oaks, Jr., J. A. Buisson, and T. B. McCaskill, "Initial Design for NTS Time Transfer Receiver," NRL Report 8312, May 1979.

3. J. Buisson, T. McCaskill, J. Oaks, D. Lynch, C. Wardrip, and G. Whitworth, "Submicrosecond Comparisons of Time Standards via the Navigation Technology Satellites (NTS)," pp. 601-627 in Proceedings of the Tenth Annual Precise Time and Time Interval (PTTI) Applications and Planning Meeting, Nov. 1978, NASA Technical Memorandum 80250.

4. "Laser Stations - Plant Facilities Development and Station Description," Goddard Space Flight Center Report MF-176, August 1983.

5. R. L. Easton, J. A. Buisson, and T. B. McCaskill, "Initial Results of the NAVSTAR GPS NTS-2 Satellite," NRL Report 8232, May 1978.

6. R. L. Easton, J. A. Buisson, T. B. McCaskill, O. J. Oaks, S. Stebbins, and M. Jeffries, "The Contribution of Navigation Technology Satellites to the Global Positioning System," NRL Report 8360, Dec. 1979.

7. S. S. Russell and J. H. Schaibly, "Control Segment and User Performance," Navigation (J. Inst. Navigation) 25(2), 166-172 (1978).

8. J. Oaks, J. Buisson, C. Wardrip - "GPS Time Transfer Receivers for the NASA Transportable Laser Ranging Network", NASA/GSFC x-814-82-6, April 1982.

9. J. Oaks, A. Frank, S. Falvey, M. Lister, J. Buisson, S. Wardrip and H. Warren, "Prototype Design and Initial Test Evaluation of a GPS Time Transfer Receiver", NRL report 8608, July 27, 1982.

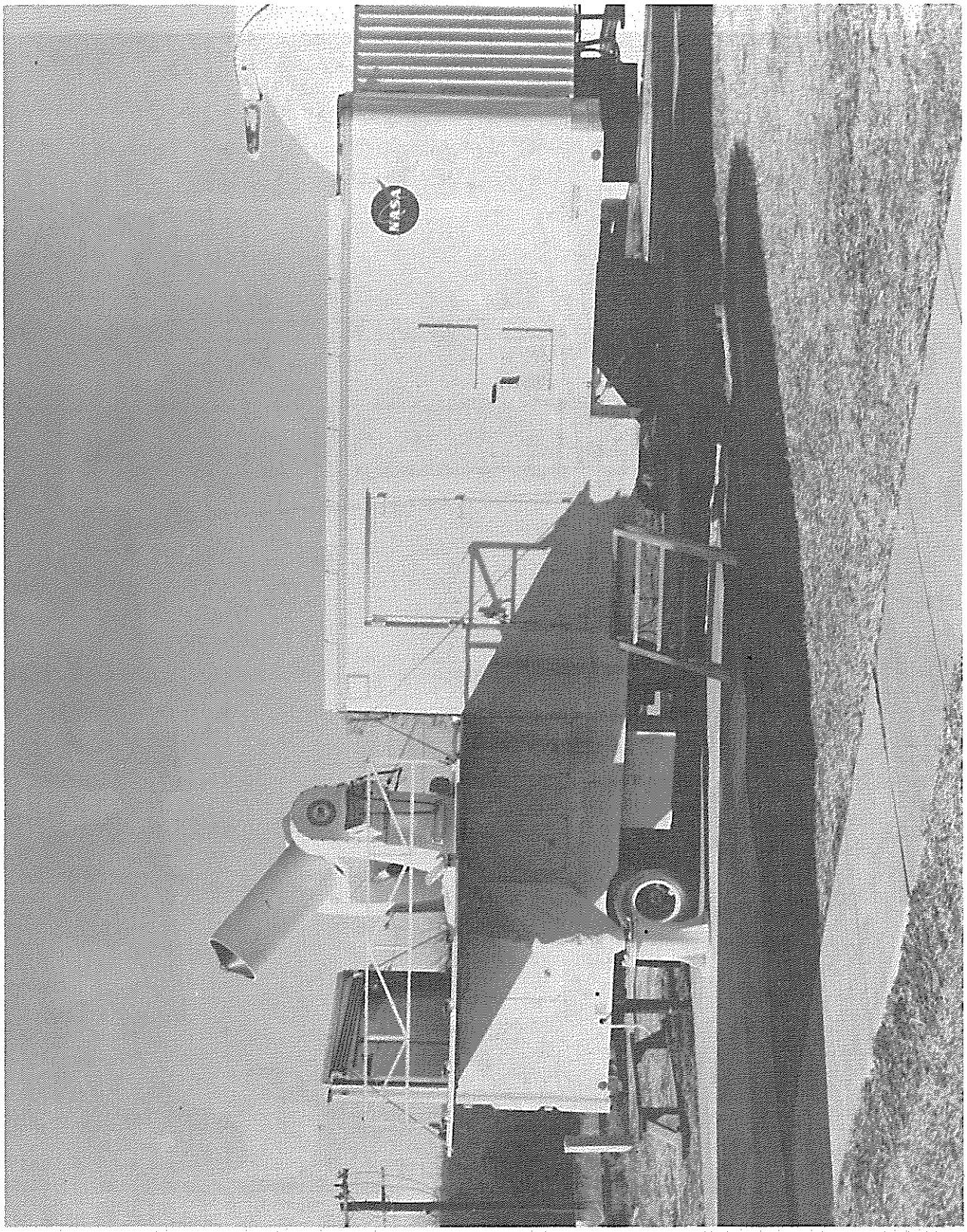

Figure 1 Mobile Laser System (MOBILAS) Van.

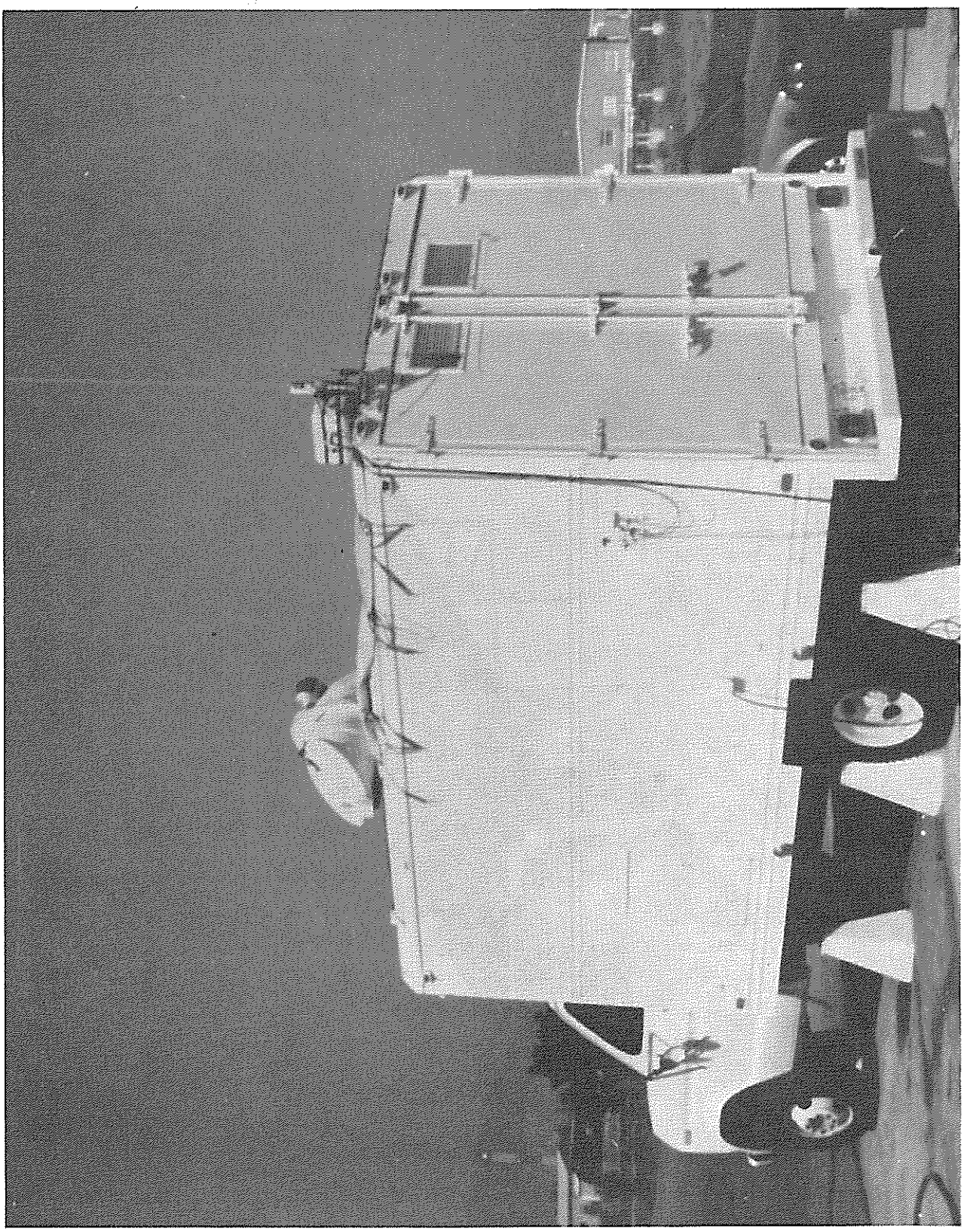

Figure 2 Transportable Laser System (TLRS-1) Van.

Figure 3 Transportable Laser System (TLRS-2) Dome.

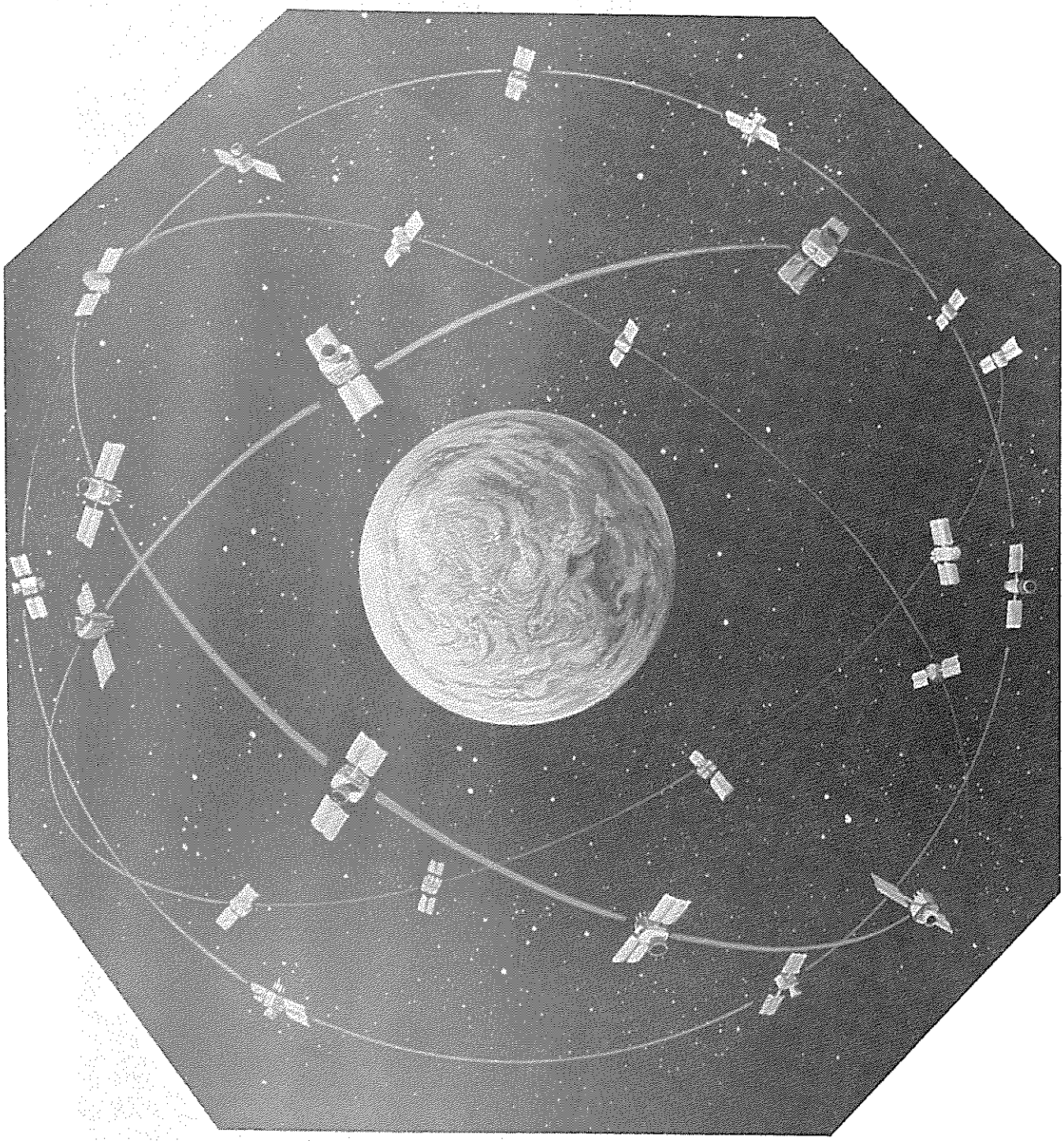

Figure 4 The NAVSTAR Global Positioning System.

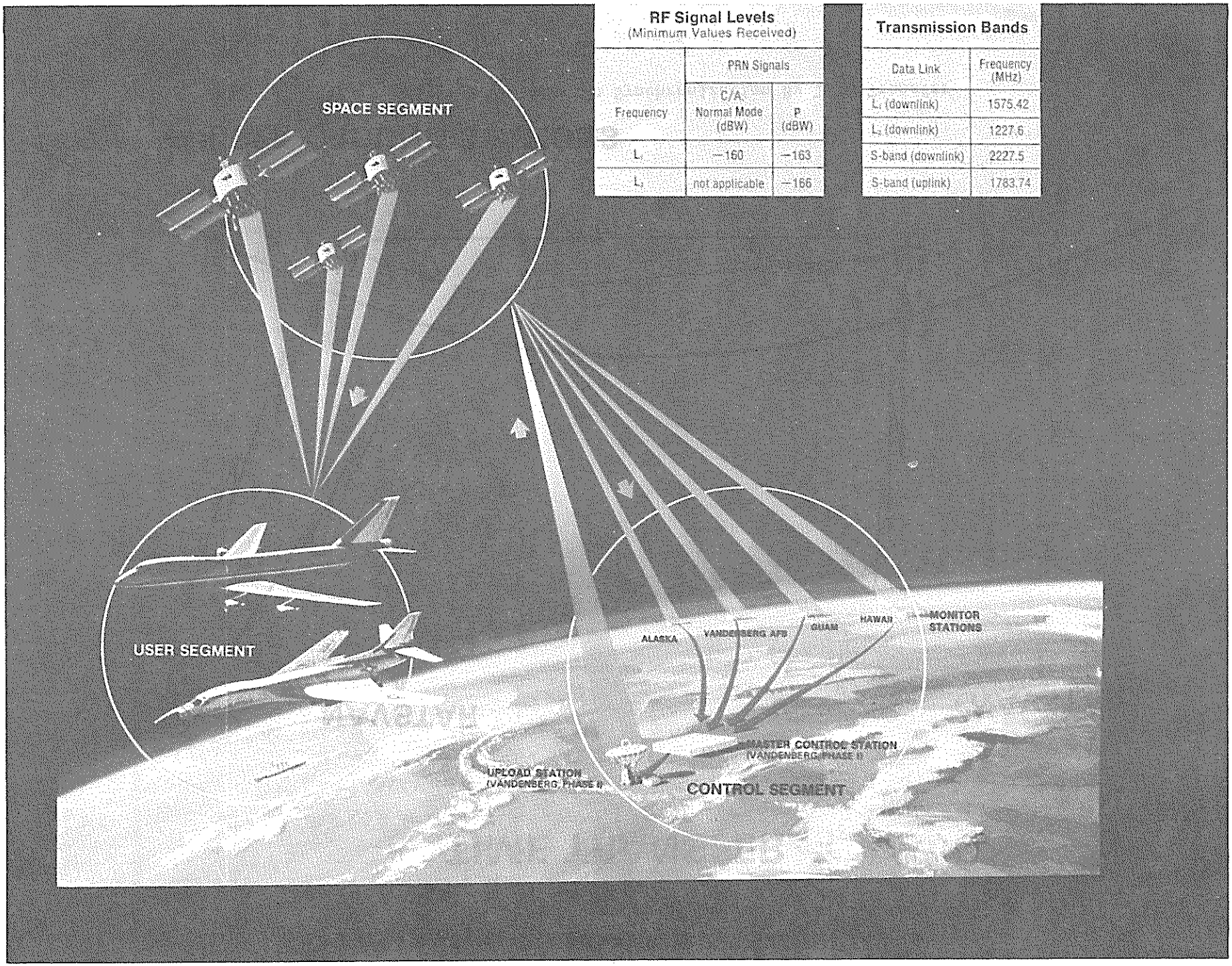

RF Signal Levels
(Minimum Values Received)

Frequency	PRN Signals	
	C/A Normal Mode (dBW)	P (dBW)
L_1	−160	−163
L_2	not applicable	−166

Transmission Bands

Data Link	Frequency (MHz)
L_1 (downlink)	1575.42
L_2 (downlink)	1227.6
S-band (downlink)	2227.5
S-band (uplink)	1783.74

Figure 5 NAVSTAR Global Positioning System Segments.

NAVSTAR GPS
STATION SYNCHRONIZATION
BY
TIME TRANSFER

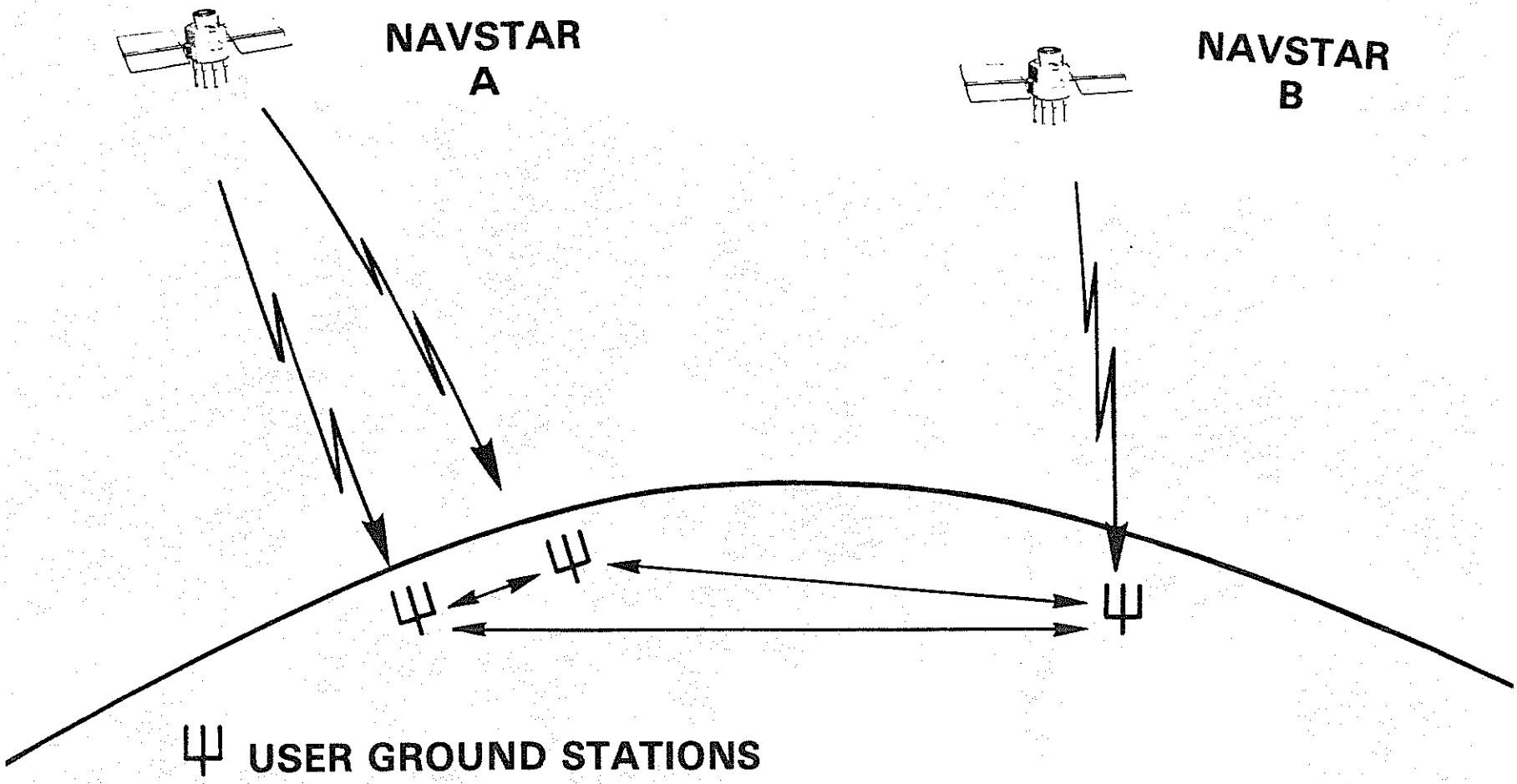

Fig. 6 NAVSTAR GPS Station Synchronization By Time Transfer

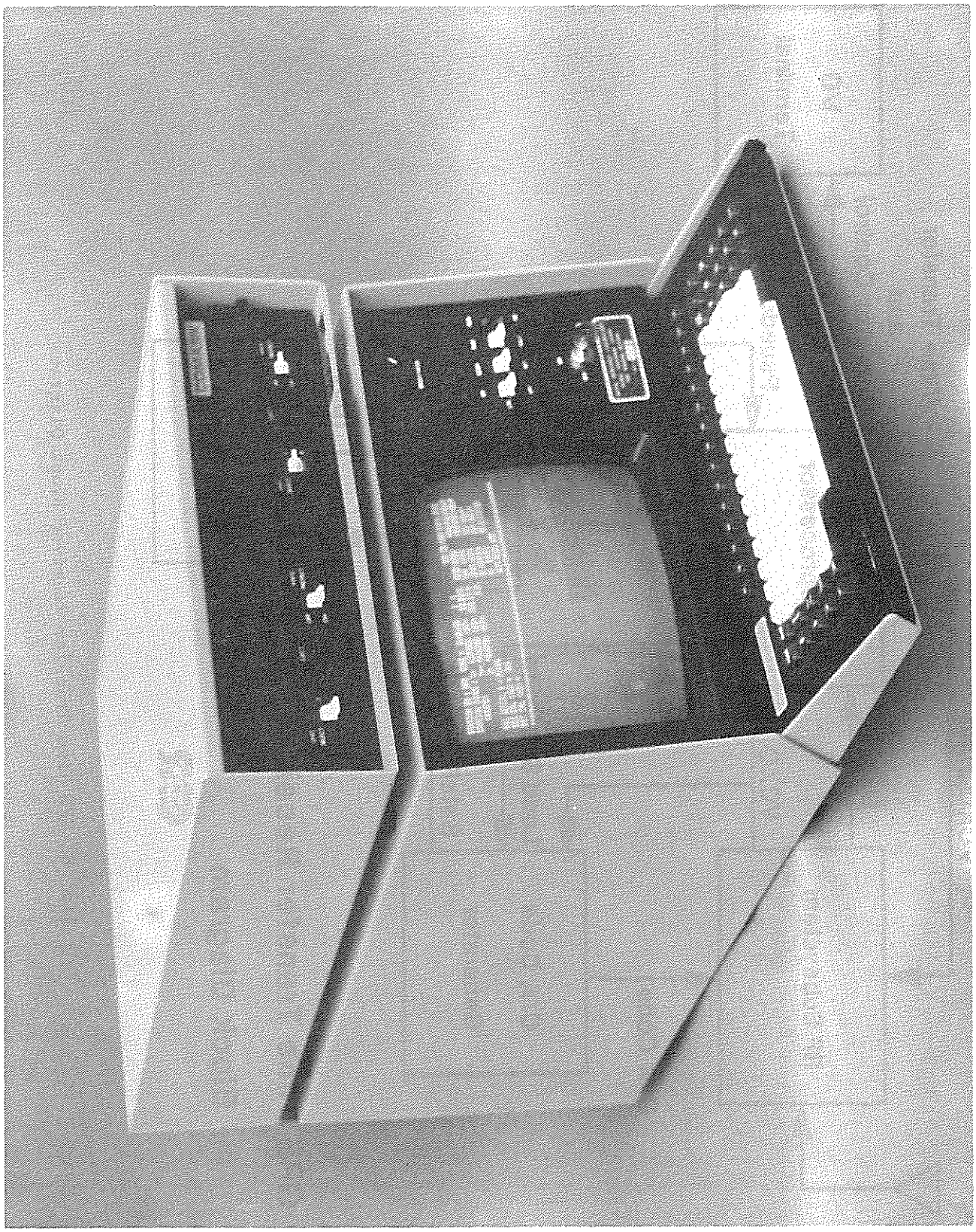

Figure 7 Naval Research Laboratory GPS Receiver.

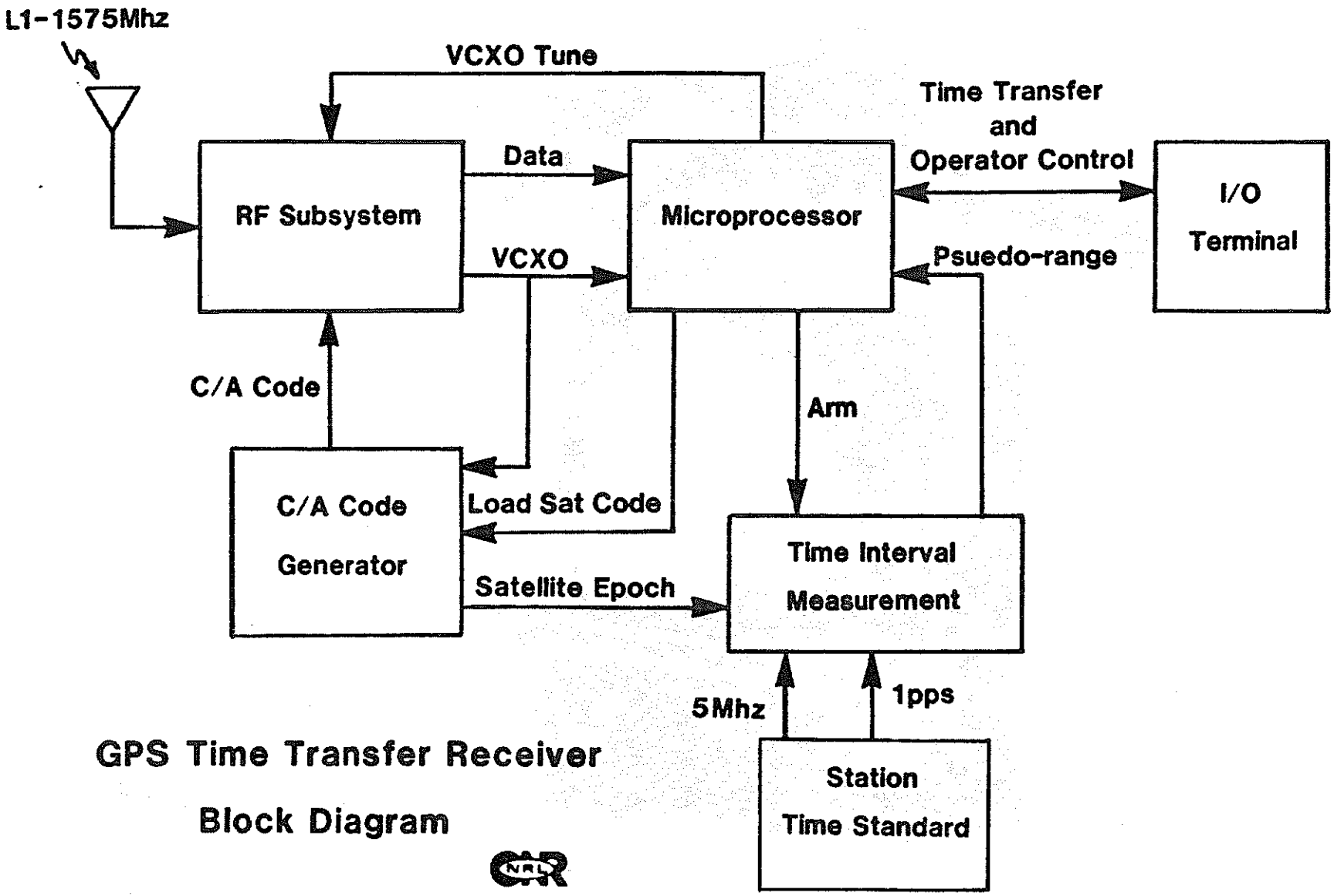

Fig. 8 GPS Time Transfer Receiver Block Diagram

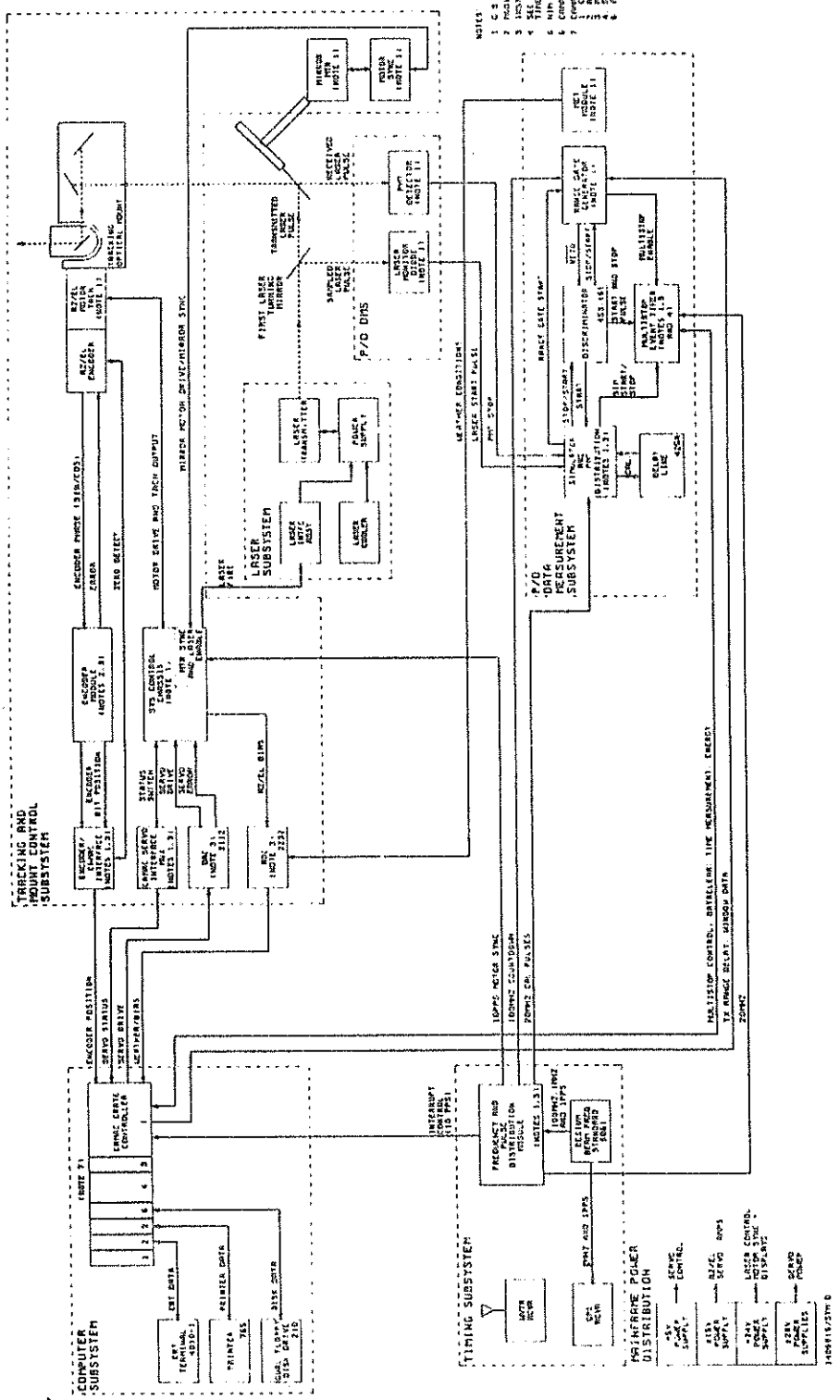

Fig. 9 TLRS-2 Overall Block Diagram

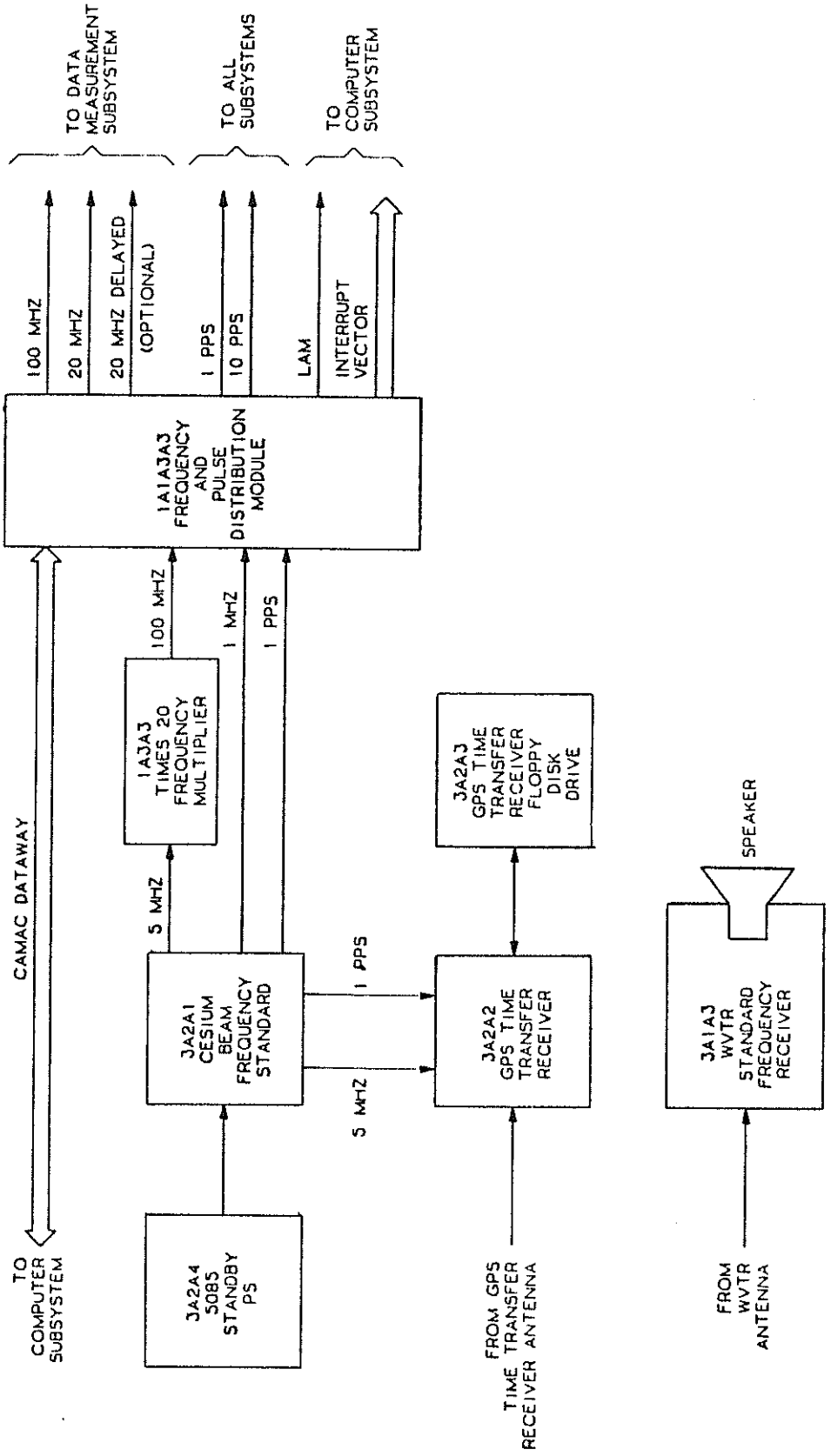

Fig. 10 Timing Subsystem, Simplified Block Diagram

NAVSTAR GPS TIME TRANSFER

EPOCH DAY 57.0 ,1984

SAT ID	TT US	FREQ PP13	AGING PP14/D	RMS NS	PTS USED	PTS FLTRD	FILTER TOL(NS)
1	.000	.00	.0	0	0	0	START 300
3	-15.682	-23.77	.0	74	11	0	PLOT
4	-15.658	-25.50	.0	48	13	0	COMP 300
5	.000	.00	.0	0	0	0	DFIT 1
6	-15.624	-24.09	.0	59	12	0	
8	-15.619	-25.54	.0	60	8	0	
9	.000	.00	.0	0	0	0	
COMP	-15.650	-24.53	.0	68	44	0	

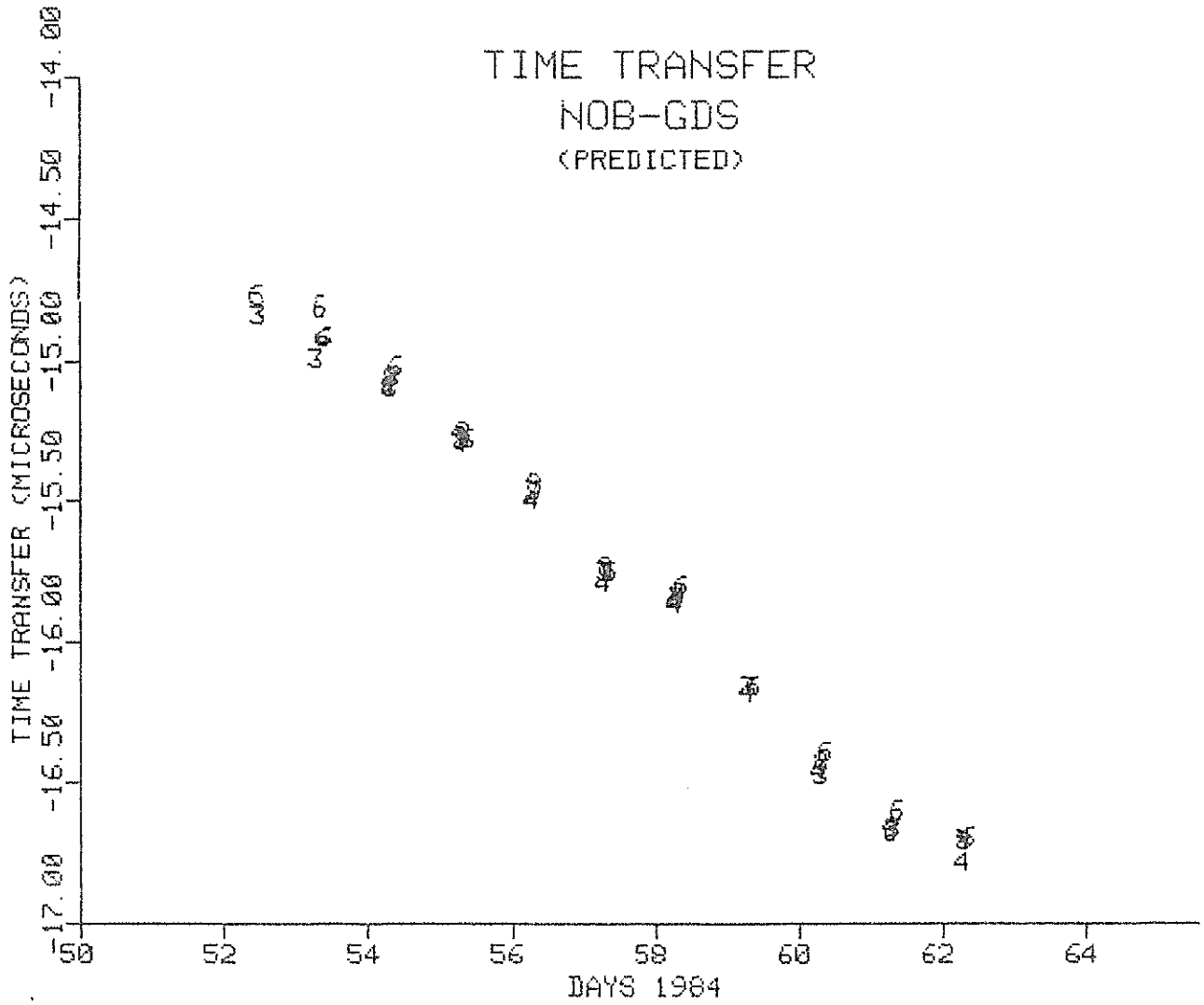

Fig. 11 NAVSTAR GPS Time Transfer

NAVSTAR GPS TIME TRANSFER

EPOCH DAY 57.0 , 1984

SAT ID	TT US	FREQ PP13	AGING PP14/D	RMS NS	PTS USED	PTS FLTRD	FILTER TOL(NS)
1	.000	.00	.0	0	0	0	STAT 300
3	-15.728	-27.63	.0	81	10	0	PLOT
4	-15.631	-23.79	.0	72	10	0	COMP 300
5	.000	.00	.0	0	0	0	DFIT 1
6	-15.625	-29.01	.0	87	10	0	
8	-15.726	-25.05	.0	56	8	0	
9	.000	.00	.0	0	0	0	
COMP	-15.671	-26.09	.0	104	38	0	

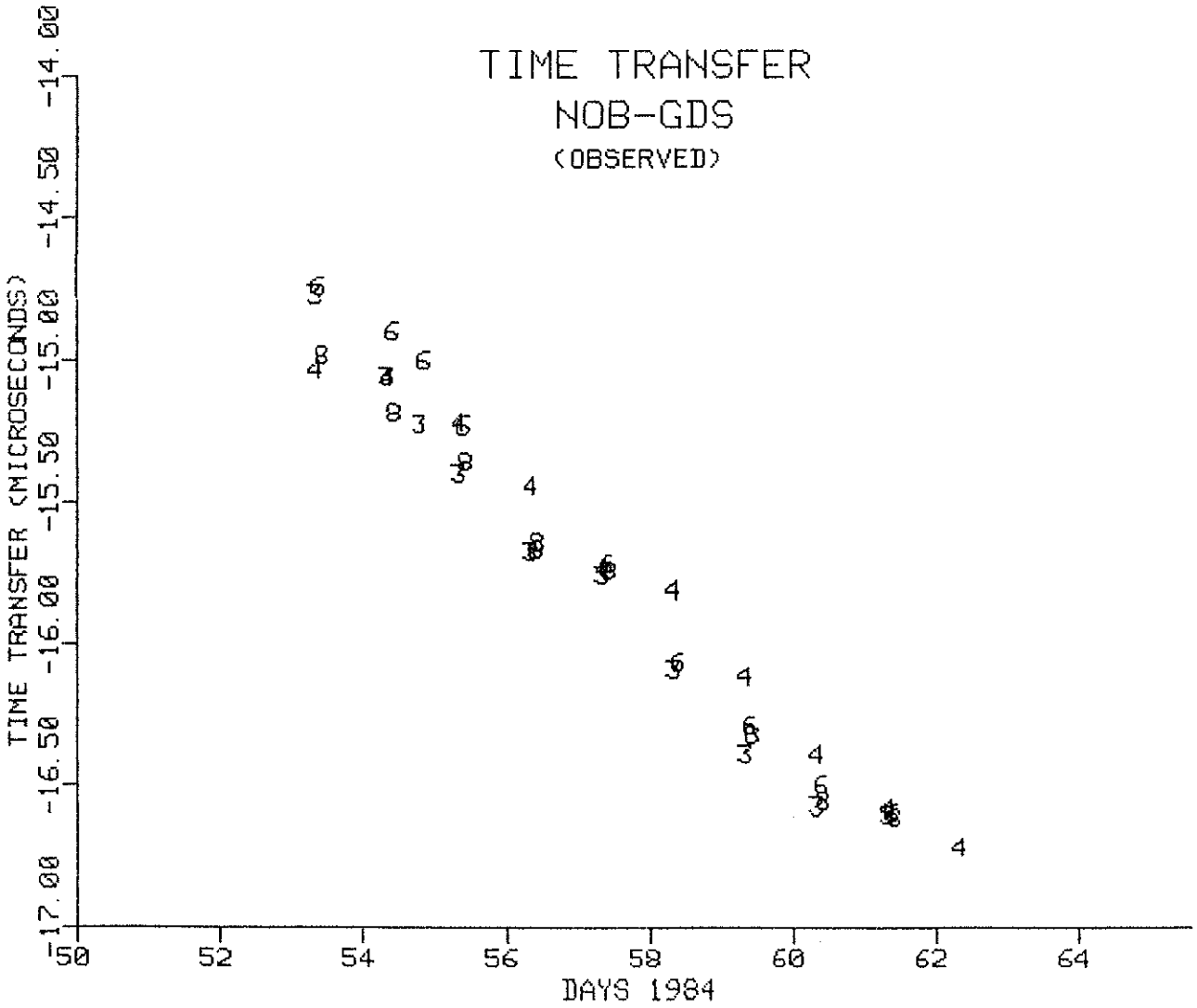

Fig. 12 NAVSTAR GPS Time Transfer

NAVSTAR GPS TIME TRANSFER

EPOCH DAY 99.5 , 1984

SAT ID	TT US	FREQ PP13	AGING PP14/D	RMS NS	PTS USED	PTS FLTRD
1	.000	.00	.0	0	0	0
3	-1.652	45.47	.0	6036	54	0
4	-3.079	42.59	.0	7191	16	0
5	.000	.00	.0	0	0	0
6	-1.205	46.06	.0	6013	52	0
8	-1.192	51.31	.0	6427	38	0
9	.000	.00	.0	0	0	0
COMP	-1.532	47.27	.0	6269	160	0

FILTER TOL(NS)
STAT 3000
PLOT
COMP 3000
DFIT 1

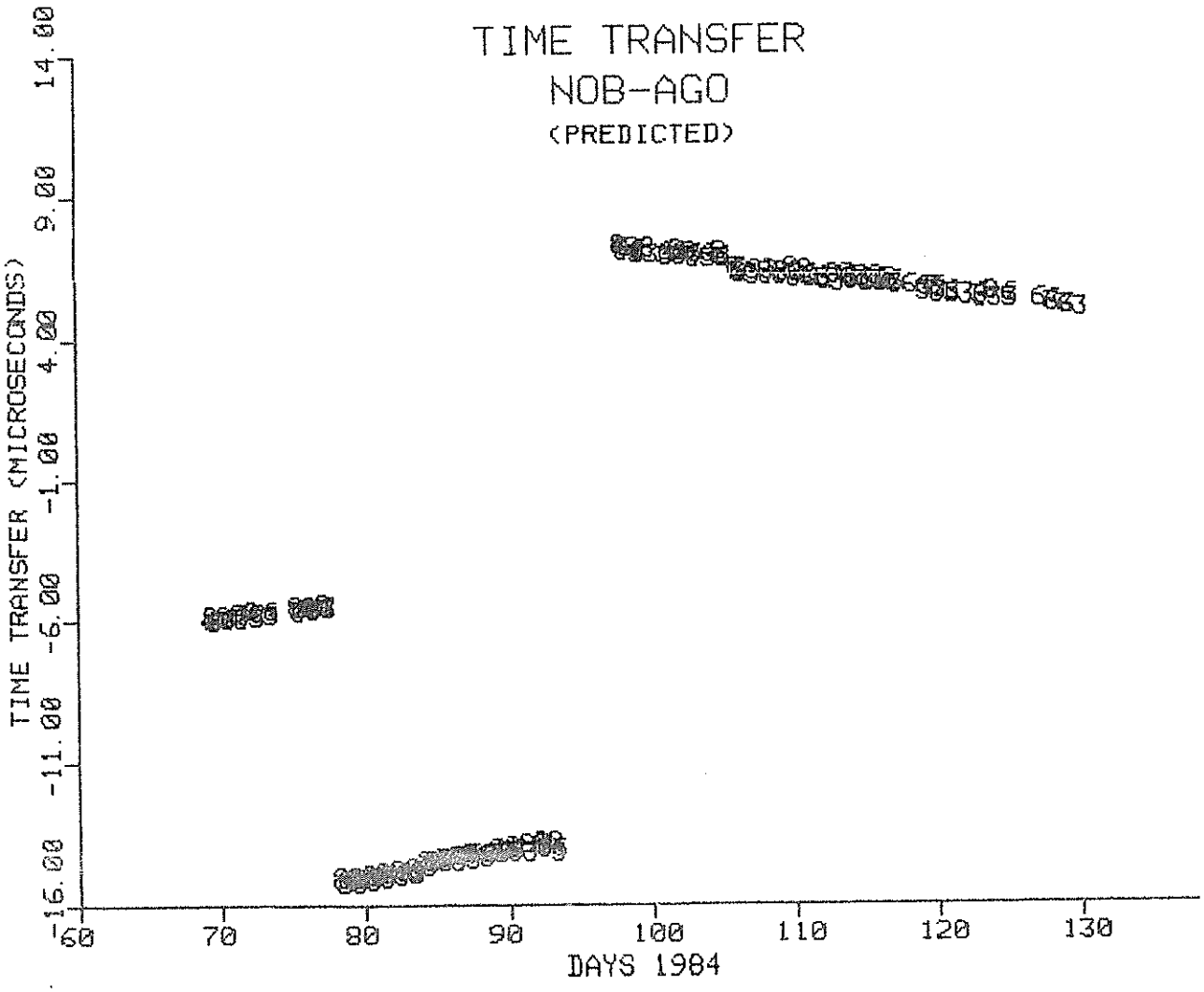

Fig. 13 NAVSTAR GPS Time Transfer

NAVSTAR GPS TIME TRANSFER

EPOCH DAY 99.5 , 1984

SAT ID	TT US	FREQ PP13	AGING PP14/D	RMS NS	PTS USED	PTS FLTRD
1	.000	.00	.0	0	0	0
3	-1.672	45.40	.0	6101	51	0
4	-2.733	56.86	.0	6958	14	0
5	.000	.00	.0	0	0	0
6	-1.580	45.60	.0	5855	49	0
8	-2.037	51.45	.0	6235	34	0
9	.000	.00	.0	0	0	0
COMP	-1.937	47.93	.0	6186	148	0

FILTER TOL(NS)
STAT 3000
PLOT
COMP 3000
DFIT 1

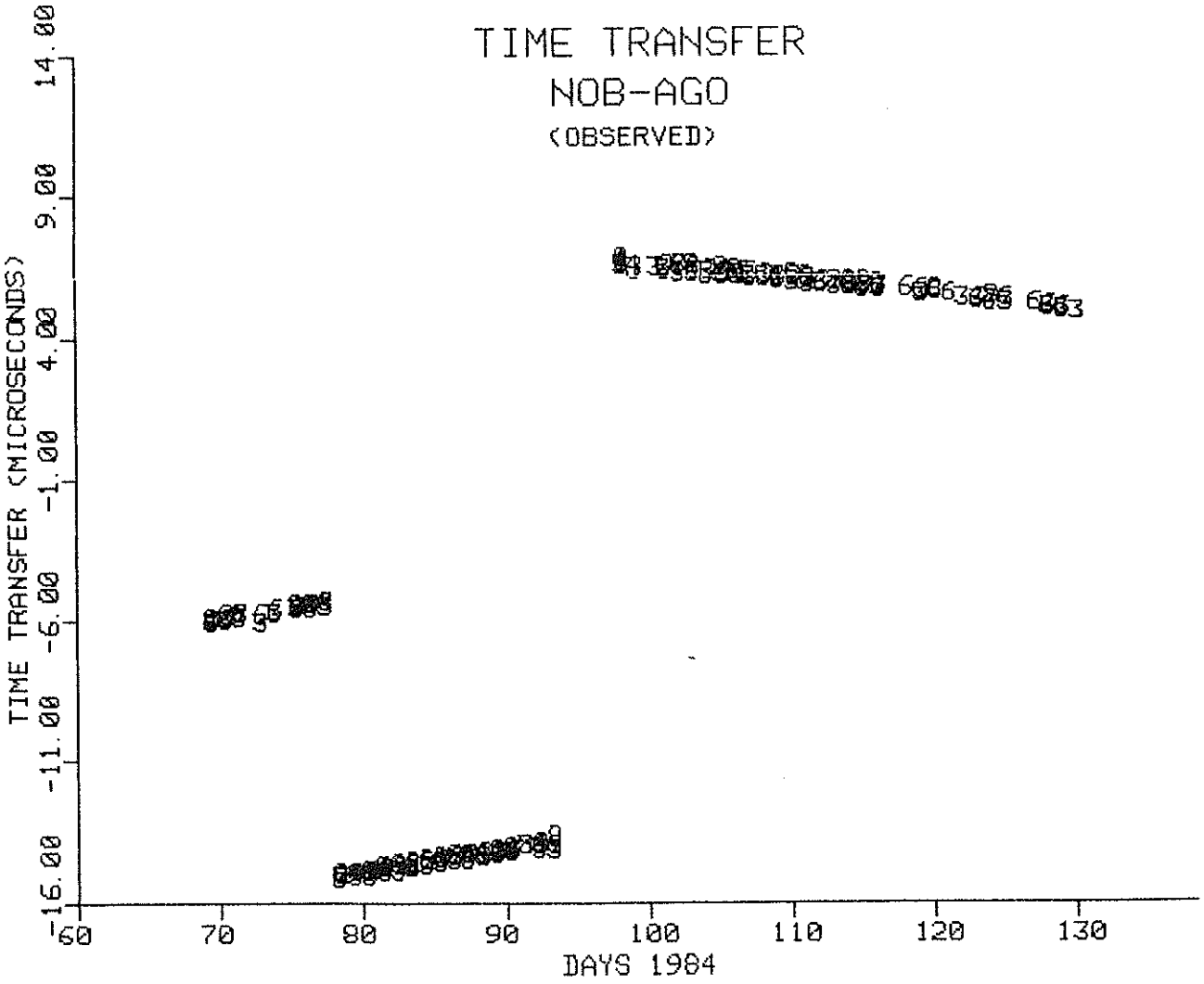

Fig. 14 NAVSTAR GPS Time Transfer

NAVSTAR GPS TIME TRANSFER

EPOCH DAY 73.0 ,1984

SAT ID	TT US	FREQ PP13	AGING PP14/D	RMS NS	PTS USED	PTS FLTRD
1	.000	.00	.0	0	0	0
3	-5.747	7.09	.0	17	8	0
4	.000	.00	.0	0	0	0
5	.000	.00	.0	0	0	0
6	-5.632	7.20	.0	44	8	0
8	-5.534	6.66	.0	14	7	0
9	.000	.00	.0	0	0	0
COMP	-5.633	7.12	.0	88	27	0

FILTER TOL(NS)
STAT 300
PLOT
COMP 300
DFIT 1

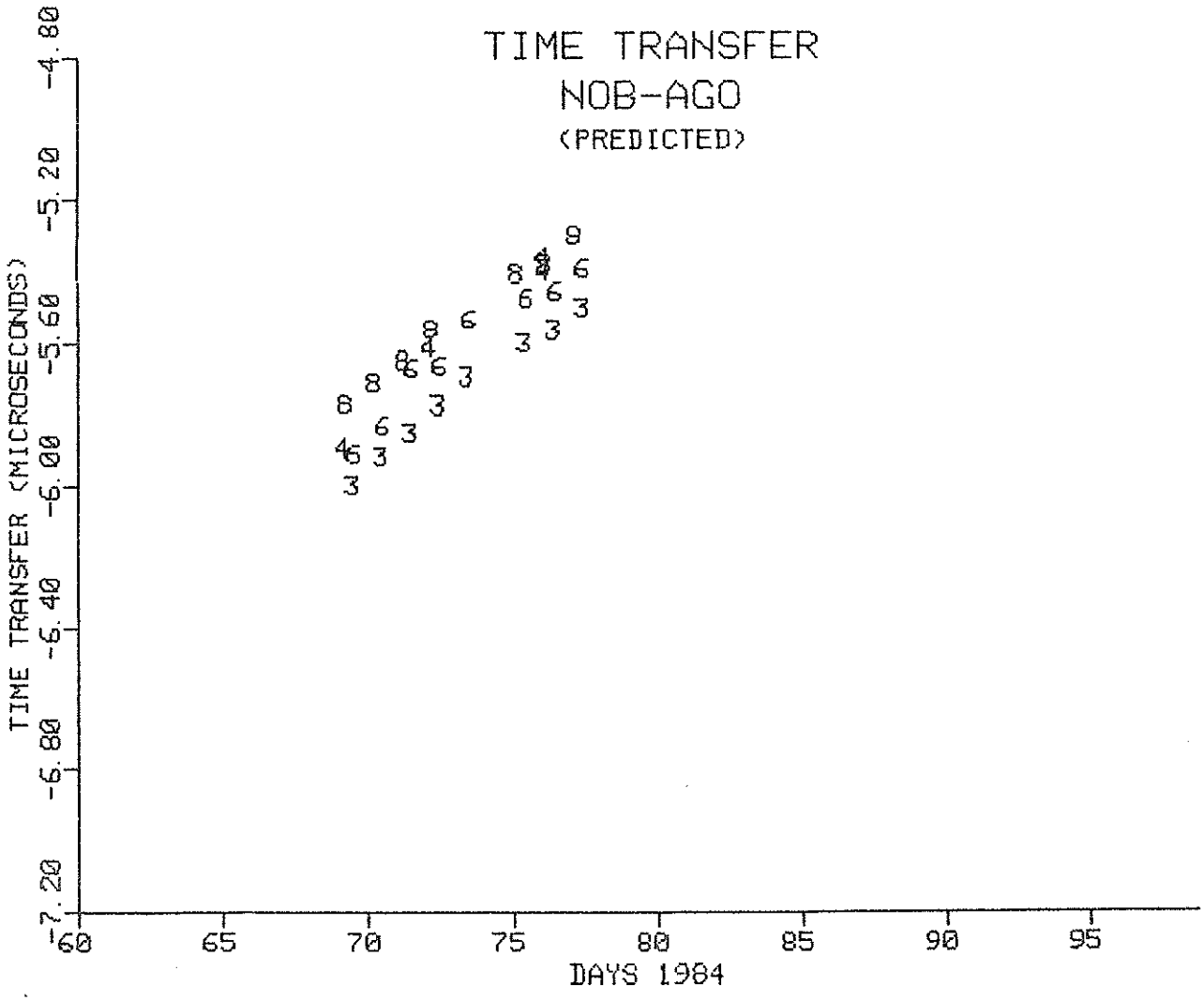

Fig. 15 NAVSTAR GPS Time Transfer

NAVSTAR GPS TIME TRANSFER

EPOCH DAY 73.0 ,1984

SAT ID	TT US	FREQ PP13	AGING PP14/D	RMS NS	PTS USED	PTS FLTRD	FILTER TOL(NS)
1	.000	.00	.0	0	0	0	STAT 300
3	-5.680	8.75	.0	17	7	0	PLOT
4	.000	.00	.0	0	0	0	COMP 300
5	.000	.00	.0	0	0	0	DFIT 1
6	-5.579	9.25	.0	42	8	0	
8	-5.501	8.08	.0	10	6	0	
9	.000	.00	.0	0	0	0	
COMP	-5.590	8.87	.0	74	23	0	

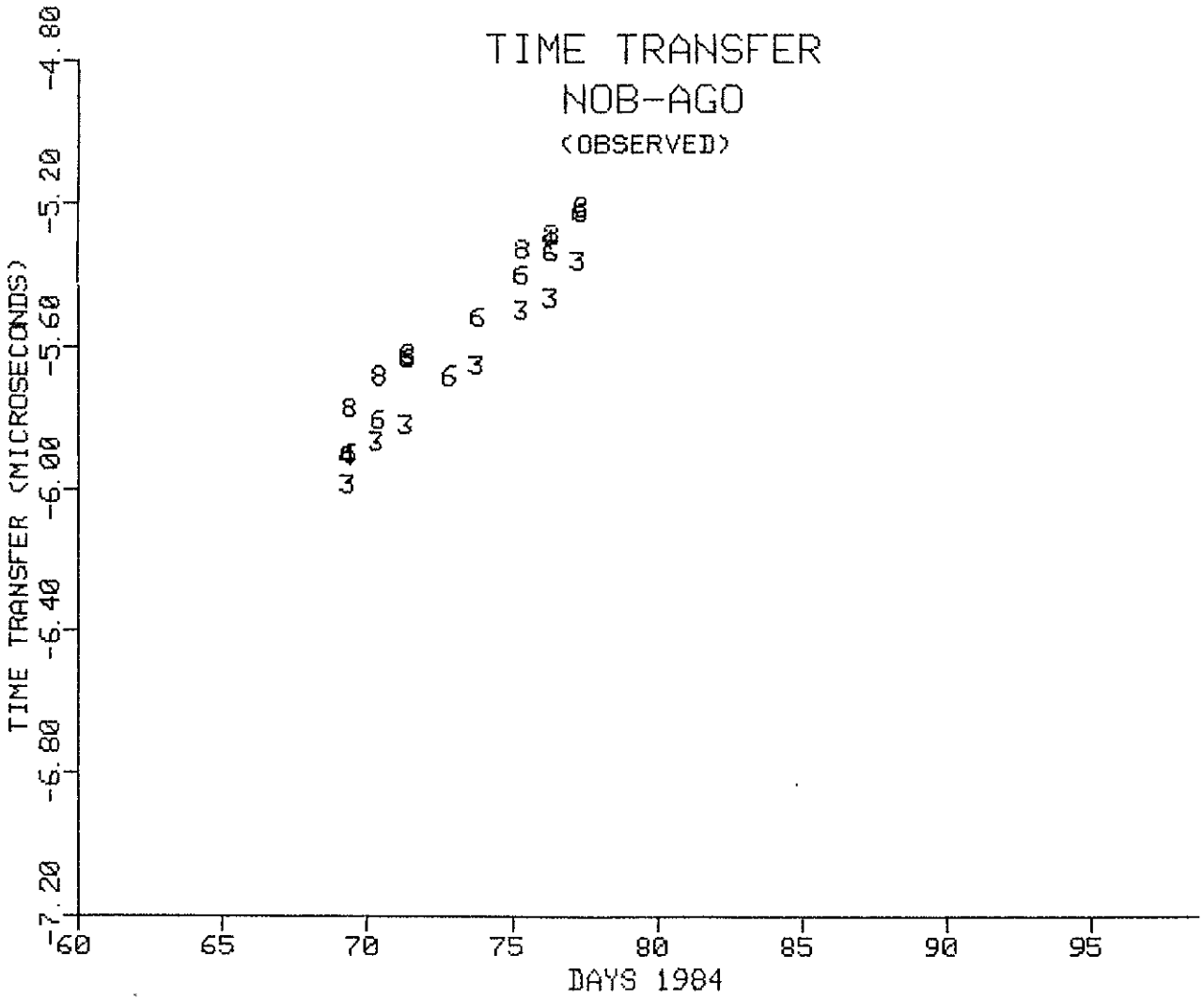

Fig. 16 NAVSTAR GPS Time Transfer

NAVSTAR GPS TIME TRANSFER

EPOCH DAY 85.0 , 1984

SAT ID	TT US	FREQ PP13	AGING PP14/D	RMS NS	PTS USED	PTS FLTRD	FILTER TOL(NS)
1	.000	.00	.0	0	0	0	STAT 300
3	-14.608	11.36	.0	69	15	0	PLOT
4	-14.412	11.37	.0	46	9	0	COMP 300
5	.000	.00	.0	0	0	0	DFIT 1
6	-14.465	11.44	.0	79	14	0	
8	-14.393	11.34	.0	60	14	0	
9	.000	.00	.0	0	0	0	
COMP	-14.475	11.33	.0	112	52	0	

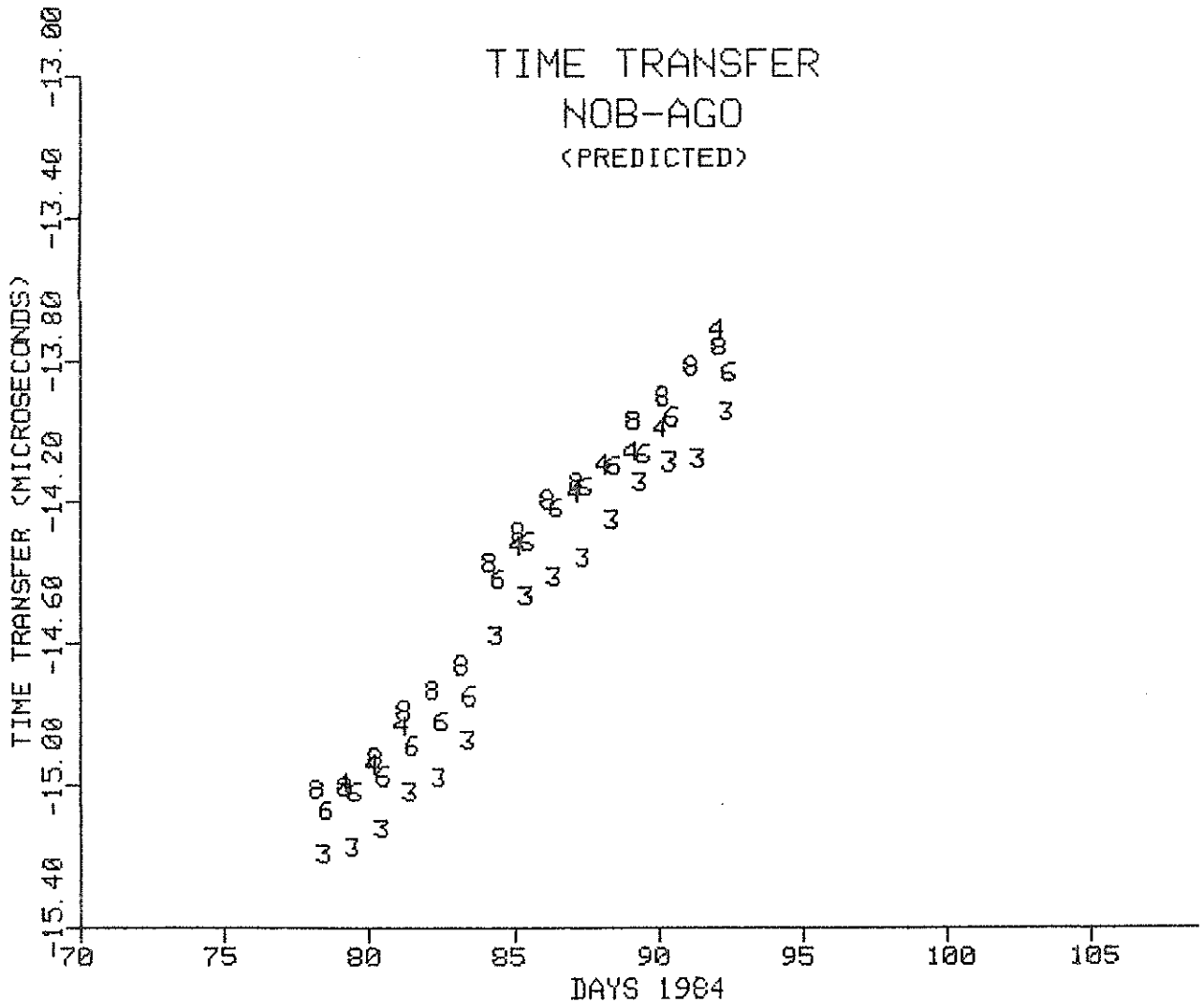

Fig. 17 NAVSTAR GPS Time Transfer

NAVSTAR GPS TIME TRANSFER

EPOCH DAY 85.0 , 1984

SAT ID	TT US	FREQ PP13	AGING PP14/D	RMS NS	PTS USED	PTS FLTRD	FILTER TOL(NS)
1	.000	.00	.0	0	0	0	STAT 300
3	-14.556	9.85	.0	58	15	0	PLOT
4	-14.426	9.24	.0	40	9	0	COMP 300
5	.000	.00	.0	0	0	0	DFIT 1
6	-14.423	9.04	.0	32	14	0	
8	-14.374	9.17	.0	24	14	0	
9	.000	.00	.0	0	0	0	
COMP	-14.448	9.33	.0	83	52	0	

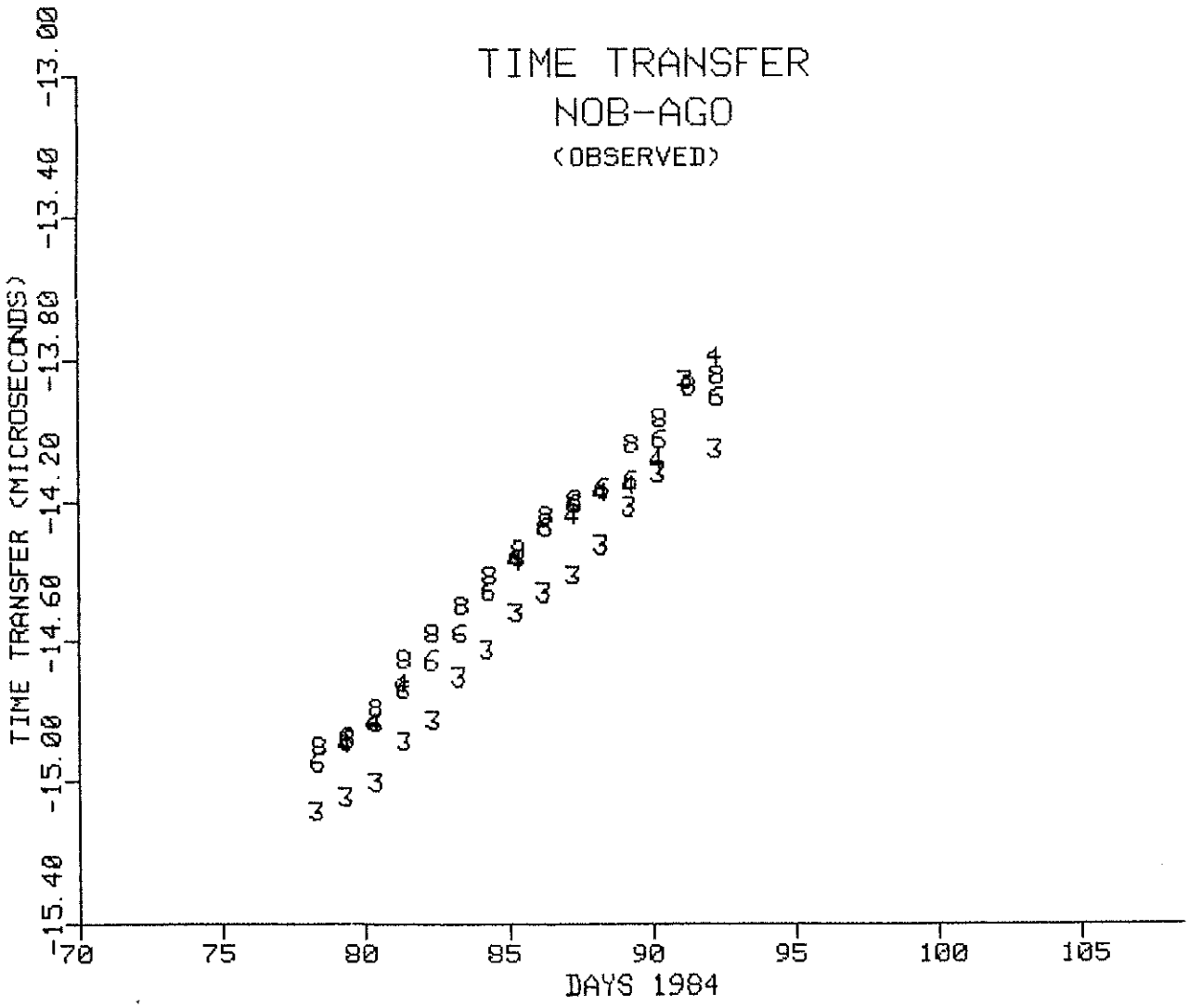

Fig. 18 NAVSTAR GPS Time Transfer

NAVSTAR GPS TIME TRANSFER

EPOCH DAY 114.0, 1984

SAT ID	TT US	FREQ PP13	AGING PP14/D	RMS NS	PTS USED	PTS FLTRD	FILTER TOL(NS)
1	.000	.00	.0	0	0	0	STAT 300
3	6.092	-7.35	.0	96	30	0	PLOT
4	.000	.00	.0	0	0	0	COMP 300
5	.000	.00	.0	0	0	0	DFIT 1
6	6.202	-7.48	.0	114	29	0	
8	6.281	-7.82	.0	101	16	0	
9	.000	.00	.0	0	0	0	
COMP	6.174	-7.62	.0	129	78	0	

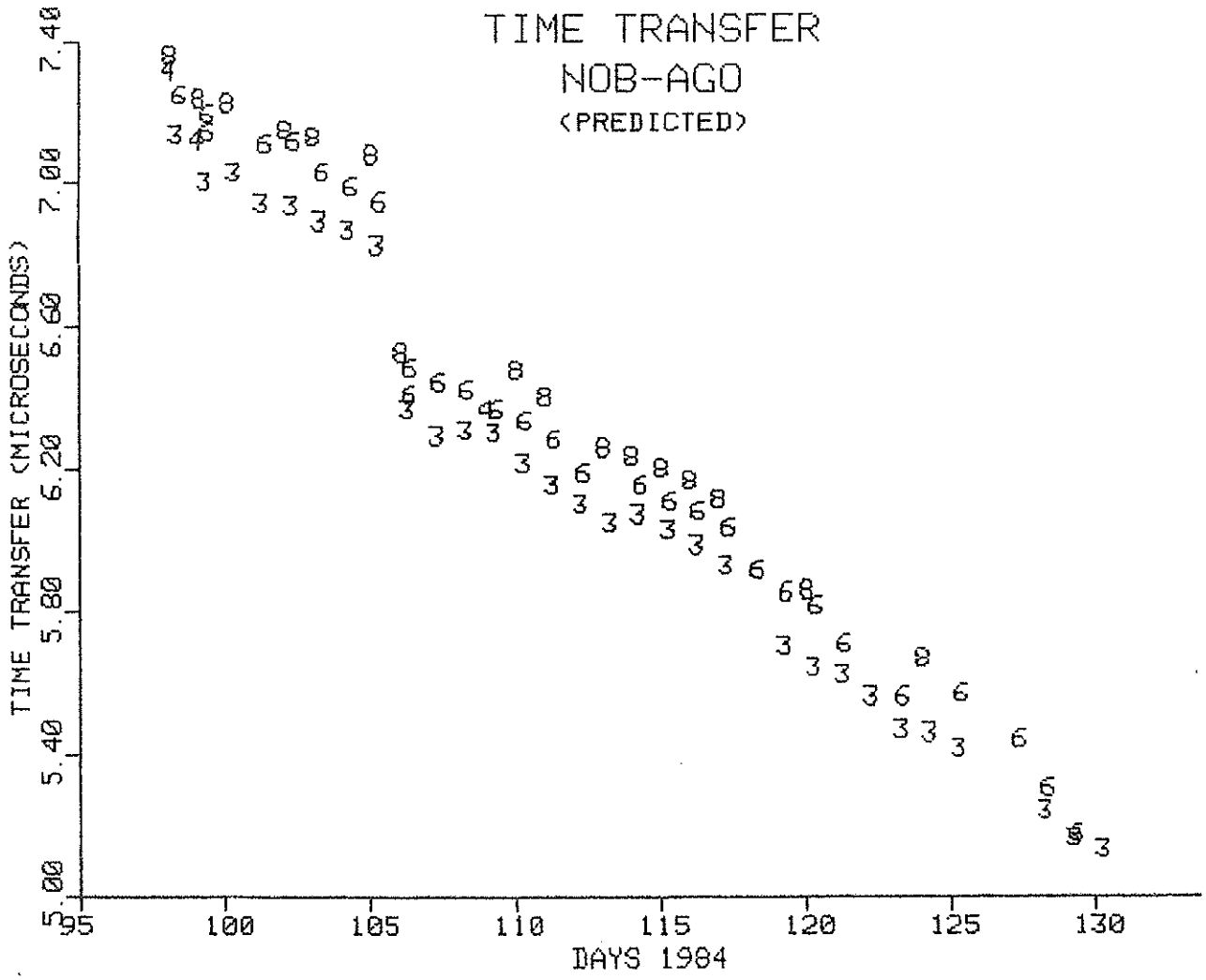

Fig. 19 NAVSTAR GPS Time Transfer

NAVSTAR GPS TIME TRANSFER

EPOCH DAY 114.0, 1984

SAT ID	TT US	FREQ PP13	AGING PP14/D	RMS NS	PTS USED	PTS FLTRD	FILTER TOL(NS)
1	.000	.00	.0	0	0	0	STAT 300
3	5.909	-5.81	.0	40	27	0	PLOT
4	.000	.00	.0	0	0	0	COMP 300
5	.000	.00	.0	0	0	0	DFIT 1
6	6.034	-5.85	.0	38	26	0	
8	6.130	-5.81	.0	26	13	0	
9	.000	.00	.0	0	0	0	
COMP	6.001	-5.87	.0	91	69	0	

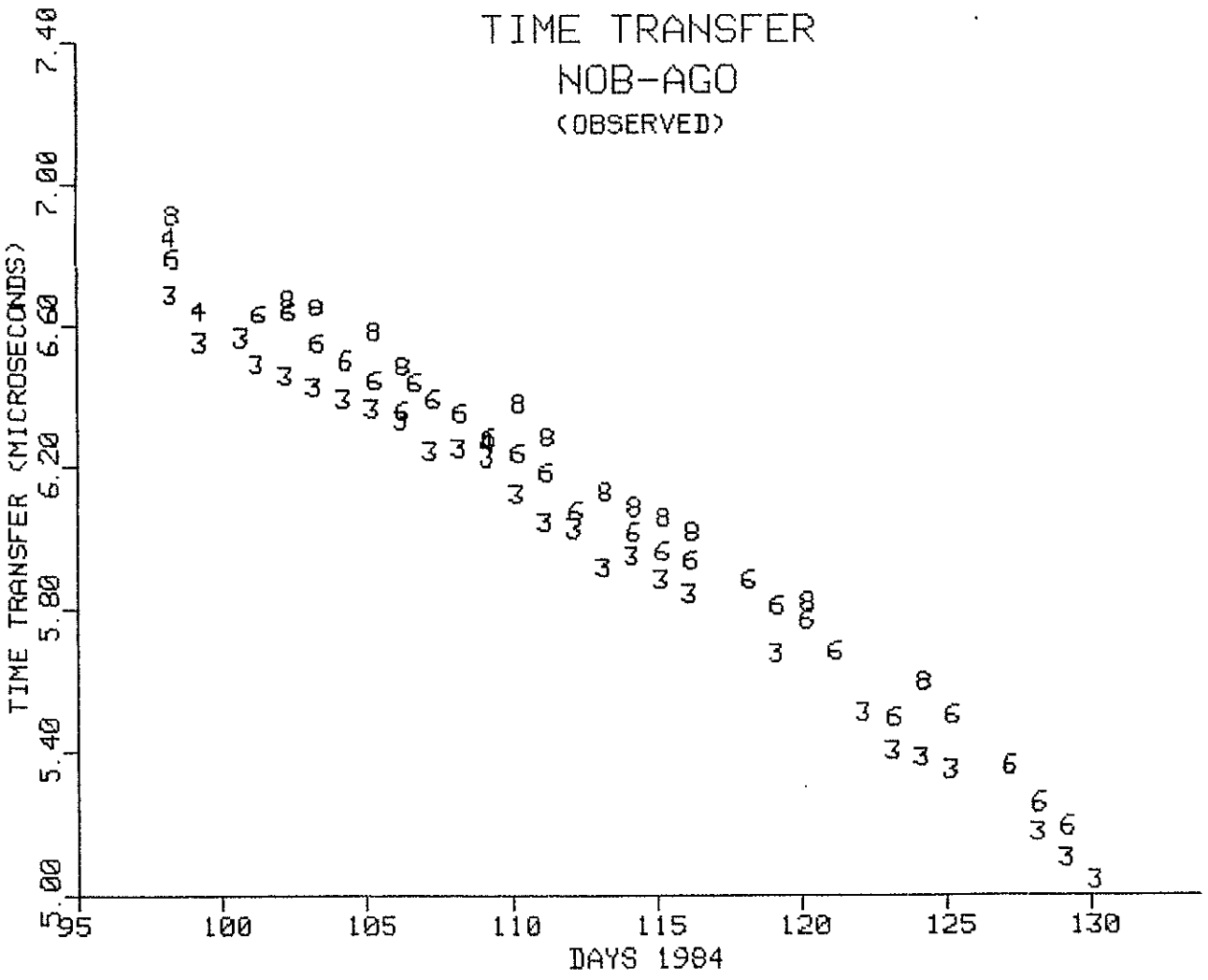

Fig. 20 NAVSTAR GPS Time Transfer

NAVSTAR GPS TIME TRANSFER

EPOCH DAY 155.0, 1984

SAT ID	TT US	FREQ PP13	AGING PP14/D	RMS NS	PTS USED	PTS FLTRD	FILTER TOL(NS)
1	.000	.00	.0	0	0	0	STAT 300
3	2.336	-11.14	.0	183	34	0	PLOT
4	.000	.00	.0	0	0	0	COMP 300
5	.000	.00	.0	0	0	0	DFIT 1
6	2.499	-13.90	.0	161	34	0	
8	2.524	-14.27	.0	186	27	0	
9	.000	.00	.0	0	0	0	
COMP	2.449	-13.05	.0	232	95	0	

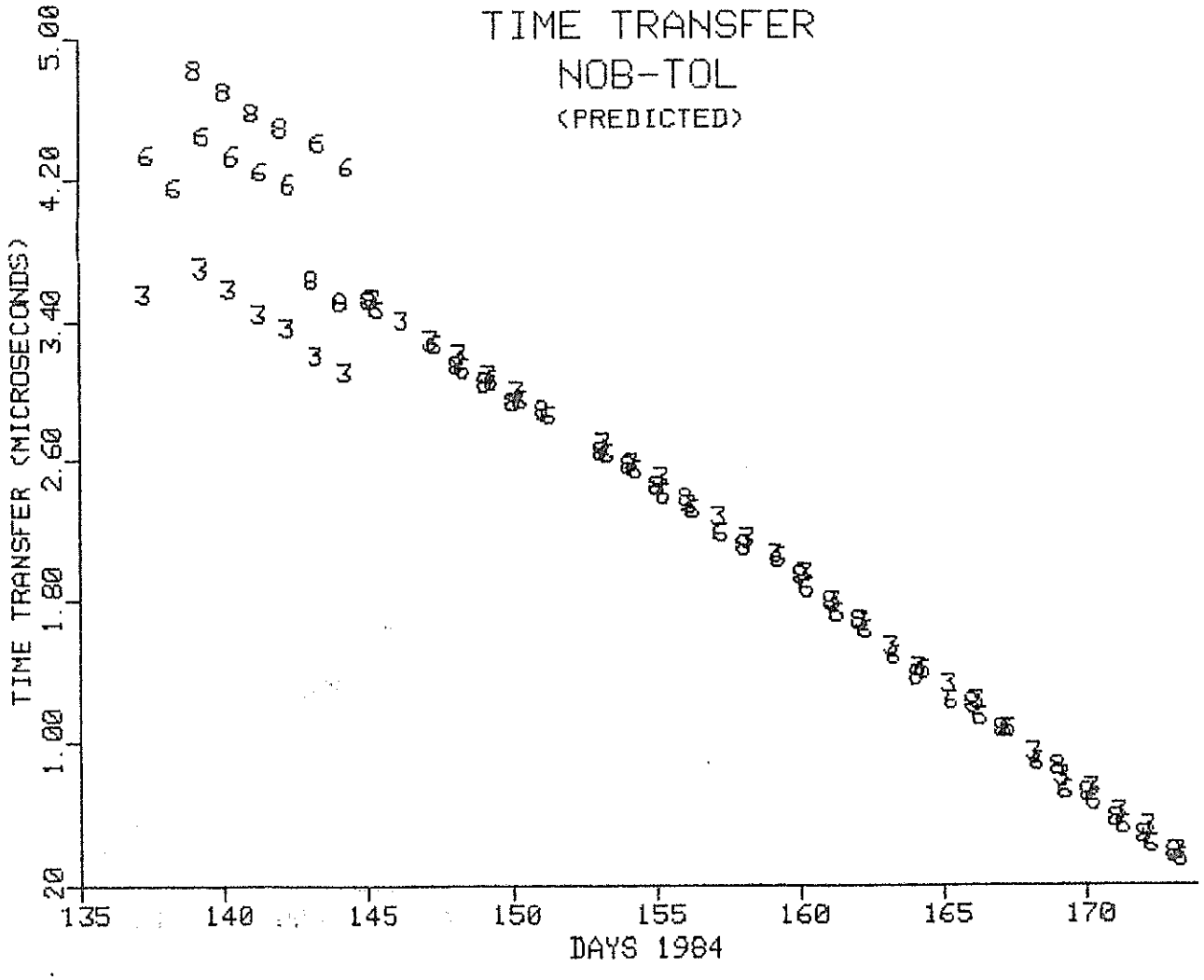

Fig. 21 NAVSTAR GPS Time Transfer

NAVSTAR GPS TIME TRANSFER

EPOCH DAY 155.0, 1984

SAT ID	TT US	FREQ PP13	AGING PP14/D	RMS NS	PTS USED	PTS FLTRD
1	.000	.00	.0	0	0	0
3	2.312	-11.06	.0	156	34	0
4	.000	.00	.0	0	0	0
5	.000	.00	.0	0	0	0
6	2.486	-14.03	.0	139	34	0
8	2.490	-13.94	.0	185	24	0
9	.000	.00	.0	0	0	0
COMP	2.426	-12.92	.0	219	92	0

FILTER TOL(NS)
STAT 300
PLOT
COMP 300
DFIT 1

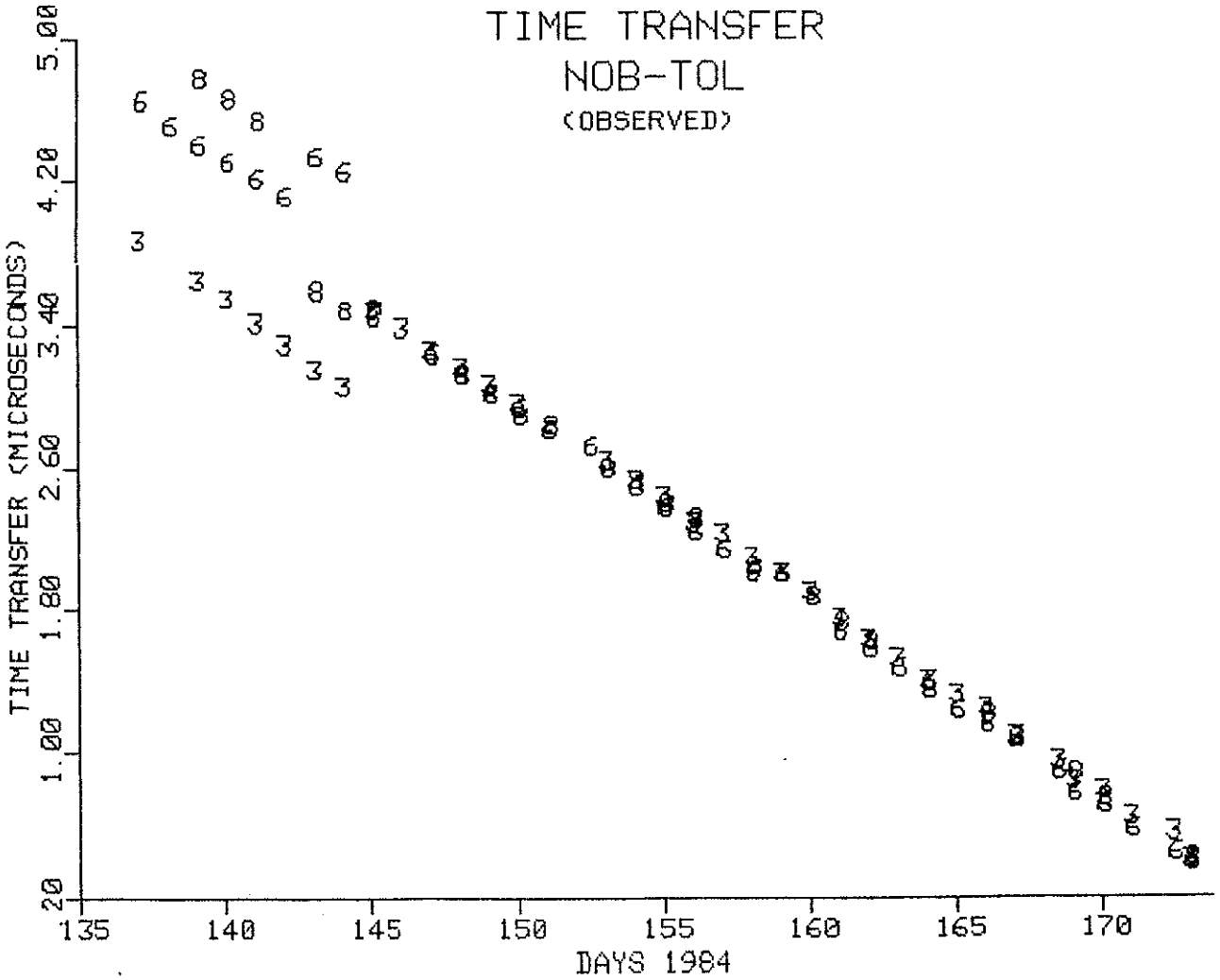

Fig. 22 NAVSTAR GPS Time Transfer

NAVSTAR GPS TIME TRANSFER

EPOCH DAY 159.0, 1984

SAT ID	TT US	FREQ PP13	AGING PP14/D	RMS NS	PTS USED	PTS FLTRD
1	.000	.00	.0	0	0	0
3	2.024	-13.08	.0	37	27	0
4	.000	.00	.0	0	0	0
5	.000	.00	.0	0	0	0
6	1.981	-13.21	.0	38	26	0
8	1.990	-13.07	.0	40	21	0
9	.000	.00	.0	0	0	0
COMP	1.999	-13.12	.0	43	74	0

FILTER TOL(NS)
STAT 300
PLOT
COMP 300
DFIT 1

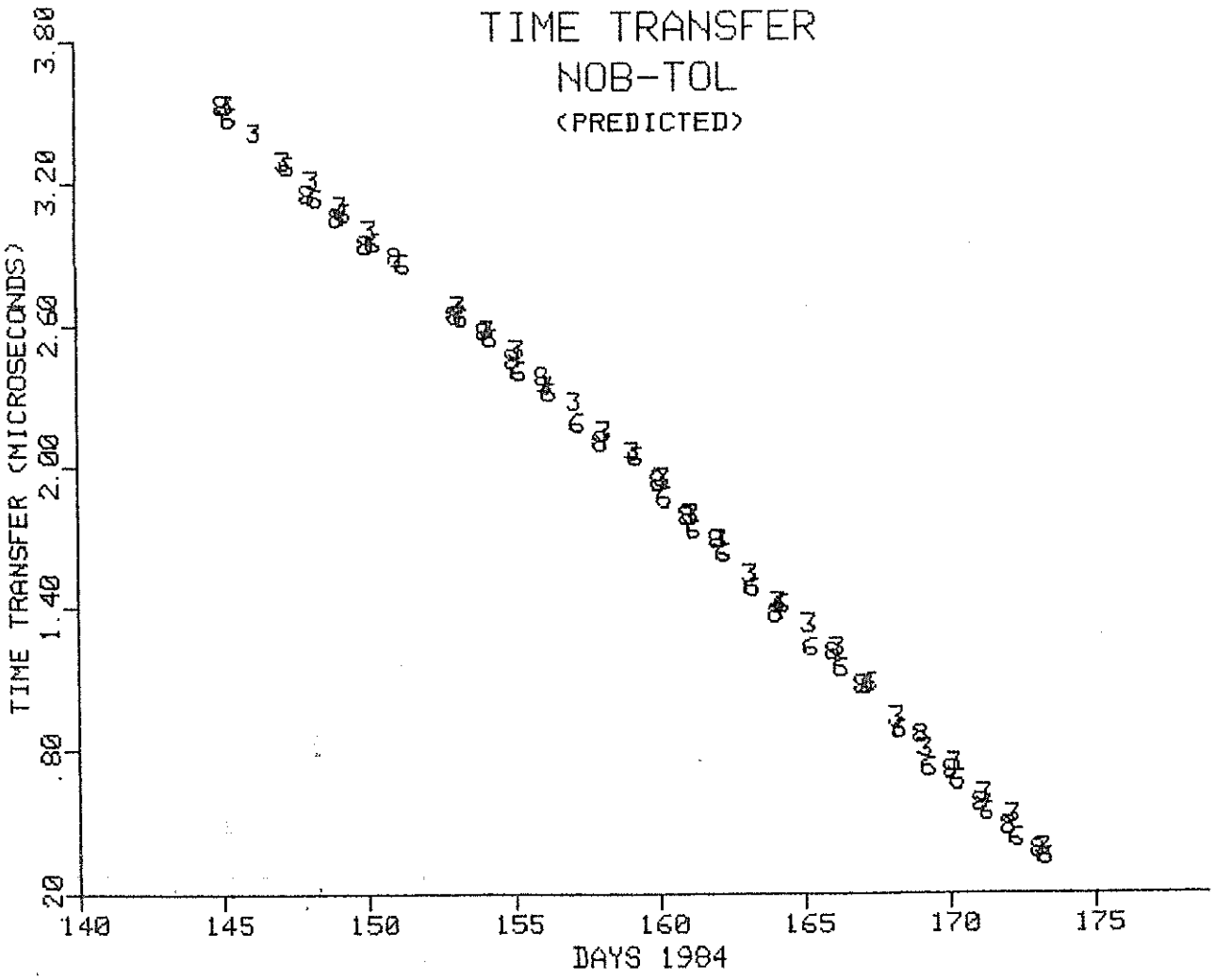

Fig. 23 NAVSTAR GPS Time Transfer

NAVSTAR GPS TIME TRANSFER

EPOCH DAY 159.0, 1984

SAT ID	TT US	FREQ PP13	AGING PP14/D	RMS NS	PTS USED	PTS FLTRD	FILTER TOL(NS)
1	.000	.00	.0	0	0	0	STAT 300
3	1.994	-12.71	.0	25	27	0	PLOT
4	.000	.00	.0	0	0	0	COMP 300
5	.000	.00	.0	0	0	0	DFIT 1
6	1.951	-12.88	.0	29	26	0	
8	1.981	-12.69	.0	25	19	0	
9	.000	.00	.0	0	0	0	
COMP	1.975	-12.77	.0	33	72	0	

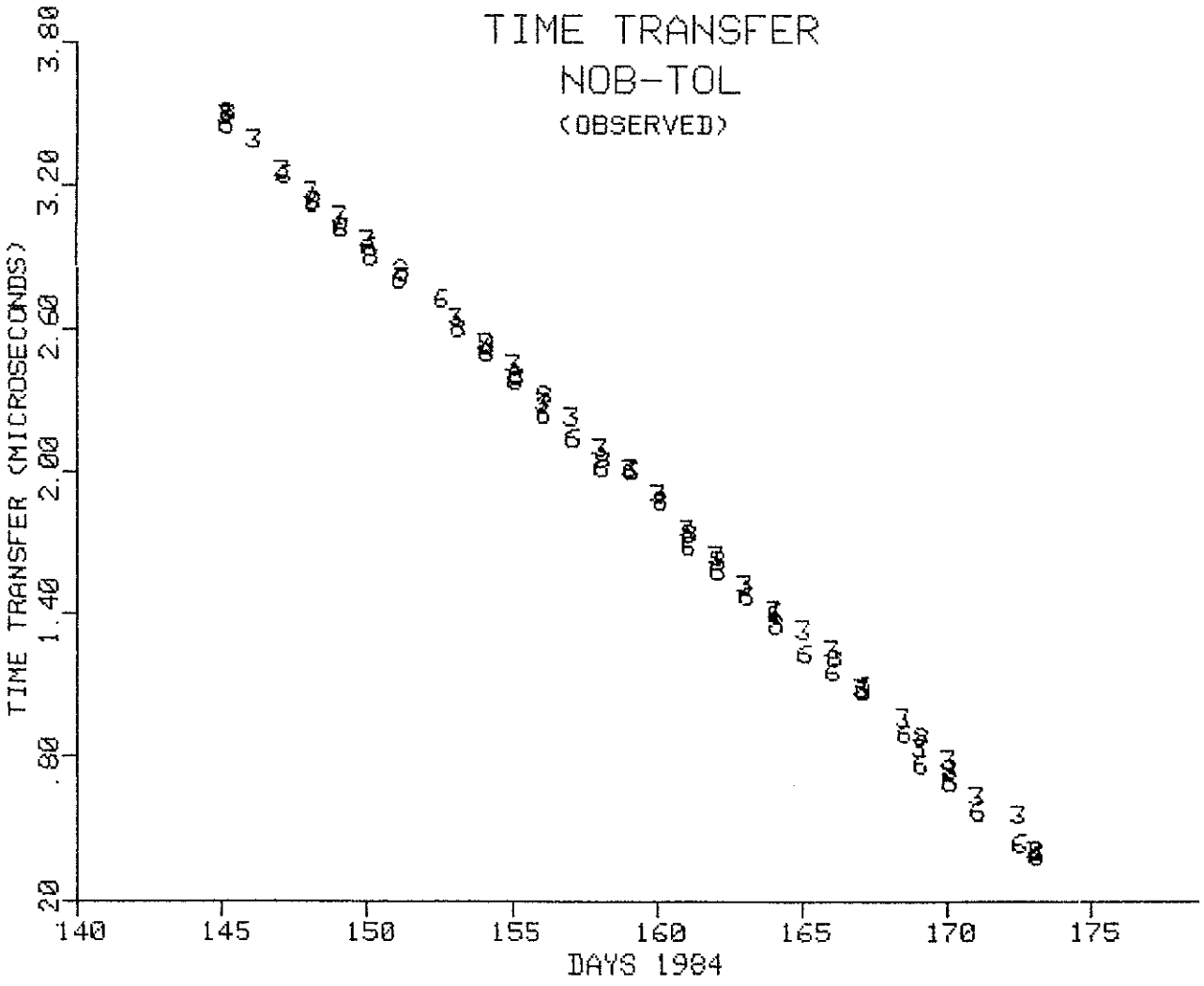

Fig. 24 NAVSTAR GPS Time Transfer

NAVSTAR GPS TIME TRANSFER

EPOCH DAY 312.0, 1983

SAT ID	TT US	FREQ PP13	AGING PP14/D	RMS NS	PTS USED	PTS FLTRD	FILTER TOL(NS)
1	.000	.00	.0	0	0	0	STAT 300
3	1.221	.20	.0	858	49	0	PLOT
4	1.078	-.46	.0	595	28	3	COMP 300
5	1.312	-.67	.0	756	14	0	DFIT 1
6	1.306	.53	.0	907	70	0	
8	1.387	1.75	.0	745	21	0	
9	.000	.00	.0	0	0	0	
COMP	1.225	.36	.0	840	183	2	

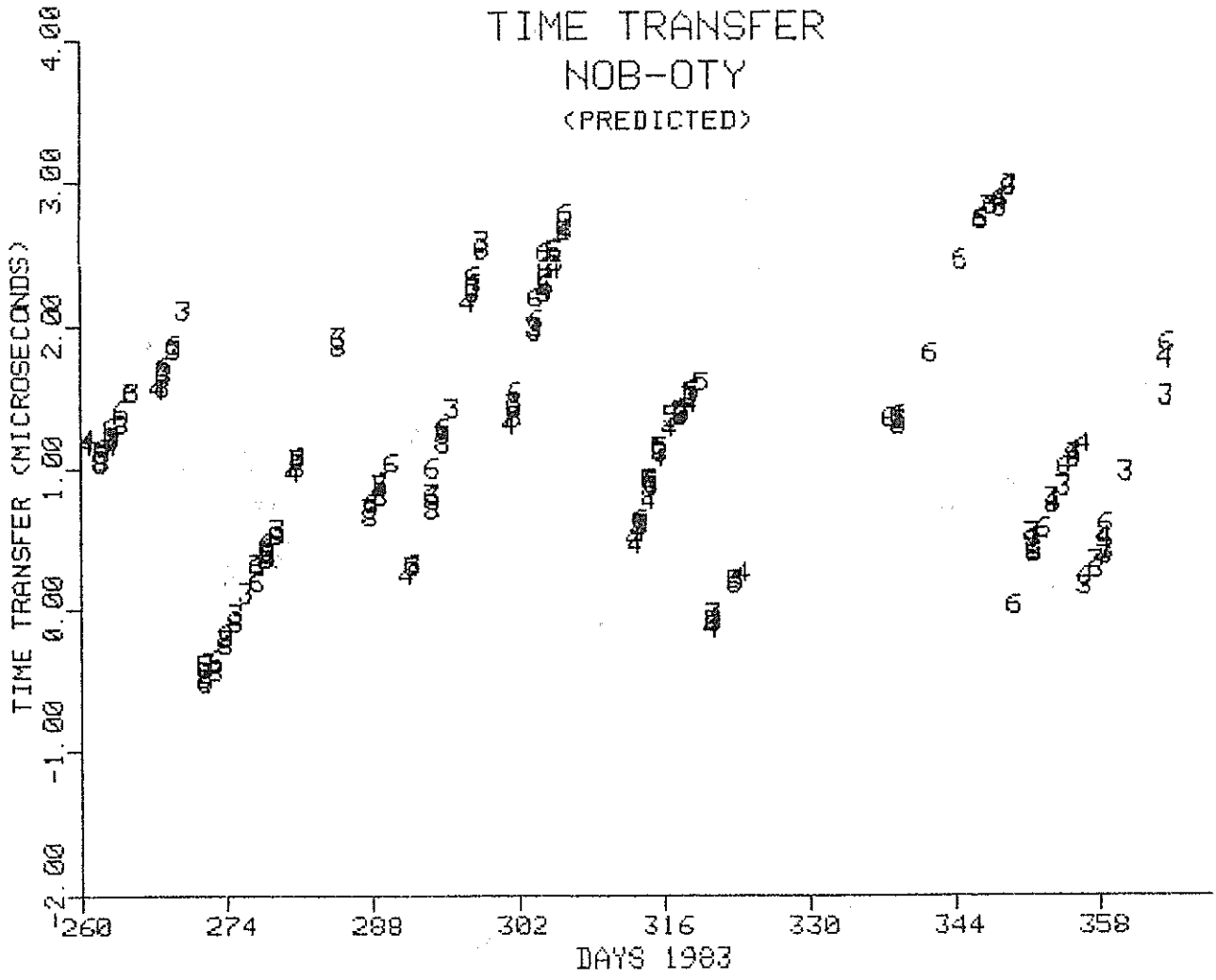

Fig. 25 NAVSTAR GPS Time Transfer

NAVSTAR GPS TIME TRANSFER

EPOCH DAY 312.0, 1983

SAT ID	TT US	FREQ PP13	AGING PP14/D	RMS NS	PTS USED	PTS FLTRD	FILTER TOL(NS)
1	.000	.00	.0	0	0	0	STAT 300
3	1.023	-.58	.0	592	36	8	PLOT
4	1.096	-.73	.0	560	21	4	COMP 300
5	1.280	-.97	.0	707	13	0	DFIT 1
6	1.273	.37	.0	901	65	0	
8	1.234	1.32	.0	796	19	0	
9	.000	.00	.0	0	0	0	
COMP	1.117	-.75	.0	592	136	30	

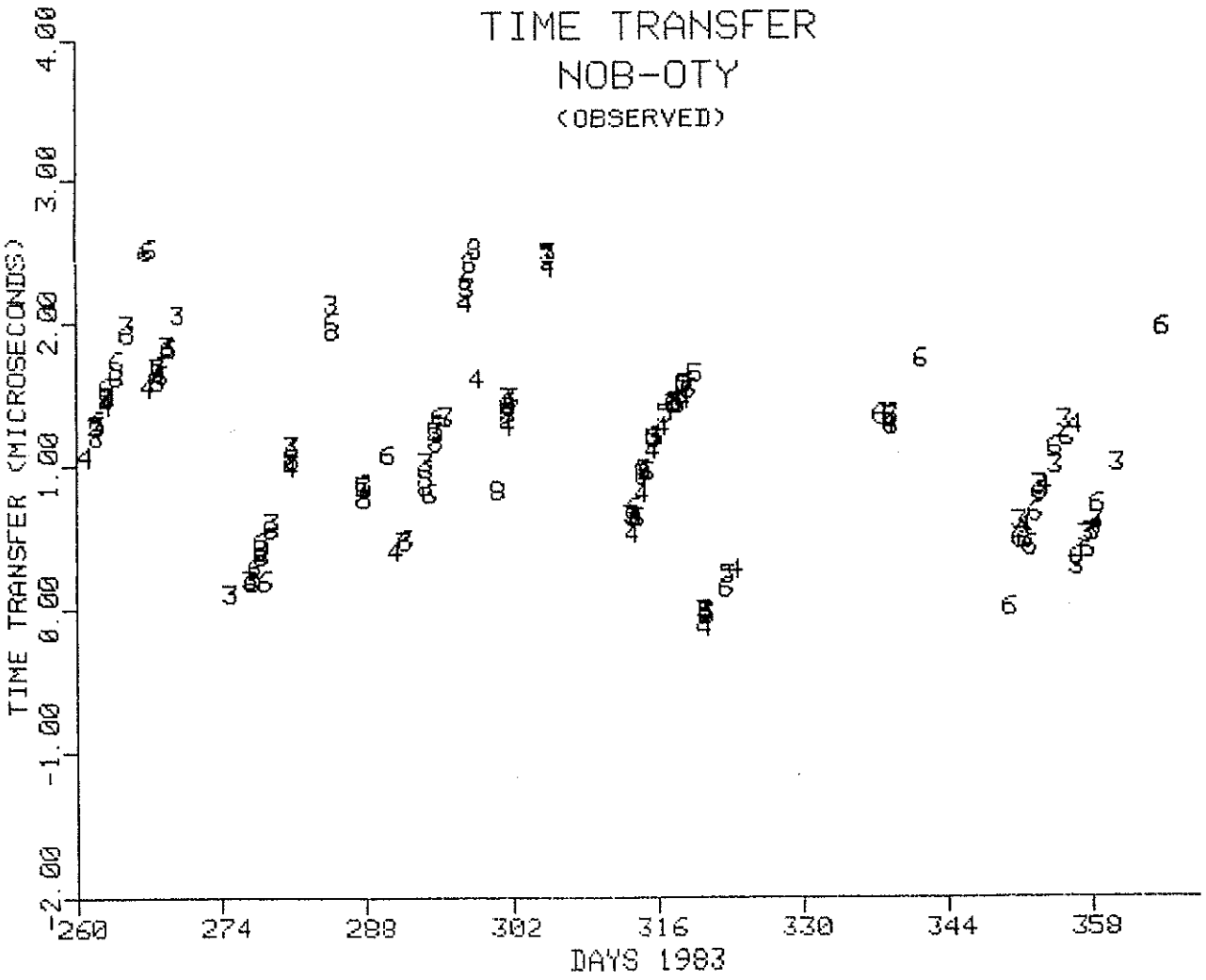

Fig. 26 NAVSTAR GPS Time Transfer

NAVSTAR GPS TIME TRANSFER

EPOCH DAY 277.5, 1983

SAT ID	TT. US.	FREQ PP13	AGING PP14/D	RMS NS	PTS USED	PTS FLTRD	FILTER TOL(NS)
1	.000	.00	.0	0	0	0	STAT 300
3	.478	20.93	.0	95	9	0	PLOT
4	.000	.00	.0	0	0	0	COMP 300
5	.000	.00	.0	0	0	0	DFIT 1
6	.488	20.74	.0	92	10	0	
8	.432	21.01	.0	87	8	0	
9	.000	.00	.0	0	0	0	
COMP	.468	20.87	.0	93	28	0	

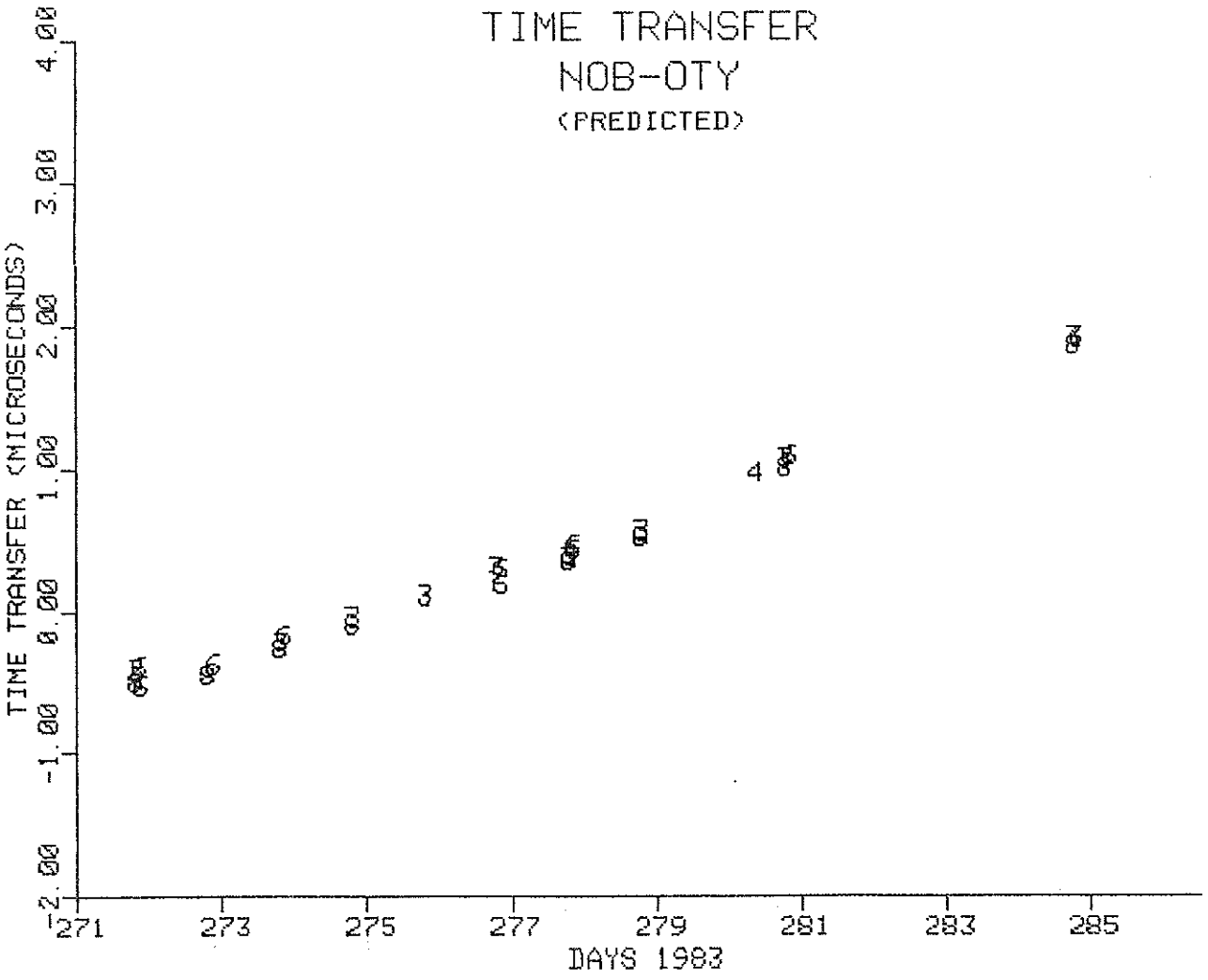

Fig. 27 NAVSTAR GPS Time Transfer

NAVSTAR GPS TIME TRANSFER

EPOCH DAY 277.5, 1983

SAT ID	TT US	FREQ PP13	AGING PP14/D	RMS NS	PTS USED	PTS FLTRD	FILTER TOL(NS)
1	.000	.00	.0	0	0	0	STAT 300
3	.506	23.72	.0	116	7	0	PLOT
4	.000	.00	.0	0	0	0	COMP 300
5	.000	.00	.0	0	0	0	DFIT 1
6	.497	22.71	.0	82	7	0	
8	.427	22.88	.0	65	8	0	
9	.000	.00	.0	0	0	0	
COMP	.476	23.13	.0	98	22	0	

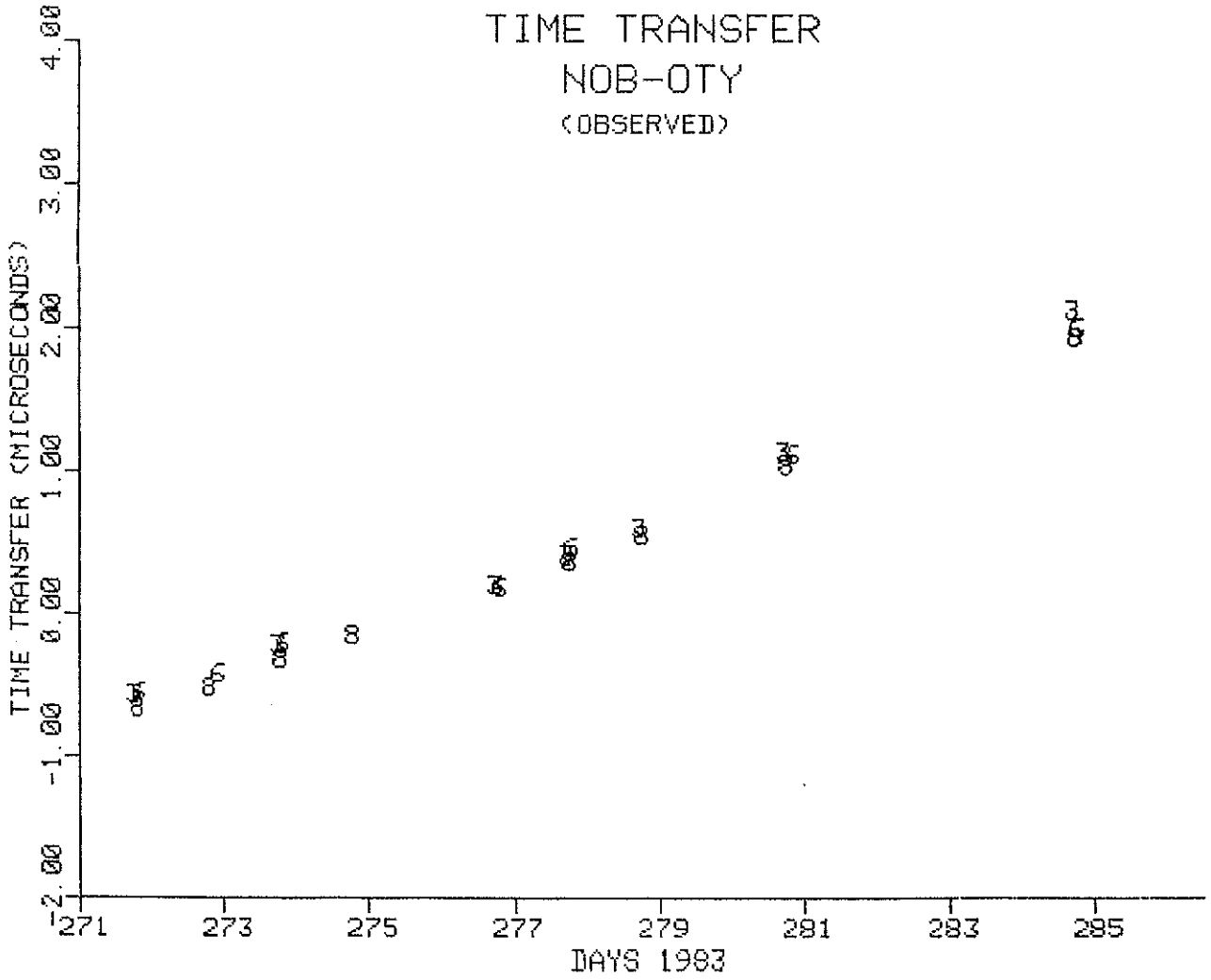

Fig. 28 NAVSTAR GPS Time Transfer

NAVSTAR GPS TIME TRANSFER

EPOCH DAY 57.0 , 1984

SAT ID	TT US	FREQ PP13	AGING PP14/D	RMS NS	PTS USED	PTS FLTRD	FILTER TOL(NS)
1	.000	.00	.0	0	0	0	STAT 300
3	.406	-10.80	.0	58	5	0	PLOT
4	.450	-9.90	.0	74	14	0	COMP 300
5	.000	.00	.0	0	0	0	DFIT 1
6	.451	-10.64	.0	74	5	0	
8	.000	.00	.0	0	0	0	
9	.000	.00	.0	0	0	0	
COMP	.442	-10.22	.0	75	24	0	

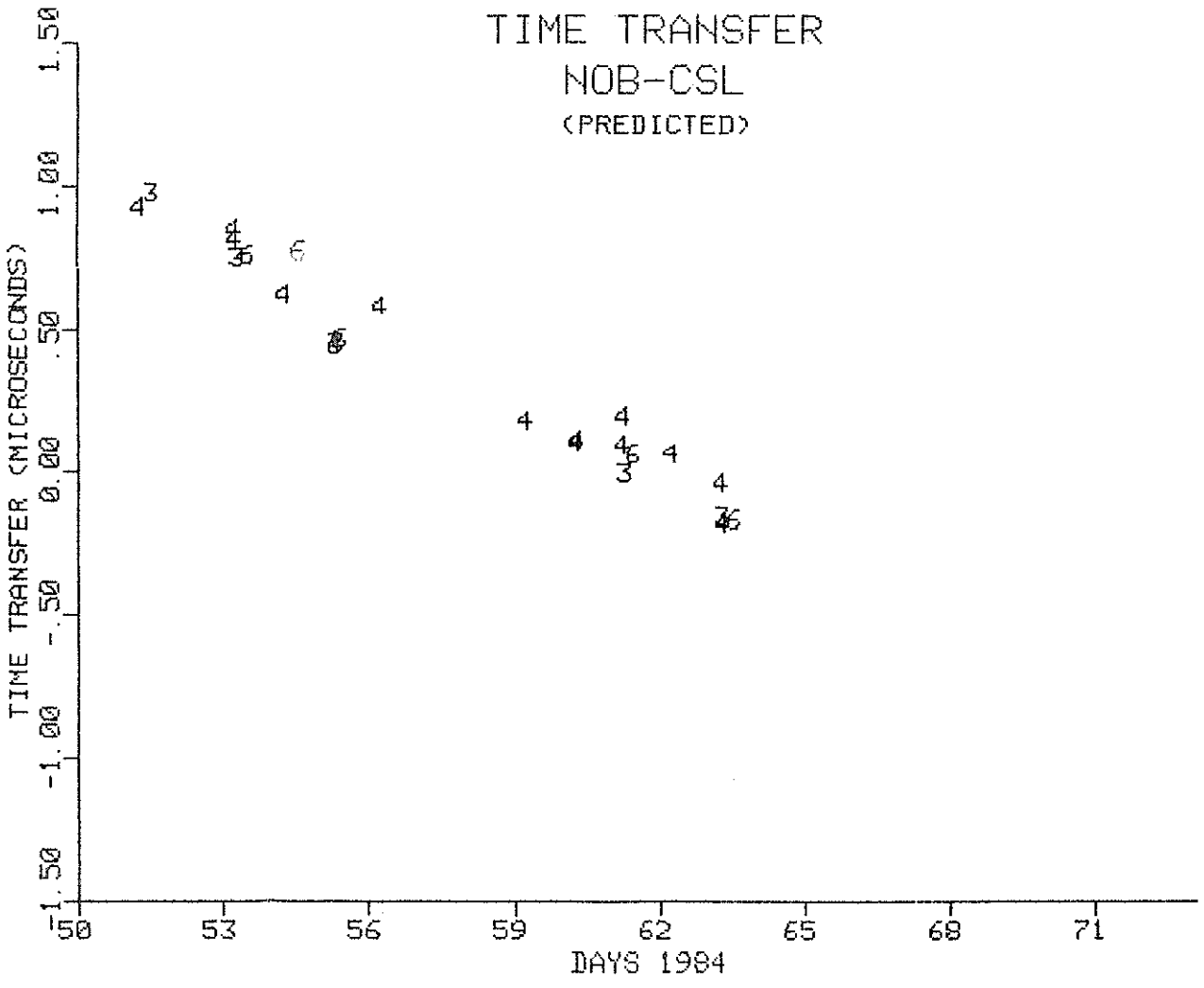

Fig. 29 NAVSTAR GPS Time Transfer

NAVSTAR GPS TIME TRANSFER

EPOCH DAY 57.0 , 1984

SAT ID	TT US	FREQ PP13	AGING PP14/D	RMS NS	PTS USED	PTS FLTRD	FILTER TOL(NS)
1	.000	.00	.0	0	0	0	STAT 300
3	.000	.00	.0	0	0	0	PLOT
4	.441	-9.98	.0	70	9	0	COMP 300
5	.000	.00	.0	0	0	0	DFIT 1
6	.456	-11.23	.0	68	5	0	
8	.000	.00	.0	0	0	0	
9	.000	.00	.0	0	0	0	
COMP	.435	-10.76	.0	79	18	0	

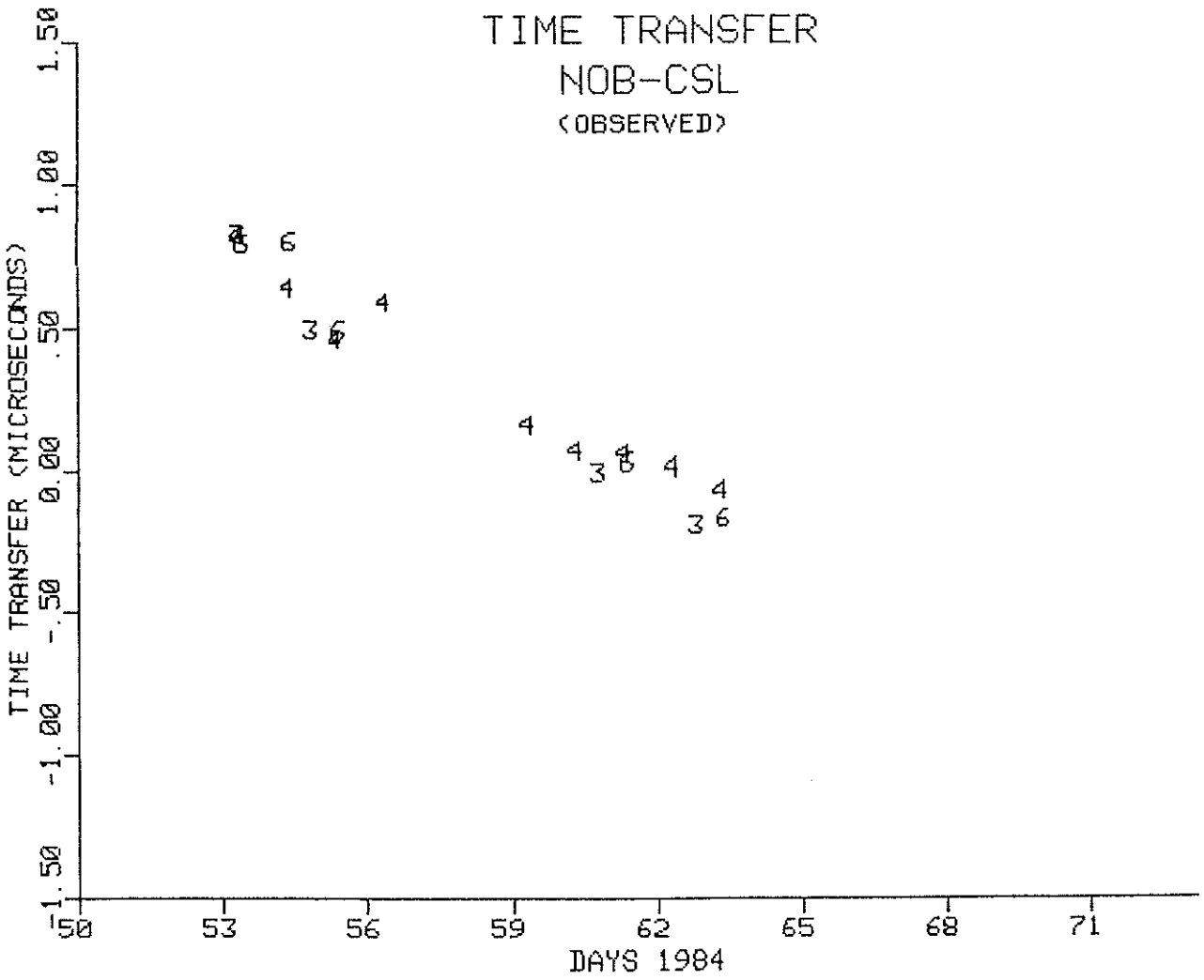

Fig. 30 NAVSTAR GPS Time Transfer

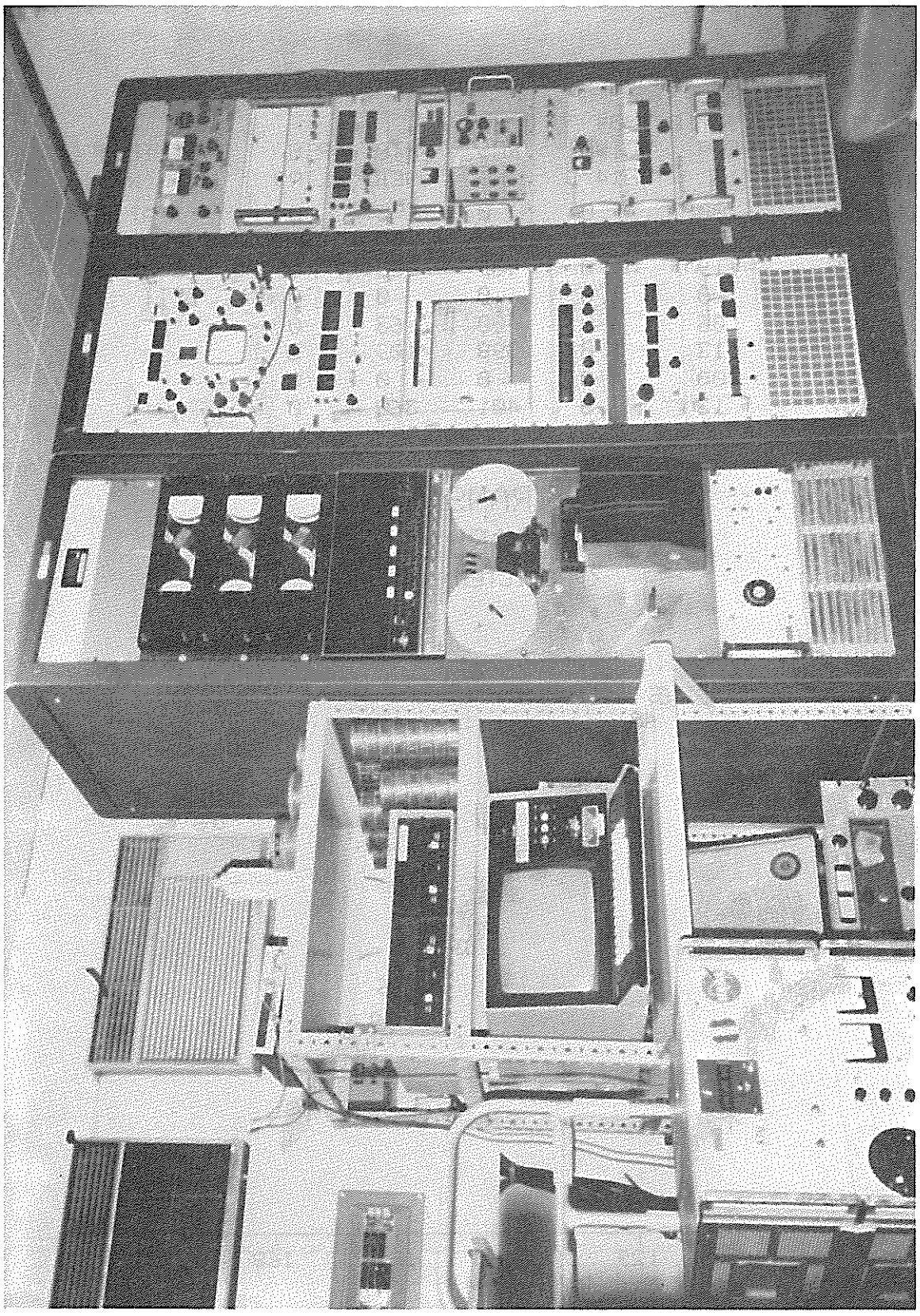

Figure 31 Arequipa, Peru Station Timing Equipment.

NAVSTAR GPS TIME TRANSFER

EPOCH DAY 137.0, 1984

SAT ID	TT US	FREQ PP13	AGING PP14/D	RMS NS	PTS USED	PTS FLTRD	FILTER TOL(NS)
1	.000	.00	.0	0	0	0	STAT 300
3	-.174	.07	.0	382	53	0	PLOT
4	-.159	.19	.0	409	135	0	COMP 300
5	.000	.00	.0	0	0	0	DFIT 1
6	-.139	.06	.0	400	63	0	
8	-.158	.13	.0	398	109	0	
9	.000	.00	.0	0	0	0	
COMP	-.157	.13	.0	401	360	0	

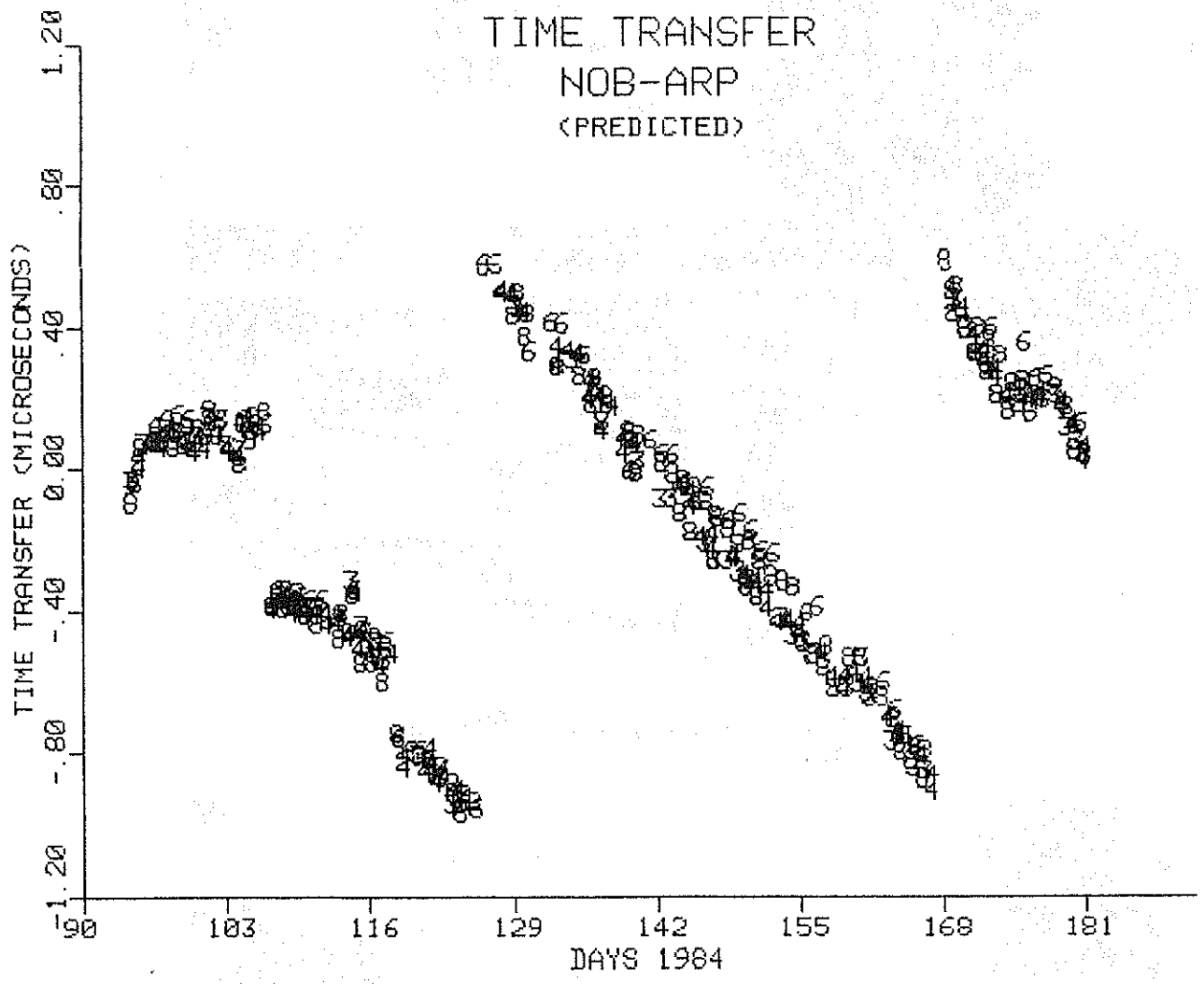

Fig. 32 NAVSTAR GPS Time Transfer

NAVSTAR GPS TIME TRANSFER

EPOCH DAY 137.0, 1984

SAT ID	TT US	FREQ PP13	AGING PP14/D	RMS NS	PTS USED	PTS FLTRD	FILTER TOL(NS)
1	.000	.00	.0	0	0	0	STAT 300
3	-.284	.59	.0	367	50	0	PLOT
4	-.279	.61	.0	382	65	0	COMP 300
5	.000	.00	.0	0	0	0	DFIT 1
6	-.228	.67	.0	377	59	0	
8	-.319	.58	.0	363	66	0	
9	.000	.00	.0	0	0	0	
COMP	-.279	.60	.0	374	240	0	

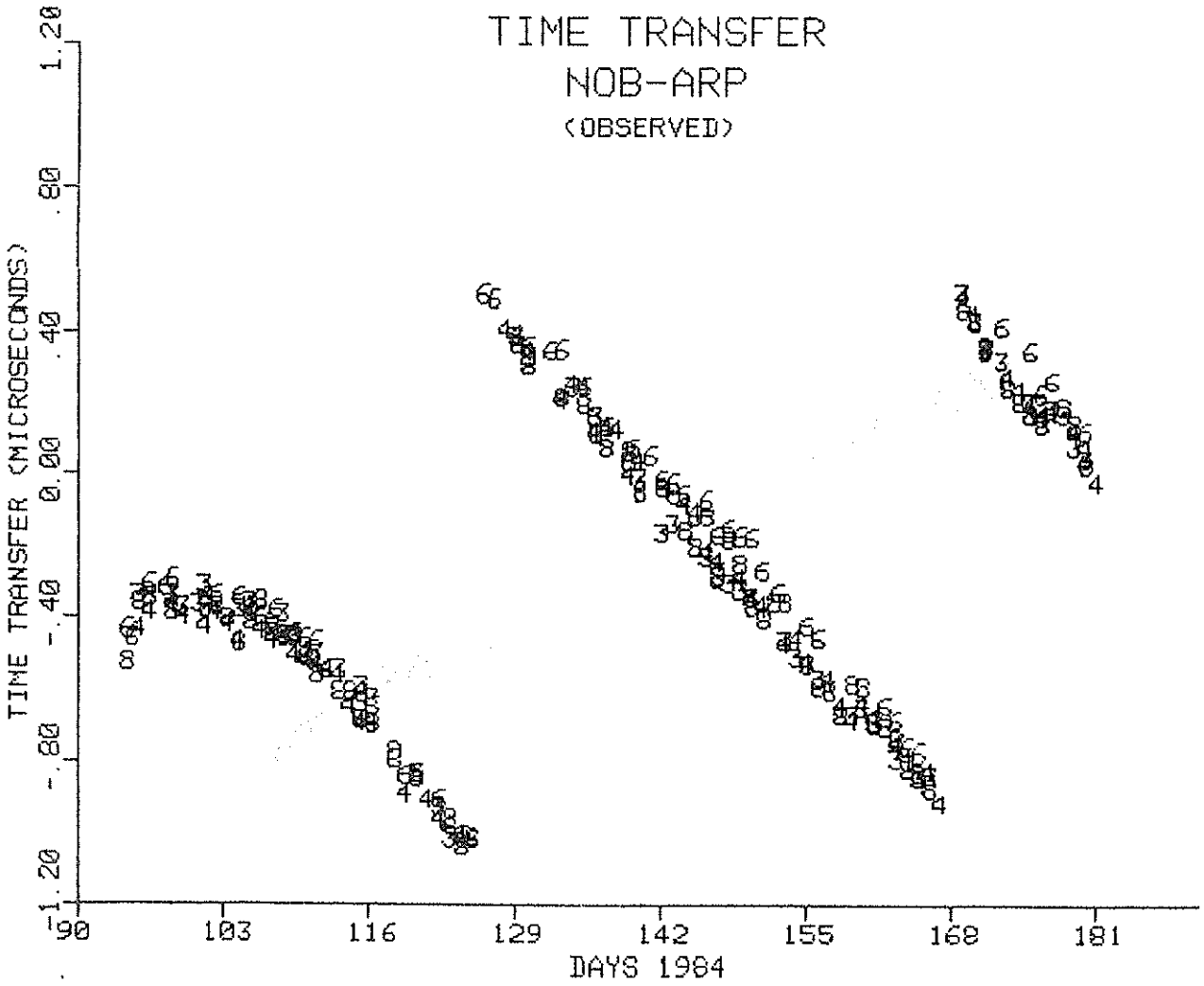

Fig. 33 NAVSTAR GPS Time Transfer

NAVSTAR GPS TIME TRANSFER

EPOCH DAY 146.0, 1984

SAT ID	TT US	FREQ PP13	AGING PP14/D	RMS NS	PTS USED	PTS FLTRD
1	.000	.00	.0	0	0	0
3	-.154	-4.06	.0	32	21	0
4	-.126	-4.09	.0	34	56	0
5	.000	.00	.0	0	0	0
6	-.069	-3.84	.0	50	30	0
8	-.118	-3.96	.0	50	48	0
9	.000	.00	.0	0	0	0
COMP	-.116	-4.03	.0	51	155	0

FILTER TOL(NS)
STAT 300
PLOT
COMP 300
DFIT 1

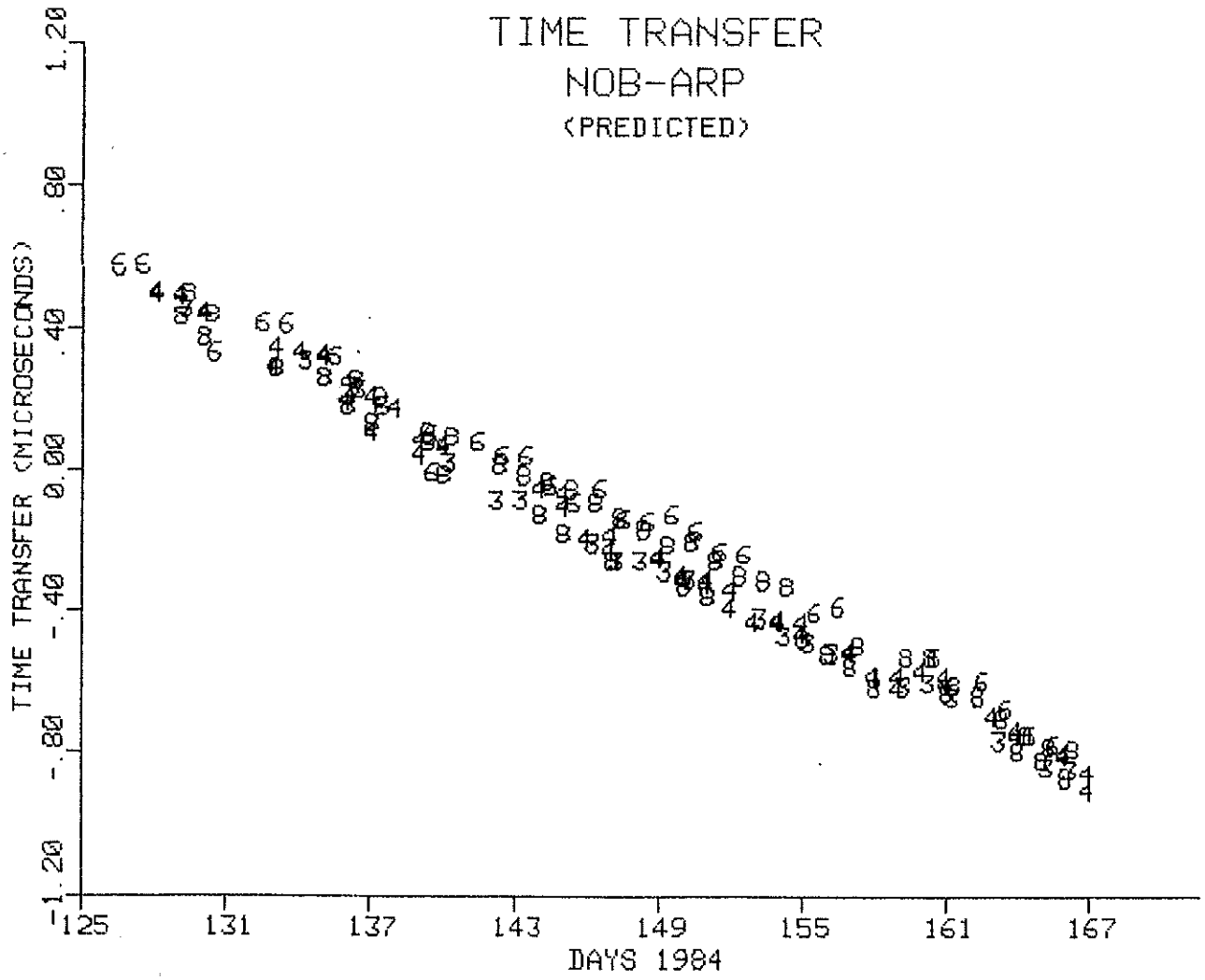

Fig. 34 NAVSTAR GPS Time Transfer

NAVSTAR GPS TIME TRANSFER

EPOCH DAY 146.0, 1984

SAT ID	TT US	FREQ PP13	AGING PP14/D	RMS NS	PTS USED	PTS FLTRD	FILTER TOL(NS)
1	.000	.00	.0	0	0	0	STAT 300
3	-.206	-3.91	.0	31	22	0	PLOT
4	-.179	-3.95	.0	32	29	0	COMP 300
5	.000	.00	.0	0	0	0	DFIT 1
6	-.114	-3.78	.0	32	28	0	
8	-.184	-3.83	.0	43	32	0	
9	.000	.00	.0	0	0	0	
COMP	-.169	-3.92	.0	49	111	0	

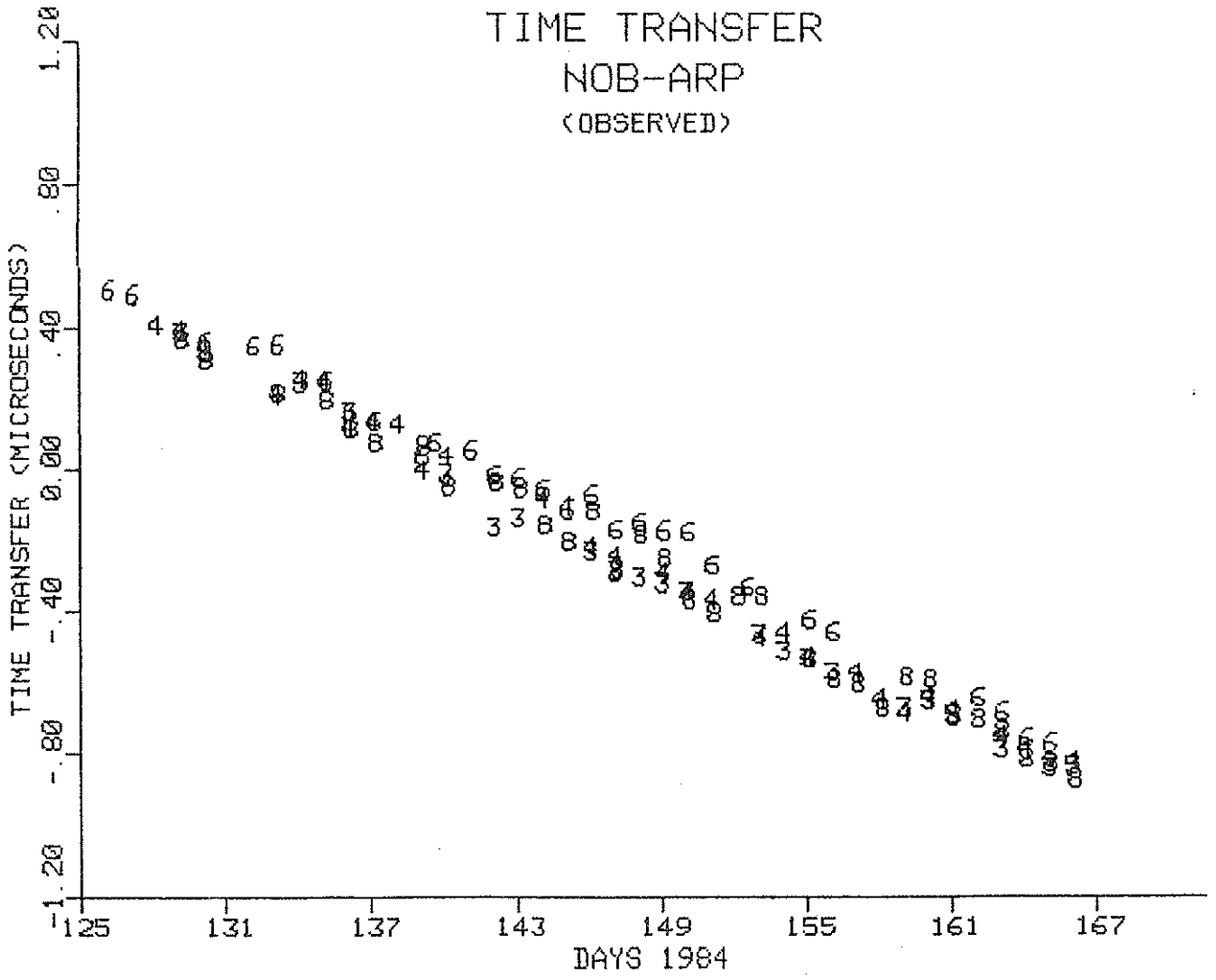

Fig. 35 NAVSTAR GPS Time Transfer

NAVSTAR GPS TIME TRANSFER

EPOCH DAY 158.0, 1984

SAT ID	TT US	FREQ PP13	AGING PP14/D	RMS NS	PTS USED	PTS FLTRD	FILTER TOL(NS)
1	.000	.00	.0	0	0	0	STAT 300
3	17.053	201.92	82.0	19	7	0	PLOT
4	17.049	201.12	81.5	35	6	0	COMP 300
5	.000	.00	.0	0	0	0	DFIT 2
6	17.064	202.30	81.3	78	12	0	
8	.000	.00	.0	0	0	0	
9	.000	.00	.0	0	0	0	
COMP	17.063	201.88	80.4	62	25	0	

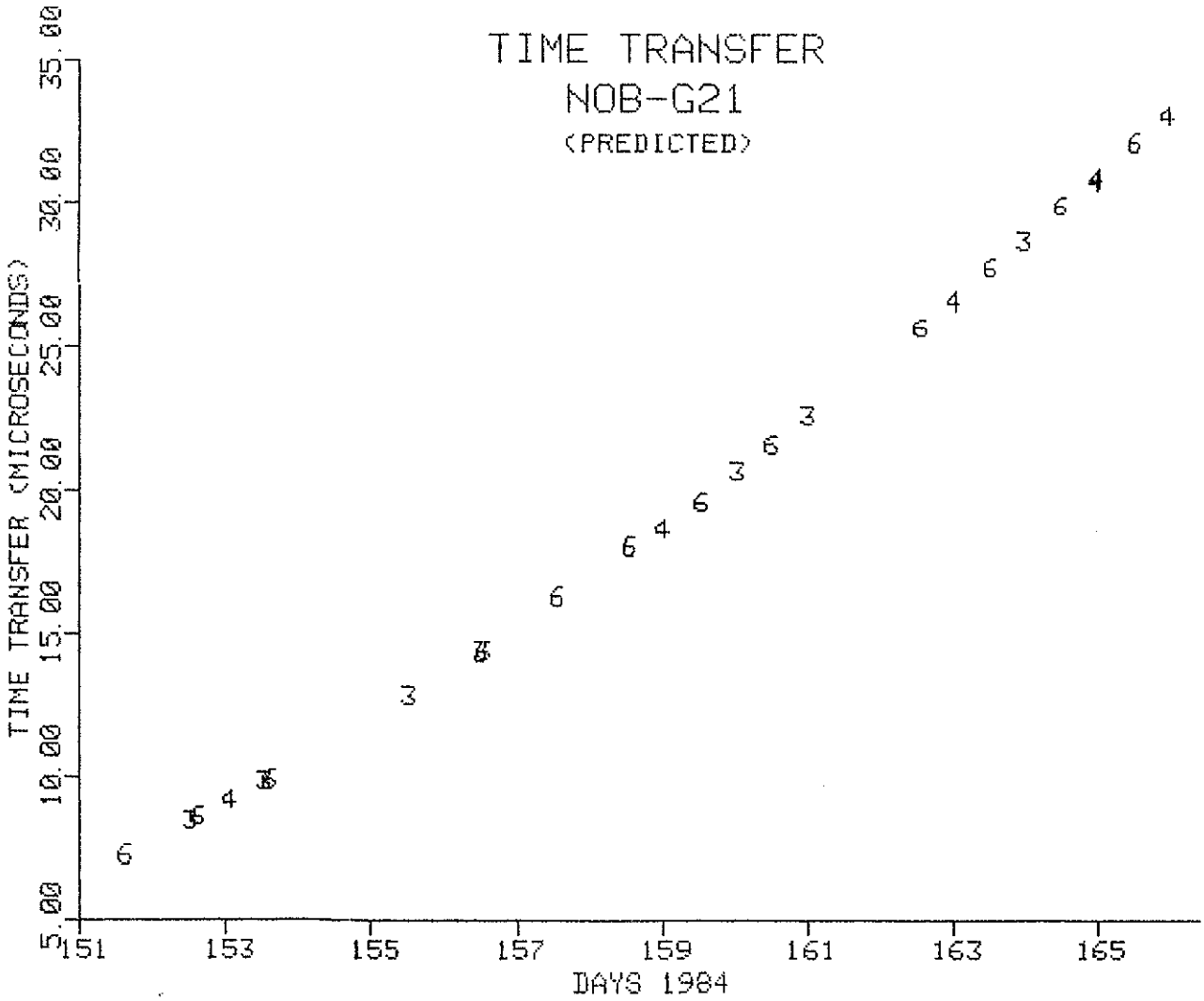

Fig. 36 NAVSTAR GPS Time Transfer

A FIBRE OPTIC TIME AND FREQUENCY DISTRIBUTION SYSTEM

D. Kirchner, H. Ressler
Institut für Nachrichtentechnik
und Wellenausbreitung
Technische Universität Graz
Inffeldgasse 12 A-8010 Graz

Telephone (0) 316 7061 ext. 7441
Telex 31221

ABSTRACT

A fibre optic time and frequency transfer system is described which is used at the Observatory Lustbühel Graz for the distribution of one pulse per second and a 10 MHz reference frequency. In developing this system special emphasis was laid on stable distribution of frequency and timing signals (good short and long term stability).

A FIBRE OPTIC TIME AND FREQUENCY DISTRIBUTION SYSTEM

INTRODUCTION

For many applications it is necessary to distribute standard frequencies and/or timing signals inside a building or between buildings. In such applications problems may arise due to ground loops and noise caused by electro-magnetic interference. Fibre optic transmissions by-pass all these problems. At the time-keeping station of the Lustbühel Observatory Graz, Austria, such a system was developed.
The system should meet the following requirements:

- Stable distribution of frequency and timing signals (good short- and long-term stability)
- Suitable for distances up to several hundred metres (adaptable to greater distances if necessary)
- Built as modular system
- Compatible with existing devices (TTL compatible signal levels, 50 ohms termination)
- Built of components available off the shelf
- High reliability
- Low price

The performance of the system should be comparable to commercially available devices in conventional technique as widely used in time-keeping laboratories.

BLOCK DIAGRAM

Fig. 1 shows the block diagrams of the frequency and the time distribution link. Although in principle it is possible to distribute both kinds of signals by the same link it is favourable to use two different links (each best suited for one of the tasks) because of the possible different duty cycles of the timing signals.
The following functional blocks are common to both systems:

- Input circuits with adjustable trigger levels
- Optic transmitter with adjustable driving current and optic receiver
- Fibre optic cable and connectors
- AC-coupled broadband amplifier with adjustable gain
- Pulse shaping circuits and line drivers

The time distribution link contains additional circuitry in the transmitter and receiver in order to be able to distribute signals of different duty cycles without changes of the throughput delay and to produce an output pulse of equal length irrespective of the input signal. In order to accommodate the link to different distances and to compensate for variations in the optic components the driving current of the optic transmitter and the gain of the amplifier in the receiver can be adjusted.

FIBRE OPTIC SYSTEM COMPONENTS

The requirements given in the introduction led to the following choice:

- Wave length: 820 nm

- Transmitter: LED with a rise time of about 10 ns and an optic output power between 5 and 25 µW at 820 nm
- Receiver: PIN-photodiode with integrated low noise transimpedance preamplifier and an output rise time of about 14 ns
- Cables: Multimode glass fibre cables (stepped index and partially graded index cables with core diameters of 200 and 100 µm, attenuation of 5 to 10 dB/km and a dispersion (pulse spreading) of about 18 ns/km
- Connectors: Factory and user installed connectors with typical insertion losses of 1.5 dB.

An important aspect for the choice of the components was the compatibility of the products of different manufacturers.

CIRCUIT DESIGN

Because of the rise times of the optic components (more than 10 ns) and in order to be compatible with widely used equipment TTL technique is used. To achieve the required low jitter values a carefully design of the print circuit boards was necessary. Besides usual filtering of the supply voltages the supply for critical components is filtered individually and the prints are designed like RF-prints (one side massive ground) to get short connections to ground (see Fig. 2). For the negative supply voltages needed for the operational amplifiers and comparators voltage inverters are used so that only positive supply voltages (5 V and 13 V) are needed. The input impedance is 50 ohms and the output signals are provided by fast line drivers delivering TTL levels into 50 ohms terminations with rise times of about 5 ns.

MAINFRAME

In order to achieve the greatest possible flexibility the device is of modular construction. The mainframe which is rack mountable (standard 19 inch rack) or for desk-top use contains the power supply (line voltage and/or 24 V DC with automatic switch-over in case of a power failure) and has space for 11 plug-ins. All available plug-ins (fibre optic transmitter and receiver for frequency and timing signals, distribution amplifiers and frequency dividers) fit in any slot of the mainframe. At the front panel signals are available which indicate if a slot is occupied and if a signal is supplied to a plug-in (front and rear panel design can be seen from Fig. 3).

PERFORMANCE

Fig. 4 shows the relation between signal jitter (standard deviation of 100 measurements of the output signal referred to the input signal), LED driving current and the length of the fibre optic link. The measurement points are for cable lengths of 10 and 100 m and driving currents of 20 and 40 mA. With the presently used optic transmitters a jitter of less than 50 ps can be achieved for distances up to several hundred metres. It is easily possible to increase the distance by the use of high efficiency fibre optic transmitters. Temperature induced changes of the throughput delay of the optic transmitter and receiver are below 30 and 50 ps/°C, respectively. Temperature induced changes of the cable delay depend on the design of the

cable used (about 5 to 17 ps/°C for a cable of 100 m length). Measurements of the signal delays on a 100 m link carried out in an air-conditioned room over a period of about one month showed no systematic changes. For several month the link is used to transmit time and frequency from the time-keeping station to the laser station of the Observatory Lustbühel and works without any problems (see the report of G. Kirchner, this issue).

ACKNOWLEDGEMENTS

The work was made possible by grants of the Austrian Council for Scientific Research and the Austrian Academy of Sciences.

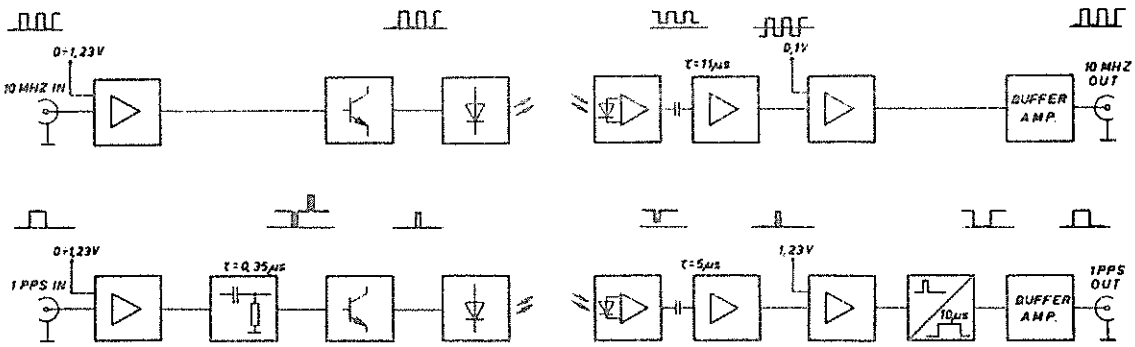

Fig. 1 Block Diagrams of the Frequency and Time Distribution Links

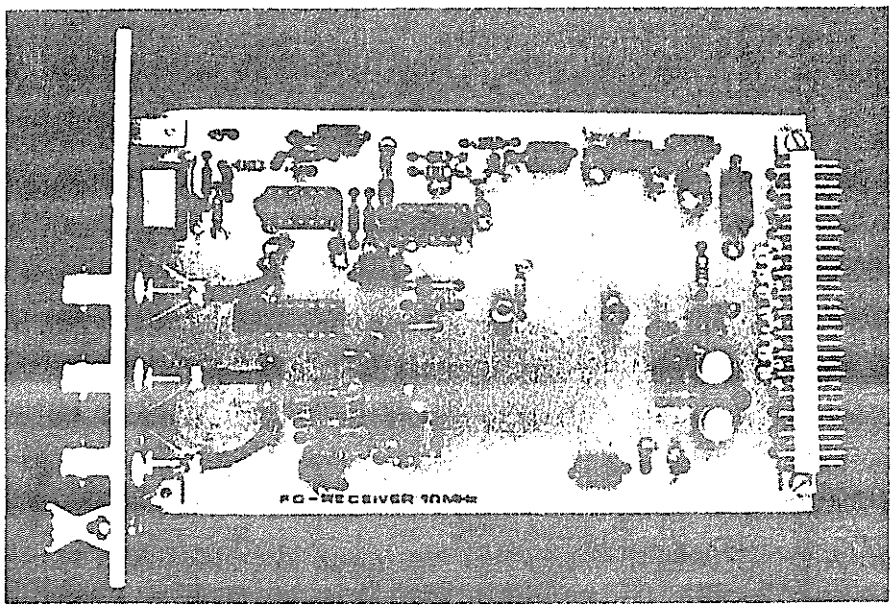

Fig. 2 Fibre Optic Plug-in (Receiver for 10 MHz)

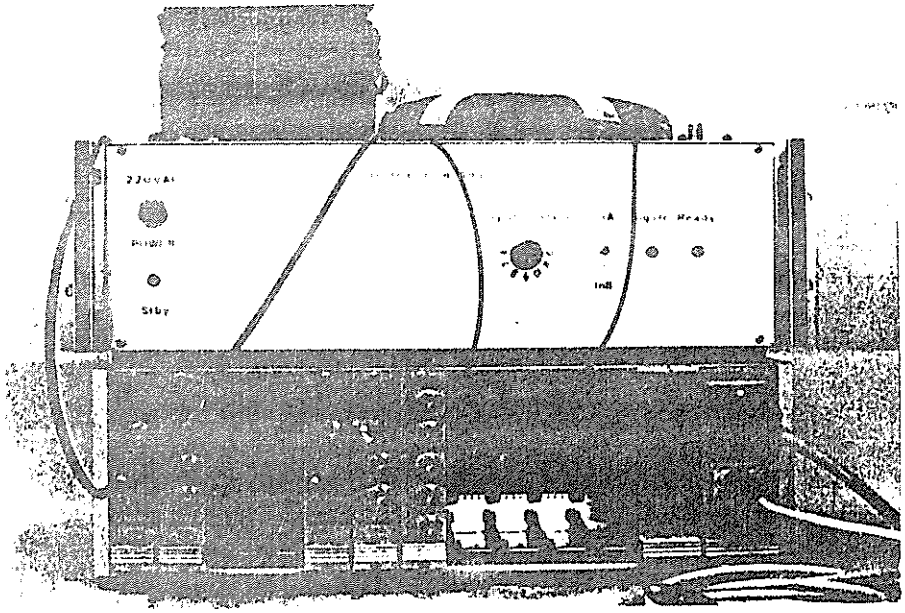

Fig. 3 Mainframe (Front and Rear Panel)

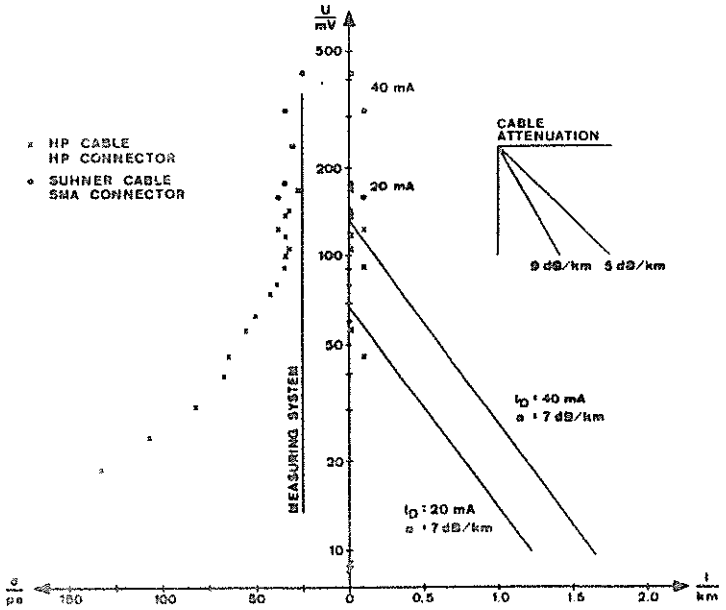

Fig. 4 Signal Jitter as aFunction of LED Driving Current, Link Length and Cable Attenuation

RECENT IMPROVEMENTS IN DATA QUALITY FROM MOBILE LASER SATELLITE TRACKING STATIONS

D.R. Edge, J.M. Heinick
Bendix Field Engineering Corporation
Data Services Group, Greenbelt, MD 20771

Telephone (301) 964 7000
Telex 197700

ABSTRACT

Since 1981 NASA's Crustal Dynamics Project has been upgrading their mobile satellite laser tracking systems (MOBLAS) to improve performance. The major hardware modifications include the installation of a short pulse high energy Quantel laser, operating at 5 hertz, with a supporting time interval unit (TIU) and a quad integrator receive energy measurement device. Calibration stability and precision as well as satellite data precision have been improved by these changes based on recent results from MOBLAS stations located in the U.S and in Australia. Full deployment of these stations will significantly improve the accuracy of the global laser data set which will lead to the more accurate determination of geophysical parameters.

Recent Improvements in Data Quality from Mobile Laser Satellite Tracking Stations

Since 1981 NASA's Crustal Dynamics Project has been upgrading their mobile satellite laser tracking systems (MOBLAS) to improve performance. The major hardware modifications include the installation of a short pulse high energy Quantel laser, operating at 5 hertz, with a supporting time interval unit (TIU) and a quad integrator receive energy measurement device. Calibration stability and precision as well as satellite data precision have been improved by these changes based on recent results from MOBLAS stations located in the U.S. and in Australia.

Full deployment of these stations will significantly improve the accuracy of the global laser data set which will lead to the more accurate determination of geophysical parameters.

Since 1981 NASA's Crustal Dynamics Project has been upgrading their mobile laser satellite tracking systems, usually referred to as MOBLAS stations. The major hardware modifications, shown to the right in Figure 1, include a new laser, time interval unit, and receive energy measurement unit. General Photonics lasers, with a pulse width of about 6 nanoseconds, are being replaced by high energy, short pulse, Quantel lasers which have a pulse width of only 2 tenths of a nanosecond. At the same time Hewlett-Packard 5370A Time Interval Units are replacing the HP5360's. The data from the HP5360's have a granularity of 100 picoseconds, or 1.5 cm in range, where as the HP5370's have a resolution of 20 picoseconds. Nonlinear Relative Energy Measurement modules measuring receive energy are being replaced with quad integrators which have a more linear scale. Also, the upgraded stations are tracking at five pps, occasionally resulting in LAGEOS passes having over ten thousand observations.

By the end of this year all but 2 of the current MOBLAS stations will have been upgraded, as shown in Figure 2. MOBLAS 1 is currently being scheduled for upgrade, while MOBLAS 2 will stop tracking and be dismantled. MOBLAS 3 is undergoing a major upgrade involving the replacement of the on-site computer in addition to the other modifications and should be back up sometime this year. The upgrades are complete on MOBLAS stations 4, 5 and 7; the upgrade with the installation of an HP5370 time interval unit later this year.

Installation of short pulse lasers greatly improved the quality of the data. In general, the calibration precision has improved by a factor of five, precalibration to postcalibration shifts have been dramatically reduced from a few tenths of nanoseconds to a few hundredths of nanoseconds, and RMS values for LAGEOS passes dropped from a range of 10 to 16 cm to the 2 to 4 cm range. This improvement in LAGEOS data can be seen in data from MOBLAS 4 in the United States and from MOBLAS 5 in Australia. Figures 3 and 4 list several LAGEOS passes taken before, and then after, the upgrades. The RMS values are plotted to the right, using the letter 'C' for combined pre- and post- calibration, and the letter 'S' for LAGEOS data. The vertical, dotted lines are at 2 centimeter intervals. At MOBLAS 4 before the upgrades, calibration RMS values were typically about 6 cm, and LAGEOS data were about 12 cm RMS. After the upgrades, calibration RMS values were down around 2.25 cm, while LAGEOS data had RMS values of about 4 cm. The improvement in the data from MOBLAS 5 was even more dramatic. Calibration RMS values went from about 5.5 cm down to 1 cm, and LAGEOS RMS values which were around 14 cm fell down to the 2 cm level.

With this large improvement in data quality it is now possible to see systematic effects at the subcentimeter level. The systematic effect from the upgraded MOBLAS stations which has received the most attention is the dependence of the range measurement on receive energy. The quad integrator allows accurate monitoring and modeling of the receive energy dependent bias and jitter of the receivers which have not yet been modified. Figure 5 is a plot of satellite data residuals versus the receive energy measurement and a plot of the receive energy distribution. The means of the range residuals in each column of the plot are plotted vertically, in centimeters, using 'X's' with one sigma error bars. The number of data points represented by each column is read downward at the bottom of the chart. The relative receive energy increases to the right. This data is from a LAGEOS pass which has an overall RMS of 2.8 centimeters, taken August 17 of this year by MOBLAS 7. As the receive energy approaches the threshold of the receive system, to the left in the plot, the delay of the system usually increases, and range measurements taken near threshold would appear to be long by a few centimeters. Also, system jitter is greater in this area, so pass RMS values increase as more data is taken near threshold. At present a large fraction of the LAGEOS data being taken by the upgraded MOBLAS systems have receive energies near the threshold limit, so it is important to monitor, model, and, if possible, correct the data based on receive energy. Upgraded MOBLAS systems now take 2000 calibration observations per pass, covering the entire receive energy range. Data has been corrected, on an experimental basis, by fitting a curve through the calibration data and then applying that curve to the satellite data, removing the bias. RMS values generally improve, some by as much as 35%, depending on the magnitude of the original biases and the distribution of data near threshold. Figure 6 is an example, a 2.7 cm LAGEOS pass taken May 13, 1984 by MOBLAS 7, was corrected based on receive energies reducing the RMS to 2.3 cm and eliminating shot by shot range biases of up to several centimeters.

To sum up, a new level of data quality has been achieved by the upgraded MOBLAS systems. LAGEOS passes now have RMS values of 2 to 4 cm, and pre- to post- calibration shifts have been greatly reduced. Data quality should improve again in the near future as new types of receivers involving microchannel plates and new discriminators are to be tested this year, and new software is being developed to handle systematic effects left in the data. LAGEOS pass RMS values should approach 1 centimeter in the near future.

LASER PULSE TIMING SYSTEM

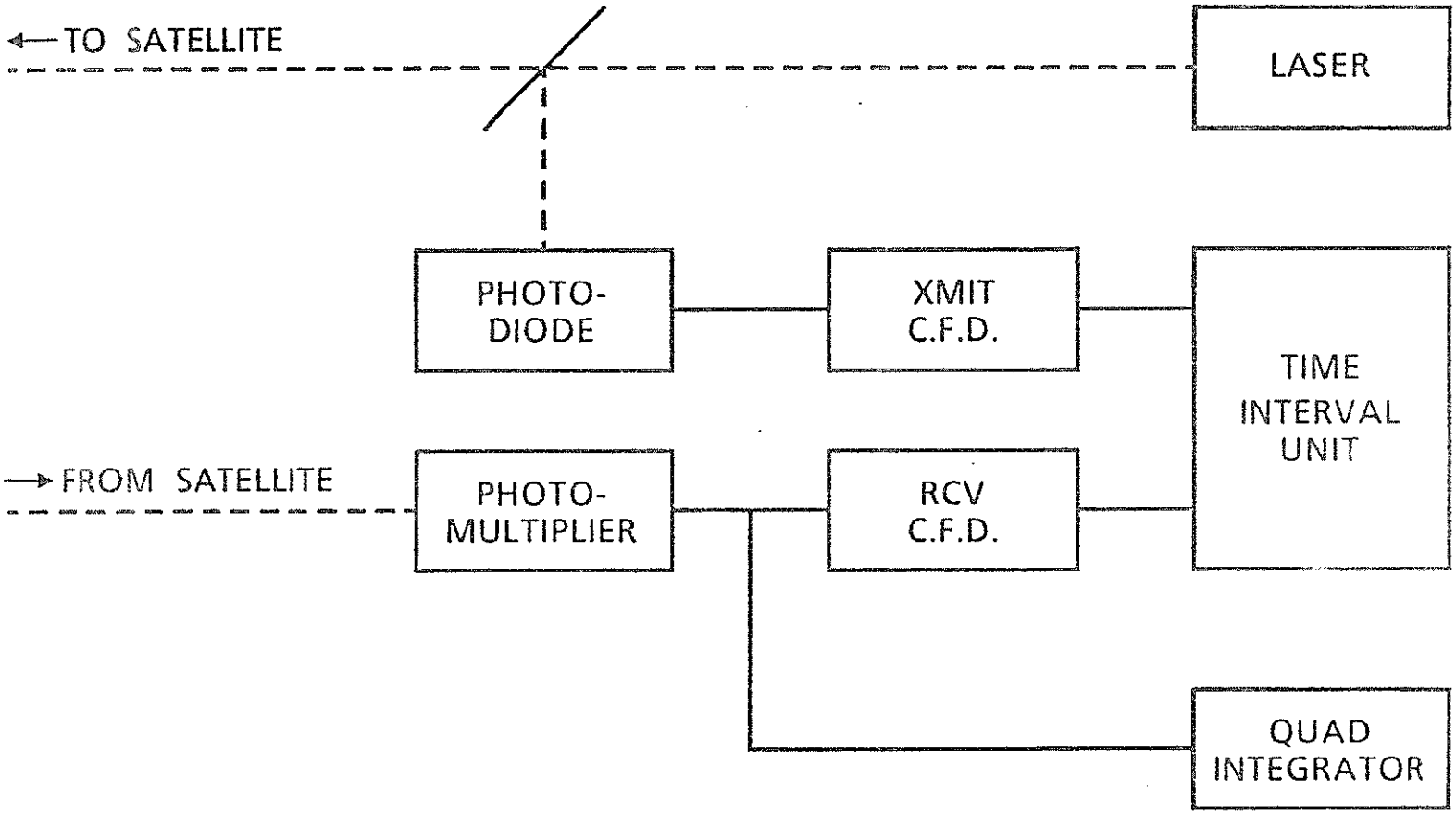

Figure 1

MOBLAS UPGRADES

STATION	LOCATION	QUANTEL LASER	HP5370 TIU	QUAD INTEGRATOR
MOBLAS 1	French Polynesia	(To be scheduled)	N/A	N/A
MOBLAS 2	Platteville, CO	(To be dismantled)	N/A	N/A
MOBLAS 3	Greenbelt, MD	1984	1984	1984
MOBLAS 4	Monument Peak, CA	1982	1982	1982
MOBLAS 5	Western Australia	1983	1983	1983
MOBLAS 6	Mexico	1984	1984	1984
MOBLAS 7	Greenbelt, MD	1983	1982	1983
MOBLAS 8	Quincy, CA	1982	(1984)	1982

Figure 2

MOBLAS 4 LAGEOS PASSES BEFORE QUANTEL

DATE	GMT		CALIBRATION ('C') AND SATELLITE ('S') RMS (CM)								
			2	4	6	8	10	12	14	16	18
9/29/82	0308	I	.	.	C.	.	.	.	S .	.	.
9/29/82	0755	I	.	.	C	.	.	.	S .	.	.
10/22/82	0328	I	.	.	C	.	.	S	.	.	.
10/23/82	0849	I	.	.	C	.	.	.S	.	.	.
10/27/82	0340	I	.	.	.	.	C .	S	.	.	.
10/28/82	0915	I	.	.	. C	.	.	.	S.	.	.
10/30/82	0306	I	.	.	.	.	.	C	S .	.	.
10/30/82	0625	I	.	. C	.	.	.	.	S .	.	.
11/03/82	0437	I	.	.	.C	. S	.	.	.	.	.
11/03/82	2349	I	.	.	.C	.	.S	.	.	.	.
11/04/82	0322	I	.	. C	.	.	.	.	.	.	S.
11/06/82	0039	I	.	. C	.	.	.	S	.	.	.

MOBLAS 4 LAGEOS PASSES BEFORE QUANTEL

DATE	GMT		CALIBRATION ('C') AND SATELLITE ('S') RMS (CM)								
			2	4	6	8	10	12	14	16	18
5/31/83	0152	I	. C	.S	.	.	.	.	.	.	.
6/02/83	1444	I	.C	S	.	.	.	.	.	.	.
6/10/83	0206	I	.C	. S	.	.	.	.	.	.	.
6/10/83	1427	I	. C	S	.	.	.	.	.	.	.
6/14/83	0025	I	. C	S	.	.	.	.	.	.	.
6/15/83	2132	I	. C	. S	.	.	.	.	.	.	.
6/16/83	0101	I	. C	.S	.	.	.	.	.	.	.
6/16/83	2354	I	C	.S	.	.	.	.	.	.	.
6/17/83	2223	I	C	S	.	.	.	.	.	.	.
6/22/83	1557	I	. C	. S	.	.	.	.	.	.	.
6/22/83	2217	I	. C	.S	.	.	.	.	.	.	.
6/23/83	1411	I	. C	.S	.	.	.	.	.	.	.
6/23/83	2102	I	C	.S	.	.	.	.	.	.	.
6/24/83	0028	I	.	S	. C	.	.	.	.	.	.

Figure 3

MOBLAS 5 LAGEOS PASSES BEFORE QUANTEL

DATE	GMT		CALIBRATION ('C') AND SATELLITE ('S') RMS (CM) 2 4 6 8 10 12 14 16 18
3/28/83	1446	I	C S
3/28/83	1817	I	C S
3/30/83	1910	I	C S
4/10/83	1448	I	C S
4/10/83	1812	I	C S
4/11/83	1648	I	C S
4/13/83	1403	I	C S
4/13/83	1738	I	C S
4/17/83	1541	I	C S
4/18/83	1754	I	C S
4/19/83	1259	I	C S
4/19/83	1628	I	C S
4/21/83	1720	I	C S
4/25/83	1856	I	C S
4/26/83	1356	I	C S

MOBLAS 5 LAGEOS PASSES BEFORE QUANTEL

DATE	GMT		CALIBRATION ('C') AND SATELLITE ('S') RMS (CM) 2 4 6 8 10 12 14 16 18
11/01/83	1341	I	C S
11/01/83	1645	I	C S
11/02/83	1517	I	C S
11/03/83	1404	I	C S
11/07/83	1532	I	C S
11/08/83	1414	I	C S
11/08/83	1741	I	C S
11/09/83	1304	I	C S
11/09/83	1615	I	C S
11/10/83	1500	I	C S
11/10/83	1830	I	C S
11/21/83	1734	I	C S
11/22/83	1254	I	C S
11/22/83	1609	I	C S
11/23/83	1449	I	C S

Figure 4

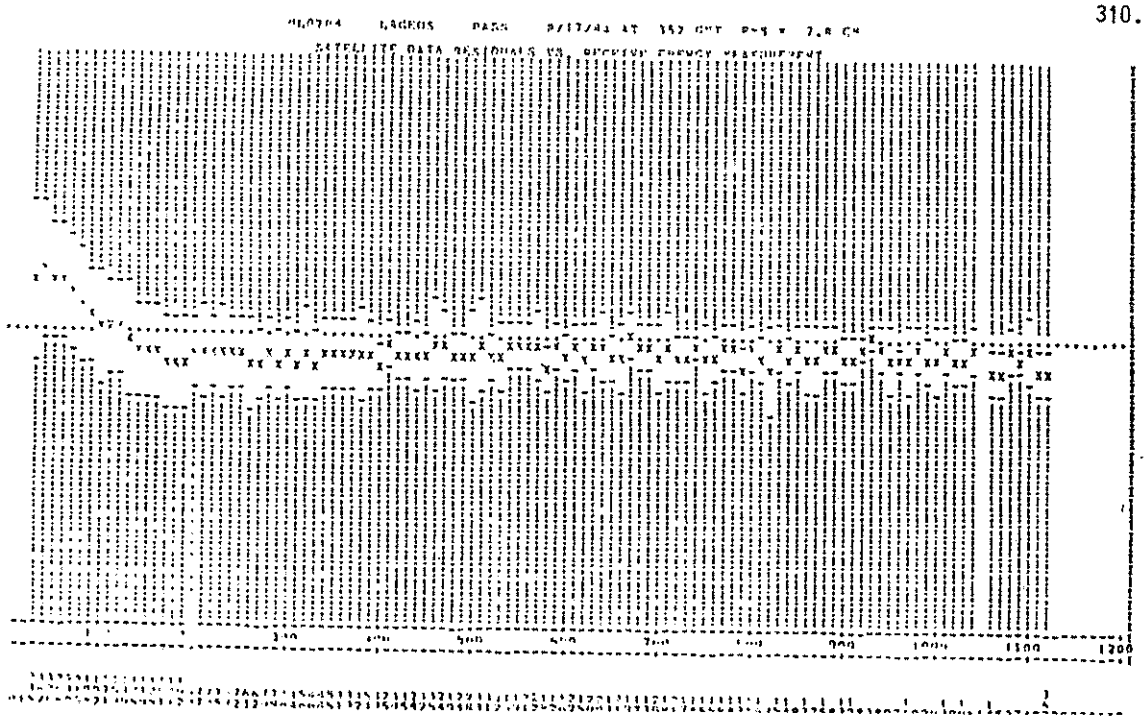

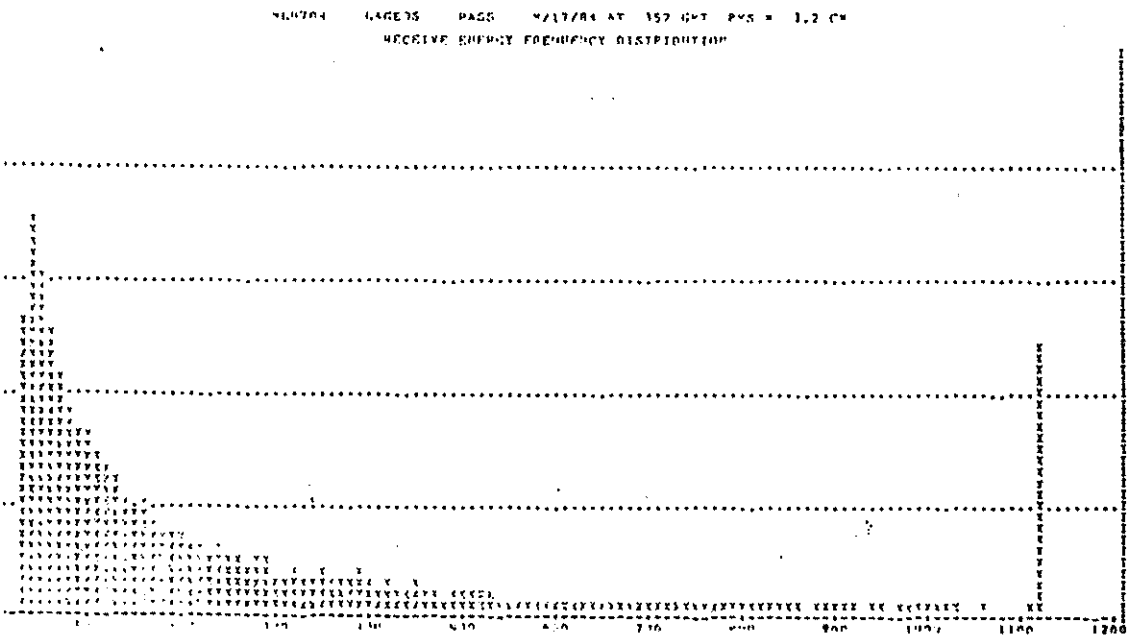

Figure 5

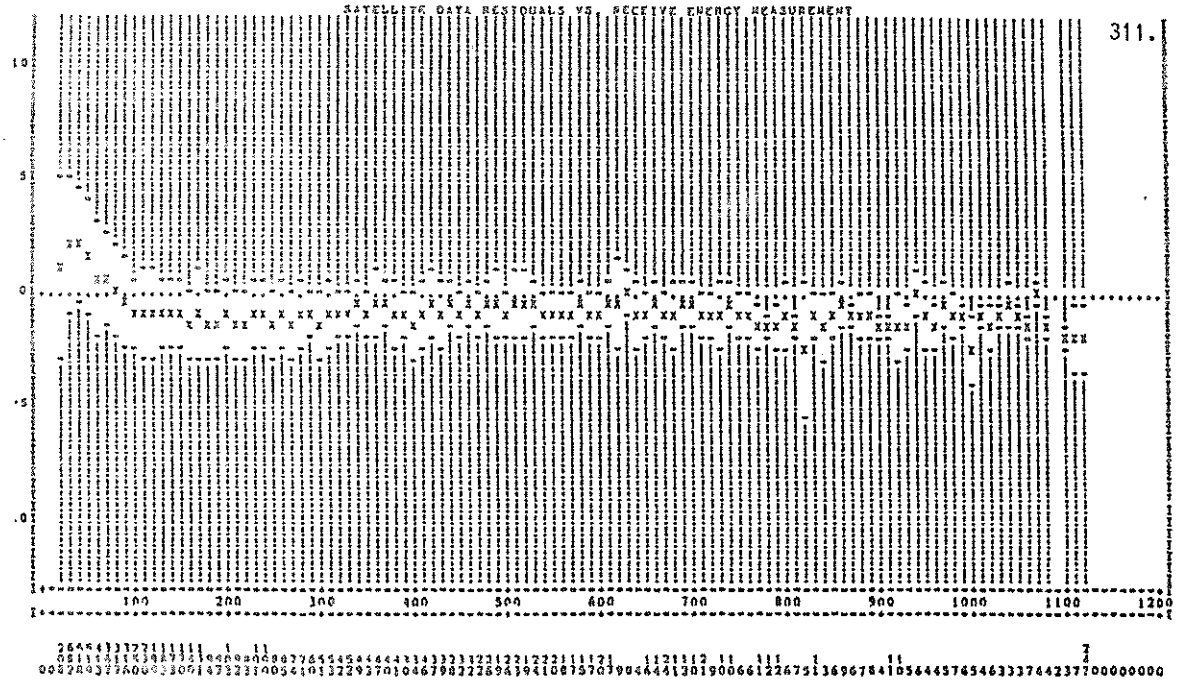
SATELLITE DATA RESIDUALS VS. RECEIVE ENERGY MEASUREMENT
100
200
300
400
500
600
700
800
900
1000
1100
1200

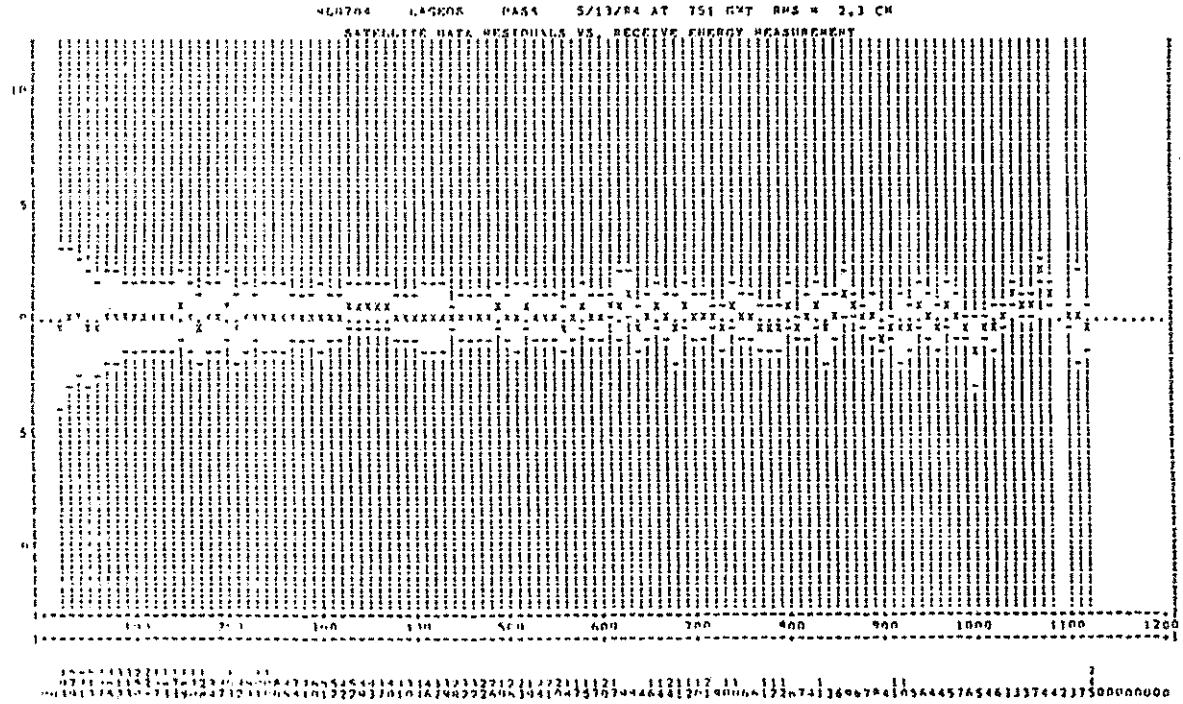
NG0704 LAGEOS PASS 5/13/84 AT 751 GMT RMS = 2.3 CM
SATELLITE DATA RESIDUALS VS. RECEIVE ENERGY MEASUREMENT
100
200
300
400
500
600
700
800
900
1000
1100
1200

Figure 6

CURRENT MOBLAS DATA QUALITY CONCLUSIONS

* LAGEOS PASS RMS VALUES HAVE BEEN REDUCED TO THE 2 TO 4 CM LEVEL.
* CALIBRATION STABILITY HAS BEEN GREATLY IMPROVED.
* CALIBRATION PRECISION HAS IMPROVED BY A FACTOR OF FIVE.
* RECEIVE SYSTEM HARDWARE DEVELOPMENT AND NEW DATA PROCESSING SOFTWARE MODELS CAN POTENTIALLY CORRECT SUBCENTIMETER SYSTEMATIC EFFECTS.
* LAGEOS PASS RMS VALUES WILL APPROACH ONE CENTIMETER IN THE NEAR FUTURE.

Figure 7

THE CONCEPT OF A NEW WETTZELL LASER RANGING SYSTEM WITH DUAL-PURPOSE CAPABILITY

W. Schlüter, G. Soltau
Institut Für Angewandte Geodäsie (Abt, II DGFI),
Richard Strauss Allee 11
D 6000 Frankfurt 70

Telephone 069 6333 1
Telex 413592

R. Dassing, R. Höpfl
Institut Für Astronomische und Physikalische Geodäsie
Der tu München
Arcisstrasse 21
D 8000 München 2

Telephone 089 2105 2409
Telex 5213550

ABSTRACT

A new Laser Ranging System with a dual purpose capability : lunar and satellites, is being discussed to substitute the present Nd/YAG System at Wettzell. The description of the conceptual design of this system is given in the following.

THE CONCEPT OF A NEW WETTZELL LASER RANGING SYSTEM WITH DUAL-PURPOSE CAPABILITY

Introduction

Some efforts have been made in the past towards Lunar Laser Ranging [1] by the group** acting within the Sonderforschungsbereich 78 - Satellitengeodäsie.

---

* MEMBER of the Sonderforschungsbereich 78 (SFB 78) Satellitengeodäsie of the Technische Universität München

** a) Institut für Astronomische und Physikalische Geodäsie der Technischen Universität München

b) Institut für Angewandte Geodäsie in Frankfurt am Main

c) Deutsches Geodätisches Forschungsinstitut (Abt. I) in München

d) Bayerische Kommission für die Internationale Erdmessung der Bayerischen Akademie der Wissenschaften in München.

e) Geodätisches Institut der Universität Bonn

A recent hardware analysis showed clearly that the Satellite Laser Ranging System designed in 1974 and operated since 1977 at Wettzell will no longer be suitable for performing operational ranging to the moon, in the manner necessary to meet the requirements of the programme for Establishment and Maintenance of a Conventional Terrestrial Reference System (Cotes) defined jointly by the IAG and IAU [2].

The new concept mainly worked out by the authors together with Dr. Greene (NATMAP) and Dr. Wilson (IfAG) foresees that the new Wettzell Laser Ranging System (WLRS) would have the capability of tracking different reflectors on the moon as well as geodynamic satellites such as LAGEOS and STARLETTE.

The design for the WLRS requires the following features:

a) ranging to lunar retroreflectors with a 20 minute normal point precision of 5 cm.

b) ranging to LAGEOS with an RMS error of less then 3 cm over 1 minute, day or night.

c) a capability of measuring to terrestrial targets.

d) sub-system modularity to allow upwards compatibility with new technology.

e) totally identical systems for ranging to lunar or satellites targets.

f) minimisation of the level of technology required to diagnose and repair faults.

g) real-time calibration of the ranging system.

h) rapid (less than 10 minutes) changeover from lunar to satellite laser ranging.

i) maximum degree of automation in operating calibrating, testing, and maintaining the system.

The WLRS-concept

The design concept for the WLRS is shown in Figure 1. It is similar to the NATMAP Lunar Laser Ranging System (NLRS) design [3].

The system will have a day/night satellite capability with the required precision, and shall be able to convert rapidly to LLR.

The measurement procedure should be identical for SLR and LLR, allowing comparisons of the data and results without a concern for systematic errors between measurement systems.

Telescope

The telescope system would have the following characteristics:

a) minimum aperture of 75 cm - clear

b) common full-aperture for transmit and receive optics

c) identical optics for transmit and receiver and guiding

d) a mechanical mount pointing error of less than 2 arc seconds referred to the transmitting aperture

e) adequate tracking and acceleration speeds for low satellites

f) high optical quality Coudé path

g) high precision servo control system to allow pointing errors (servo only) of < 0.5 arc second and track rate errors of < 0.25 arc sec/sec

h) mount configuration: ALT/AZ

i) mount position readout precision of better than 1.0 arc second RMS on both axes

j) a field of view, unvignetted, at the Coudé room entry port, of 3 to 5 arc minutes

k) total hemispheric sky coverage

l) minicomputer control of servo system

m) transmission efficiency of 10% from Coudé room entry port (similarly for receiving)

n) simple adjustment facilities

o) prevention of condensation on the optical parts

p) elevation range -5^{o} to 185^{o}

q) operating conditions in temperature of -20^{o} to 40^{o} C and up to 95% humidity.

Telescope and mount should be computer controlled, and they should be connected via a Coudé path to the guiding station, T/R-system, laser, and receiver placed in a controlled environment.

Guiding System

The prime data acquisition mode is planned to be final the absolute guiding mode. However, other guiding systems are necessary for development of the absolute guiding capability as well as for backup, system diagnostics, and real-time checking of the system's optical parameters.

The WLRS proposed guiding systems consist of

a) a wide-field finder TV mounted on a small (10 cm) auxiliary telescope. This system can also be mounted at the Cassegrain position, with a smaller field of view.

b) an eyepiece placed at a guiding station in the Coudé room (field of view 5 arc min).

c) a TV imaging system placed in the guiding station to allow electronic image enhancement for manual guiding.

d) a star tracking system (eg. quadrant detector) placed at the guiding station also.

The guiding station concept is shown in figure 2. The eyepiece is always available for use. The beamsplitter is used to optically switch between star tracking system and TV (lunar tracking).

The WLRS would initially become operational with manual guiding for LLR from the guide station. Absolute guiding should be possible as soon as the mount model is improved to give an RMS error overall of less than 4 arc seconds.

T/R-Switching System and Receiver System

The requirement for a transmit/receive switching system (T/R) arises because common optics would be used for transmitting and receiving. The requirements for the transmit/receive switching system (T/R) are:

a) to connect the Coudé path to the laser during time of fire.

b) to connect the Coudé path to the receiver at the time of expected returns.

c) high efficiency in the transmitting and receiving mode.

d) to operate at high laser pulse rate of max. 10 Hz.

Filters for the receiver will be employed between the T/R and the receiver

e) suitable spacial filters.

f) suitable spectral filters.

The receiver system should consist of

a) a suitable photomultiplier (RCA 8850 or MCP/Micro Channel Plate) and

b) a matched preamplifier and discriminator.

Laser

A Quantel Nd:YAG Laser, Model YG 402 DP, would be chosen. This Laser can work in the following 4 modes:

	Mode 1	Mode 2	Mode 3	Mode 4
No. of pulses/shot	1	4	8	1
Pulse width	100 ps	50-250 ps	50-250 ps	3 ns
Pulse spacing	-	8 ns	8 ns	-

	Mode 1	Mode 2	Mode 3	Mode 4
Pulse energy	100 mJ	250 mJ	350 mJ	350 mJ
Mean Power	1 W	2,5 W	3,5 W	3,5 W

Further parameters:

Pulse repetition rate	0.3 - 10 Hz
Wave length	532 nm
Beam diameter	9,5 mm
Beam divergence	< 0.7 mrad

The single pulse (mode 1) would be used for SLR. The other 3 modes are for LLR. It is expected that mode 3 would be the most frequently used when the WLRS is in its final configuration.

Timing System

Reference to UTC within 0.1 µs (1 pps) and a stable 5 MHz-reference-frequency (H-Maser) is available from the existing timing system of the station. The internal timing system of the Laser should be driven and synchronized by the time system of the station. The epoch of Laser ranging events is determined by combining a real time determination of UTC (accurate to 0.1 µs) with a relative determination using time interval techniques (± 100 ps).

The system would have the following components:

a) time interval counters for multiple-event-counting (± 125 ps; Le Croy time interval unit) or the new high resolution (± 20 ps) Le Croy TDC if available.

b) time interval counter (HP 5370B) for calibration.

Software

The following software components are foreseen:

a) SLR prediction software, for the generation of telescope point angles and range predictions for satellite ranging, based on daily IRV inputs.

b) LLR prediction software, for the generation of telescope point angles and range predictions for lunar ranging, based on a lunar ephemeris.

c) A real-time laser ranging programme for the acquisition of lunar and satellite range data.

d) Pre-processing software to produce quick-look data files to GSFC specification, and full rate data magnetic tape for analysis and archiving.

e) Software drivers for all devices to be interfaced to the main computer (CAMAC-CRATE, Telescope- and Dome Control System, T/R and Receiver, Timing Range Gate and Range Window electronics).

f) Stand-alone diagnostic programs for each interfaced device, to allow testing of individual devices, interfaces, and drivers.

g) Mount modelling software (option).

h) Calibration software for off-line calibration.

i) Calibration software for simulated ranging, terrestrial target calibration, differential path calibration, and real-time calibration whilst ranging (incorporated into c)).

j) Software aids for system alignment, laser monitoring and testing, weather monitoring.

The software would be installed on a HP-A900 computer system in order to be compatible with the NATMAP software development.

Electronics

The WLRS control electronics visualised consist of the following (cf. fig. 1):

a) Laser Ranging Controller (LRC).

b) CAMAC Controller and electronic interface to HP-A900 computer.

c) Guiding system electronic interface to HP-A900 computer.

d) Telescope system electronic interface to HP-A900 computer.

e) T/R control system and electronic interface to HP-A900 computer.

f) Dome control system and electronic interface to HP-A900 computer.

g) Timing system for laser ranging, including electronic interface to HP-A900 computer.

h) Wideband signal processing electronics.

The electronics for the WLRS should be designed and constructed to operate in cohesive and integrated fashion so as to allow software control and monitoring of the entire laser ranging process.

The major electronics sub-systems are shown in figure 1, WLRS OVERVIEW. In this figure, the receiver system incorporates the active spectral filter control, the telescope system includes the dome control and interface, the signal processing electronics are distributed between the CAMAC system and the LRC, and the ranging timing system between the LRC and the CAMAG system.

References

[1] Peter Wilson: Zur Erweiterung des Nd:YAG Laserentfernungsmeßsystems der Station Wettzell für Entfernungsmessungen zum Mond. - Veröff. d. Bayer. Kommiss. f. d. Internationale Erdmessung, Heft 38, München 1978.

[2] MERIT/COTES Joint Working Groups: MERIT Campaign, Connection of Reference Frames. - BIH, Paris, 1983.

[3] John Mck. Luck: NATMAP Laser Ranging System. - CSTG Bulletin No. 5 (1983).

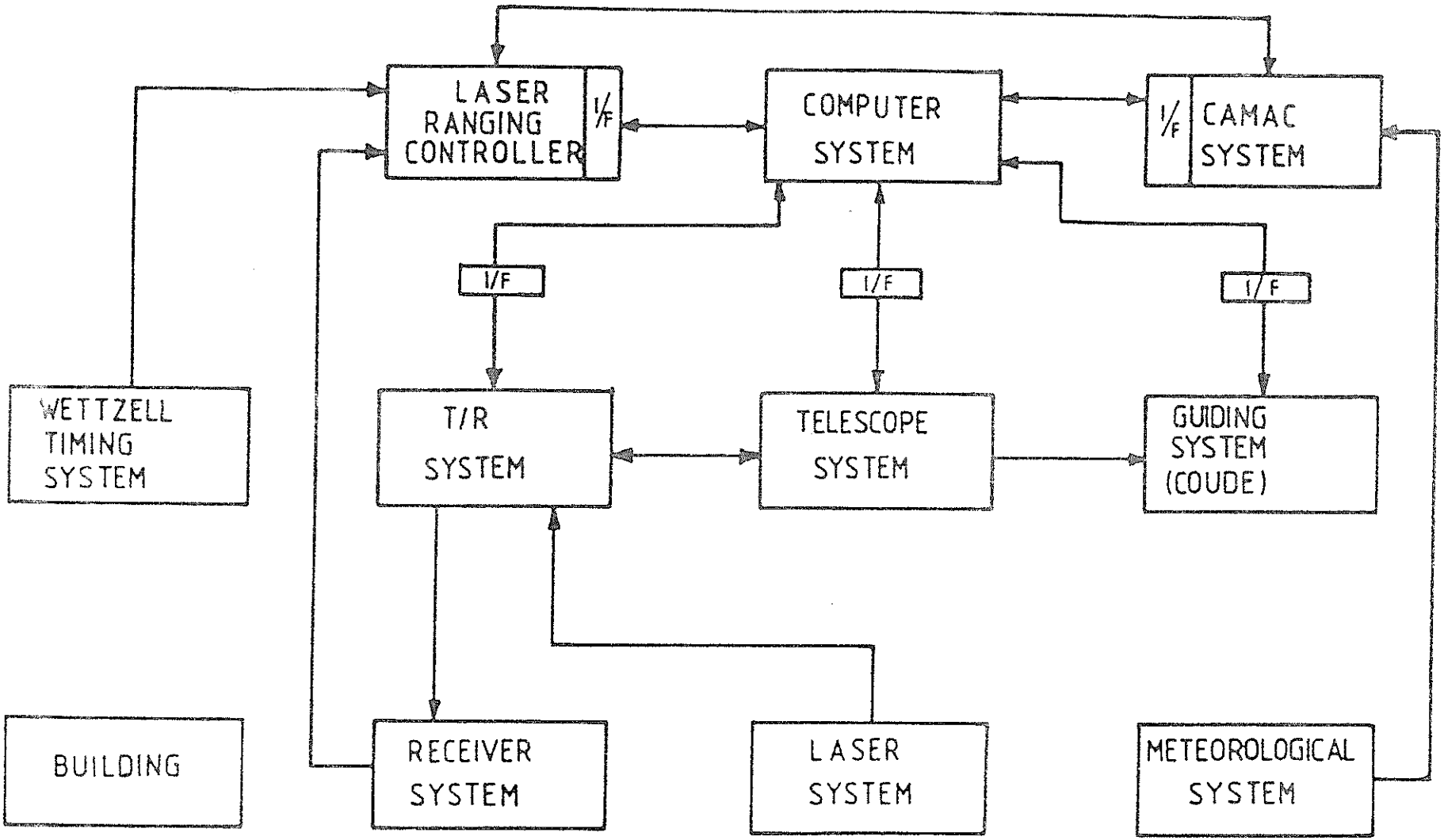

Figure 1 WLRS OVERVIEW

Figure 2

GUIDING STATION CONCEPT

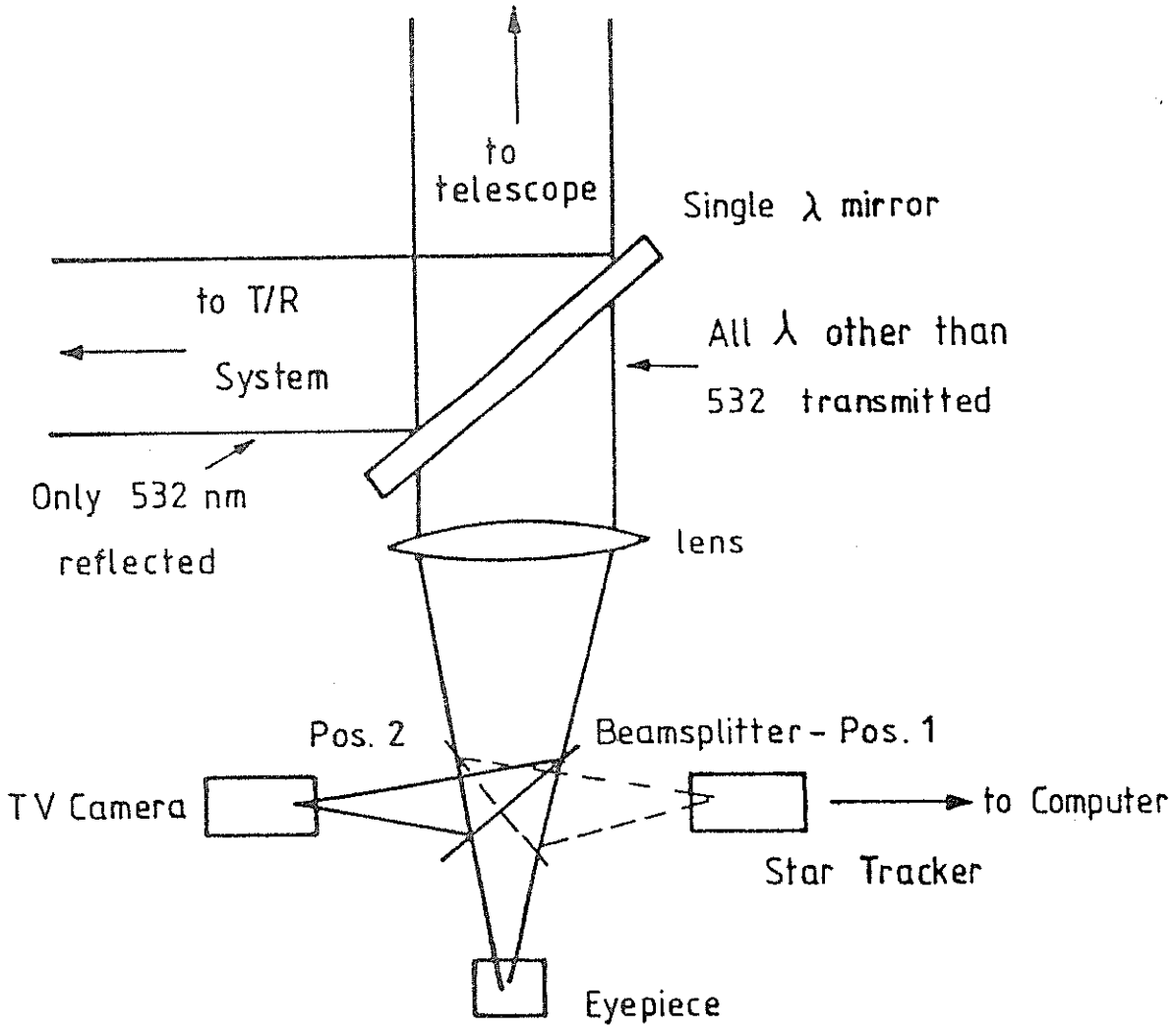

THE TRANSPORTABLE LASER RANGING SYSTEM MARK III

T.S. Johnson
Instrument Electro Optics Branch
NASA Goddard Space Flight Center
Greenbelt, Maryland 20771

Telephone (301) 344 7000
TWX 710 828 9716

W.L. Bane, C.C. Johnson, A.W. Mansfield, P.J. Dunn
EG & G WASC,
6801 Kenilworth Avenue, Riverdale, Maryland 20737

Telephone (301) 779 2800
Telex 590613

ABSTRACT

The transportable laser ranging system (TLRS-3) has been designed to take advantage of the latest developments in satellite ranging instrumentation and techniques. Satellite returns at the single photo-electron level are detected from low power laser light transmitted trough a compactly designed mount. Modular construction efficiently integrates the computer system, with terminal entry, disc sotrage and graphic display and a time transfer system driving a precise frequency standard. Station, star and satellite acquisition data are read from floppy discs, which can also be used as the final medium for shipping the ranging data. An azimuth/elevation tracking mount can be calibrated from visual observations of automatically selected stars. A single shot rms noise level of a few centimeters is observed on satellite at a return data interval around one second. The light-weight system consumes little power and requires no more than two operators for a normal satellite tracking shift.

THE TRANSPORTABLE LASER RANGING SYSTEM MARK III

The transportable laser ranging system (TLRS-3) has been designed to take advantage of the latest developments in satellite ranging instrumentation and techniques. Its architecture is based on that of TLRS-2, which has successfully completed campaigns in Greenbelt in 1982 and on Easter Island and Otay Mountain in 1983, and is now making measurements at other normally inaccessible and undeveloped sites. Collocation tests have demonstrated agreement between the ranging observations taken by the transportable machines and high power laser systems at the centimeter level. A single shot r.m.s. noise level of a few centimeters is observed on satellite ranges at a return data interval around one second. Mount pointing repeatability of a few seconds of arc can be maintained during an occupation period of several weeks.

Satellite returns at the single photo-electron level are detected from low power laser light transmitted through a compactly designed mount. The modular construction efficiently integrates the computer system, with terminal entry, disc storage and graphic display and a time transfer system driving a precise frequency standard. Station, star and satellite acquisition data are read from floppy discs, which can also be used as the final medium for shipping the ranging data. An azimuth/elevation tracking mount can be calibrated from visual observations of automatically selected stars. During the satellite pass, a three-level interrupt sequence coordinates the computer's system control, prediction and data recording functions. The light-weight system consumes little power and requires no more than two operators for a normal satellite tracking shift.

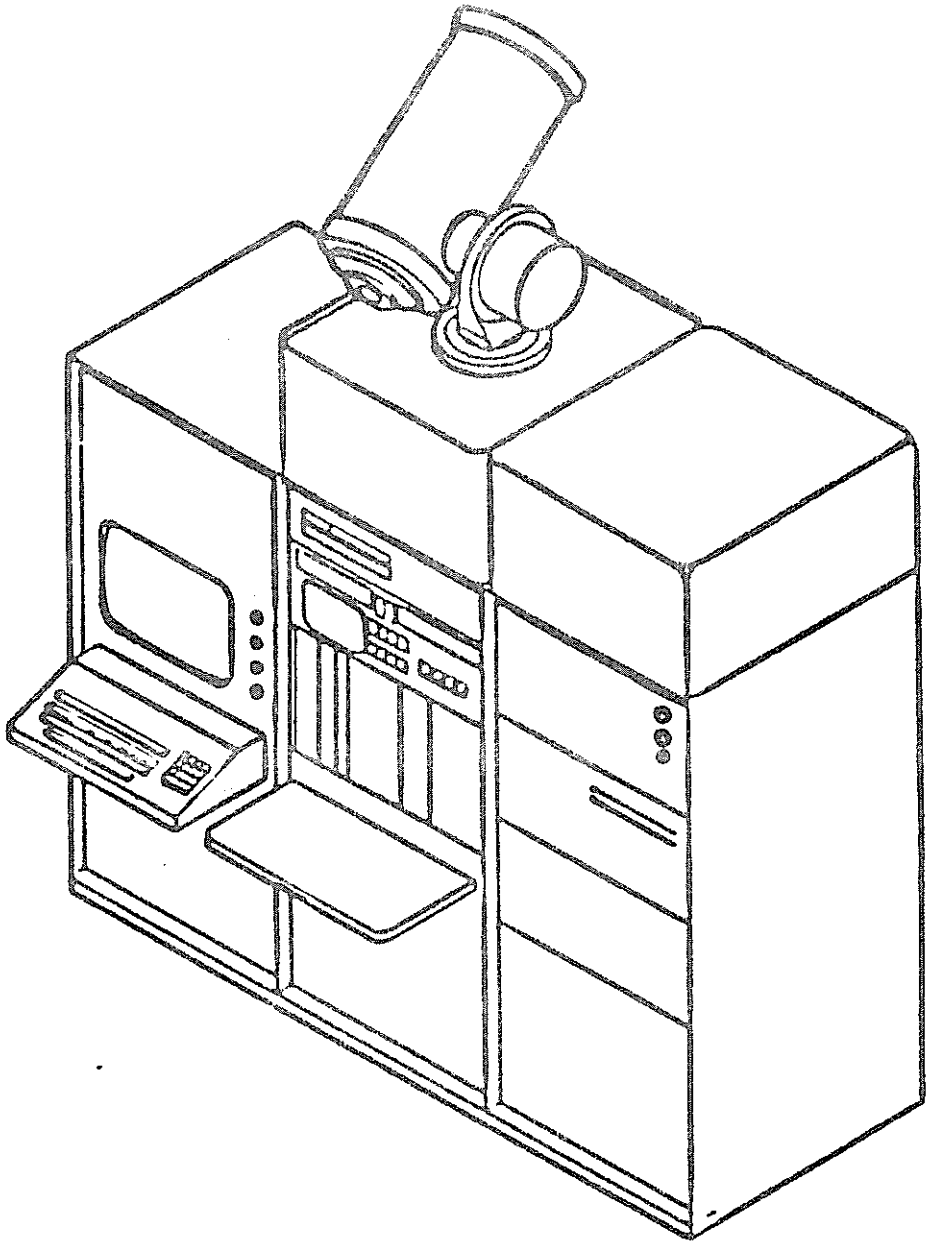

In the configuration shown, the laser is mounted in its shipping container above the rack to the right, which contains the chiller and power supply, with the optical path folded within the central case which also covers the pedestal. Below the mount in the central rack, the microprocessor with disc storage units and the ranging and mount control electronics are housed. The console panel includes a small graphics display screen, digital readout devices and control switches. A timing system is mounted in the third unit.

TRACKING MOUNT

A 280 mm. aperture optical telescope with near diffraction limited optics and f/10 focal ratio is mounted off the axis of an azimuth elevation mount to give a common transmit/receive path for the light signal. A mirror within the telescope deflects the light path along the elevation axis and into the mount support where a second mirror turns the path down the azimuth axis. The mount is positioned with motor/tachometer/inductosyn encoder assemblies for azimuth and elevation control. A mirror inside the pedestal, rotated by a motor synchronized with the laser firing sequence, deflects the transmitted signal up the azimuth axis, after it has been sampled with a pellicle mounted in the horizontal path of the laser output.

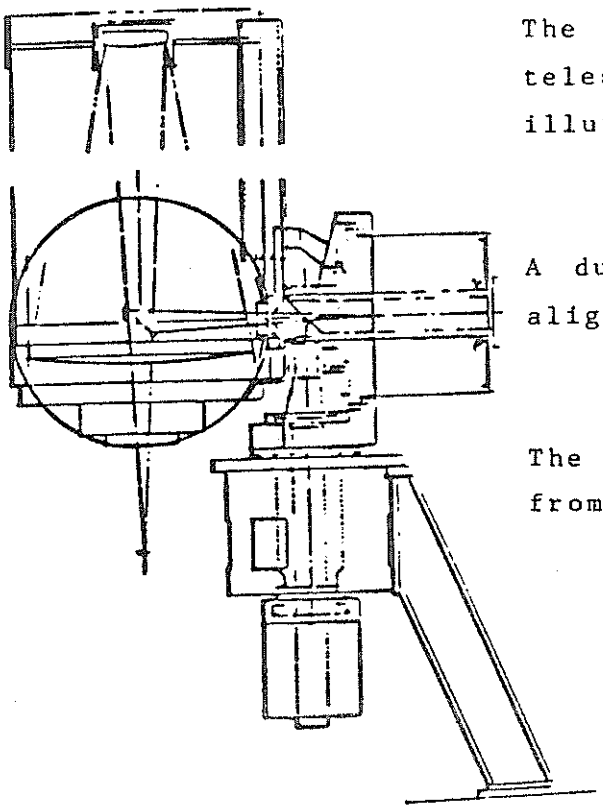

The modified Schmidt-Cassegrain telescope is sectioned in this illutration.

A dual-bearing mount allows easy alignment of the optical system.

The pedestal tripod is constructed from aluminum weldments.

TIMING SYSTEM

A master oscillator provides primary timing signals at 20 MHz, 1 MHz and 1 pps to a module which distributes frequency and pulse information throughout the system. The difference between the system 1 pps clock and a GPS receiver is used to establish epoch time to within one microsecond of a master clock.

LASER SYSTEM

The transmitter consists of a passively mode-locked Neodynium-YAG laser with a pulse slicer and double-pass amplifier. The fundamental frequency of 1062 nm. is doubled to produce green light at 10 pulses per second. The transmitter is supported by capacitor banks, a control unit, power supply and a cooler carrying deionized water to dissipate heat generated by the flash lamps and laser rods.

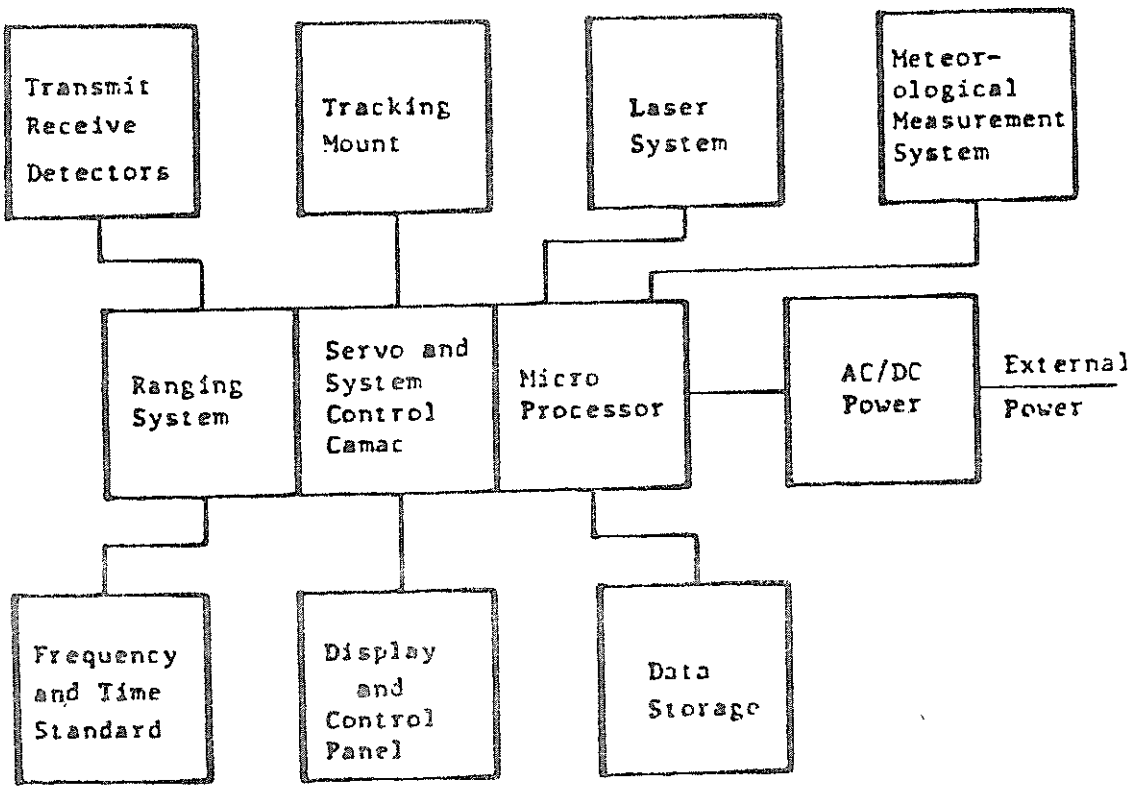

SERVO AND SYSTEM CONTROL

The central control sytem uses a 20 pps interrupt timing signal from the frequency and pulse distribution module to position the optical axis of the tracking mount. Angle error commands are received from the computer through a digital-to-analog converter and compared with shaft encoder position signals. The correct speed and direction of travel for the azimuth and elevation motors can then be specified to the servo amplifiers.

TRANSMIT/RECEIVE DETECTORS

A laser monitor diode triggers a start pulse when it detects the light transmitted through a dichroic mirror placed in the optical path of the laser transmitter. The green light reflected by the dichroic mirror passes through a negative laser coupling lens before the rotating mirror reflects it into the tracking optics. The received laser pulse is detected by a photomultiplier and arrives at the PMT distribution unit after the start pulse. Constant fraction discriminators separately shape the start and stop pulses which are transmitted to the ranging system.

RANGING SYSTEM

The range measurement system is driven by the system 10 pps interrupt signal and consists of a multichannel 50 picosecond resolution time interval counter. A common start signal is received from the transmit discriminator and up to seven separate signals may be accepted from the receiver discriminator in any measurement cycle. In addition, the ranging system measures the amplitude of each individual start or stop signal as well as the epoch time of the start signal and the mean background rate (the number of noise photo electrons/sec).

COMPUTER SUBSYSTEM

The computer communicates with the other subsystems through a CAMAC dataway. Control and service routines are driven by hardware-generated interrupts in foreground. Trajectory computation is performed as a background task, with display and data recording scheduled for execution by foreground routines. Computer peripheral input/output operations are controlled asynchronously.

A numerical integration scheme is used to compute the orbit for a satellite pass based on a power series representation. The travel time for a particular laser pulse and the range gate window needed to accurately measure the return time is predicted, as well as the pointing angle required to place the target within the laser beam. The computer system also operates in a star tracking mode for mount error calibration and computes cable delay corrections from both internal and external targets. A ranging analysis software package allows on-site analysis of data for quality control and a comprehensive set of diagnostic routines support the field operation.

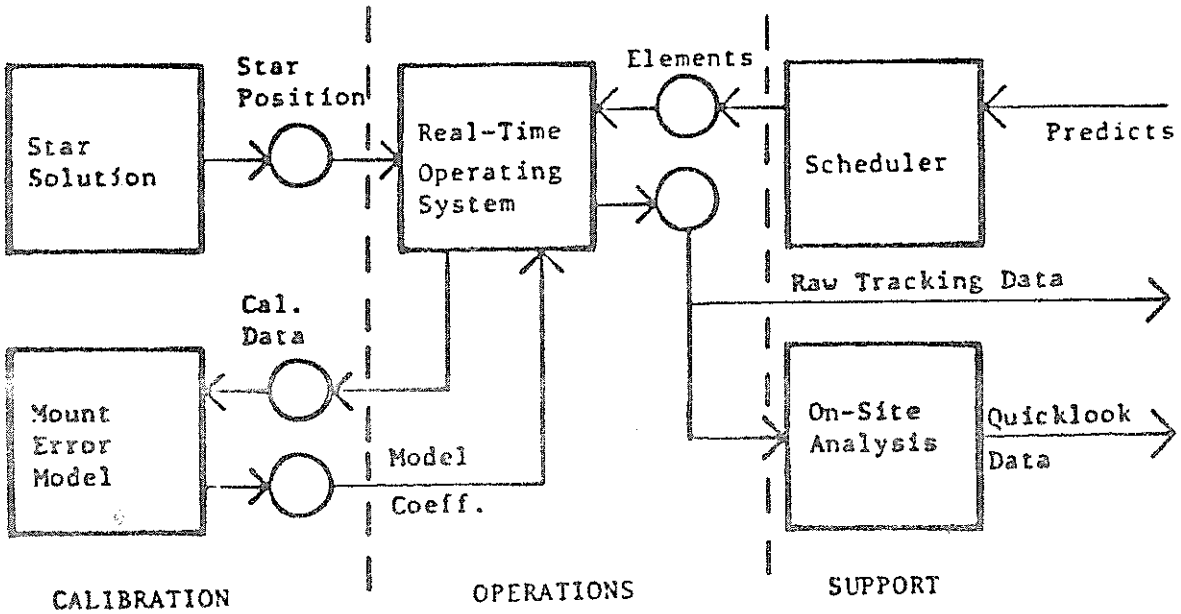

TRACKING OPERATION

Passive star calibration and active ground and satellite ranging are conducted under computer control. A console panel allows operator tuning of each mode of operation based on information displayed on the screen, and contains switches to initiate the required mode. Angle biases can be applied to star observations to derive a mount error model, and to compensate for any target position errors during tracking. The dominant satellite positioning error is along the orbit track and is compensated by applying a bias to the epoch of the laser pulse's predicted travel time. In the illustration, range residuals to a satellite with a small along-track orbit prediction error are shown on the screen.

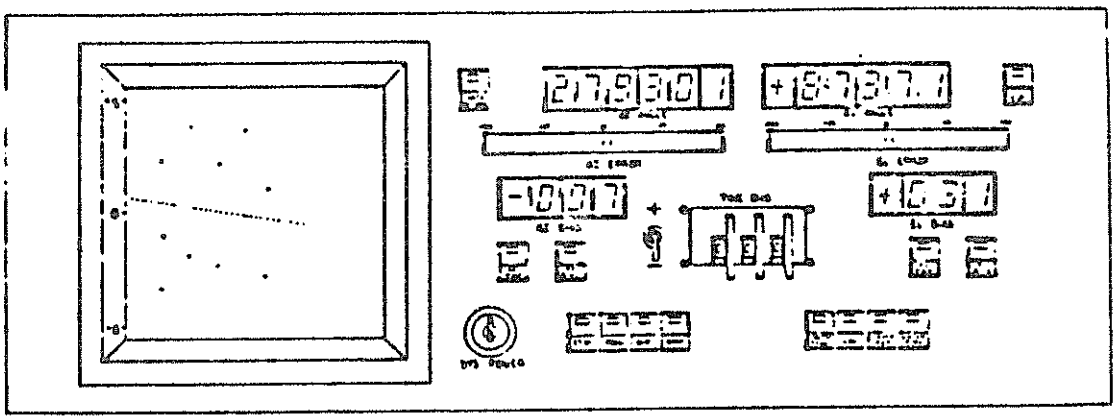

The details of each transmitted pulse are recorded together with enough data on the returns to properly monitor system performance. Automatically recorded measurements of the pressure, temperature, and relative humidity at the site accompany the tracking data to allow the measurements to yield their intrinsic accuracy at the centimeter level.

THE SOFTWARE SYSTEM FOR TLRS II

P.J. Dunn, C.C. Johnson, A.W. Mansfield
EG & G WASC,
6801 Kenilworth Avenue, Riverdale, Maryland 20737

Telephone (301) 779 2800
Telex 590613

T.S. Johnson
Instrument Electro-Optics Branch
NASA Goddard Space Flight Center
Greenbelt, Maryland 20771

Telephone (301) 344 7000
TWX 710 828 9716

ABSTRACT

The Transportable Laser Ranging System Mark II has been designed for accurate satellite tracking operations with low power consumption. The performance of the system can be regularly monitored with software which also provides on site capability to assess data quality and to confirm that the system is working at the single photoelectron return level. This short report briefly describes the software suite and illustrates the date quality assessment procedure for satellite and ground target observations.

THE SOFTWARE SYSTEM FOR TLRS II

The Transportable Laser Ranging System Mark II is a new type of highly mobile laser satellite tracking system. It is designed for rapid deployment to normally inaccessible and undeveloped sites within the laser network operated as part of the Goddard Space Flight Center Crustal Dynamics Project. The system is packaged in shipping containers which will fit in the cargo holds of normal passenger jet airlines, and emphasises modular construction and low power requirements. A single photoelectron system receives returns on seven channels through a 25 cm. aperture refractive optical system from a passively modelocked, frequency doubled Nd:Yag laser transmitter.

System control, pointing, data recording and post-flight data analysis is accomplished with a CAMAC packaged microprocessor. The principal interfaces for the software suite are shown in Figure 1, and the three functions of calibration, operation and support are categorized. An overview of the Real-Time operating system is presented in Figure 2, which also provides details of the hardware configuration. A flow chart of the main control routine for real-time operation is given in Figure 3 and indicates the procedure by which the system is prepared for satellite acquisition or star tracking for mount calibration.

The instrument has completed successful campaigns at Greenbelt, Maryland, Easter Island, Otay Mountain and Cabo San Lucas, Mexico. The capabilities of the on-site data analysis software have helped to control data quality and to indicate occasional system malfunctions. The performance of

the post-flight analysis software is the focus of this report and is illustrated in Figures 4, 5 and 6.

The post-flight recontruction of the real-time screen display for a pass of LAGEOS taken at Cabo San Lucas in March 1983 is shown in Figure 4. The vertical scale has been set to 50 nanoseconds in round-trip flight time to show the noise level of the returns, although the range gate actually used for acquisition was one microsecond. The horizontal scale is in seconds from the predicted point of closest approach and the pattern of returns is caused by orbit prediction error which in this case amounts to a few meters. The increased background noise visible as the pass progresses is caused by the occurrence of sunrise. The histogram of returns shown to the right of the screen display is redundandant in this reconstruction and the statistics listed below the histogram apply to all of the information on the screen. Options to display quicklook data, to fit low order polynomials to selected points, change plot scales and redefine plotting variables are available to the operator as part of the quality control procedure.

In Figure 5, three consecutive screen displays are shown to illustrate the sequence used by the operator to assess the data quality. A low order polynomial is fitted to the screen pattern to produce a symmetrical histogram of returns. Although manual editing capability is available, in this example, automatic editing based on the observed noise level of the data was applied to produce the final display of acceptable returns. The noise level of 487 measurements taken from all channels of the receiver system amounted to 10.4 centimeters. This is higher than expected

and is partly due to the application of nominal interpolator scale factors to each of the channels.

The screen display of Figure 6 shows returns detected in a single channel from three separate horizontal targets. The noise level is 5.7 cm for 588 observations, which is close to nominal for the system, but will include some survey error for the targets at the centimeter level. The horizontal target calibration establishes the system delay at 4.93 m. and this value was maintained consistently throughout the occupation. Figure 6 also shows a plot of range against return power amplitude to establish that the system is operating at the single photon level for which it was designed, and which corresponds to about 60 units on the horizontal scale. A histogram of returns as a function of return power is also shown and exhibits a Poisson distribution with peaks at the multiple photoelectron levels.

The TLRS-2 quality control software has been found to efficiently indicate any aberrations in the system which might lead to adjustments to improve the performance of the laser, the discriminators or the operating power level. It has efficiently assisted the operators in their efforts to maintain the accuracy of this new transportable instrument.

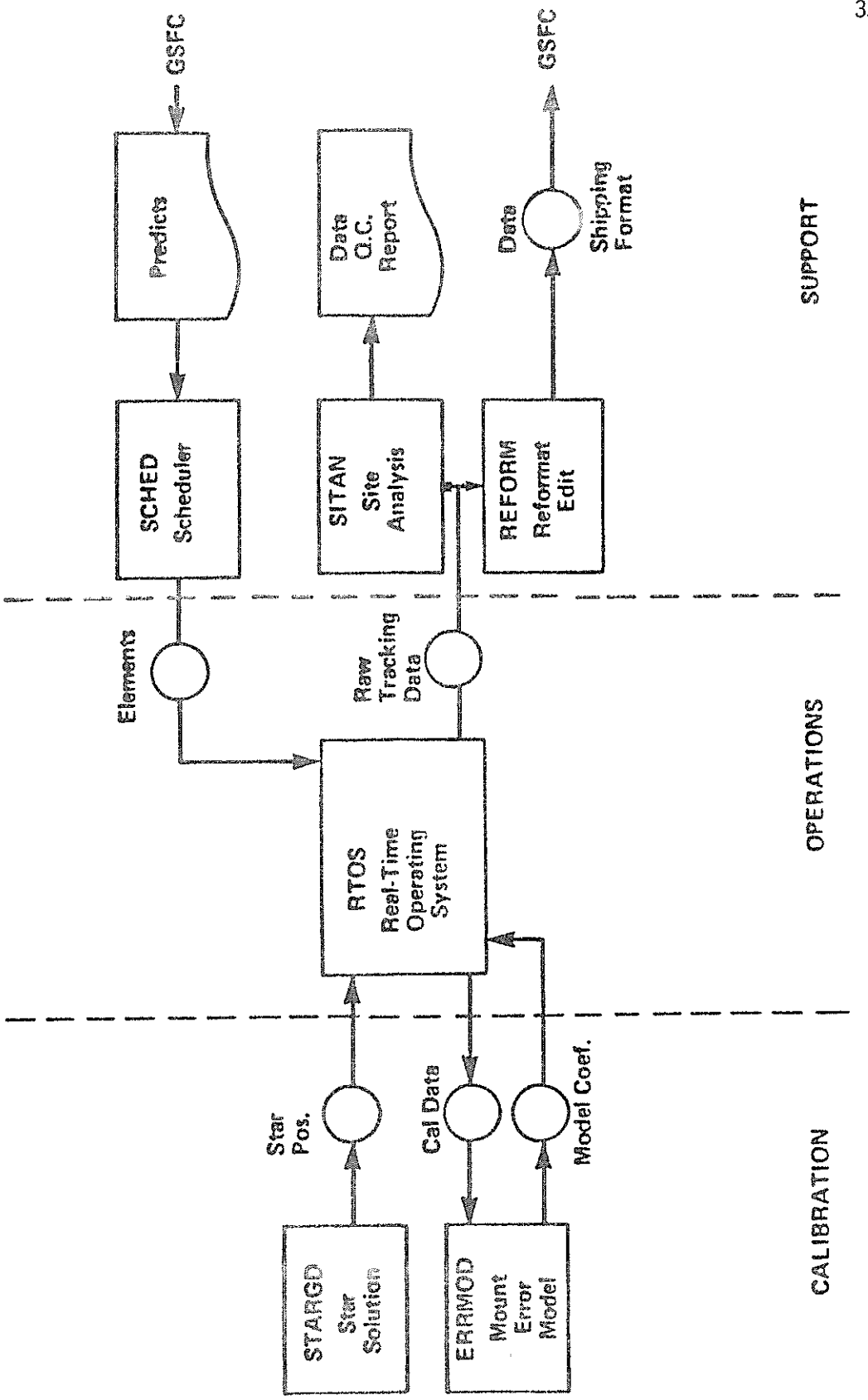

FIGURE 1. TLRS-II SOFTWARE ORGANIZATION

FIGURE 2. TLRS–II REAL–TIME OPERATING SYSTEM

Language:	FORTRAN ≈1600 Lines Executable Code ASSEMBLY ≈1100 Lines Executable Code + Resident System Routines	
Machine Environment:	CAMAC – Packaged Standard Engineering Corp. MIK 11/23 Microprocessor–based functional equivalent to PDP–11 32K storage (16-bit words) (volatile) KEF–11 Floating Point Option RT–11 SJ Operating System	
Trajectory Computation Strategy:	Numerical integration of power series orbit representation J2, J3, J4 Real-time steps of 1 sec Interpolated to 20 pps for servo bandwidth constraints	
Core Utilization:	Essentially 100%, but without overlays	
Real-Time Mechanization:	Foreground:	Control and service routines driven by 1, 10 and 20 pps hardware-generated interrupts.
	Background:	Trajectory computation, display and data recording scheduled for execution by foreground routines.
	Asynchronous:	All computer peripheral I/O: display terminal and disk.
Additional Modes:	Star tracking for mount calibration. Fixed-target mode for target-board ranging electronics calibration.	
Graphic Ranging Display:	Timing bias, AZ–EL position and range residuals.	

FIGURE 3. CONTROL ROUTINE FOR REAL-TIME OPERATIONS

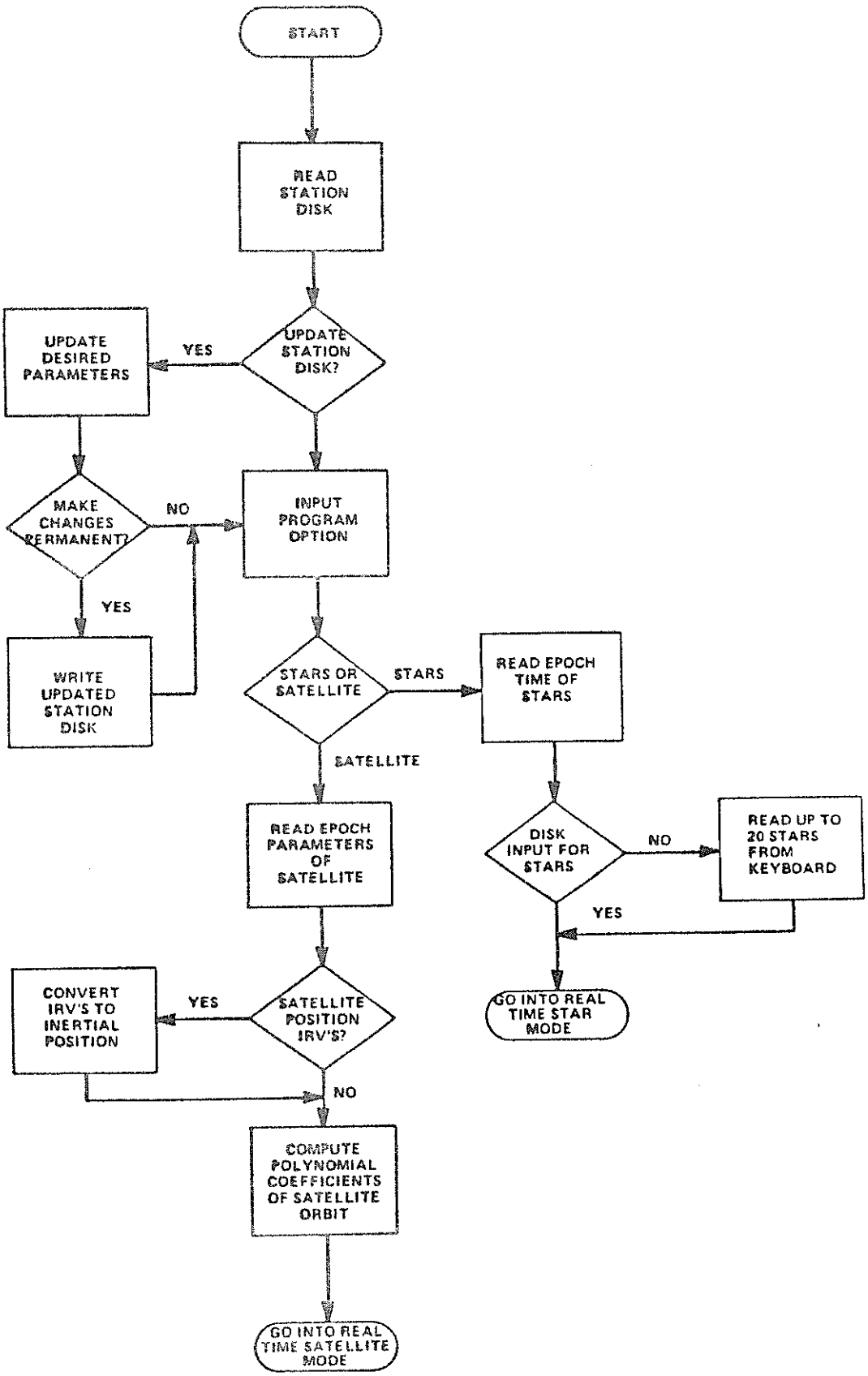

FIGURE 4. RECONSTRUCTION OF A LAGEOS PASS

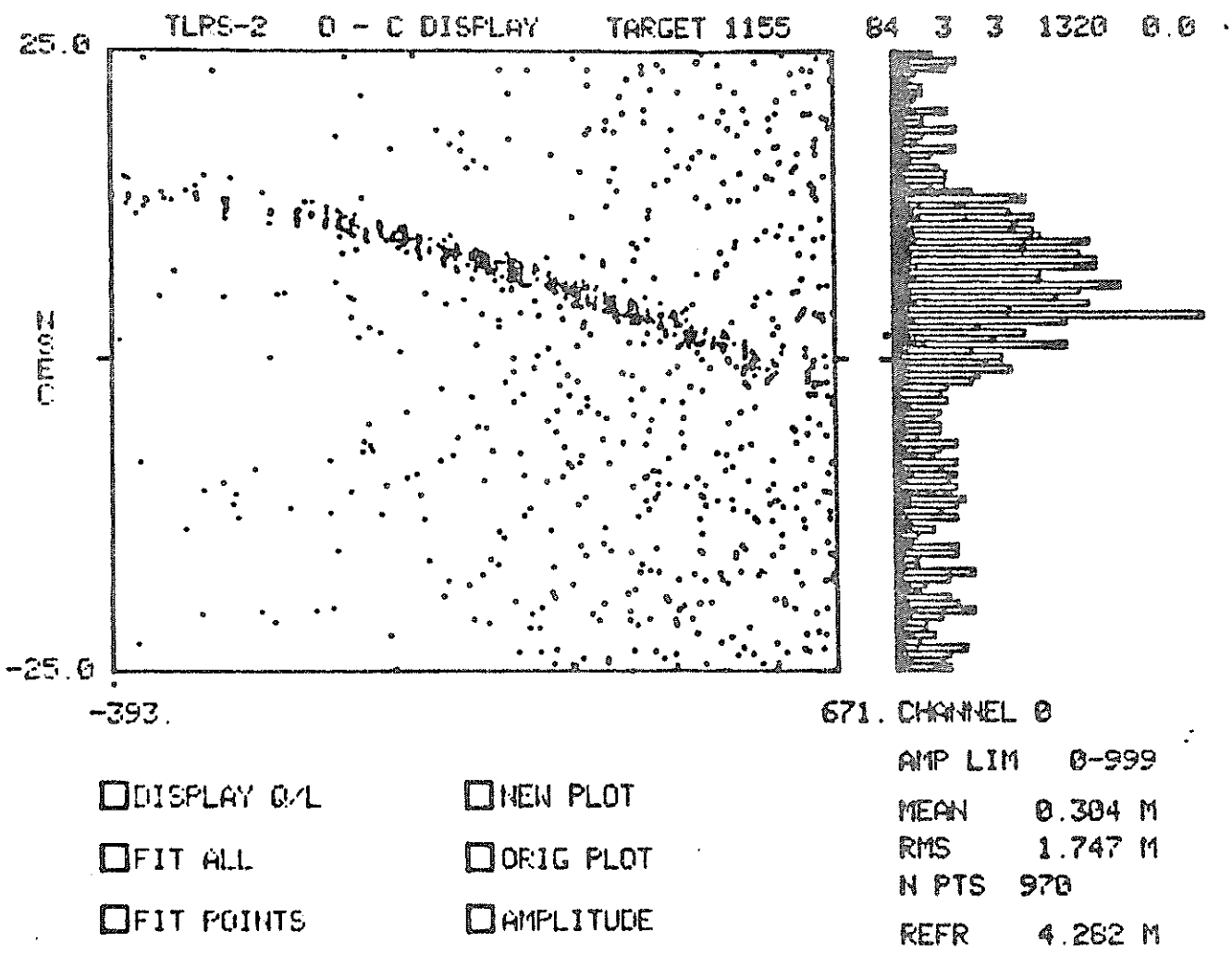

FIGURE 5. DATA QUALITY ASSESSMENT FOR A SATELLITE PASS

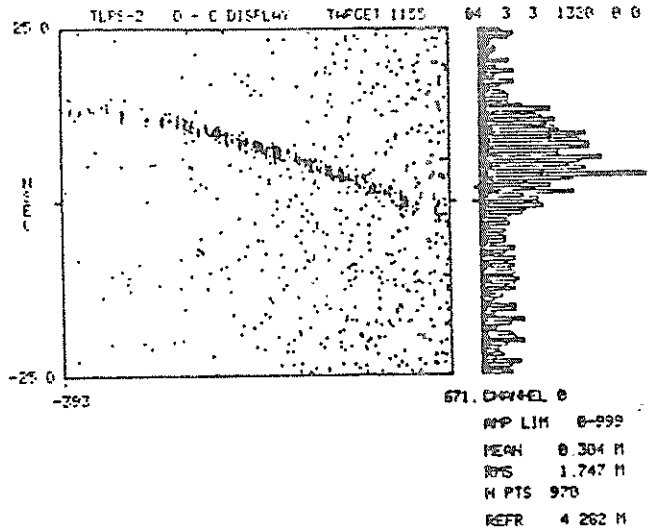

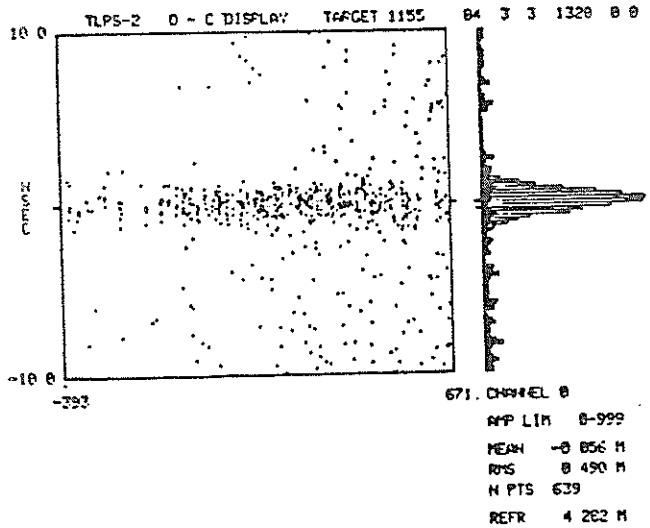

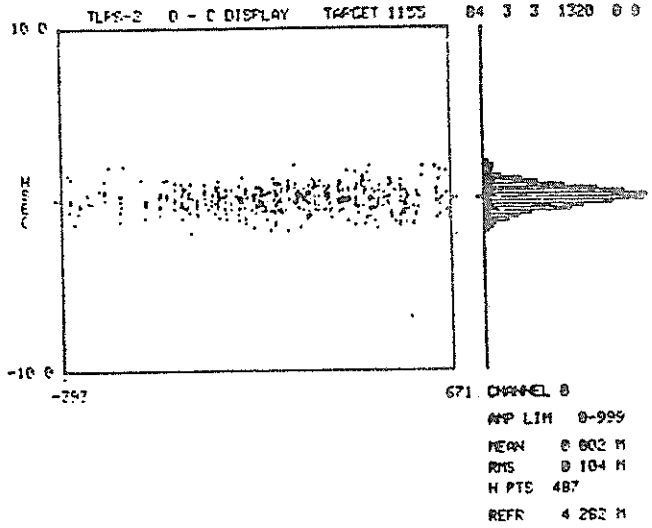

FIGURE 6. DATA QUALITY ASSESSMENT FOR A HORIZONTAL TARGET CALIBRATION

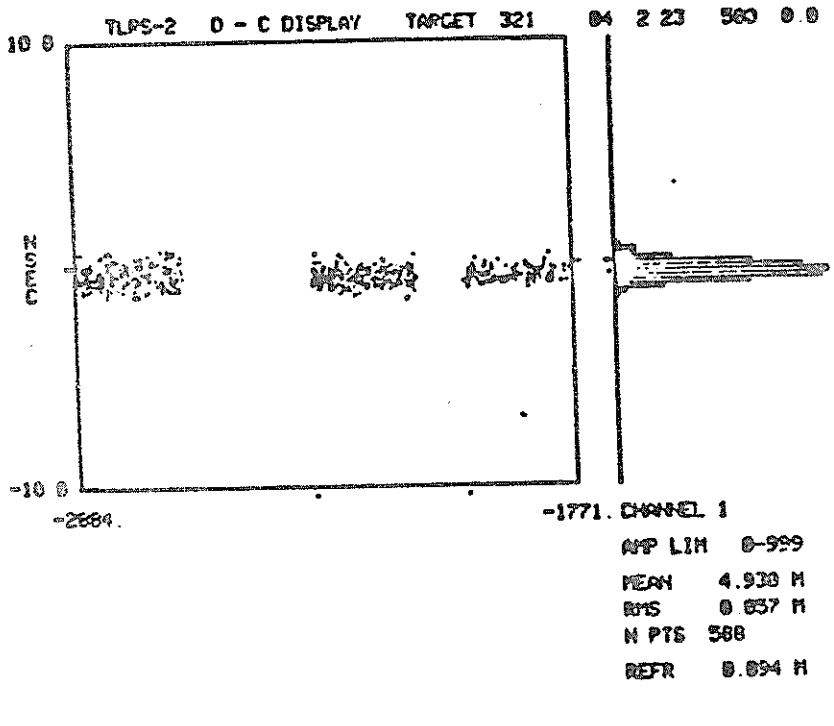

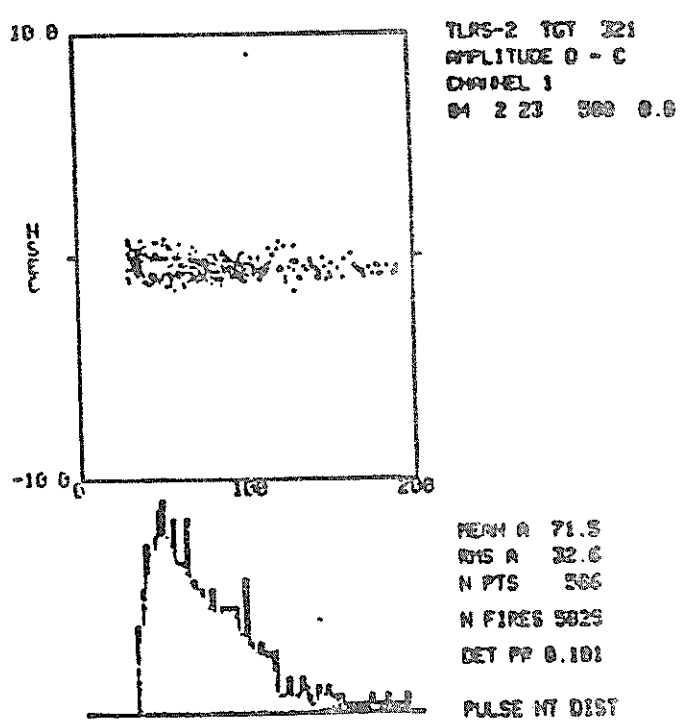

MTLRS SOFTWARE AND FIRMWARE

E. Vermaat, K.H. Otten
Department of Geodesy
Delft University of technology
Thijsseweg 11
2629 JA Delft, The Netherlands

Telephone 057 69 341
Telex 36442

M. Conrad
Institute for Applied Geodesy
Richard Strauss Allee 11
6000 Frankfurt / M, F.R.G.

Telephone 069 63 331
Telex 413592

ABSTRACT

This paper reviews the software and firmware which has been developed to date for the Modular Transportable Laser Ranging System (MTLRS). Four major tasks are identified some of which involve real time communication with the system hardware. One of the main characteristics of the overall system design is the separation of the computer hardware into three independent but mutually cooperating microprocessors. Consequently the software and firmware package of MTLRS has a modular design.

1. Introduction

The computer configuration of the Modular Transportable Laser Ranging System (MTLRS) is primarily characterized by the deployment of three microprocessors: an HP 1000 L main processor and two Motorola M6809 slave processors. The main processor together with its peripherals can be used stand-alone for any computing task, whereas the real time utilization of the total ranging system also involves the two slave processors, each addressing an independent task.
Therefore the software designed for MTLRS always involves the main processor and only in some cases requires the use of the two slave processors.
Due to the limited memory capacity of the main processor and of the external storage devices, the total amount of software developed for the system is separated into four major tasks, each requiring an individual bootstrap loading of the operating system.

2. The hardware configuration

The computer configuration (figure 1) comprises one HP 1000 L model 5 16-bit microsystem and two Motorola 8-bit microcomputer systems.
The HP 1000 computer or main processor has 128 Kbytes of RAM at its disposal for the operating system and the real time programs. The data communication with the two diskette units and the two Motorola microsystems is established through two IEEE-488 interfaces. An HP 2623 graphics terminal with an internal hardcopy unit functions as system console. Support for data communication over public telephone lines is feasible by a Silent 700 terminal with 20 Kbytes of bubble memory and acoustic coupler. All programs are executing under control of the disc based RTE-XL operating system.
The two Motorola microcomputer systems, i.e. the predictor processor and the formatter processor, are slaved to the main processor. Each of the processors comprises one 5 MHz microcomputer board based on an M6809 MPU, one IEEE-488 listener/talker i/o board with two additional 8-bit PIA's (parallel interface adapter) providing for interprocessor and MTLRS electronics data i/o. A memory board with 16 Kbytes of RAM installed, is available to each of the slaves and is used for real time program data storage. An APU (arithmetic processing unit) board based on an AMD 9511 is attached to the predictor processor and an additional IEEE-488 listener/talker board is modified to provide for the controller function of the data communication link between the formatter processor and the two HP 5370 range counters.

The real time programs of the slave processors are supported by a selfmade operating system. The operating system as well as the real time programs are installed in EPROM.

3. The real time software system

The MTLRS is controlled by three cooperating microprocessor based computer systems. Each processor hosts a task, executing a well defined function to achieve a minimum of interaction between the processors. These three functions can be described as:

- final prediction and correction of the direction and the speed of movement of the optical axis of the telescope,
- collection and formatting of the observational data into a compact data format,
- data acquisition during and control of the observational activities.

The first two functions are performed by the predictor and the formatter processor respectively while the last one is carried out by the main processor because of its complexity and variety concerning data handling. The predictor as well as the formatter task are programmed in assembler to meet the requirements of time dependency during real time operation whereas the task of the main processor has been established in Fortran IV. For overall synchronization of the different processors, the start-up procedure and the observational activities have been broken down into several levels, each of them representing a certain state of operation. A change of state is mainly caused by a binary command string from the main processor's monitor program to the predictor and formatter processors, but also by the detection of a certain condition by either processor. At all times both slave processors notify the monitor program about a change of state, while during the real time operation also the predictor and formatter processors interchange state information. In this section the major states of operation of both the predictor (figure 2) and formatter processor (figure 3) will be discussed in some detail.

Start-up The predictor and formatter processor system command handlers are entered after power-up, ready to receive a command from the main processor's monitor program for system function initiation like memory dump, program loading and (real time) program execution. At this level diagnostics may be loaded and executed.

On behalf of the observational activities the real time predictor and formatter programs residing in EPROM are started by the monitor program. Both programs

examine all the communication links they are going to use, reset the encoders of both the telescope's axes as well as the range counters after which they automatically proceed to the next state.

Session idle The session idle state is defined as a resting-point for both the predictor and formatter real time programs to allow off-line operation of the main processor.
At this level there is no interaction with the MTLRS guiding and detection system and between both slave processors. For future use, functions like telescope encoder readings and time synchronization of the main processor may be added to the predictor and formatter programs, callable by monitor user commands.
To leave the session idle state, the monitor program may issue a user command to return to the processor system command handler or to proceed to the session initiate state for the execution of a series of observational activities.

Session initiate All data transfers between the main processor and the slave processors will be performed under interrupt control from this state onwards to guarantee that the 10 Hz operation rate of the predictor and the formatter programs will not be disturbed.
After receipt of the initiation command by both slaves, the predictor program receives a set of equally spaced topocentric predictions from the monitor program. The predictions are to be used for target tracking (satellite path) or fixed target pointing (ground targets), the latter one mostly being time independent. In the case of time independent pointing the movement from one target to another is performed under monitor command. Optionally the directional mode of observation may be chosen instead of the ranging mode.
To maintain azimuth angle accuracy of tracking predictions at higher elevation, the predictor program defines separate coordinate systems for adjacent groups of four satellite points utilized during real time 3rd degree interpolation.
Concurrently the formatter program optionally initializes the two range counters and prepares observational data formatting. Before entering the session active state the predictor and formatter program synchronize for the first 0.1 second observation cycle, as will be described in the next section.

Session active Three major tasks have to be performed during a 0.1 second observation cycle, i.e.

- calculation and correction of a prediction,

- synchronization of the predictor processor and the formatter processor,
- formatting of the observational data records.

The prediction calculation and correction task is carried out by the predictor program. The predictor program subsequently passes through three substates during the session active state. The first one is the prediction ready state while it waits for the first prediction epoch. It remains in the prediction valid state until the last prediction epoch is encountered, whereafter the prediction exhausted state is entered. In the prediction ready state the telescope's direction is moved to the first predicted point, being a satellite position or a ground target. The prediction valid state comprehends either the selection of a pointing prediction or the interpolation of a tracking prediction and the correction of that prediction, to be used for the next observation cycle. While in the prediction exhausted state, telescope pointing in the direction of the last calculated position is maintained.
The predictor and the formatter programs synchronize every 0.1 second observation cycle, by using the well defined epoch whereupon the mount positioner accepts a prediction message from the prediction program. The predictor program then transmits a synchronization message, including the current prediction to the formatter program and in turn receives a message from the formatter program containing the corrections to be applied to the next prediction.

The formatting of the observational data records is performed by the formatter program. The observational data is received from the multiplexor and one of the two range counters which are alternatingly used every 0.1 observation cycle. Three different types of 8 byte records may repeatedly appear in an observation message, i.e. the time record, the direction record and the observation record.
The time record contains the absolute epoch and appears every 25.6 seconds in the stream of observation messages. Every 1.6 seconds the current elevation and azimuth of the telescope are formatted into a direction record. If a successful observation is detected, an observation record is formatted, including time fractions of the laser firing epoch, the simultaneous calibration and the range count. Because the MTLRS can be utilized for direction observations, the observation record may contain azimuth and elevation angles instead of ranging data. Both the direction and the observation record contain unambiguous time offsets of their epoch. Every 1.6 seconds, the currently formatted observation message, together with an optional multiple-stop timer message are submitted to the interrupt system for transmission to the main processor.
Calibration mode of ranging may be selected during the whole session active state

with either the telescope being directed to a predefined point or with the telescope continuing to point or track. The session active state may be terminated at all times by user command to the predictor program whereafter both the predictor and formatter programs return to their respective wait state.

4. Task 1: Site Installation

Mobile laser ranging involves frequent moves of a laser ranging system between site locations. Before the actual ranging can start upon arrival at a new site, a variety of activities has to be performed, such as orientation, a lignments, system checks, etc. Some of these activities allow automation especially if they involve data taking utilising the system, data reduction or data storage. A software system has been designed combining the computer aided installation activities in one task (figure 4). This task is made up of four subtasks:

a. the astronomical orientation of the telescope mount axes together with the determination of astronomical latitude and longitude,
b. the positioning of the mount relative to local markers,
c. the initialization of terrestrial range targets and finally
d. the recording of data and results obtained from these subtasks on selected external storage devices.

Geodetic astronomy A high accuracy orientation is required for tracking a predicted satellite orbit with a laserbeam of 10 arcsec. minimum divergence. Therefore this subtask first determines the orientation of both the azimuth and elevation encoder system in an astronomical reference frame. Since, the reach of hand paddle corrections in elevation and azimuth in tracking mode is limited to $\pm$0.127 degrees, the orientation is obtained in two steps.
An initial azimuth orientation is determined from star observations in static pointing mode, manually operating the mount positioner. Subsequently accurate azimuth and elevation orientations are obtained observing optimally selected meridian stars in tracking mode, making full use of the computer controlled systems for mount positioning and data recording. The data reduction results are tested statistically and if these results are not accepted, the observational procedure is re-scheduled immediately.

If the orientation is satisfactory the subtask secondly determines astronomical latitude and longitude simultaneously, by observing zenith distances of optimally

selected ex-meridian stars in tracking mode.
Latitude and longitude are required to obtain baseline corrections in a global reference frame from locally obtained eccentric positions of the system, as well as for proper transformation of predicted satellite positions to topocentric coordinates.

Survey local markers This second subtask determines the position of the telescope mount relative to a number of survey markers available on the site pad. A positioning device is utilised to obtain azimuth and elevation readings to these markers, employing the computer controlled mount-positioning system and data recording system. If four or five optimally arranged markers are observed (Vermaat and Van Gelder, 1983) the positioning of the ranging system can be obtained with sub-millimeter precision from a specially designed data reduction method (Vermaat, 1984).

Initialize range targets If terrestrial range targets are going to be observed in a lateration mode, these targets will be identified in the third subtask. This very simple process involves manual pointing at a target utilising the mount-positioning system and the subsequent reading and recording of the telescope position under computer control. This initial identification facilitates the ranging to any of these targets employing the ranging task and the real time software system.

Finish the installation task OK-bits identifying each of the previously described subtasks will be set as soon as the particular subtask has been completed satisfactorily. If all OK-bits are set, i.e. if the complete installation task has produced acceptable results, the present termination subtask will perform a specific process of data storage. First, all observations obtained during any of the previous subtasks will be stored in a uniquely identified site log file on a specific data diskette. This enables the reconstruction of the complete installation task at any time, using the original observations. Subsequently, site identification parameters such as site number and occupation number together with the results from the installation process, e.g. astronomical latitude and longitude, the baseline correction vector, etc., will be stored on the system diskettes of all subsequent tasks. This procedure safeguards these subsequent tasks against the use of wrong site dependent

data and requires each of these subsequent tasks to start with a check on the identity of the current site.

5. Task 2: Satellite prediction

Satellite ephemerides must be available in the form of inertial state vectors (comprising position and velocity components) at an epoch close to the rise time of the satellite for a particular site. Thus each satellite pass for a site requires one state vector. These state vectors can be obtained from any established method of orbital prediction, performed by the authority responsible for the deployment of the system. To facilitate the use of any available data communication method, the state vectors are required in an ASCII-character format.

The task performing the satellite prediction comprises two subtasks: the re-formatting of newly received ephemerides and the actual prediction of individual satellite passes (figure 5).

Processing of new ephemerides This subtask checks the ASCII-character input data for transmission errors and subsequently re-formats the data into a compact binary internal format. This binary format allows efficient use of storage space on diskette as well as efficient access to the data by the prediction software.

Pass prediction This subtask performs a numerical integration of the satellite pass from the input state vector over the time-span of visibility at the site. Due to the limited time-span a very simplified force model can be employed for the equations of motion. The parameters for the integration have been tuned to minimise computing time on the HP-1000 L processor and to maintain the excellent prediction capability of the laser geodynamics satellite LAGEOS, utilising input state vectors derived from ephemerides provided by the Center for Space Research of the University of Texas (Schutz, et al., 1981). The software produces topocentric satellite positions at a satellite dependent constant time spacing. This time spacing has been tuned to the real time 3rd degree interpolator in the prediction processor. The predictions are stored in a binary format in data files on a prediction diskette, and are thus readily available for the ranging task.
At the hardcopy unit of the HP 2623 A graphics terminal an alert list is produced, summarizing the rise- and set times of the satellite in the predicted period.

6. Task 3: Ranging

The ranging task (figure 6) employs several programs, some of them may be called optionally, e.g. to update ranging parameters, others are necessary during ranging and are designed to reduce delay times of data transmission. The real time ranging activities are executed by three programs, i.e. the range program, the alarm program and the disk program. The overall control of the ranging activities is performed by the range program, which schedules the alarm and disk programs to become memory resident before real time operation. The alarm program is scheduled on a time interval basis. It repeatedly polls the predictor and formatter processors for pending data messages, which it routes to the range program. The disk program is reactivated by the range program every time the observation buffer is filled with observational data to be recorded on diskette.

The range program initiates the observation activities selecting a set of predictions from diskette, prepared in the previous task. The predictions are sent to the predictor processor and are also recorded on the observation diskette for use in the data evaluation task. The calibration mode of ranging is selected when the predictor and formatter program indicate their readiness for pre-calibration. Because calibrations are taken using a prism mounted to the front end of the telescope, the direction of the telescope is moved to a predefined point to eliminate effects caused by the possibly inhomogeneous wave front of the laser beam. When sufficient calibration observations have been collected, satellite ranging mode is turned on and tracking is automatically started on the first satellite prediction epoch. During satellite ranging, the multiple-stop timer counts, four of every 0.1 second observation cycle are displayed on the system console to aid in optimizing the prediction corrections. Six different corrections are possible during tracking, i.e. time-, cross track-, azimuth-, elevation-, range gate delay- and window correction. A histogram of the simultaneous calibration provides a permanent indication of the stability of the system. After pass termination and post-calibration all observational data is available on the observation diskette for data evaluation.

7. Task 4: Data evaluation

Processing of observed data Reliable deployment of mobile satellite laser ranging equipment calls for the availability of a method of data evaluation on-site. This method must basically aim at:

a. the determination of the noise level of satellite data and the search for outliers,

b. the validation of system performance,

c. the updating of orbital parameters.

The software designed to meet these requirements for MTLRS (figure 7) initially produces range residuals, i.e. the differences between observed and predicted ranges. These residuals are displayed on the HP 2623 A graphics terminal, facilitating the visual recognition of the satellite ranges among noise data. Optionally a range window can be defined about the predicted ranges by selecting a time- and range bias and a window size. All residuals outside this window will be flagged for rejection. This simple technique of editing enables the elimination of a large portion of the noise data facilitating the subsequent analysis, especially at a high level of noise data. The accepted range residuals are then subjected to a curve fitting utilizing orthogonal polynomials followed by a procedure of iterative statistical testing (Aardoom, et al. 1982). The resulting residuals are displayed on the graphics terminal and the range data is flagged according to the result of the tests. This powerful method of datafiltering automatically discriminates satellite returns from noise data. Pre- and post calibration data obtained from the optional retro-reflective calibration mirror at the telescope as well as simultaneously obtained calibration data from the Le Croy counter can be analysed utilising the same filtering technique. All data editing only effects 2-bit flags available in each range record in the data file, thus no data will be lost or altered and the data-evaluation of each pass of data can be replayed any number of times.

Accepted residuals define an RMS value which is a measure for the precision of the obtained ranges. The accepted satellite ranges are also used to evaluate a time- and a range bias for the particular pass. These biases allow the updating of satellite predictions for future passes and thus enhance the data acquisition capability of the system, especially in the case of low satellites.

List data summary This task consists of a procedure for listing a summary of all data obtained at the current site, enabling the crew to appreciate the progress made to date.

Select quick-look data A third subtask selects quick-look data from previously evaluated passes. A selection is made out of all accepted satellite ranges. This data is corrected for system delay estimated from the processed pre- and post calibration data.

8. Concluding remarks

The aim to build a highly mobile and field operational satellite laser ranging system has been realized in the hardware and software of the MTLRS. The MTLRS has demonstrated its reliability and quality during the collocation experiment at the satellite observatory in Kootwijk in spring 1984. About 3000 single photo-electron observations taken with a single shot precision better than 6 cm RMS represent the normal results of a Lageos pass during clear sky conditions.

The choice to subdivide the observation task into three subtasks, each of them executed almost independently by a separate microcomputer has an important positive impact on the reliability of the MTLRS.
The two relatively small 8-bit Motorola M6809 microcomputers, hosting the EPROM resident real time prediction and formatting tasks, provide complete and efficient control of all time-critical observational activities.
Consequently the third microcomputer, i.e. an HP 1000 L 16-bit microsystem with the RTE-XL operating system, is relieved from the time critical aspects, being left with routinely data acquisition during and overall control of the observational activities. This multi processor set-up and consequent modular task design will facilitate easy future software upgrading.

A software system designed to determine the astronomical orientation of the telescope mount axes together with the astronomical latitude and longitude has been used successfully. The scrupulous approach to positioning the mount relative to local markers has proven its value. The technique deployed to merge site dependent parameters automatically with all data files produced, enhances the reliability of the data output of the MTLRS.

State vectors derived from the ephemerides for Lageos, provided by the Center for Space Research of the University of Texas and utilized in the advanced integration program of the MTLRS, enable field missions of several months without receiving prediction updates from the outside world. Time biases to be applied to the epoch of the state vectors and information to monitor system performance during a mission are derived from the data evaluation program.

References

Aardoom, L., B.H.W. van Gelder and E. Vermaat, 1982. "Aspects of the analysis and utilization of Satellite Laser Ranging Data at the Kootwijk Observatory". In: Forty years of thought... Anniversary volume in honour of Prof. Baarda's 65th birthday, Delft 1982, pp. 275-317.

Vermaat, E. and B.H.W. van Gelder, 1983. "On the eccentricity of MTRLS". Delft University of Technology. Reports of the Department of Geodesy, Mathematical and Physical Geodesy, No. 83.4.

Vermaat, E. 1984. "Establishing ground ties with MTLRS; performance and results". Preprint. Delft University of Technology. Reports of the Department of Geodesy, Mathematical and Physical Geodesy, No. 84.3.

Otten, K.H., 1984. Microprocessor controlled real time operation of the MTLRS". Delft University of Technology. Reports of the Department of Geodesy, Mathematical and Physical Geodesy, No. 84.5.

Schutz, B.E., B.D. Tapley, R.J. Eanes, B. Cuthbertson, 1982. Lageos ephemeris predictions. Proceedings of the IV International Workshop on Laser Ranging Instrumentation, 12-16 October 1981, University of Texas, Austin, Texas, USA. University of Bonn, 1982, pp. 145-171.

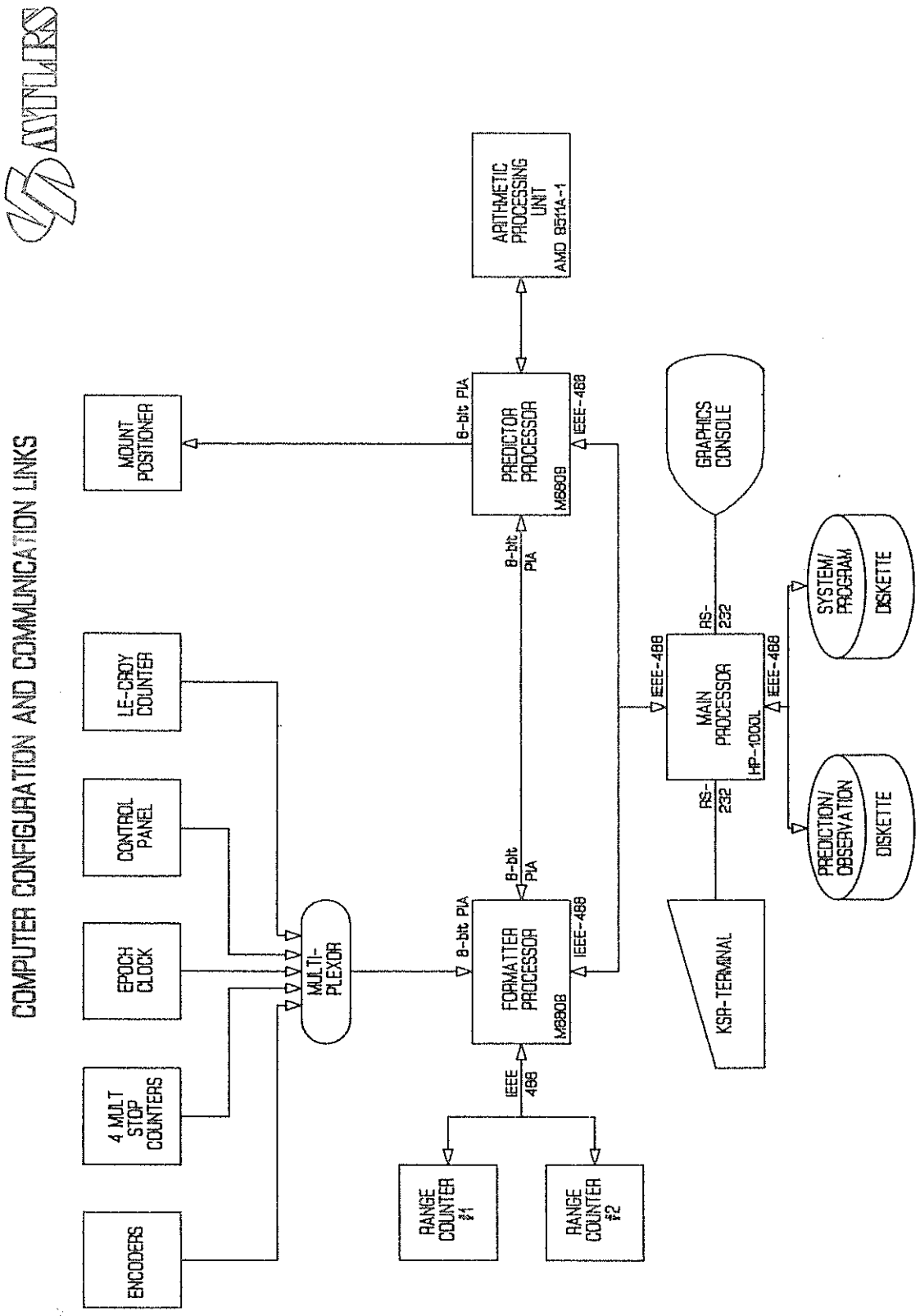

figure 1 Configuration diagram of the three MTLRS microprocessors including the communication links to the peripherals and the MTLRS hardware.

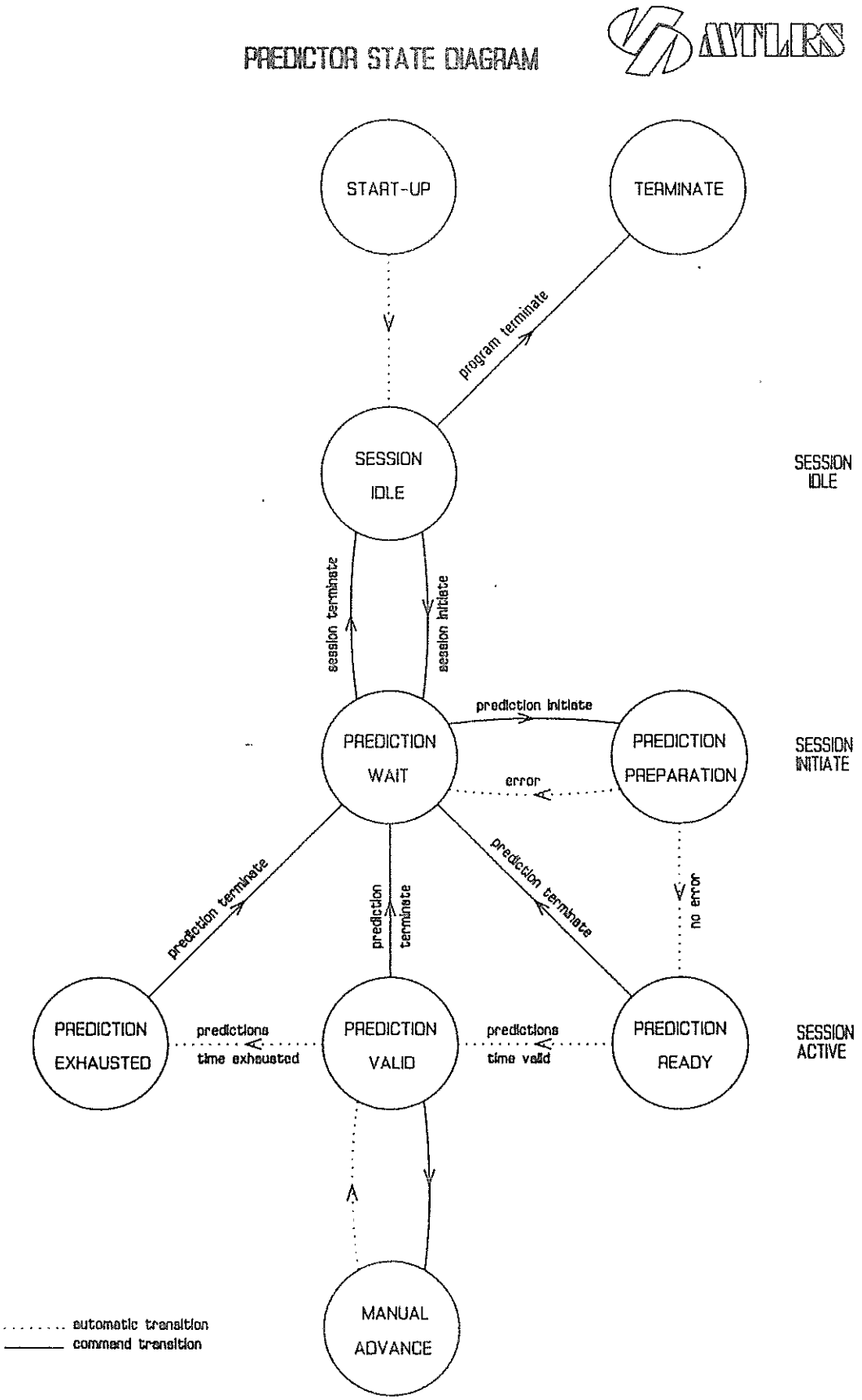

figure 2 State diagram of the real time predictor program including the commands and conditions causing the state transitions.

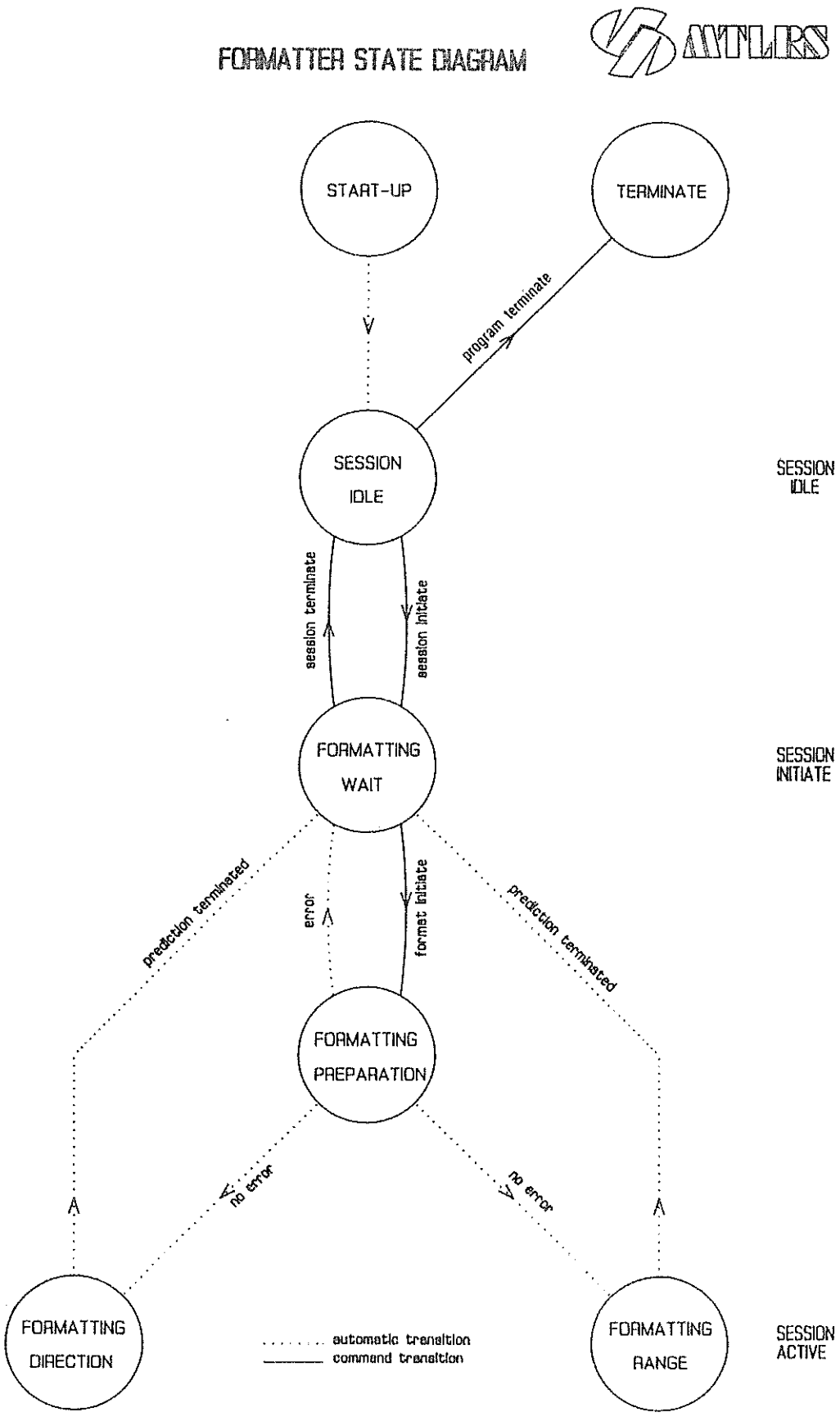

figure 3 State diagram of the real time formatter program including the commands and conditions causing the state transitions.

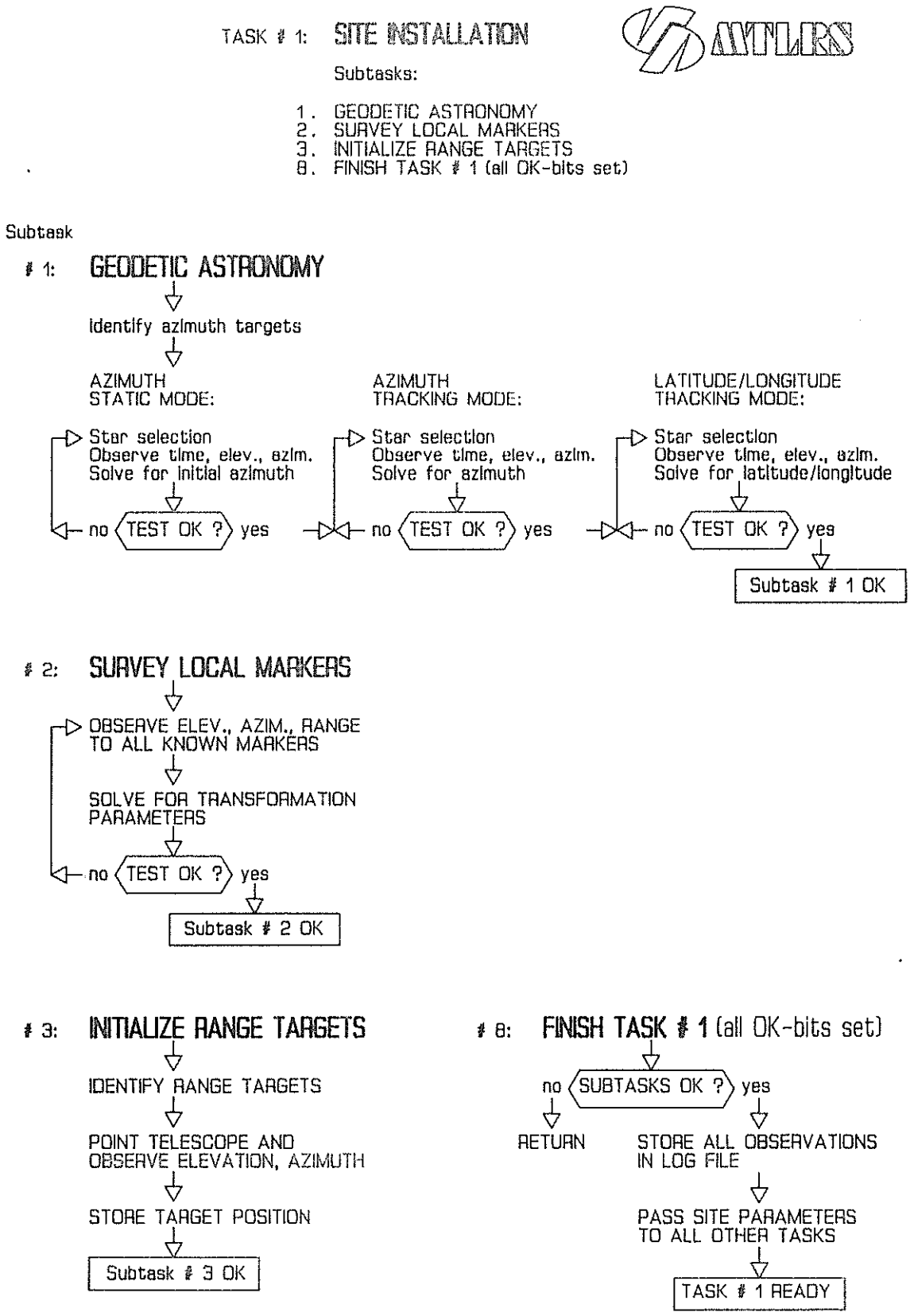

figure 4 Task-1: Diagram of the site installation activities and the procedure followed to determine the site parameters by using the MTLRS direction mode of observation.

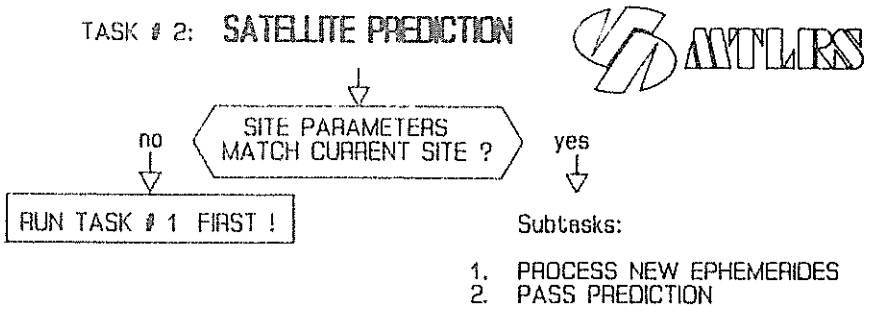

Subtask

1: PROCESS NEW EPHEMERIDES

CHECK AND RE-FORMAT
ASCII STATE VECTOR FILE
INTO BINARY EPHEMERIDES FILE

SUMMARIZE STATE VECTORS
PER SATELLITE

2: PASS PREDICTION

REQUEST: satellite
time bias
time period

INTEGRATE EACH PASS INDIVIDUALLY
integration stepsize 300 sec
integration order 5
gravity field 5 X 5

EVALUATE TIME, ELEVATION, AZIMUTH AND RANGE AT FIXED TIME SPACING
spacing 30 sec for LAGEOS
5 sec otherwise

STORE PREDICTIONS

figure 5 Task-2 Diagram of the satellite-pass prediction calculation using specific state vectors supplied for every single pass.

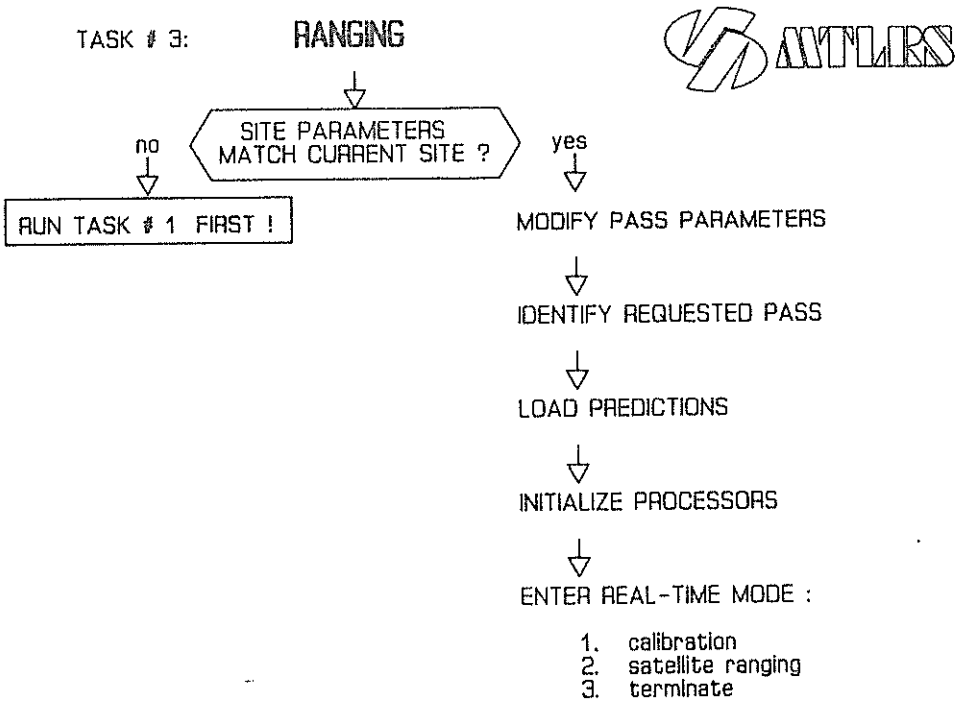

figure 6 Task-3: Diagram of the satellite ranging activities.

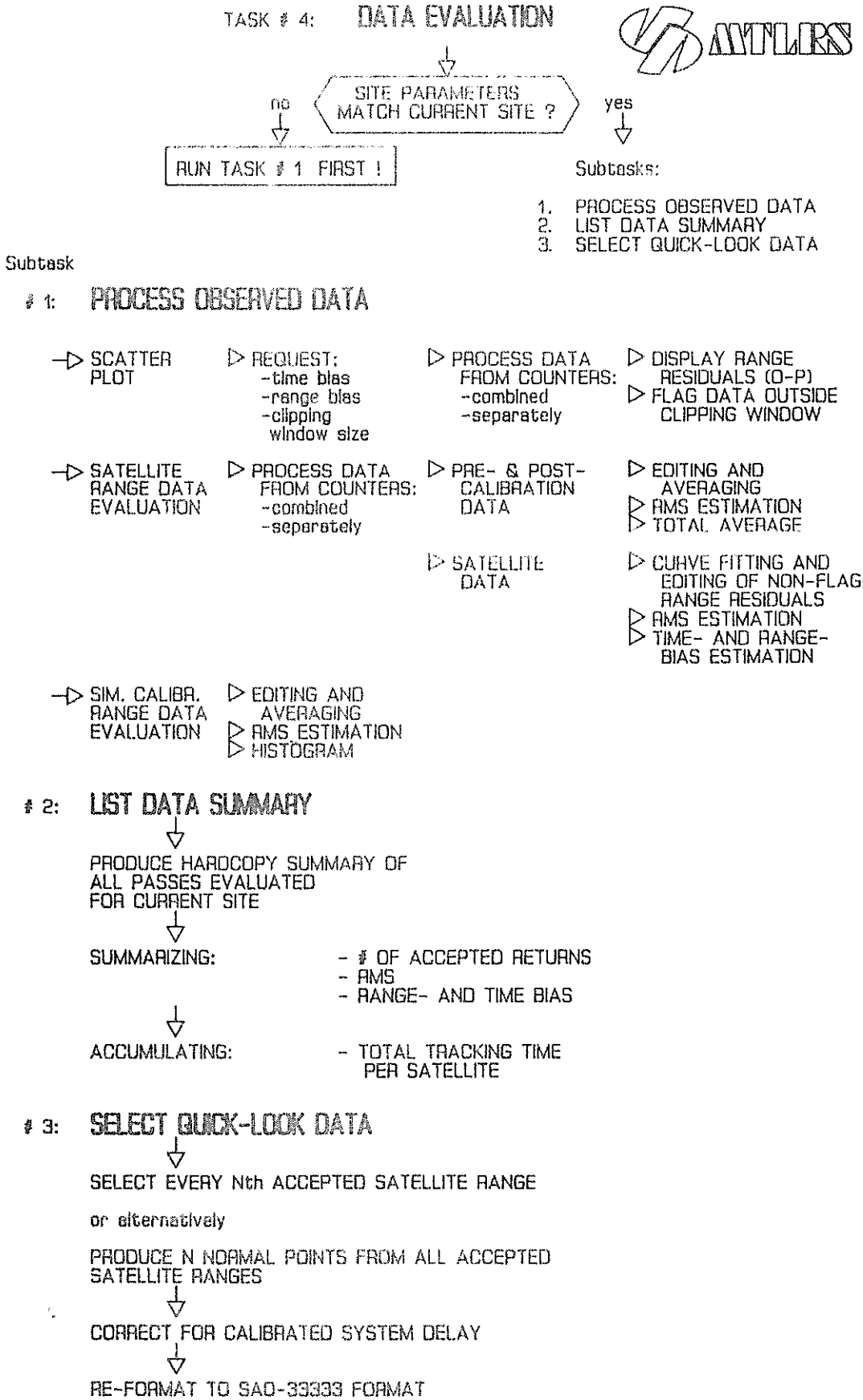

figure 7 Task-4: Diagram of the satellite-ranging and calibration data evaluation and the selection of quick-look data.

THE COMPUTER SYSTEM AT MLRS

R. L. Ricklefs
University of Texas
RLM 15.308
Austin, Texas 78712 USA

Telephone (512) 471 4462
TWX 910 874 1351

J.R. Wiant
McDonald Observatory
Fort Davis, Texas 79734 USA

Telephone (915) 426 3263
TWX 910 879 1351

ABSTRACT

The MLRS station computer firmware and software are described. Hardware that directly affects programming is highlighted.

COMPUTER SYSTEM

1 Introduction

The following document describes the computer system of the McDonald Laser Ranging System (MLRS) which was constructed by The University of Texas McDonald Observatory under NASA Contract NASW-3296. The station is located about 17 miles north of Fort Davis, Texas at longitude 255.9841, geodetic latitude 30.6770 N, and altitude 1963.41m. The system is a dual purpose installation designed for both artificial satellites and lunar targets. It takes advantage of many of the same design used in the 30 cm Transportable Laser Ranging System (TLRS) constructed earlier and the techniques developed in the 12 year old 2.7 meter lunar system about 800 meters away.

2 Functions Performed

Lunar and Satellite Position Determination: The computer must produce an ephemeris in both direction and range, suitable for tracking satellites and lunar sites in real time during each pass, Figure (◇a). These preprocessed initial conditions are produced either by integrating from a tape of Inter-Range Vectors (IRVs) (◇b) generated by an outside computer (for artificial satellites) or by internally computing an ephemeris based on either an MIT or JPL export lunar and planetary ephemeris (for the moon) (◇c). The preprocessed positions are produced at intervals which are commensurate with the apparent paths of the satellites and the moon to the required tracking precision.

Real Time Pointing and Tracking: In real time, the computer must perform 6th order interpolation of the pointing and ranging tables to generate rates for the 76 cm telescope, Figure(△a), and range predictions to open the receive gate (△b) and interpret the returning pulses (△c). Real time tracking utilizes position dependent functions to correct for telescope mount orientation errors (◇e). The hand paddle (△d) is used to input point angle offsets as well as time offsets, the latter modifying range as well as point angles. The system also responds to a number of interlocks and status word inputs. Tracking status, including point angles, are displayed on the Matrox monitor (△e), while error messages appear on the system console (△f).

Satellite pointing and tracking are accomplished by reading the absolute encoders (△g) through the CAMAC interface (△k). Lunar pointing is accomplished by visually pointing at known lunar features and then using differential offsets through the incremental encoder CAMAC interface (△h).

Stellar Object Tracking: The computer is able to slew the telescope to the position of known stellar objects and begin tracking at stellar rates. In this mode the system is sensitive to position changes, via the handpaddle (△d), and to focus commands only. An abridged version of the FK4 (◇d) supplies star positions, although positions may be entered manually by the operator (△f). Stellar observations are used to determine the telescope orientation error model (◇e).

Telescope Servo System: The beam director servo system (△l) is controlled by the NOVA 4X computer (△j) via a CAMAC interface unit (△h). Through the CAMAC unit the computer has continuous access to the positions of both the incremental encoder units (△l) and the absolute encoders (△g) and is able to select drive rates on each axis over the full rate capability of the system. As many as seventeen limit switches are available on both axis with which the computer may sense both the observing limits of the system as well as the mechanical stops in each axis. A manual handpaddle (△m) is provided to move the beam director independently of the computer CAMAC system.

Laser Firing Control: During laser firing it is necessary for the computer to rotate the transmit-receive switch (▵n) and the attenuator to the appropriate positions, calculate the laser firing times, and fire the laser (▵o) at the correct repetition rate. During firing, the computer accesses the corrected returns, calculates the residual error between the observed and predicted flight times, and displays the results on the screen (▵f) for operator interaction. Calibration data is automatically recorded and displayed (▵f) during the real time firing. All relevant data is saved (▵p) for later analysis.

Time of Flight: The time of flight system (TOF) is designed around a latchable timer (▵q), an EGG time digitizer (▵r) and a CMOS clock (▵D). The time digitizer (▵r) measures the interval between any event and the next pulse in a 5-megahertz pulse train with 100-picosecond accuracy. The latchable timer (▵q) records which pulse was used. The CMOS clock (▵D) contains the time of day from 1 second to 1000 days. The timer (▵q) and the time digitizer (▵r) are phased together with delay boxes to remove the one count uncertainty in the time of flight. The time latch on the timer (▵q) has five gateable inputs which are selectable from the computer. They are; four external TTL-compatible inputs (▵s, ▵s), and one internal, computer triggerable input. The timer (▵q) maintains the time standard from 200 nanoseconds to at least 53 seconds. It also has two computer-selectable outputs which occur upon the coincidence of the timer count train with a computer-loadable latch; one TTL laser firing output (▵t), and one variable width NIM compatible gate pulse (10 microseconds nominal width)(▵u).

Data Log Processing: The computer permits the entry of interactive log information (◇f), the editing of this information(◇n), the inclusion of internally regenerated sets of information, and allows for the storage on disk(▵p), or hard copy (▵B) and the subsequent review of the log information at a later time.

The Dynamic Process Monitoring: The dynamic processes in the system are monitored at all times (◇s). These processes include weather (◇g)(▵v), system interlocks, scaler data, clock frequency drift (◇h)(▵w), and the NASCOM line (◇i)(▵x).

System Operator Tutoring: The system is designed to tutor a non-sophisticated user such that he can access the proper commands, by answering a menu of questions at each phase (▵f).

Initialization Functions: Since nearly all of the ranging system dynamic processes are under computer control, a number of programs are needed to aid the operator to determine and input parameters required for laser ranging. These include the programs to develope the telescope orientation parameters from star observations (◇e), to input, check, and convert satellite and lunar ephemeris and stellar positions information (◇j,◇j), to set the hardware and software clocks, to enter new clock transfer information (◇k), site coordinates (◇l), and ground target positions.

Range Data Processing: Sometime after acquiring range data (◇m) and entering the pertinent log (◇f) information, the operator must generate files (◇v,◇w,◇x,◇y) containing this data for use elsewhere. The programs which the operator invokes (◇n) allow displaying (▵f) the old data, windowing it, and transferring it to disk (▵p), tape(▵y), etc., in the appropriate format for further use. In addition, a permanent archival copy is made of the raw data file itself.

NASCOM: The computer allows the easy preparation, editing and sending of all standard NASCOM messages including Status, TOR, and Quick Look (◇o). It also monitors the line (◇i)(▵z) for incoming messages and routes them to appropriate holding files on the disk (▵p).

Debugging: Several programs have been written to facilitate debugging the hardware and software unique to MLRS. These include programs to manually set parameters for the CAMAC modules, exercise the telescope drive, exercise the rotating mirror and attenuator, and to print binary data files in a useful format. These supplement a host of computer-vender supplied diagnostic programs.

3 Inputs to Computer

1. Telescope absolute axes encoders (◇p)(△g)--from CAMAC (△k)
2. Telescope incremental encoders(◇p)(△l)--from CAMAC (△h)
3. Handpaddle(◇q)(△d)--from CAMAC (△A)
4. User commands and response--from keyboard (△f)
5. Epoch--from CAMAC (△D,△q,△r)
6. Ephemeris data(◇b,◇c) for object (star, satellite,etc.)--from disc(△p), keyboard(△f)
7. Site constants--from keyboard (△f)
8. Telescope orientation parameters--from disc (△p)
9. Overrides, condition detectors and interlocks to the telescope--from CAMAC (△h,△A)
10. Weather (△v) information--from CAMAC (△E)
11. Previous return data(◇m)--from magnetic tape(△y) and disc(△p)
12. Status information from guiding (△d) and detecting packages (△q)--from CAMAC (△A)
13. Orbit time coefficients--from manageltic tape(△y)

4 Outputs from Computer

1. Track rates to telescope axes(△a)--through CAMAC (△h)
2. Pulses to each telescope axis(△a)--through CAMAC (△h)
3. Slew commands to the telescope(△a)--through CAMAC (△h)
4. Keyboard (△f) responses and prompts
5. Display of statistics (△f)--CRT graph
6. Return information--disc(△p), tape(△y), printer(△8)
7. Estimated fire times (△t)--through CAMAC (△q)
8. Transmit/receive control(△6)--through CAMAC (△A)
9. Dynamic information(◇r)--TV monitor (△e)

5 Mode of Use

The MLRS operating system is disc resident (△p) with a backup system on tape (△y). Startup is initiated through a vendor-supplied operating system (RDOS) . After system initialization, the monitor program (◇s) begins to execute in the Forground partition (◇t) and the Command Line Interpreter (CLI) begins to execute in the Background partition (◇u) and awaits operator commands (△f).

6 Environment

Hardware: The software system operates in a computer system configuration which can include any or all of the following:

1. One Nova 4X CPU with 128K 16 bit words of semi-conductor memory, power fail protect, a real-time clock, automatic program load, hardware arithmetic, and floating point options (▵j)
2. Two 10-megabyte disc subsystems, with removable 5-megabyte cartridges (▵p)
3. One 640X by 476Y point graphic/alphanumeric CRT terminal, 6.4" by 9" display area, with 75 to 9600 baud rate (9600 is used) (▵f)
4. One telephone modem, 300 baud rate, for NASCOM, RS232 (▵z)
5. A CAMAC interface (▵F) to the locally built hardware which includes a CRT monitor (▵e) for real time information displays
6. One 9-track, 800 BPI, 10-1/2" reel magnetic tape unit (▵y)
7. One line printer (▵B)

Operating System: The vendor-supplied operating system used is the Data General Real Time Disc Operating System (RDOS). This system provides software drivers for all vendor-supplied peripherals. It allows the user to compile, assemble and build the controlling software system on the single computer system. During real time operation, the system handles multiple priorities of user hardware interrupts on a task oriented basis. RDOS has been modified locally to handle the Matrox display (▵e)and TOF timers as system devices (▵q,▵r,▵D).

Note: On Figure ▵ , the symbol

Ψ

indicates that these devices were designed and built by McDonald Observatory. Other device were available commercially.

7 Main Software

The following programs are available for routine operator usage and can be called by name by the operator from the system standby state (CLI). Indented entries are programs swapped in by the previous program.

BCDEPH	-Converts ASCII JPL Lunar and Planetary Export Ephemeris tape into NOVA-Compatible binary file
CALTD8	-Determines TD811 time digitizer calibration constants.
CLEANUP	-RDOS command file which cleans up debri after system crash
CLKCOR	-Allows operator to access clock data
CPYRDF	-Copies range data file between disk and tape
CYB9	-Writes blocked tapes for use by other computers such as the C.D.C. Cyber
FIXEPH	-Applies current time to ephemeris file for testing
FIXLEPH	-FIXEPH for lunar ephemeris files
FMAILER	-Creates ASCII laser mailing tape, quick look, and lunar Z & P files from windowed ranging data
GLOGGER	-Logs satellite passes
GTE	-Generates test ephemeris for range tests
INTRDF	-Initializes a range data file for (re)use
INITSAT	-Integrates IRV to produce satellite ephemeris
KEYCAMAC	-CAMAC diagnostic program
LMTCHECK	-Produces report of ASCII Laser Mailing Tape contents
LMTOP	-Converts FMAILER binary LMT to ASCII mag tape file
LUNRANGE	-Lunar range data acquisition program
MFORMIRV	-Reformats & verifies checksums on raw IRVS (Goddard & UT Metric)
MOUNT	-Telescope mount orientation data acquisition & fitting
MNTGRA	-Graphics program used by MOUNT
LSQFIT	-Least-squares fitting program used by MOUNT
MONITOR	-Foreground program to monitor & update time, clock differences, encoder, & environmental information
MSATPATH	-Prints listing of satellite positions (X,Y) from ephemeris file
MTAR	-Records fixed target positions for later use
NBRCMP	-NASCOM message number comparison
NCEDIT	-NASCOM message editor
PRECLI	-Setup program executed at system start-up
PREDCNTRL	-Lunar ephemeris generation program
PREDICT	-Produces intermediate lunar ephemeris
TABFORM	-Converts intermediate lunar ephemeris to MLRS lunar format
PRNTEPH	-Prints satellite positions (X,Y,Range) from ephemeris file
READX	-Read IRV format tape
RET	-Request for NASCOM re-transmission
RSCLK	-Re-syncs software clock to CAMAC CMOS clock
SATRANGE	-Satellite range data acquisition
SENDQL	-Sends Quicklook Data message
SITE	-Allows entry of site coordinates and eccentricities into system
STAT	-Writes status report (to Joe Miller, BFEC) onto NASCOM
TDUMP	-Dumps binary JPL ephemeris to line printer
TBR	-Sends time bias report over NASCOM
TOR	-Sends tracking observation report over NASCOM
XSHORT	-Creates short version of binary JPL ephemeris for routine use

In addition, the following is a list of files and file naming conventions for MLRS.

I. Satellite Ranging

--------.BI	-Binary IRVs (output of FORMIRV, input to INITSAT)
--------.RC	-Eye-readable recap of contents of BI file, including IRV number,date,& time
--------.EP	-Ephemeris File (output of INITSAT, input to SATRANGE)
GEMION	-Geophysical and physical constants input to INITSAT
RDFn	-Range Data File (shared w/lunar)

II. Lunar Ranging

LSITES.PC	-Lunar observatory site coordinate file
LFEAT.PC	-Lunar surface feature file
LREFL.PC	-Lunar reflector file
LMODEL.PC	-Lunar model parameters file
LCONTOL.PC	-Lunar control parameters file
PROCTRL.PC	-Current lunar control parameter file
--------.IE	-Intermediate lunar ephemeris file
--------.EP	-Lunar ephemeris file (output from PREDCNTRL, input to LUNRANGE)
RDFn	-Range data file (shared w/ satellite)
DE111S	-Shortened binary JPL lunar and planetary ephemeris

III. Star Pointing

FK4PKD	-FK4 star catalog edited and packed as a binary file
STARS	-Eye-readable list of brightest stars and corresponding numbers

IV. NASCOM

RLOG	-Receive log; lists message number, file where placed, date/time received
NASCOM	-All other messages
TLOG	-Transmit log

V. Others

SVFILE	-Station variables files. Used by monitor and most user programs
FEATPKD	-Ground target position file
FILES	-List of file names and naming conventions (this list)

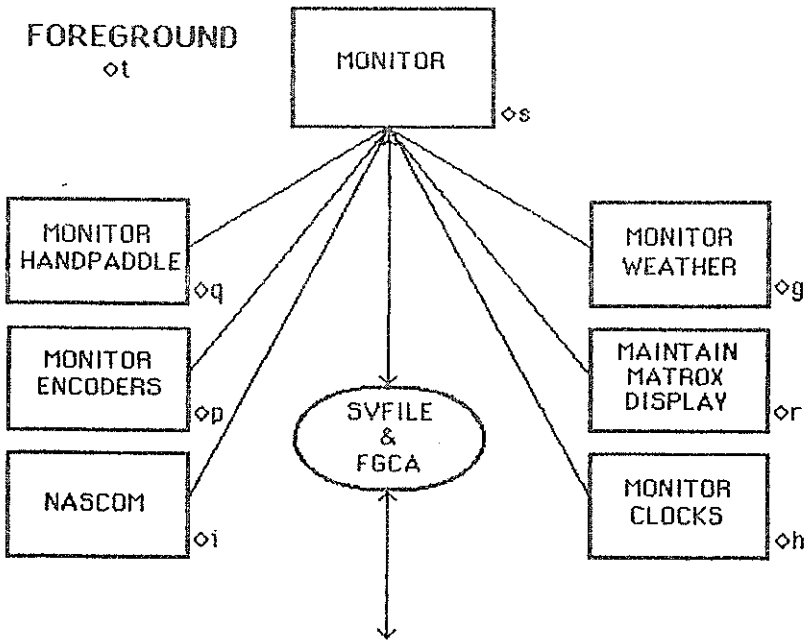

PROGRAM & FILE OVERVIEW

FIGURE ◇

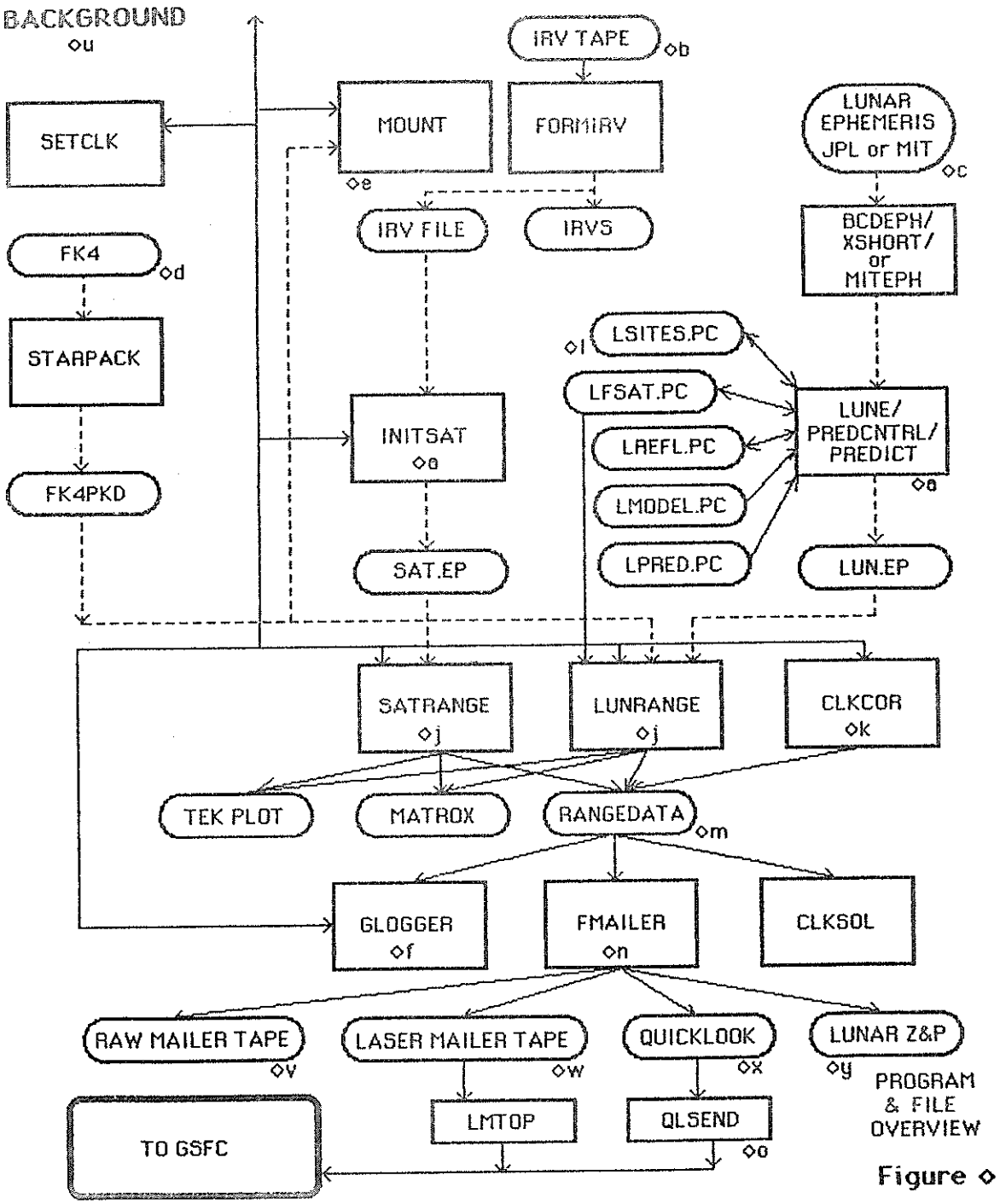
BACKGROUND
◇u
IRV TAPE
◇b
SETCLK
MOUNT
FORMIRV
◇e
LUNAR EPHEMERIS JPL or MIT
◇c
IRV FILE
IRVS
BCDEPH/ XSHORT/ or MITEPH
FK4
◇d
STARPACK
◇l
LSITES.PC
LFSAT.PC
INITSAT
◇a
LREFL.PC
LUNE/ PREDCNTRL/ PREDICT
◇a
LMODEL.PC
FK4PKD
SAT.EP
LPRED.PC
LUN.EP
SATRANGE
◇j
LUNRANGE
◇j
CLKCOR
◇k
TEK PLOT
MATROX
RANGEDATA
◇m
GLOGGER
◇f
FMAILER
◇n
CLKSOL
RAW MAILER TAPE
◇v
LASER MAILER TAPE
◇w
QUICKLOOK
◇x
LUNAR Z&P
◇y
PROGRAM & FILE OVERVIEW
TO GSFC
LMTOP
QLSEND
◇o

Figure ◇

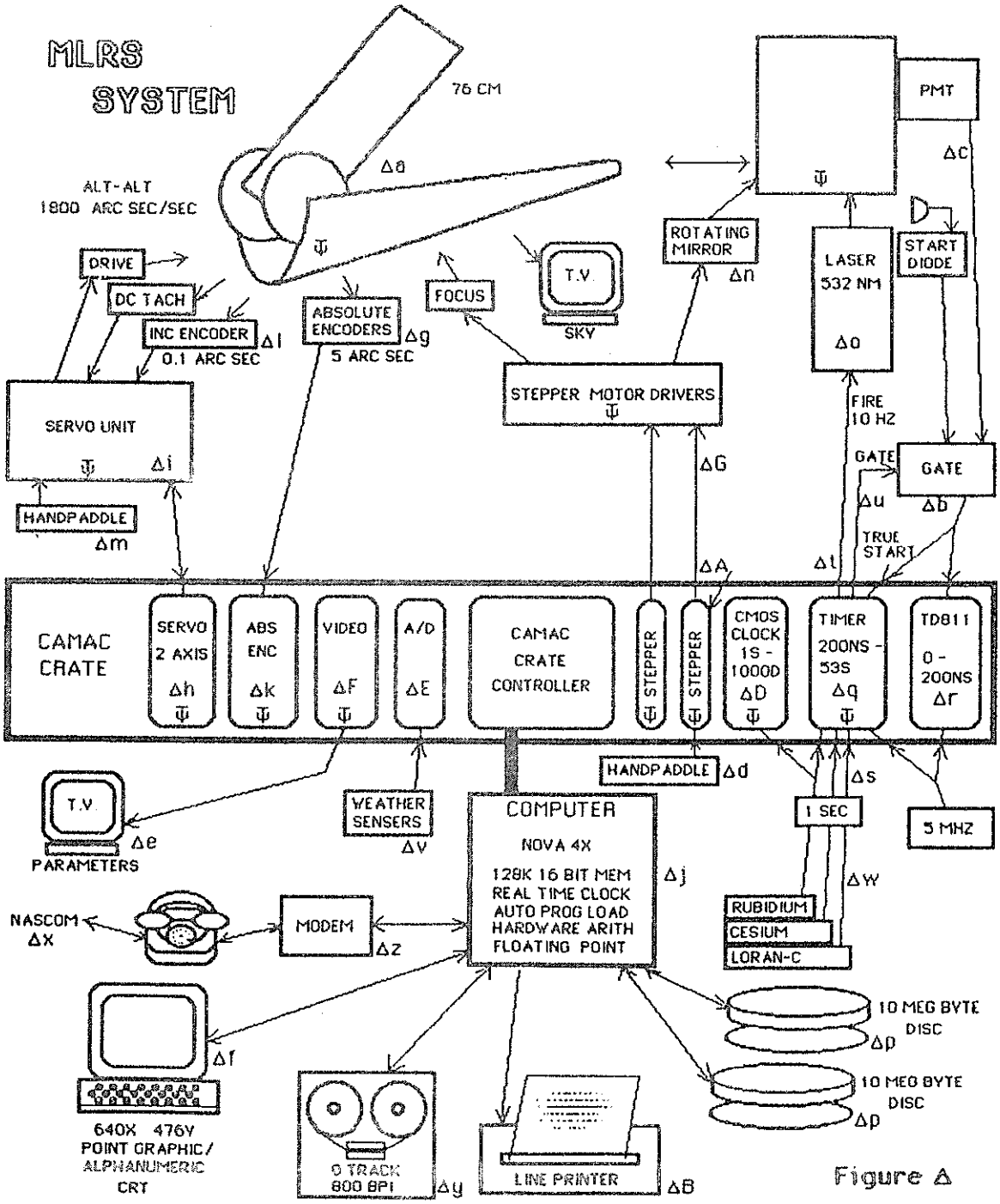
MLRS
SYSTEM
76 CM
Δa
ALT-ALT
1800 ARC SEC/SEC
Ψ
DRIVE
DC TACH
INC ENCODER
Δl
0.1 ARC SEC
ABSOLUTE
ENCODERS
Δg
5 ARC SEC
FOCUS
T.V.
SKY
ROTATING
MIRROR
Δn
Ψ
PMT
Δc
LASER
532 NM
Δo
START
DIODE
SERVO UNIT
Ψ Δi
HANDPADDLE
Δm
STEPPER MOTOR DRIVERS
Ψ
ΔG
FIRE
10 HZ
GATE
GATE
Δu
Δb
TRUE
START
Δt
ΔA
CAMAC
CRATE
SERVO
2 AXIS
Δh
Ψ
ABS
ENC
Δk
Ψ
VIDEO
ΔF
Ψ
A/D
ΔE
CAMAC
CRATE
CONTROLLER
Ψ STEPPER
Ψ STEPPER
CMOS
CLOCK
1S -
1000D
ΔD
Ψ
TIMER
200NS -
53S
Δq
Ψ
TD811
0 -
200NS
Δr
T.V.
Δe
PARAMETERS
WEATHER
SENSERS
Δv
COMPUTER
NOVA 4X
128K 16 BIT MEM
REAL TIME CLOCK
AUTO PROG LOAD
HARDWARE ARITH
FLOATING POINT
Δj
HANDPADDLE
Δd
Δs
1 SEC
5 MHZ
Δw
RUBIDIUM
CESIUM
LORAN-C
NASCOM
Δx
MODEM
Δz
10 MEG BYTE
DISC
Δp
10 MEG BYTE
DISC
Δp
Δf
640X 476Y
POINT GRAPHIC/
ALPHANUMERIC
CRT
9 TRACK
800 BPI
Δy
LINE PRINTER
ΔB

Figure Δ

A DESCRIPTION OF THE MT. HALEAKALA SATELLITE AND LUNAR LASER RANGING SOFTWARE

E. Kiernan, M.L. White
Institute for Astronomy
University of Hawaii
P.O. Box 209
Kula, HI 96790

Telephone (808) 244 9108
Telex 7238459

ABSTRACT

The Mt. Haleakala Satellite and Lunar Laser Ranging System utilizes a LSI-11/23 processor manufactured by the Digital Equipment Corporation. The satellite and lunar software programs are written in Fortran and Macro-11. The RSX-11M, version 3.2 operating system is used for both program development and real time execution. This operating system allows several programs to execute concurrently and to interact with each other in real time by means of global system flags ans shared regions of memory.

A DESCRIPTION OF THE MT. HALEAKALA SATELLITE AND LUNAR LASER RANGING SOFTWARE

1.0 INTRODUCTION

This paper describes SATCAL version 6.0, satellite laser ranging software, and the LURE version 7.0, lunar laser ranging software used at the University of Hawaii, Haleakala Observatory. The SATCAL and LURE systems consist of several programs which run on an LSI-11/23 processor manufactured by the Digital Equipment Corporation. The processor has 128K words of memory, the upper 2K being used for the video graphics display. The RSX-11M operating system, version 3.2, is used to execute the tasks and control inter-task communication and synchronization. The SATCAL and LURE software has been written in FORTRAN and MACRO-11 languages.

2.0 SATCAL

The SATCAL version 6.0, satellite ranging software consists of the following programs:

1. SATCAL is a small task which prompts the operator for the desired activity, performs initializations, and starts execution of the DESIGN task.

2. DESIGN is the main program for satellite and target board ranging. It starts up all of the other tasks, goes into a one-second real-time ranging loop, and exits when ranging is done.

3. INLIZE is started up by DESIGN, and initializes the variables needed for satellite and target board ranging.

4. RANGE runs only during the real-time ranging cycle. It contains a loop which runs N times a second, N being a number set by the operator. N can be any number from 1 to 10, but due to the structure of the laser, the only numbers which can be used are 1, 5, or 10. 5 is the number used at present for satellite ranging. RANGE fires the laser and arms the Event Timer for the return pulse.

5. UTIPR is the task which interfaces with the Hewlett Packard 5370A Universal Time Interval Counter (referred to henceforth as the UTI). It contains a loop which is activated whenever a return pulse is expected, up to N times per second. It reads the UTI and arms it for the next return.

6. INTEG runs during the real-time cycle. It contains a loop which is executed every 2 seconds. Every other loop (i.e. every 4 seconds) it integrates the IRV vector in order to get the current azimuth, elevation, and range for the satellite. It also performs the necessary corrections for refraction, mirror offsets, etc.

7. IOPRG runs during the real-time cycle and prompts the operator for commands such as: fire laser, record the data, etc.

8. SYSCOM is a common region which is shared by all of the tasks. It contains constants, inter-task semaphores (called "event flags" by RSX-11M), and variables shared by the tasks.

9. VIDCOM is a system common region which corresponds to the video graphics display memory. Once a second, DESIGN writes to this region, in order to update the display.

These tasks are described in detail in the following paragraphs.

SATCAL is a small task which is invoked directly by the operator by the command RUN SATCAL. It initializes the display on the operator's VT100 console. It also initializes the video graphics display. It reads the file CONFIL. DAT, which contains several SYSCOM constants, such as current temperature, humidity, telescope tiltmeter readings, etc. CONFIL. DAT is edited by the operator to update the appropriate values, before the start of each satellite run. SATCAL prompts the user for the activity desired (range to a satellite, range to the target board only, range to the corner cube, or exit program). SATCAL starts up (i.e., spawns) the DESIGN task, and then waits patiently for DESIGN to exit. It then goes back and prompts the user for the next activity.

DESIGN is the main task for satellite and target board ranging. It starts up the INLIZE task, which initializes SYSCOM

values and prompts the operator for several parameters. DESIGN waits for INLIZE to finish, and then proceeds to create and open the output data file. It asks the operator if target board ranging is desired. If so, it calls the subroutine CALIBR, which performs real-time target board ranging. (CALIBR is described in detail below).

After target board ranging is complete, if the operator has requested satellite ranging, DESIGN starts up INLIZE again, this time to compute the initial telescope positions and range for the satellite for a time a minute or two from now. After INLIZE is done, DESIGN points the telescope to this initial position, using the telescope's "position" mode. It then starts up the following tasks: RANGE, IOPRG, INTEG, and UTIPR. Then it goes into a loop, which is executed once a second. In this loop, during which all of the tasks are executing and performing the necessary activities for laser ranging, DESIGN does the following:

1. Wait for an event flag to be set by the RANGE task, and then clear it.

2. If the current time is less than the initial time, then go back to step 1 and wait again.

3. Point the Lunastat, in telescope "digital rate" mode. If using the Lurescope to receive ranges (this is rarely done), point it too.

4. Write the previous second's data to the data file.

5. Point the dome if necessary. (Is done every 10 degrees of azimuth).

6. Every 2 seconds, set a flag for the INTEG task to begin its loop.

7. Every 4 seconds, take the values just calculated by INTEG, and put them in the interpolation tables.

8. Interpolate the az, el, and range for 2 seconds from now.

9. Update the video graphics display.

10. Go back to the first step and wait.

This loop will continue indefinitely until the operator has indicated "exit" to the system via IOPRG.

At the termination of this loop, DESIGN asks the operator if target board post-calibration is desired, and if so, calls CALIBR again. Then, it closes the data file, stops the telescopes, sets several event flags to ensure that all of the other tasks have stopped, sets a flag to signal to SATCAL that it is done, and exits.

CALIBR is a subroutine called by DESIGN, to perform target board ranging. It also does corner cube ranging, which is exactly like target board ranging, except that the telescope is pointed to a slightly different position. CALIBR first initializes the appropriate local and common variables, points the telescope to the target board, and starts up the tasks RANGE, UTIPR, AND IOPRG. It then enters a one-second real-time ranging loop, which is very similar to the one in DESIGN.

INLIZE is executed before a satellite and/or target board ranging run. It calls routines which read in SYSCOM values from various files, and other routines which prompt the operator for ranging parameters. For satellites, it calculates the initial satellite position and range from the IRV vector. It corrects these values for refraction, the mount model, and mirror offsets. It also checks if the satellite is too near the sun, and calls sun avoidance routines if necessary. It sets up and initializes tables which will be later used by INTEG to interpolate the azimuth, elevation, and range.

RANGE runs only during the real-time ranging cycle. It connects to an interrupt card which provides interrupts at N times a second. N is set by the operator, and is usually set to 5, for satellite ranging. It executes a loop N times a second, during which the following things are done:

1. Wait for an event flag to be set by the interrupt card, and then clear it.

2. Fire the laser.

3. Read the time of laser fire (start diode time).

4. Compute the time at which to open the range gate. The range gate is opened just before the satellite return pulse is expected back, and closed just after.

When the range gate is open, the return pulse can be detected by the receive equipment.

5. Arm the Event Timer to open the range gate at the proper time.

6. Calculate the predicted range for the next cycle.

7. After the range gate has been opened, set an event flag to signal to the task UTIPR. UTIPR will read the UTI for the range value.

8. Go back to the first step and wait.

UTIPR is a task which interfaces to the UTI. When it is first started up, it connects to the UTI, initializes it, and arms it to receive the first satellite range. It then goes into a loop, which is executed every time a flag has been set by RANGE. RANGE sets this flag whenever it has gotten a laser start and is expecting a return pulse. Therefore UTIPR's loop is executed up to N times a second. During this loop, the following happens:

1. Wait for the flag to be set by RANGE, then clear it.

2. Check event flags which indicate whether or not a return range has been received. Continue checking until we time-out, in which case we haven't gotten a return pulse.

3. If a range has been received, read it from the buffer.

4. If a range has been received, read the Receive Energy Module (REM) and save this value in SYSCOM.

5. Clear out the buffer.

6. Re-arm the UTI to receive the next range.

IOPRG runs during the real-time cycle. It simply displays a prompt on the VT100 console, and waits for the operator to type in a command. The commands can be abbreviated. The following is a list of the available commands. The upper case letters indicate the minimum

possible abbreviation, and the lower case letters are optional. (In the actual program, the commands consist of all upper case letter).

1. Fire - Start to fire the laser.

2. NOFire - Stop the laser firing.

3. Record - Record the data on the data file.

4. NORecord - Stop recording.

5. WRITEall - Write to the data file, whether or not there have been any return ranges.

6. LScan - Change Lunastat scanning mode. Available modes are:

    1. PADdle - Read the paddles and calculate the cross-track and long-bias, based on the readings.

    2. SPiral - Change the cross-track and the long-bias automatically, in a spiral pattern.

    3. TIMscan - Use the paddle readings to calculate the cross-track and the time-bias.

    4. STop - Stop the spiral.

    5. CLear - Set the cross-track and long-bias offsets to zero.

7. MLtscan - Change the scanning mode for the Lurescope. The modes are the same as for the Lunastat.

8. EXit - Stop the real-time ranging cycle.

9. Carriage return - same as a "nofire".

10. RBias - Change the range bias.

11. TBias - Change the time bias.

INTEG runs only during the real-time ranging cycle. It contains a loop which is activated every two seconds. During this loop, it does the following:

1. Wait for an event flag to be set by DESIGN, then clear it.

2. If the operator is using the hand paddles to change vector time bias, then read the paddles and calculate the time bias.

3. Read the Analog-to-Digital Card for environmental information, such as temperature, etc. (However, at this writing, the A-to-D card is disabled).

Every other cycle, i.e., every 4 seconds, INTEG also does the following:

1. Integrate the IRV vector to 4 seconds in the future.

2. De-inertialize the vector.

3. Modify the vector cross-track and/or long-bias, either by reading the hand paddles or changing them in a spiral pattern. (The operator selects which mode to use for cross-track and long-bias scanning).

4. Calculate the azimuth, elevation, and range for 4 seconds from now.

5. Checks the azimuth and elevation of the sun. If the satellite position is within 15 degrees of the sun, then modify the satellite position to go around the sun, and stop firing the laser. It is necessary to avoid pointing the telescope directly at the sun, since it could be destructive to the receive equipment.

6. Correct the elevation and range for refraction.

7. Convert the azimuth and elevation from satellite angles to Lunastat mirror angles.

8. Correct the azimuth and elevation for the mount model.

9. Place the calculated values in the interpolation tables.

3.0 LURE

The LURE version 7.0, lunar ranging software consists of the following programs:

1. SYSCOM is a common region of shared memory.

2. MOON is a main control program for lunar ranging.

3. INITSK initialized values in syscom.

4. POINT fires the laser and points the telescope.

5. ETINT arms and reads the event timer.

6. IOPRG updates the video display and accepts user commands.

7. HISTO displays residuals on the histogram.

These tasks are described in detail in the following paragraphs.

SYSCOM is a common region of memory which is shared by all of the programs. It contains values which are used by all of the programs, such as constants. It provides a means for the programs to pass values to each other. VIDCOM is another shared region of memory, however, it is only used by the IOPRG program. It corresponds to a region of the memory which is connected to a MATROX video display card, therefore, writing to this region will update the display.

MOON is the main program which initiates the lunar ranging sequence. Its first task is to start up the program INITSK. MOON suspends its own execution until INITSK is done. After INITSK has completed and exited, MOON proceeds to open the output data file on

the disk. If target board pre-calibration ranging is requested by the operator, the calibration routine is called. MOON reads in the lunar ephemeris, which is calculated by another program prior to the lunar run. MOON uses the ephemeris to calculate an initial position and range for the moon for a time a couple of minutes in the future. It then points the two telescopes to this initial az and el, using "position drive" mode. MOON now starts up the program POINT, IOPRG, and HISTO. Then, MOON enters a software loop which is executed once a second. This loop will be referred to as the "real-time ranging cycle". So, once a second, MOON does the following:

1. Wait for a flag to be set by the POINT program. This flag is set once a second, to signal to MOON that it is time to do its loop.

2. See if any lunar data has been obtained. If so, write it to the data file.

3. If there was lunar data, also signal the HISTO program so it can be plotted.

4. Predict the lunar position (az, el) and range, for 2 seconds from now. This is done by interpolating the ephemeris values.

5. Correct the az, el, and range for the following: refraction, Lunastat mirror angles, and mount model.

6. Go back to the first step and wait.

This loop will continue indefinitely, until the operator indicates that the lunar run is over. When the loop is terminated in this manner, the POINT, IOPRG, and HISTO programs all exit. MOON now will perform a post-cal on the target board if the operator so requests, and then closes all of the input and output files and exits.

INITSK, as mentioned above, is started up by MOON. Its only function is to initialize the values in SYSCOM. It obtains these values from user input and several disk files.

POINT is a program which runs only during the real-time ranging loop. It starts up the ETINT program, then enters a loop which is executed 5 times a second. This loop does the following things:

1. Wait for an interrupt to come in from the interrupt card. The card is connected to the Cesium clock, and can be programmed to give an interrupt at 1 to 10 times a second.

2. If the range gate is open, wait until it is closed. This is done to avoid any possible conflicts between the laser fire and the lunar return coming back, since the same event timer is used for both events. The range gate is usually open for 1 microsecond.

3. If the "laser fire" flag has been set to "Yes" by the operator, fire the laser and read the start time.

4. If there is a return coming in during this cycle, send a signal to the ETINT program.

5. Once every 5 cycles, (or once a second) point the telescopes. The current position of the telescope is compared against the position at which it should be in one second, and the corresponding rate command is sent to the telescope.

6. Once every second, set event flags to start up the MOON and IOPRG programs.

7. Calculate whether or not a return is coming in during the next cycle.

8. Go back to the first step and wait.

ETINT is a small program which runs only during the real-time cycle. It is active only when a return range is expected during the 200 millisecond cycle. Therefore, it usually runs 5 times a second. It waits for a flag from POINT. When the flag is set, it arms the Event Timer for the expected range. After the range has been received, it processes the Event Timer readings and places the results in a buffer. It then goes back and waits for another flag from POINT.

IOPRG only runs during the real-time cycle. It is activated once a second by the POINT program. It updates the video display, which

contains current values for az, el, range, time, number of data obtained thus far, and other values useful to the operator. IOPRG also interacts with the operator at the console, accepting the various commands such as fire the laser, stop firing, exit from the lunar run, etc.

HISTO is activated only when the MOON program has determined that some lunar data has been received. Therefore, HISTO runs once a second or less. It takes the residual values (Observed range minus Calculated range) and plots them on the histogram display. This provides real-time feedback to the operator, since many returns in the same bin of the histogram would indicate possible lunar ranges.

4.0 DISCUSSION

The LSI-11/23 with 128 kilowords of memory using the RSX-11M operating system has proven adequate for satellite and lunar laser ranging at 5 p.p.s. However, due to the somewhat elaborate executive overhead of the RSX-11M operating system, program execution timing conflicts can arise on lower orbit satellites such as Starlette and BE-C.

REFERENCES

Documentation Kit RSX-11M Version 3.2, Digital Equipment Corporation, Maynard, Massachusetts, 1979.

Microcomputer Interface Handbook, Digital Equipment Corporation, Maynard, Massachusetts, 1980.

Microcomputer Processor Handbook, Digital Equipment Corporation, Maynard, Massachusetts, 1979.

AN OVERVIEW OF THE NLRS RANGING SOFTWARE

R.J. Bryant*, J.P. Guilfoyle**
Division Of National Mapping
Department of Ressources and Energy
Canberra, Australia

Telephone *62 52 52 77 ** 62 35 72 85
Telex 62230

ABSTRACT

The Division of National Mapping in co-operation with NASA have undertaken an upgrade of the National Mapping ranging facility to enable Satellite Laser Ranging as well as a Lunar Ranging to be performed at the site. Because the new system was to be so dramatically different from what existed, this upgrade provided a unique opportunity to design from basics a complete integrated system to fulfil this dual role. This paper provides a brief outline of the ranging system hardware used and an overview of the software system to control it. It should not be taken as a recipe for instant success or necessarily the best way but as an outline of the approach taken by National Mapping to achieve the goal of routine high accuracy ranging.

AN OVERVIEW OF THE NLRS RANGING SOFTWARE

Introduction

The Division of National Mapping in co-operation with NASA have undertaken an upgrade of the National Mapping ranging facility to enable Satellite Laser Ranging as well as a Lunar Ranging to be performed at the site.

Because the new system was to be so dramatically different from what existed, this upgrade provided a unique opportunity to design from basics a complete integrated system to fulfil this dual role.

This paper provides a brief outline of the ranging system hardware used and an overview of the software system to control it. It should not be taken as a recipe for instant success or necessarily the best way but as an outline of the approach taken by National Mapping to achieve the goal of routine high accuracy ranging.

Ranging System Hardware

Telescope and Telescope Control:

The telescope is a 60 inch clear aperture Cassegrain telescope mounted in an X-Y configuration. The telescope control electronics consists of a Contraves-Goerz MPACS system with an absolute encoding system providing a resolution of 0.36 arc seconds. The telescope's position can be read under computer control and it can be driven in both position and rate modes.

The MPACS system is interfaced to the computer system through a locally designed and built interface (MPACS Interface).

Automated dome control is implemented by means of this interface together with a guiding handpaddle which provides a manual offset of the computed telescope position. Four push buttons provide long and cross track corrections for satellite ranging. These same push buttons provide X and Y corrections when used for Flexure Mapping of the telescope. Incorporated in the Handpaddle is an 'on target' switch which is also used for Flexure Mapping.

Laser Ranging Controller:

The NLRS uses epoch determination rather than time interval measurements for establishing the time-of-flight. Coarse epoch consisting of days, hours, minutes, seconds and decimal seconds to the 100 nanosecond level is obtained from a locally designed and built Laser Ranging Controller. Fine resolution epochs to ten picoseconds are obtained by merging the coarse epoch with readings taken from 2 Lecroy 4202 Time to Digital converters which are controlled by the same pulses as the Laser Ranging Controller's clock. The Lecroy modules are housed in a standard Camac crate.

The LRC provides a) the Range Gate function for the system; b) in conjunction with a Hewlett Packard 5359A Time Synthesiser two software selectable off-line system calibration modes; c) a T/R system monitor; d) a Station Clock which can be used under computer control to determine epochs of selected events other than ranging operations together with Laser Control, Diode/PMT gating logic and the necessary computer hardware interface.

CAMAC Crate:

A standard CAMAC crate is used to house the following modules:

a) Kinetic Systems crate controller

b) Locally developed computer Interface

c) Dataway display module for diagnostic purposes

d) Discriminator and Logic modules for Timing System

e) Lecroy 4202 TDC modules

f) T/R stepping motor controller

g) A/D Converter module for Meteorological system.

Transmit/Receive System:

A T/R system of the same design employed by the McDonald Observatory MLRS is used in the NLRS. A spinning disc mirror with 2 diametrically opposed holes is used to switch the optical path between laser transmission from the telescope and returning signal into the PMT. A spinning 'dog-bone' is used as a protective shield for the PMT. The mirror disc and the 'dog-bone' have to be synchronised and rotated at the same speed for system operation.

Locally developed hardware is used to detect that the T/R system is in position for the Laser to fire. This is used in conjunction with a master Laser Enable signal generated by the computer through the LRC to fire the laser.

The T/R system is controlled by the computer via a module in the CAMAC crate.

Computer Hardware:

There are two Hewlett Packard A-Series computers on site.

The Ranging is currently run on the A-700 system which is configured with 1Mb of memory, hardware floating point, 65Mb Winchester disc drive, 400 lpm printer, 1600 BPI magnetic tape drive, graphics VDU, system console VDU.

The second system comprises an A-900 system with 1.5Mb memory, hardware floating point, 132Mb Winchester disc, 1600 BPI magnetic tape drive, 200 LPM printer, 2 graphics VDU's and a system console VDU.

All non-standard peripherals on both systems are interfaced using Hewlett Packard 16 bit parallel interface cards. Although Hewlett Packard supply a software driver for this card our approach has been to develop our own. This has allowed us to customise the drivers and provide a means whereby the complexity of the hardware control and interrupt routines are removed from the actual ranging and utility programs.

Both computer systems run the standard Hewlett Packard RTE-A Real Time operating system which is unmodified in any way. The relevant software drivers for the locally developed hardware interfaces are 'generated' into the system and these devices are accessed from then on as any other standard peripheral using high level language calls.

All locally developed drivers are written in Assembler language (H.P. MACRO). The Ranging software and all other utility software is written in FORTRAN 77.

Ranging System Software

Satellite Prediction System:

The NLRS prediction software is based on that used at McDonald Observatory. Ephemeris data arrives at the site on magnetic tape in the form of daily IRV's for about a 6 month period. They are read from tape and stored in a variable record length disc file.

As required program FORMIRV is run against this disc file to create a random access binary file or IRV's to cover the desired period. FORMIRV performs checksum verification and the necessary reformatting. It is capable of accepting IRV data from either Goddard or U. of T. Experience at the McDonald site leads us to believe that the U. of T. IRV's have a better long term stability.

Periodically the SATPREDICT program is run to produce an ALERT file for a period as well as a PREDICTION file for each satellite pass where the satellite will rise above a 20 degree horizon. Data in the prediction file consists of a file header containing the relevant IRV from which it was generated, daily time bump information as supplied by the network (U. of T.) and for every 1 minute point in the pass a satellite position in Azimuth, Elevation and Range.

Operator inputs to program SATPREDICT are:

a) File name of checked daily IRV's

b) Starting date and number of days predicts required

c) Whether program can expect a new IRV for each day's processing or has to extrapolate from only one IRV

d) Whether PREDICT files are required

e) Whether an ALERT file is required.

Where there is a missing IRV the program can extrapolate across the gap.

Ranging Software:

The Ranging system comprises 3 separate programs, INITIAL, RANGE and CLEANUP.

Program INITIAL performs the following sequence of operations:

a) Initialise the inter-program communication memory area.

b) Access the ALERT's file to determine which pass is the relevant one, obtain the name of the PREDICT file and create and initialise the observation data file.

c) Read in from a disc file the current flexure parameters for the telescope.

d) Obtain the current weather parameters from the meteorological system.

e) Loop through the PREDICTION file data applying refraction corrections to predicted elevation and range; azimuth corrections for dome positioning; corrections for X-Y axes offset and optical path lengths to system fundamental point; corrections for telescope flexure.

f) Store in the inter-program communication area the corrected prediction data together with all other default parameters such as range gate window width, firing repetition rate, real time display parameters etc.

E M P T Y P A G E

Program RANGE is the actual data acquisition program. It is basically a supervisory program which directs the various hardware systems to perform the requested actions in a sequential fashion. This sequence is as follows:

a) Initialise all hardware modules, position dome for start of pass.

b) Synchronise T/R stepping motors.

c) Initialise real time display.

d) Verify all variable parameters with user.

e) Ramp up the T/R system to require repetition rate.

f) Determine theoretical telescope and dome positions. Output them to MPACS. Wait 100msec then read in telescope position from MPACS. Evaluate new theoretical position and calculate error vector. If error vector is less than 0.02 degrees then proceed otherwise repeat this step.

g) Issue the Master Laser Enable signal to the LRC.

h) Read in from the LRC and CAMAC timing modules the epoch of the laser diode pulse and PMT calibration pulse.

i) Evaluate predictions for theoretical range.

j) Output Range Gate Epoch to LRC.

k) Read in from MPACS the current telescope position, time and handpaddle data.

l) Determine theoretical position, drive rates and dome azimuth.

m) Calculate actual drive rate for ensuing period by adding in to base rate corrections for handpaddle.

n) Output pointing information to MPACS.

o) Read in current weather details from CAMAC module.

p) Read in from the LRC and CAMAC timing modules the epoch/s of returning photons.

q) Calculate and display Residuals on real time display.

r) Journal data to disc file.

Steps (h) through (r) are repeated for the duration of the pass. The system can be halted at any time to enable the user to vary such things as firing rate, range gate window width, range gate offset, real time display parameters and also to display a histogram of the current real time calibration data. Once this is done control goes back to step (h) and ranging is resumed.

The one minute IRV's held in the inter-program communication area are interpolated using Bessel's Central-Difference Formula of degree 5 to provide theoretical range at step (i) and telescope position and dome azimuth at steps (f) and (l).

Steps (h) and (p) are the only occasions when the software system has to wait for a hardware interrupt from an external device.

Program CLEANUP is true to its name. Essentially it filters the ranging data and reformats it to make up the QUICKLOOK, MAILING and ARCHIVING files. It operates in the following manner:

Low noise passes

Three iterations of a two step stripping process are employed on each 1 minute block of returns. The two steps are:

a) Residuals are histogrammed (at a bin width of 10 nanoseconds on the first iteration an 1/2 sigma on subsequent iterations). The highest bin is determined. Data in bins of height less than a nominated fraction (typically 25%) of this maximum are rejected.

b) A straight line is fitted through the remaining residuals. Results more than 3 standard errors away are rejected.

In practice this procedure converges satisfactorily and the final histogram has a reasonably normal distribution out to 3 sigma. The standard error is often 0.3 nanoseconds and 67 - 80% of all data points are accepted.

High Noise Passes

A preliminary estimate of the starting point and slope of the real trace in the first minute of the data has to be obtained from the real time ranging display. All data points more than 32 nanoseconds away from this line are then stripped out. The low noise procedure outlined above is then performed. The resulting straight line is then used as the reference for the next 1 minute of data.

Future Development

The system described is the satellite ranging software system. For Lunar ranging the same concepts - indeed almost the same programs - are being used. The inter-program communication area will be expanded to hold data for the several lunar targets, some of the internal loops of program RANGE will need to be modified to allow for multiple photons in flight and the

user will be given the ability to switch from one target to the other without having to reinitialise the system. The hardware will require no modification nor will the software drivers that interface them to the computer. It is intended to include into the system one or two video monitors for the real time display instead of using the graphics VDU. This will enable the display of both residuals and calibration simultaneously.

Conclusions

The Hewlett Packard computer system used has proven adequate. Once an integrated hardware/software design for the system was reached both streams were able to proceed in parallel. The ability to 'hide' the complex hardware control within the operating system makes the high level code easy to write and maintain. If software drivers need to be changed then a new system has to be generated but since this takes on average half an hour it is not seen as a problem. It facilitates the testing of individual parts of the system using various locally written high level utility routines which proved extremely helpful in the debugging phase of the project.

One of the main design aims in the software has been to make the system user friendly to the extent that specialists are not required for the routine operation of the site. For satellite ranging this goal has been achieved and National Mapping's Laser Ranging System is now in full production.

NLRS Data Flow

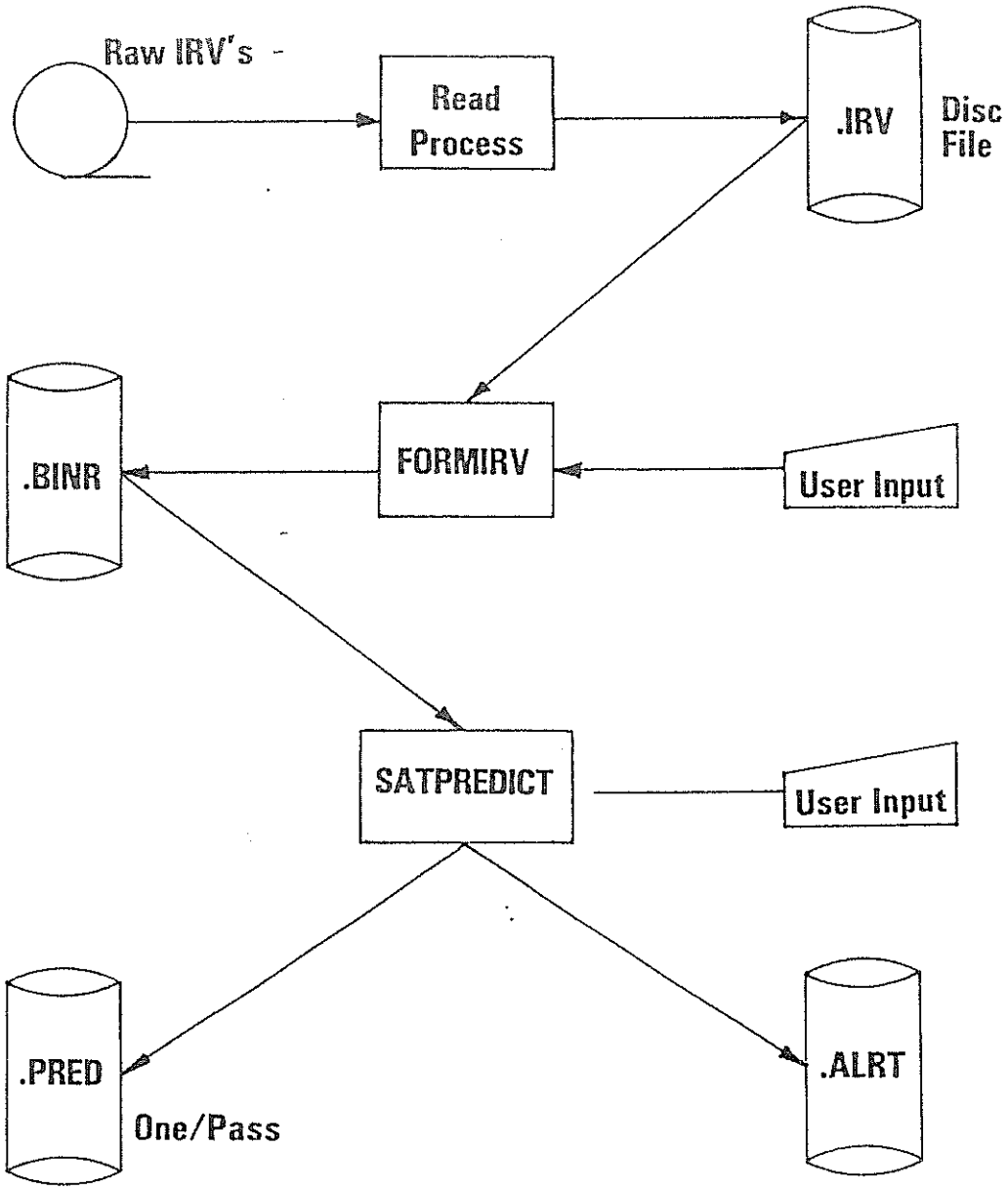

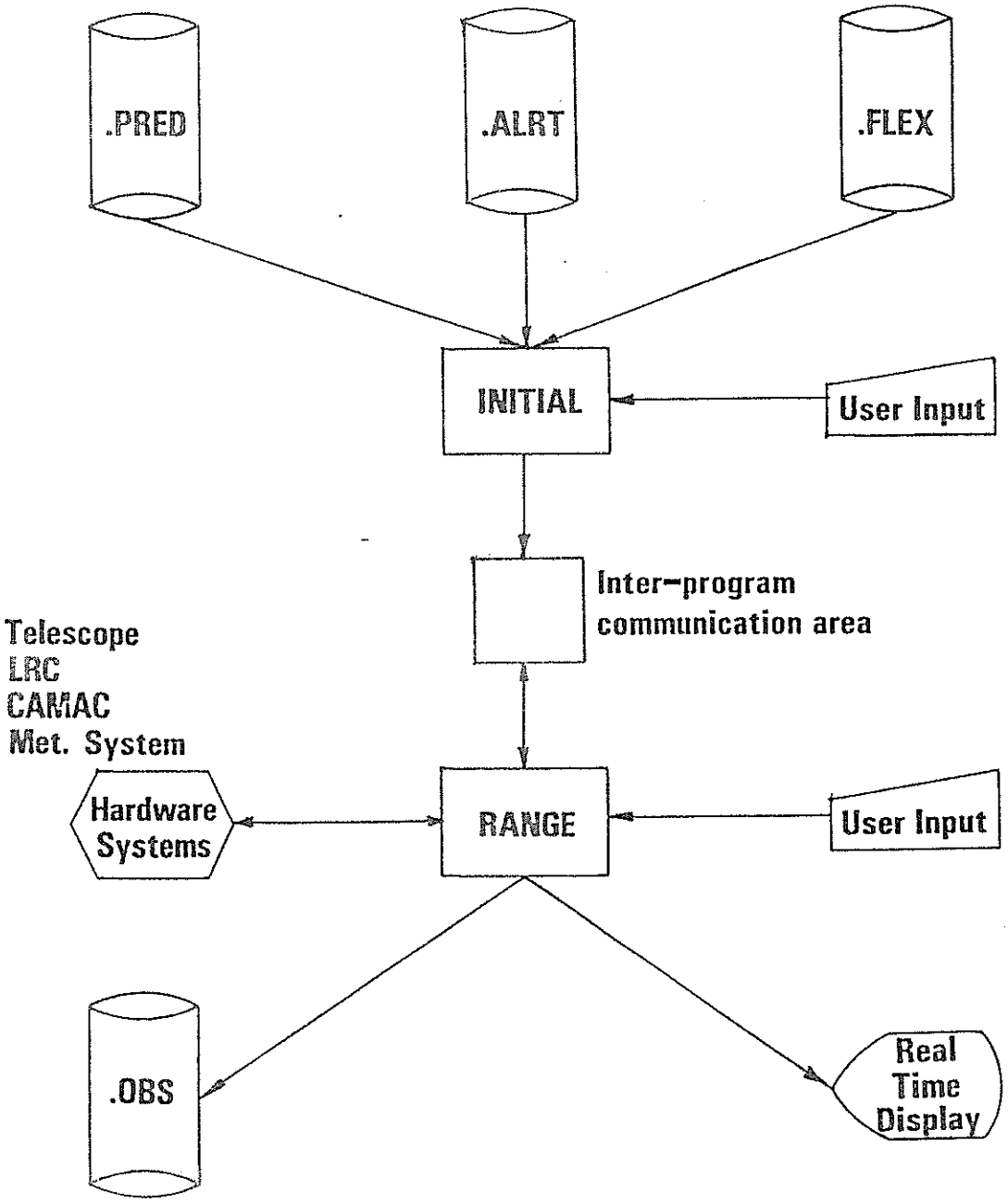
.PRED
.ALRT
.FLEX
INITIAL
User Input
Inter-program communication area
Telescope
LRC
CAMAC
Met. System
Hardware Systems
RANGE
User Input
.OBS
Real Time Display

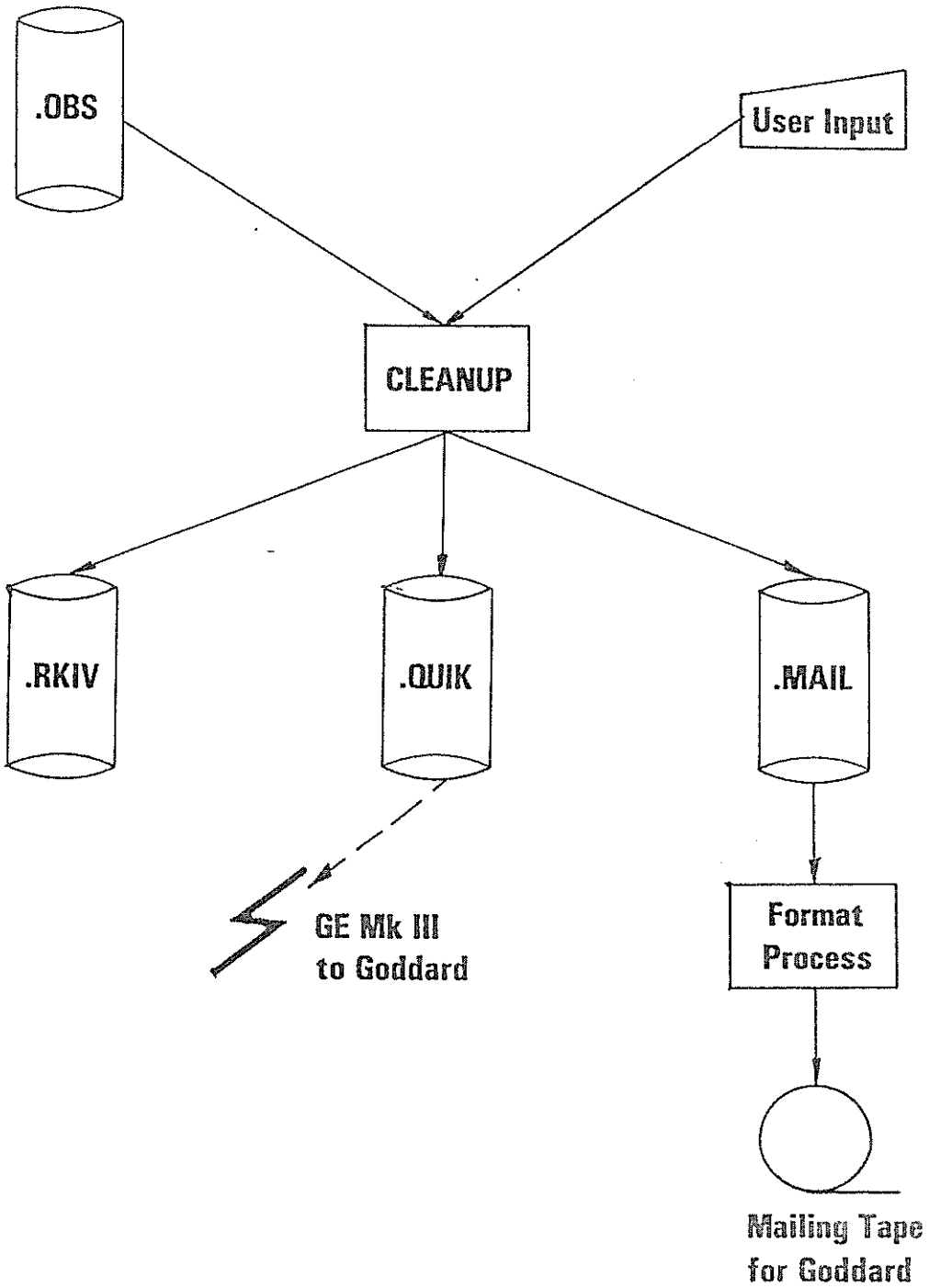
.OBS
User Input
CLEANUP
.RKIV
.QUIK
.MAIL
GE Mk III
to Goddard
Format
Process
Mailing Tape
for Goddard

UPGRADING THE COMPUTER CONTROL OF THE INTERKOSMOS LASER RANGING STATION IN HELWAN

A. Novotny, I. Prochazka
INTERKOSMOS
Faculty of Nuclear and Physical Engineering
Czech Technical University
Brehova 7, 115 19 Prague 1 Czechoslovakia

Telephone (2) 84 8840
Telex 121254

ABSTRACT

To fulfill the requirements on the laser ranging systems, the soft/hadware package of the Helwan station was significantly modified in period 1982-84. The max. ranging reprate was increased up to 5 pps. The mount pointing accuracy was increased implementing the mechanical inaccuracies software model. The automatical comparison of the time base to the Loran C signal was put into operation.

UPGRADING THE COMPUTER CONTROL OF THE INTERKOSMOS LASER RANGING STATION IN HELWAN

Software package for the Satellite Laser Ranging Station in Helwan, Egypt was presented at the 4th Workshop, Austin 1981 /1/. This software was used untill June 1983. The significiant modification and expansion were carried out in the period 1983-84.

SATELLITE POSITION PREDICTION

It is based on SAO prediction routines. The new perturbation calculation scheme (GRIPE) was inplemented /2/. The prediction program memory requirements were reduced (<32Kbytes), the special operating system for prediction is not required more.

To make the prediciton algorithm more effective, two step interpolation of predicted position is used. In the prepass phase, the satellite position (x,y,z) is computed - 10 points per pass only. The satellite position is then interpolated onto 150 points, the satellite topocentric coordinates are computed, the mount mechanical inaccuracies are software compensated (program PPP). In the on-line phase, the quadratic interpolation is used.

CONTROL SOFTWARE PACKAGE

The control software package was significantly modified mainly because of the ruby laser transmitter replacement by Mode Locked Train YAG Laser /3/. The software had to take into account that:

- higher repetition rate of laser firing is required,
- 30 arcsec positioning accuracy must be achieved,
- only the single photo-electron echoes are acceptable.

CALIBRATION

The main features of calibration program include:

Programmable reprate up to 10 Hz, parallel reading and raw data processing from two ranging counters (HP5360A, HP5370B), independent time ranging gates for both counters in two ranges (fixed target ~500m, internal pass ~2m), statistical check of the single photo-electron level determined on-line by the ratio : transmitted laser pulses to detected pulses. The ratio must be higher than 5:1.

The calibration results confirm that present accuracy of the Helwan system is determined mainly by single photo-electron PMT jitter

/4/. The ranging counter HP5370B is used for calibration only.

SATELLITE TRACKING

There are two programs simultaneously loaded into memory, which share the system common block for data handling. Using a different priorities and Resource Number flag, the synchronism of the programmes execution is guaranteed.

The segmented background programme STY keeps the structure of the older SATEL. The tracking segment of this programme uses a 4 second loop. During one loop:

- results are avaluated and stored into disc file
- range residuals are displayed on the operator CRT console and transmitted into HP85 for on-line graphics display,
- computation of 4 mount settings and gate positions are carried out,
- on the console is displayed : time, mount setting, no. of stops within the gate for the last 10 shots, range residuals.

The small foreground program has a higher computing priority. Timing of its internal loop is checked by flag derived from the laser trigger pulse. The trigger pulse is generated and synchronised to Station Time Base by Laser Clock. This programme transmits data to Step Motors Controller and Time Gate Window Unit and reads results from Laser Clock (epoch timer) and range counter.

The internal structure of the loops in this programme depends on applied repetition rate of the laser triggers, which can be 1 pps, 2.5 pps and 5 pps.

GRAPHICS

Working with a train of picosecond pulses at the single photo-electron level implies poor signal to noise ratio. In this cases the graphical output of range residuals versus time is simple method to reccgnize the retrosignal from noise on-line and off-line, as well.

The personal computer HP85F (graphical CRT and graphical printer build in) was installed. The range residuals (+/- 3usec for low satellites, +/-1usec for Lageos) are displayed on the screen , 15 or 30 minutes of tracking per screen.

MOUNT ORIENTING AND ERROR COMPENSATION

To increase the mount positioning accuracy, the mount pointing accuracy is checked, the error model is computed. The mount error model is taking into account:

- the mount gears eccentricities	4 parameters
- the nonperpendicularities	2 parameters
- the coordinates offsets	2 parameters

The first four parameters are determined on the basis of mechanical measurements and ground aiming tests, the others are determined on the basis of the star observations. Ten to thirteen suitably distributed

stars are used. The interactive program (Stars) is used for the star catalogue manipulations, selecting of the observing star sequence etc. Program Sky is used for the mount control during star observations. The star position is monitored visually using an aiming telescope (50mm). The program MMP evaluates the (four) mount parameters on the basis of the star observation results /6/.

TIME BASE

Station time base is based on the HP5061 Cs frequency standard/clock. As the epoch reference, the Loran C signal (Mediterranean chain) is used. Laser Clock is synchronized from cesium clock. Propagation dalays of the LORAN C transmitters (Master, Slaves X,Y,Z) were calibrated in 1983 by cesium flying clock.

An automatical comparison of the local time base to the LORAN C signal was developed. The system consist of:

- LORAN C signal receiver + LORAN C rate generator
- delay generator
- oscilloscope
- epoch timer (Laser Clock) + computer + programme LORNT.

Principle of operation:

Output from LORAN C rate generator is connected to input of epoch timer instead of Laser START pulse. The phase of the generator is adjusted to correspond to the phase of the received Loran signal. The oscilloscope is used for this pupose. Recording the phase of the rate generator by the epoch timer, taking into account the delays, one can compute the difference between the station time base and the Loran C timing signal.

The program LORAN is running in the loop and is resposible for:

- reading the data from the Epoch Timer (Ti) - computing of the nearest Time of Coincidence (TOC) ,
- computing the time difference (Di) according to the formulas:

  $Di = (Ti - TOC - n*P)$

  $-P < Di < P$

  where P is the Loran period and n is an integer.
- computing the mean of ten readings,
- identifying the transmitter according to the value of Di,
- applying the corresponding delay.

Copleting the procedure for all the transmitters available, the weighted mean is computed, the protocol is printed.

POSTPASS RANGING DATA ANALYSIS

This part of the Station Software Package was significantly expanded. The programs for noise rejection and orbital fitting programs were completed. The accuracy of the raw results from calibration and satellite ranging (2-4nsec rms) is given by the laser pulse train envelope. Using the "Mode Locked Train YAG Laser Ranging Data Processing" software peckage /5/ the data are converted into "like single pulse" form and the subdecimeter rms level is achieved.

References

/1/ A.Novotny, I.Prochazka, Software package for station SAO N0.7831 Helwan,Egypt, in Proceedings of the Fourth International Workshop on Laser Ranging Instrumentation,held at Austin,USA,1981,p.89

/2/ J.H.Latimer,D.M.Hills,S.D.Vrtilek,A.Chaiken,D.A.Arnold and M.R.Pearlman, An evaluation and upgrading of the SAO prediction technique, in /1/, p.94

/3/ H.Jelinkova, Mode Locked Train YAG Transmitter in this Proceedings

/4/ K.Hamal, I.Prochazka, J.Gaignebet,Mode Locked Train YAG Laser Calibration Experiment, in this Proceedings

/5/ I.Prochazka, Mode Locked Train YAG Laser Ranging Data Processing, in this Proceedings

/6/ R.L.Ricklefs, Orienting a Transportable Alt-Azimuth Telescope in /1/, p.289

MODE LOCKED TRAIN YAG LASER RANGING DATA PROCESSING

I. Prochazka
INTERKOSMOS
Faculty of Nuclear Science and Physical Engineering
Czech Technical University
Brehova 7, 115 19 Prague 1, Czechoslovakia

Telephone (2) 84 8840
Telex 121254

ABSTRACT

The method of processing of laser ranging data collected using the passively mode locked YAG train laser is decribed. The algorithm for resolving of individual peaks in measured ranges histogram and system internal noise determination is explained together with the crosscorrelation methods for system calibration constant evaluation. The low satellites, Lageos and calibration ranging results are included.

MODE LOCKED TRAIN YAG LASER RANGING DATA PROCESSING

The INTERKOSMOS satellite laser ranging station in Helwan is using the passively mode locked train YAG laser transmitter since late 1982 /1/. The laser generates the train of pulses, 70psec each, spaced at fixed distance 2.0 nsec, most of the energy is concentrated within 3 pulses. The ranging system operates on the single PE signal level only. The software package for the mode locked train (MLT) laser ranging data processing was developed. Its final goal is:

a/ to find out the ranging data sets internal structure, to resolve the echoes from the individual laser pulses within the train,
b/ to determine the calibration constant and system internal noise,
c/ to convert the ranging data into the "like single pulse" form.

In comparison with the TLRS 1 /2/, the spacing of the pulses in the train is much smaller. It is dictated by the laser construction and stability requiremets /5/. However, decreasing the MLT pulses spacing, the analysis of the measured signal becomes more critical. Several laser transmitters with MLT pulses spacings 1.6-2.2nsec were tested during 1982-84. The value adopted (2.0 nsec) is a compromise between the laser stability and the data analysis limitations.

The fundamental procedure in the MLT ranging data processing is to find out the function, describing the distribution of measured values. Suppose the hypotetic ranging system using an individual short laser pulse, single PE ranging. The distribution of the measured ranges may be described by the Gaussian distribution function. Its offset determines the measured range, its dispersion the system noise. For a ranging system using the MLT laser, the problem is more complex. Keeping in mind the shape of the train of transmitted pulses, START discriminator /4/, single PE ranging, one may conclude: the measured values distribution function will be a superposition of the Gaussian distribution functions of unknovn amplitudes, equal dispersion and offsets, differing one to another in the value of pulses spacing within the train.

$$F(t) = \sum_{k=-N}^{N} a_k \cdot \exp\left(-(t-o-k.r)^2/(2.s^2)\right) \qquad (1)$$

where
a_k ... amplitudes,
o ... offset,
s ... dispersion
r ... pulse spacing in the train.

Thus, having a set of measured data, one can find out the unknovn parameters s,o,a. (For the system, in which most of the energy is contained in 3 pulses, the value N=2 was found to be optimal.) The measured data distribution is expressed in the form of a histogram, the unknovn parameters of the function (1) are computed using the non linear least square fit process.

On figures 1 to 4 are the prints out of the ranging data analysis precedure for calibration, low satellite and Lageos, respectivelly. The upper histogram corresponds to the measured data distribution, the lower ones to the computed distribution function F. To check the solution stability and confidence, the whole procedure is repeated for different histogram constructions /cell width, starting point/, totaly 5x4=20 solutions are calculated.

The complete ranging data analysis is carried out in 3 steps:
- the satellite ranging residuals are evaluated using algorithm /3/, the distribution functions for the ranging and calibration are found,
- the calibration constant is determined : extremely simple /and fast/ algorith is used to crosscorrelate the ranging and calibration data and to assign to each ranging data histogram peak the corresponding one from the calibration data set. The accurate value of the calibration constant is evaluated from the computed calibration data offset adding/substracting integer multiples of the train pulses spacing.
- the measured values are folded.

Conclusion

The mode locked train laser ranging data analysis procedures were tested by a large number of numerical simulations, indoor calibration tests and real satellite ranging and calibration runs. The minimal number of echoes required for analysis depends on the system noise and the pulse train length. Typicaly, 50 range measurements are sufficient to form a stable solution, although the succesfull data analysis for the set of 30 echoes occured.

The ultimate limit of the ranging system internal noise, for which the mode locking structure may be resolved with the acceptable confidency within the ranging data is 0.32 times the pulse spacing within the train.

Special attention was given to the uncertainty caused by the multipulse character of the laser transmitter. It may cause a systematic error in range measurement of integer multiples of the spacing of the pulses within the train /4/. Calibration tests to internal and/or external targets were carried out to find the calibration constant determination confidence during 1984 mission. It was found, that in at least 90% of the mesurement series, the calibration costant was determined correctly. In the remaining cases, the errors +/- 2.0 nsec occured. On fig.5 there is histogram of pre-postpass calibration differencies /6/, the distribution of the systematic errors may be seen.

If the mode locking structure can not be resolved within the ranging data set, the data may be treated as beeing acquired by the

MODE-LOCKED YAG LASER RANGING DATA PROCESSING
****

EXTERNAL TARGET CALIBRATION 84.7.3. UT 23: 6

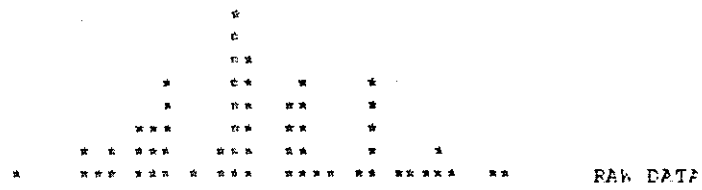

RAW DATA

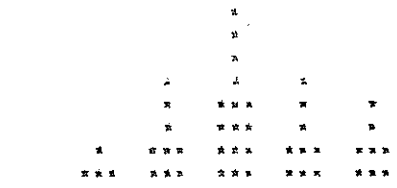

SOLUTION

B.SPACING : .40
OFFSET (ns): 3402.66
SIGMA (ns): .32
AMPLITUDES : 2.6 4.6 6.1 5.1 3.6

INTEGRAL TREATMENT RESULTS
MEAN VALUE 3403.24 SIGMA 3.37 (NSEC)

B.SPAC. .500 OFFSET 3402.64+/- .01 SIGMA .26 .38 .32 .32 NSEC
B.SPAC. .400 OFFSET 3402.66+/- .01 SIGMA .25 .57 .29 .29 NSEC
B.SPAC. .333 OFFSET 3402.64+/- .03 SIGMA .59 .34 .22 .61 NSEC
B.SPAC. .286 OFFSET 3402.63+/- .07 SIGMA .18 .60 .33 .33 NSEC
B.SPAC. .250 OFFSET 3402.66+/- .02 SIGMA .28 .22 .26 .23 NSEC

RESULTING : OFFSET 3402.64+/- .04 SIGMA .32 NSEC
SOLUTION CONFIDENCE 1.00

Fig.1

MODE-LOCKED YAG LASER RANGING DATA PROCESSING
****

INTERNAL PASS CALIBRATION 84.7.16. UT 22:34

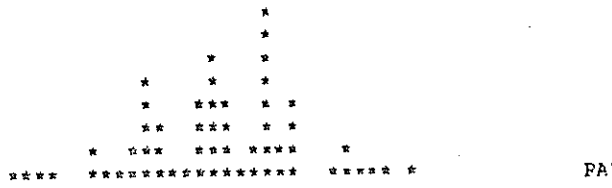

RAW DATA

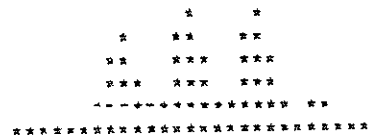

SOLUTION

B.SPACING : .40
OFFSET (ns): 136.31
SIGMA (ns): .48
AMPLITUDES : .6 4.1 5.6 5.4 1.6

INTEGRAL TREATMENT RESULTS
MEAN VALUE 136.26 SIGMA 2.90 (NSEC)

B.SPAC. .500 OFFSET 136.31+/- .02 SIGMA .44 .46 .39 .39 NSEC
B.SPAC. .400 OFFSET 136.36+/- .04 SIGMA .44 .40 .39 .37 NSEC
B.SPAC. .333 OFFSET 136.32+/- .02 SIGMA .45 .35 .41 .41 NSEC
B.SPAC. .286 OFFSET 136.32+/- .02 SIGMA .39 .48 .39 .39 NSEC
B.SPAC. .250 OFFSET 136.31+/- .01 SIGMA .40 .43 .42 .42 NSEC

RESULTING : OFFSET 136.32+/- .03 SIGMA .41 NSEC
SOLUTION CONFIDENCE 1.00

Fig.2

Mode locked train laser ranging data processing, calibration series.

MODE-LOCKED YAG LASER RANGING DATA PROCESSING

SATELLITE 6503201 64. 7. 16. UT 22:20

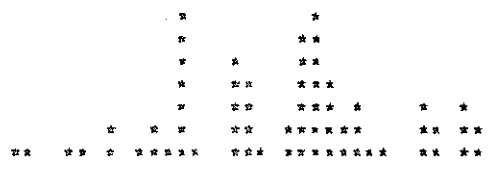

RAW DATA

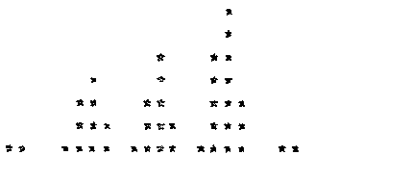

SOLUTION

```
R.SPACING  :          .46
OFFSET (ns):         1.09
SIGMA  (ns):          .46
AMPLITUDES :      1.3     4.7     4.5     7.7     1.4

INTEGRAL TREATMENT RESULTS
MEAN VALUE          -.05  SIGMA   3.41 (NSEC)

R.SPAC. .500 OFFSET     1.09+/- .04 SIGMA .52 .57 .50 .50 NSEC
R.SPAC. .400 OFFSET     1.14+/- .02 SIGMA .52 .49 .51 .51 NSEC
R.SPAC. .333 OFFSET     1.12+/- .01 SIGMA .53 .50 .57 .57 NSEC
R.SPAC. .286 OFFSET     1.07+/- .04 SIGMA .59 .49 .49 .49 NSEC
R.SPAC. .250 OFFSET     1.09+/- .02 SIGMA .49 .53 .51 .49 NSEC
-------------------------------------------------------------

RESULTING : OFFSET      1.10+/- .04 SIGMA      .52        NSEC
SOLUTION CONFIDENCE     1.00
```

Fig.3

MODE-LOCKED YAG LASER RANGING DATA PROCESSING

SATELLITE 7603901 83.10.30. UT 22:50

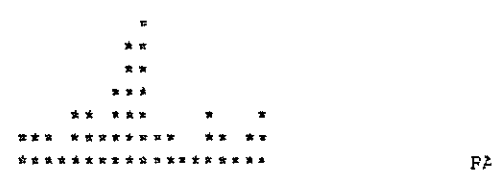

RAW DATA

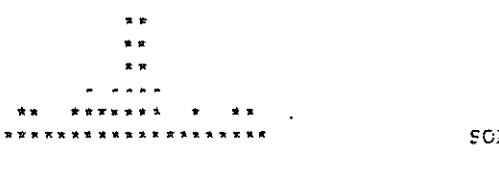

SOLUTION

```
R.SPACING  :          .45
OFFSET (ns):         -.02
SIGMA  (ns):          .57
AMPLITUDES :      2.0     2.9     6.6     1.5     2.4

INTEGRAL TREATMENT RESULTS
MEAN VALUE            .00  SIGMA   2.32 (NSEC)

R.SPAC. .454 OFFSET     -.02+/-0.00 SIGMA .57 .63 .64 .64 NSEC
R.SPAC. .363 OFFSET      .05+/- .07 SIGMA .62 .57 .56 .56 NSEC
R.SPAC. .303 OFFSET      ---+/- --- SIGMA .63 .65 .64 .64 NSEC
R.SPAC. .259 OFFSET      ---+/- --- SIGMA .56 .67 .60 .60 NSEC
R.SPAC. .227 OFFSET      .02+/- .00 SIGMA .59 .60 .56 .56 NSEC
-------------------------------------------------------------

RESULTING : OFFSET      .03+/- .06 SIGMA      .56        NSEC
SOLUTION CONFIDENCE     .30
```

Fig.4

SLR working with the single pulse of few nsec length. In such a case, the system internal noise (RMS) ranges from 2 to 3 nsec.

References

1/ B.Kvasil,K.Hamal,H.Jelinkova,A.Novotny,I.Prochazka,M.Fahim, B.Baghos,A.G.Massevich,S.K.Tatevian, Interkosmos Laser Radar Version Mode Locked Train, in this proceeding
2/ E.C.Silverberg, The Feedback Calibration of the TLRS Ranging System,proceedings of the Fourth International workshop, held at Austin,Texas,1981,published in Bonn,1982
3/ I.Prochazka, Ranging Data Analysis Procedure, FJFI Preprint Series No.82/143 Prague, 1982
4/ P.Wilson , private communication, 1984
5/ H.Jelinkova,Mode Locked Train YAG Laser Transmitter in this proceeding
6/ M.R.Pearlman,N.Lanham,J.Thorp,J.Wohn,SAO Calibration Techniques, in /2/, Vol.II, p.323

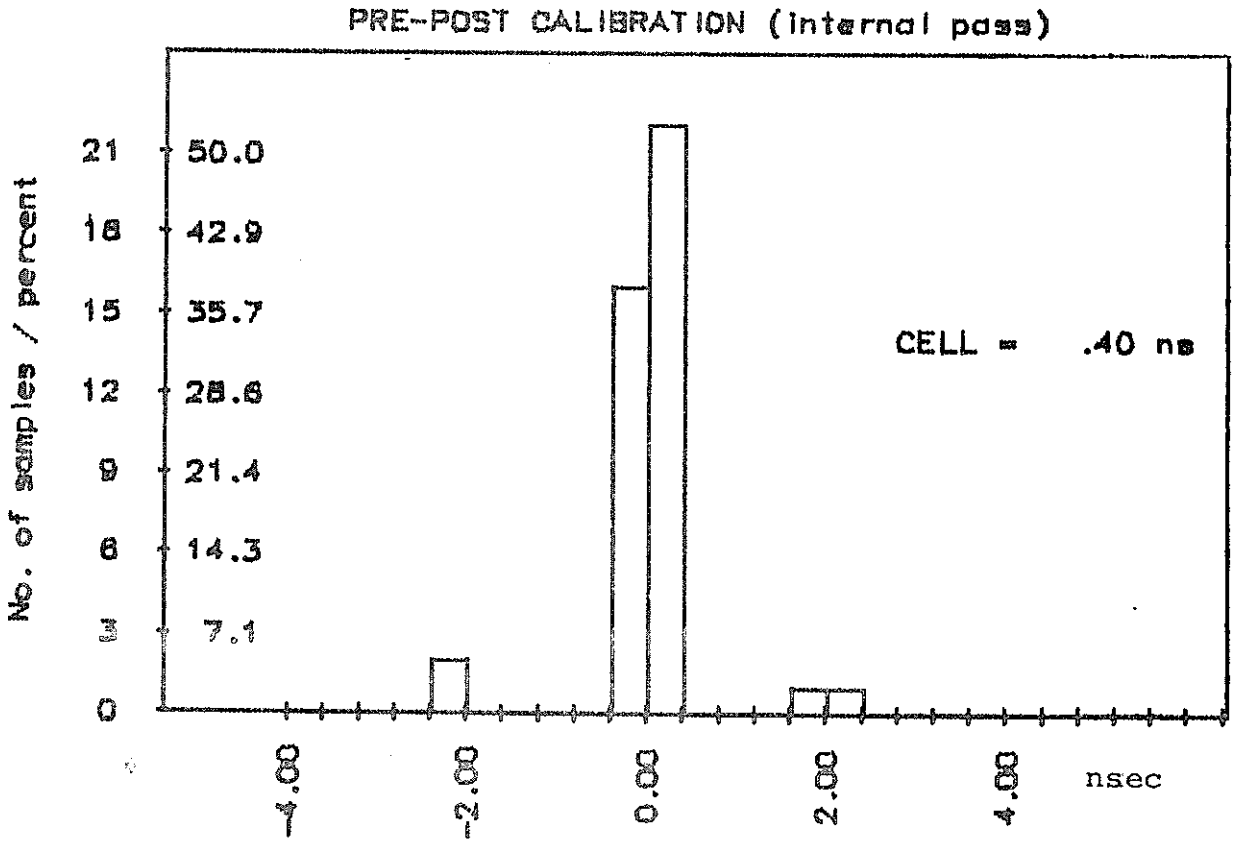

Histogram of pre-postpass calibration differencies internal calibration pass,station Helwan,July 1984

Fig. 5.

GLTN LASER DATA PRODUCTS

D.R. Edge
Bendix Field Engineering Corporation
Data Services Group, Greenbelt Md. 20771

Telephone (301) 344 7530
Telex 197700

ABSTRACT

The Goddard Space Flight Center (GSFC) Laser Data System supports and manages the flow of laser data products from satellite laser ranging stations to the international laser data user community. The GSFC Laser Data System performs quick look data management, operational orbit determination, orbital data analysis in supporting the acquisition message and scheduling requirements of the international laser tracking community. The Data System supports the production and distribution of laser data products including quick look data, the monthly global full rate MERIT 1 data tape, and eventually aggregate laser data. The production and distribution of laser data through the GSFC Laser Data System involves supporting stations, GLTN Communications System, the GLTN Bendix VAX Computer System, the Crustal Dynamics Project Data Information System (DIS), and the Crustal Dynamics Project Investigators.

GLTN LASER DATA PRODUCTS

DATA FLOW

The Goddard Space Flight Center (GSFC) Laser data System supports and manages the flow of laser data products from satellite laser ranging stations to the international laser data user community. The GSFC Laser Data System supports and is supported by laser stations from around the world including the Goddard Laser Tracking Network (GLTN), Australian Laser Network (ALN), Participating Laser Network (PLN), Cooperating Foreign Laser Network (CFLN), and others. Attachment 1 is a data flow schematic of the GSFC Laser Data System, which includes supporting stations, the GLTN Communications System, The GLTN Bendix VAX Computer System, the Crustal Dynamics Project Data Information System (DIS), and the Crustal Dynamics Project Investigators.

The GLTN Communications System receives and transmits quick look data, tracking operations reports, quick look analysis results, acquisition data, scheduling information, and other station information. The GLTN Communications System uses a Micronet 8 to support communications between the laser stations, the GLTN VAX Computer System, and Investigators through Direct Distance Dialing (DDD), TELEX, GE Mark 3, or NASCOM.

The GLTN VAX Computer System supports the management, processing, analysis, and quality control of satellite laser data. Raw satellite data from GLTN, ALN, and PLN stations is managed, processed and merged with processed data from CFLN and other supporting stations to produce a montly global data tape in the MERIT 1 format. The GLTN VAX Computer System also supports quick look laser data management, operational orbit determination, and orbital data analysis used for acquisition message generation and network scheduling. Data processing and orbital analysis results and supporting data quality information from tracking stations and investigators are used on the VAX Computer System to produce data quality evaluation information which supports the quality control of the monthly global MERIT 1 data tape and other laser data products.

The Crustal Dynamics Project Data Information System manages, distributes, and archives processed laser data to support the laser data user community. In managing laser data, laser data information and investigator results, the DIS is the primary interface between the laser data production community and the laser data user community.

The laser data user community is comprised of Crustal Dynamics Project investigators and other scientists doing research in Crustal Dynamics, earth rotation, orbit determination, instrument calibration, data evaluation, and other scientific applications.

MERIT DATA VOLUME (Attachment 2)

Laser data productivity has increased sharply during the MERIT Campaign which began in September 1983. The GSFC Laser Data System has received quick look data from 28 different international laser stations and full rate data from 22 different international laser stations since the beginning of the MERIT Campaign. During the MERIT Campaign the monthly global processed data tapes have averaged over 600 satellite passes and over one half million satellite ranging observations per month.

LASER DATA PRODUCTS

Satellite laser ranging observations have been traditionally available to users in either quick look or full rate form, quick look data meeting the requirements for users needing immediate access to data and full rate meeting the requirements of users who need the complete precision data set. The recent increases in worldwide laser data productivity have led a number of users to investigate data compression techniques to improve computer efficiency in using very large full rate laser data sets. Statistically compressed or aggregate data is needed as a new laser data product. Operational production of aggregate laser data to supplement the quick look and full rate data products is very likely in the near future. Attachment 3 highlights important characteristics of the quick look, full rate, and aggregate data types.

Quick look data is typically produced on site using generic calibration techniques, and is transmitted to the GLTN Communications System daily, making it available to users within approximately 48 hours. Quick look data is generally randomly sampled with only gross filtering to provide a good representation of the full rate data set. Quick look precision and accuracy is generally comparable to full rate. Intermittent data problems occasionally impair quick look data accuracy. Many of these problems are corrected during full rate processing. Quick look data quality is adequate to support scientific applications and orbital maintenance. Operational quality control using quick look data can be very effective if on site data editing does not compromise the representation of the full rate data set.

Full rate data is typically produced offsite using analytic calibration techniques and is generally available within three months. Data editing is limited to provide the most information in a complete precision data set. The primary advantage of full rate data is that it has the necessary data visibility to perform precision data quality control. Full rate has been traditionally used to support scientific applications.

LASER DATA PRODUCTS con't

Aggregate data will probably be produced offsite from full rate data and should also be available within three months. Aggregate data will be produced by using a statistical model to compress the full rate data set into a much smaller precision data set. Aggregate data accuracy should be virtually identical to full data accuracy. The improved computer efficiency of aggregate data will make it ideal for scientific applications. Quality control of laser data using the aggregate data set will be very efficient and should lead to improved techniques using orbital analysis of the global data set. Precision data problems requiring special investigation can be resolved by referring back to the full rate data set. Improved data compression techniques or specialized data compression requirements are likely to evolve in the future. The archived full rate data set can be reprocessed to meet new future aggregate data requirements.

G L T N L A S E R D A T A F L O W

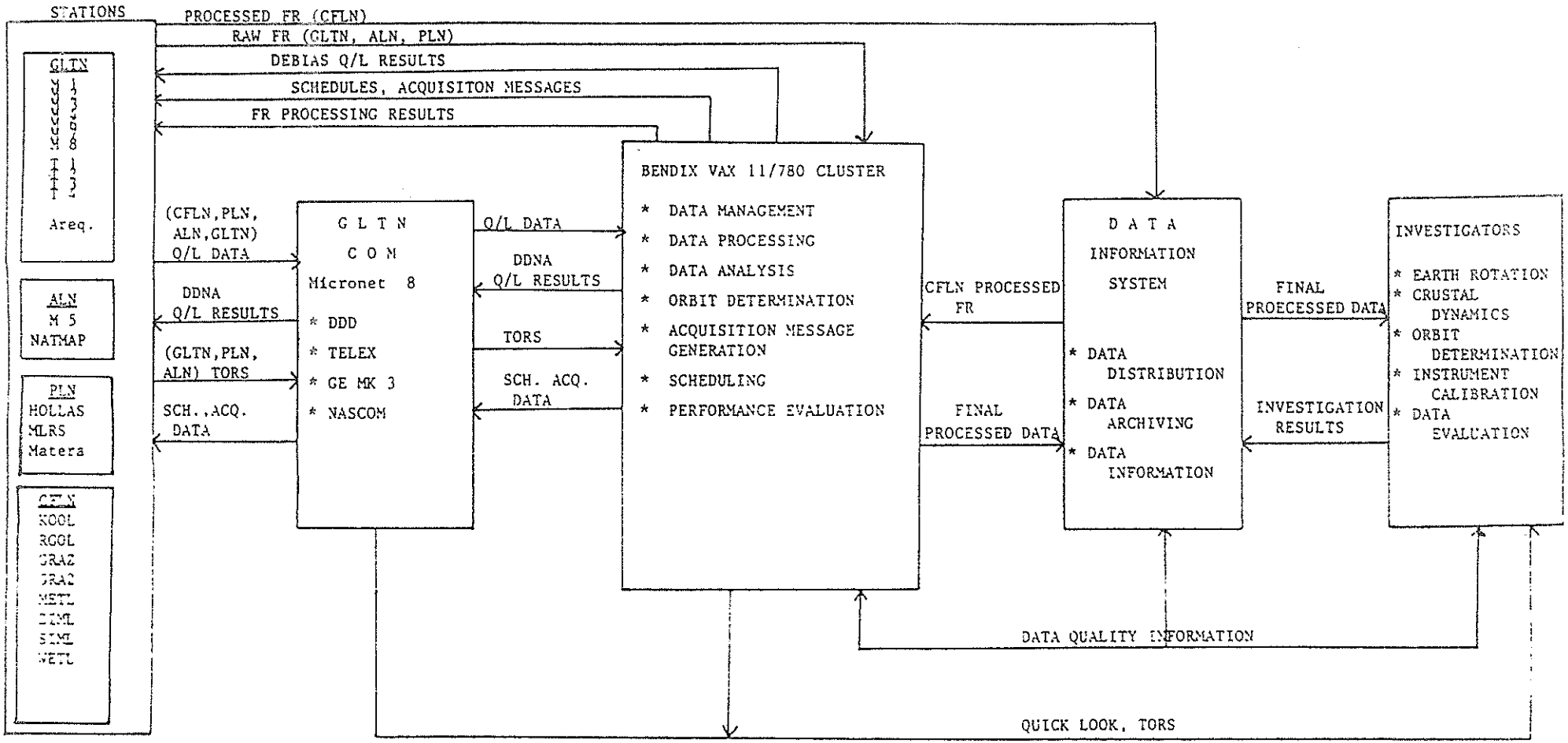

GLTN LASER DATA PRODUCTS

	FULL RATE	QUICK LOOK	AGGREGATE(FUTURE)
PRODUCTION	OFFSITE PROCESSING	ONSITE PROCESSING	ONSITE/OFFSITE PROCESSING
CALIBRATION	ANALYTIC	GENERIC	ANALYTIC/GENERIC
AVAILABILITY	3 MONTHS	48 HOURS	TBD
USE	SCIENTIFIC PRECISION DATA Q/C	SCIENTIFIC, ORBIT MAINTENANCE, OPERATIONAL Q/C	SCIENTIFIC, GROSS DATA Q/C
DATA SELECTION	N/A	RANDOM/ GROSS FILTER	STATISTICAL MODEL
ADVANTAGES	DATA VISIBILITY	TIMELY	COMPUTER EFFICIENCY
DISADVANTAGES	COMPUTER EFFICIENCY	ACCURACY	DATA VISIBILITY

M E R I T L A S E R D A T A V O L U M E

* QUICK LOOK DATA FROM 28 STATIONS
* FULL RATE DATA FROM 22 STATIONS
* 600 SATELLITE PASSES PER MONTH
* 500,000 RANGING OBSERVATIONS PER MONTH

PERFORMANCE AND EARLY OBSERVATION OF THE SECOND-GENERATION SATELLITE LASER RANGING SYSTEM AT SHANGHAI OBSERVATORY

Y. Fumin, Z. Youming, S. Xiaoliang, T. Detong,
X. Chikun, S. Jinyuan, L. Jiaqian
Shanghai Observatory Academia Sinica
Shanghai, China

ABSTRACT

The satellite laser ranging work at Shanghai Observatory has been presented on the Fourth International Workshop on Laser Ranging Instrumentation held in Austin, Texas in 1981. The development of the second-generation SLR system at Shanghai Observatory was begun in 1978, and has been supported by the Academia Sinica. It is a product of the combined efforts of several institutes under the Academia Sinica. The system design demands and scheme were presented at Shanghai Observatory. The mount of the system was designed at our observatory in collaboration with the Changchun Satellite Observation Station, and manufactured by the Changchun Institute of Optics and Fine Mechanics. The servo subsystem, torque motors and tachometers were developed and fabricated by the Shenyang Automation Institute. The Nd:YAG frequency-doubled laser was built by the Shanghai Institute of Optics and Fine Mechanics. The receiver, timing system, hardware and software of the computer control system were developed at our observatory. The mount was installed at Zo-Se Section of Shanghai Observatory in March 1983. The integration of the system and measurements of ground target were followed. The experimental ranging to satellites was started in October, and the first echo from LAGEOS was successfully received on November 7.

Performance and Early Observation of the Second-Generation Satellite Laser Ranging System at Shanghai Observatory

I. Introduction

The satellite laser ranging work at Shanghai Observatory has been presented on the Fourth International Workshop on Laser Ranging Instrumentation held in Austin, Texas in 1981.[1] The development of the second-generation SLR system at Shanghai Observatory was begun in 1978, and has been supported by the Academia Sinica. It is a product of the combined efforts of several institutes under the Academia Sinica. The system design demands and scheme were presented at Shanghai Observatory. The mount of the system was designed at our observatory in collaboration with the Changchun Satellite Observation Station, and manufactured by the Changchun Institute of Optics and Fine Mechanics. The servo subsystem, torque motors and tachometers were developed and fabricated by the Shenyang Automation Institute. The Nd:YAG frequency-doubled laser was built by the Shanghai Institute of Optics and Fine Mechanics. The receiver, timing system, hardware and software of the computer control system were developed at our observatory.

The mount was installed at Zo-Se Section of Shanghai Observatory in March, 1983. The integration of the system and measurements of ground targets were followed. The experimental ranging to satellites was started in October, and the first echo from LAGEOS was successfully received on November 7.

II. Performance

The characteristics of the system are listed in Table 1. The main observation object of the second-generation SLR system is LAGEOS, so that the receiving telescope is specially designed for two purposes: one is for receiving the laser return signals, the other for visual detection of the faint satellites, such as LAGEOS. The coude optics is prepared so as to install conveniently the high power Nd:YAG laser and to ensure its stabillity. In order to operate smoothly the mount at low angular velocity and reduce the error of mechanic drive, two axes of the mount are directly coupled with torque motors. The optical encoders have 20-bit resolution (1.2 arc second).

The optics of receiving telescope is of Ritchey-Chretien configuration and the field-of-view for receiver is adjustable from 30 arc seconds to 7 arc minutes in seven steps and the field-of-view for visual detection is 30 arc minutes. The width of interference filter is 10A. The type of photomultiplier adopted is GDB-49, a kind of tube made by the Beijing

Nuclear Instrument Factory, Beijing, China, which has a 1.7-1.9 nsec risetime, a gain of 3×10^7, and a 200 psec transit time jitter. The measured time walk of the receiver electronics, including PMT, pre-amplifier, constant fraction discriminator and computing counter, etc., is less than 0.5 nsec.[2] The Nd:YAG laser has been continuously operated for nine months without any heavy repairs, such as replacement of rods or mirrors. The maximum output energy in 5320A is 330 mj in 4-5 nsec duration time (FWHM), and the efficiency of frequency doubler is about 45 per cent. The maximum repetition of the laser is 3 Hz, but only 0.5 or 1 Hz is adopted in routine operation.

The wobble in each axis of the mount is held to 1 arc second, and the pointing accuracy of the mount is better than 10 arc seconds with systematic errors not being corrected. The alignment of the coude mirrors and transmit optics is made with the aid of a lateral transfer prism set, which will be added at the front ends of both the receiving telescope and the transmitter, if need be. It has been shown in the experiment that the drift of the transmit beam arose from the rotations of two axes of the mount is less than 5 arc seconds and the parallelism between the transmit axis and the receiving one is better than 6 arc seconds.

Fig. 1 is the block diagram of the SLR system at Shanghai Observatory.

Fig. 2 is the block diagram of the SLR servo subsystem.

Fig. 3 is the optical scheme of the Nd:YAG frequency-doubled laser.

III. Preliminary Observation Results

The first echo from LAGEOS was received on November 7, 1983. The visual tracking mode with joystick had been used, because the software of the microcomputer had not been completed yet, so that the number of successful observations per pass was only 10-20. The maximum range we obtained was 7100km, and the lowest elevation angle of LAGEOS was only 40 degrees.

We have transmitted the quick-look data of LAGEOS to NASA/Goddard Laser Tracking Network, United States. These preliminary observation data have been analysed by the Center for Space Research. The university of Texas at Austin.[3] Table 2 is the summary of residuals of LAGEOS quick-look data obtained from Nov. 7 to Dec. 4, 1983, Shanghai SLR station. Fig. 4 is a typical range residuals of LAGEOS, taken by Shanghai station, Dec. 3, 1983 and it has shown that the accuracy of our data for signle shot is about 16 cm. Only using the above 7 passes LAGEOS data, a preliminary adjustment of our station coordinate has been done by the same center (Table 2).

It was rain season during the intensive observation period (April to June, 1984). Thus only a dozen successful observation passes have been obtained from Nov. 1983 to July 1984. Afterward, we have got the long-term precise prediction ephemeris of LAGEOS and relevant software from the Center for Space Research, the University of Texas at Austin, and adopted the "position mode" for LAGEOS ranging. The azimuth, elevation of telescope and range gate (0.5-1.5μs) have been mannually set by observers every 30 seconds. The single photoelectron receiving system has been developed. The first blind track to LAGEOS was obtained on Sept. 3, 1984. Since then, above-mentioned limitations have been broken free from, and the successful observaton passes have been greatly increased. We have obtained 21 passes, 341 observations during 571 minutes of tracking to LAGEOS (no editing) in September, and 13 passes, 264 observations during 342 minutes for Oct. 1 to Oct. 26 (the writing moment). Up to now, the maximum range is about

8542 km, the lowest elelvation angle of LAGEOS is 20 degrees and the maximum number of the observations in a pass is 61, and the longest tracking arc of LAGEOS in a pass is 45 minutes.

IV. Future Plans

By the end of this year, we hope that the computer control system will be available, and the SLR system will be automatically operated. Further improvement on the performance is under consideration. A contract to build a Nd:YAG frequency-doubled mode-locked system that nominally produces up to a 30 mj, 200 psec FWHM pulse with repetition rates up to 10 pulses per second has been signed with the Shanghai Institute of Optics and Fine Mechanics, and the new laser will be delivered to the observatory in 1986. In the meanwhile, a new 16-bit microcomputer system will be added to improve the control and data collection capabilities of the present system. Therefore, we hope that a third-generation SLR system will be in operation in 1986-1987, and do more contributions to the geodynamics applications.

Acknowledgement: The second-generation SLR system would have not been operated if we had not been in cooperation with before-mentioned those institutes and had not had many colleagues' help in the work. The authors are indebted to each of them. The authors would like to express their gratitude to Prof. B.E. Schutz, the University of Texas, at Austin, for his kind help in data analysis.

References

[1] Yang Fumin et al., Satellite Laser Ranging Work at Shanghai Observatory, Proceedings of the Fourth International Workshop on Laser Ranging Instyrumentation held at Austin, Texas, pp. 65-79, (1981).

[2] Su Jinyuan et al., The Receiver System of the Satellite Laser Ranging System with Decimeter Level Precision, Annals of Shanghai Observatory, Academia Sinica, No. 4, pp. 271-278 (1982).

[3] B.E. Schutz, Private Communication, (1983).

Table 1 Performance of the second-generation SLR system at Shanghai Obs.

I. LASER SUBSYSTEM		III. MOUNT	
material	Nd:YAG	aperture of receiver	600mm
output wavelength	5320Å	type of mount	alt-az &Coudé optics
output energy	250mj		
width of pulse	4-5nsec	optical encoder	20 bits(1":2)
repetition	1pps	range of travel	-5^{c}—$+185^{c}$ in alt 600^{c} in azimuth
aperture of transmitting telescope	150mm	static pointing accuracy	10"(without systematic corrections)
beam divergence	0.2-2mrad		
II. TIMING SUBSYSTEM		resonant frequency	45Hz
filter bandwidth	10Å	max. angular velocity	15°/sec in az. 8°/sec in alt.
type of photomulti.	GDB-49(chinese type)		
quantum effeciency	10%	max. angular accelera.	$20^{\circ}/sec^{2}$ in az. $10^{\circ}/sec^{2}$ in alt.
risetime	1.8nsec		
resolution of timer	0.1nsec	IV. COMPUTER	
threshold detecter	constant fraction	Dynabyte microcomputer system(Z80 CPU)	
freqency standard	rubidium	8 bit, 64KB	
synchronization	Loran-C	disk, printer	
accuracy of synchr.	2μs		

Table 2 SUMMARY OF LAGEOS QUICK-LOOK DATA RESIDUAL

SHANGHAI SLR STATION*

+SHANGHAI STATION COORDINATES:

ALTITUDE = 29.0230 Meters
LONGITUDE = 121.191740599 Degrees
LATITUDE = 31.097527357 Degrees

REFERENCE ELLIPSOID FOR STATION COORDINATES:

A_E = 6378137.0 Meters
1/F = 298.2570

STATION WAVELENGTH:

λ = 5320.0 Angstroms
$f(\lambda)$ = 1.025792

STA ID	NO OF PASSES	TOTAL OBS	EDITED OBS++	PCT EDITED	GOOD OBS	RAW RMS	RB TB RMS	PRECISION ESTIMATE
7837 SHANGHAI	7	82	5	6.1	77	54.9	17.7	17.7cm

++20 meters edit criteria imposed

STA ID	NO OF PASSES	NO OF NPTS	PTS/ NPT	NPTS/ PASS	EPSIG	NPT WRMS	APSIG	NPT RMS
7837 SHANGHAI	7	24	3.2	3.4	9.5	11.7	16.1	14.9cm

*Obtained from Nov.7 to Dec.4,1983, and analysed by Center for Space Research, University of Texas at Austin.

+Preliminary Station Coordinate solution, LPM8402

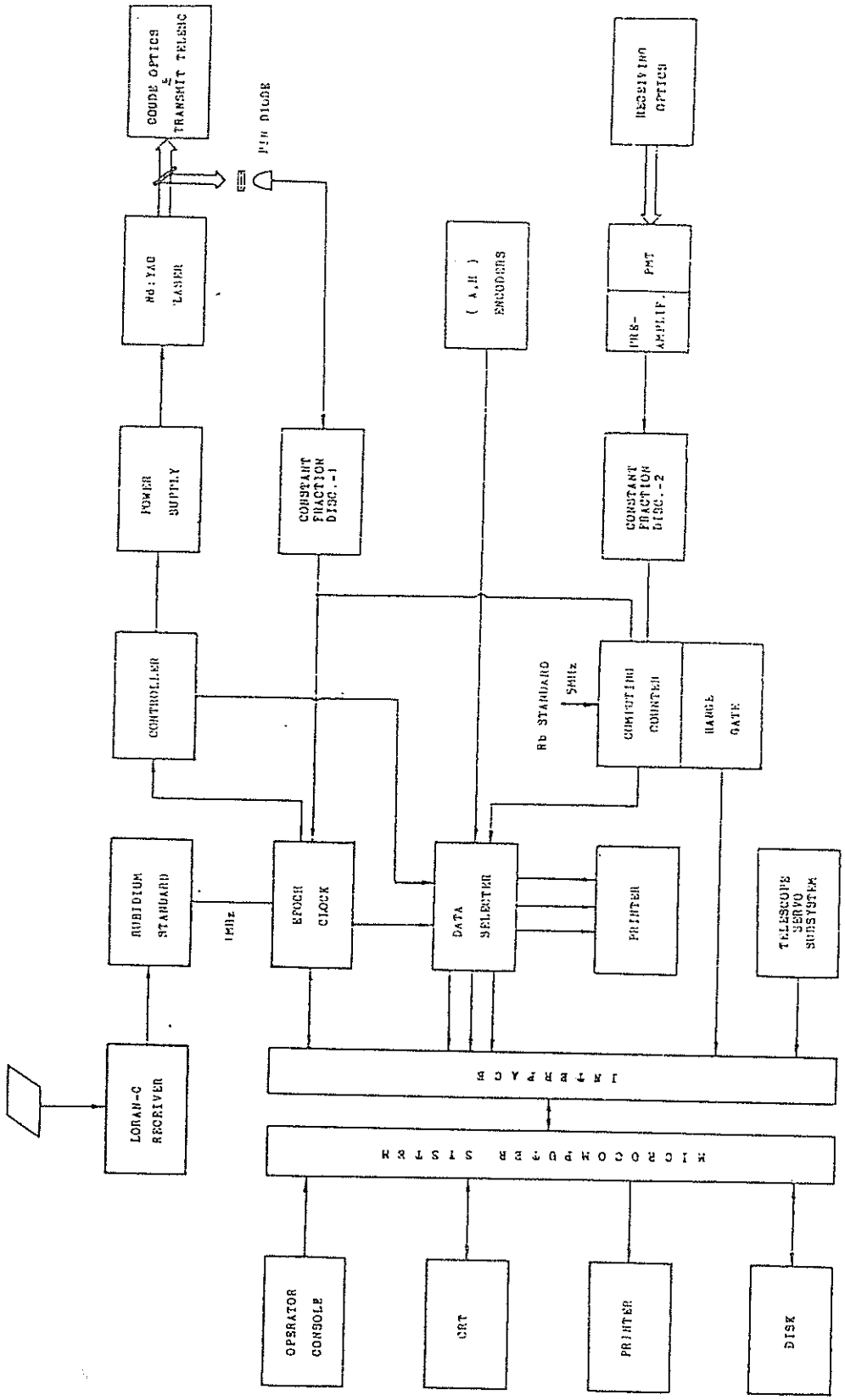

Fig.1 Block Diagram of Second-Generation SLR system at Shanghai Obs.

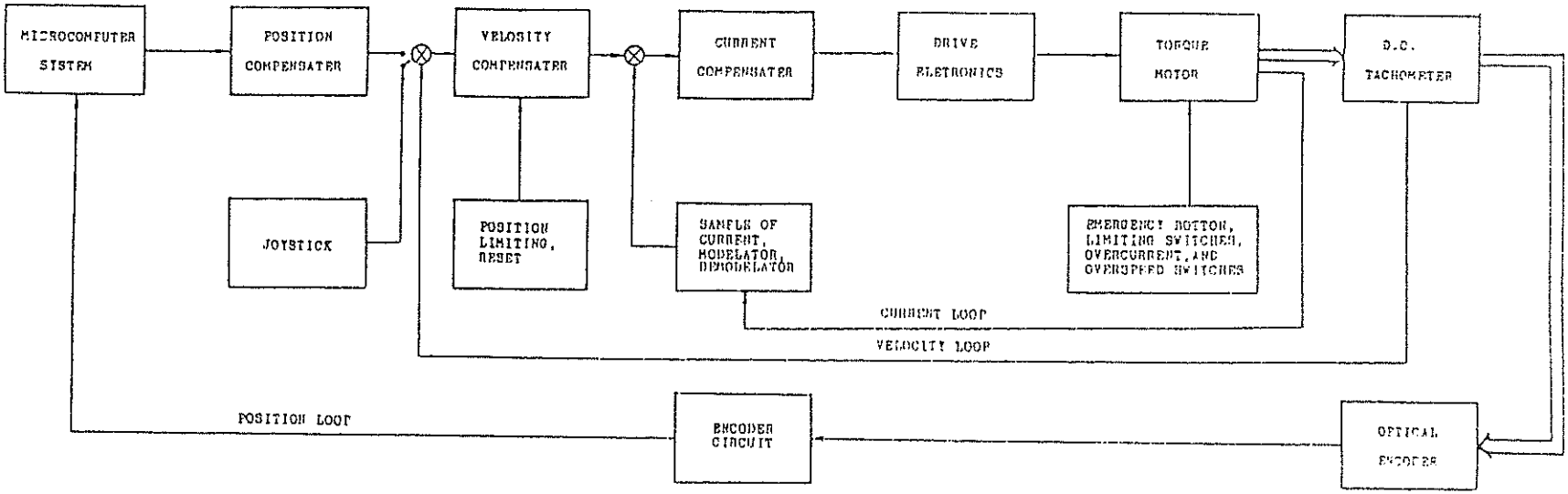

Fig.2 Block Diagram of the Servo Subsystem

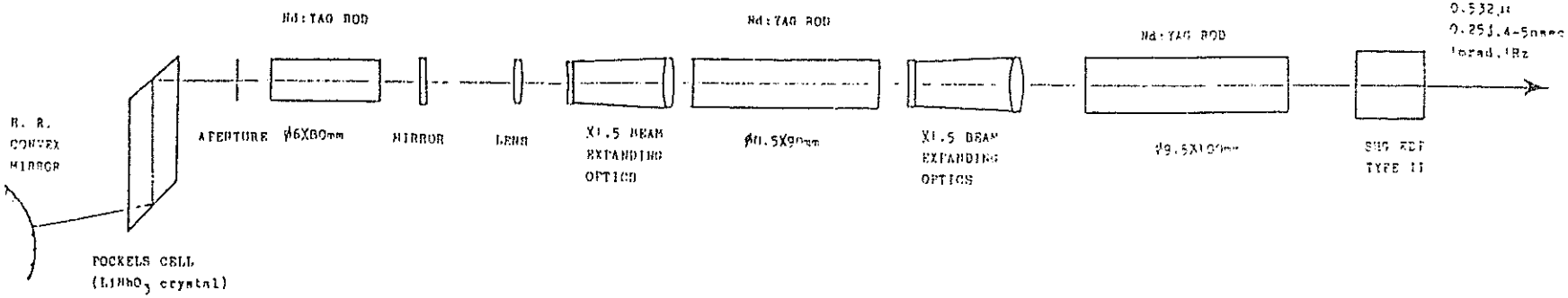

Fig.3 Optical Scheme of the Nd:YAG Laser

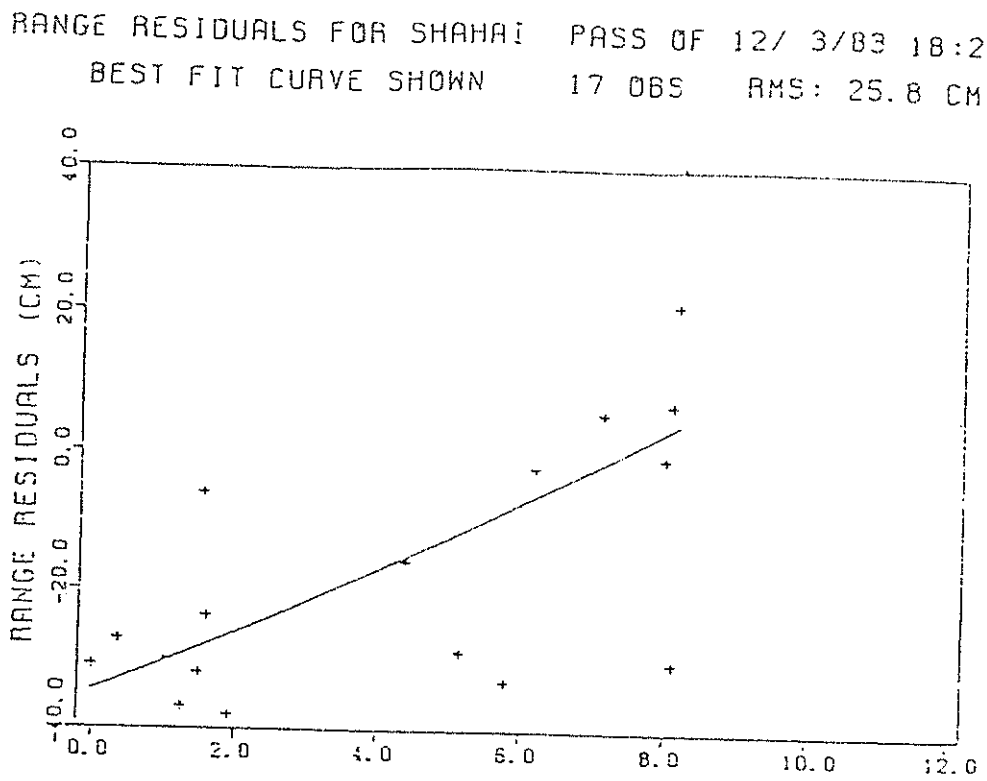
RANGE RESIDUALS FOR SHAHAI PASS OF 12/ 3/83 18:25:43
BEST FIT CURVE SHOWN 17 OBS RMS: 25.8 CM
RANGE RESIDUALS (CM)
40.0
20.0
0.0
-20.0
-40.0
0.0
2.0
4.0
6.0
8.0
10.0
12.0

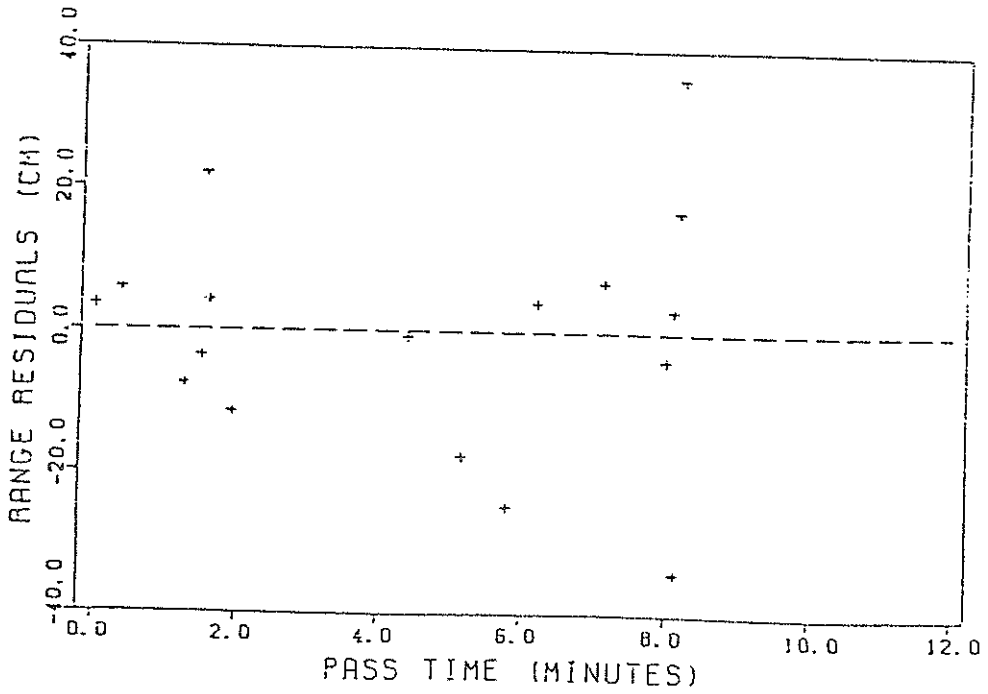
RESIDUALS AFTER FITTING RMS: 16.3 CM
RANGE RESIDUALS (CM)
40.0
20.0
0.0
-20.0
-40.0
0.0
2.0
4.0
6.0
8.0
10.0
12.0
PASS TIME (MINUTES)

Figure 4

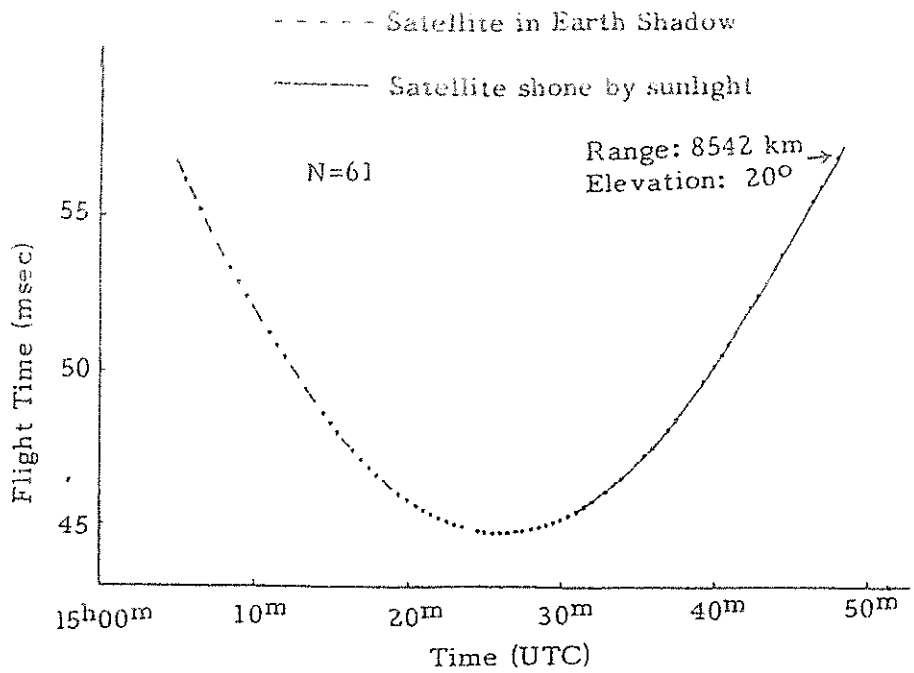

Fugure 5. A LAGEOS Pass Obtained by Position Mode at Shanghai Station (Oct. 18,1984)

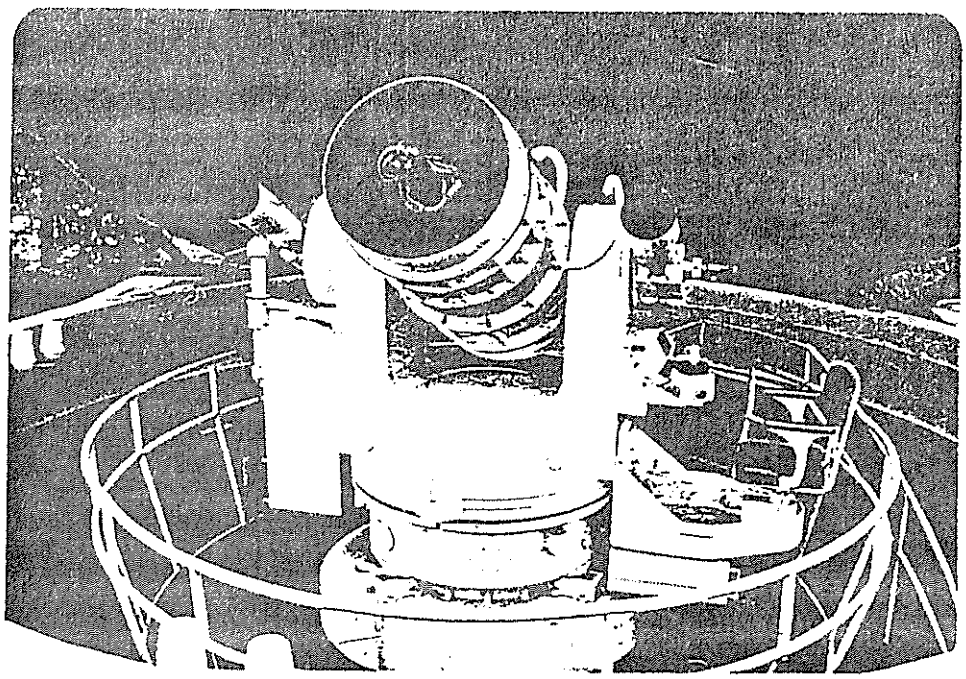

Figure 6. Shanghai SLR Sytem Telescope

REPORT OF THE ACTIVITIES OF THE LASER STATION GRAZ-LUSTBUEHEL

G. Kirchner
Observatory Lustbuehel
Lustbuehelstr. 46
A-8042 Graz Austria

Telephone (0) 316 42231
Telex 31078

ABSTRACT

An overview of the laser ranging activities at the observatory Graz-Lustbuehel during the last two years is given; modifications of the system and their result on the measurements accuracy are described.

REPORT OF THE ACTIVITIES OF THE LASER STATION GRAZ-LUSTBUEHEL

In the year 1979 the installation of a third generation satellite laser ranging system was initiated at the observatory Graz-Lustbuehel. First test measurements to LAGEOS started in April 1982. Since October 1982 the laser station Graz is fully operational.

Up to now about 450 passes of LAGEOS, STARLETTE and BEACON-C have been measured (fig. 1). The single shot RMS jitter of the measurements is now in the range of +/- 2 cm to +/- 4 cm for all satellites (fig. 2).

The laser measurements can only be made during night time (from midnight to 6^{00} in the morning) due to restrictions from the aircraft authorities.

Laser

The laser system, made by QUANTEL, consists of a passive mode-locked Nd:YAG laser (100 ps pulse width; 10 Hz/5 Hz/2.5 Hz repetition rate; 100 mJ per pulse at 532 nm) and an additional ruby laser (passive Q-switched; up to 0.25 Hz; 3 ns/2.5 J or 6 ns/4 J).

All results up to now have been obtained with the Nd:YAG laser at a 2.5 Hz repetition rate; most times the single pulse energy is kept in the 30 to 50 mJ region; this provides enough energy for LAGEOS while keeping power densities at mirrors etc. low. Some passes of LAGEOS and STARLETTE have been measured with pulse energies of about 2 to 5 mJ without major problems (the last amplifier of the Nd:YAG laser was switched off).

Mount, telescope, detection package

The mount and telescope system (CONTRAVES) has proven high reliability; one of the most useful features is the ISIT-camera. About 2/3 of all passes allow visual observation of the satellite (night time); therefore the absolute pointing accuracy requirements can be somewhat diminished, while still allowing blind tracking, if necessary. Furthermore, it reduces the necessary re-alignment work: Although there is some drift of the mirror mountings in the Coude path, readjustment of these mirrors is done only in intervalls of about 6 months or more.

The detection package still uses the relatively slow RCA 8852 PMT, a conventional HF amplifier and the Ortec 934 constant fraction discriminator. During the last year some effort has been made to optimize this package (adjustment of the discriminator, use of different amplifiers, different high voltages of the PMT etc.). As a consequence, the RMS jitter of the measurements went down from the initial +/-5 cm to +/- 8 cm and more to around +/-2 cm to +/-4 cm (fig. 2).

The Ortec 934 discriminator still produces some time walk, especially for the multi-photon-electron returns of the lower satellites; therefore a Tennelec TC454 constant fraction discriminator has been bought and will be installed during the next months. With this and some other modifications

it is hoped to reach an even better single shot accuracy.

Timing and calibration

Some improvements have been made in the timing system. The 1-Hz-pulse and the 10 MHz standard frequency are transmitted via fibre optics from the TUG time laboratory (within the observatory) to the laser room; there the standard frequency is distributed to all instruments.

The transmission and distribution of the standard frequency introduced some noticeable jitter into the measurements; therefore a new fibre optic transmission and distribution system was developed and built by the TUG time laboratory; this new unit was installed at the end of August 1984, lowering the RMS jitter of the laser measurements again (fig. 3, RMS jitter of the calibration values; notice the step at the end of August 1984). Details of this unit are described in another paper (D. Kirchner).

Pre- and post-calibration measurements are done to a fixed target in about 400 m distance; during calibration, the laser is attenuated to about 2.5 micro-Joules before transmission via two mirrors; this results in single photon-electron detection, as with satellites, and avoids the sometimes dangerous full power ranging to terrestrial targets.

Differences between pre- and postcalibrations are most times less than 1 cm, but show a systematic trend of about 0.4 cm in the average, probably caused by some temperature effects within the system, but up to now not clearly enough identified.

Pass-to-pass variations of the calibration measurements are within a few centimeters, caused mainly by small variations of the initial manual setting of the PMT high voltage; if this voltage remains unchanged, the variations are below 1 cm.

Conclusion

The Graz laser station has now operated for almost two years on a seven days per week schedule. The most severe restriction during this time was the small allowed time of observation between midnight and 6^{00} (restriction from aircraft authorities); the lack of observations in May and July 1983 (fig.1) is due to the absence of any satellite passes within this allowed observation time; other periods with no observations have been caused by more or less continuous bad weather. About 5 % of all possible passes have been lost due to technical problems.

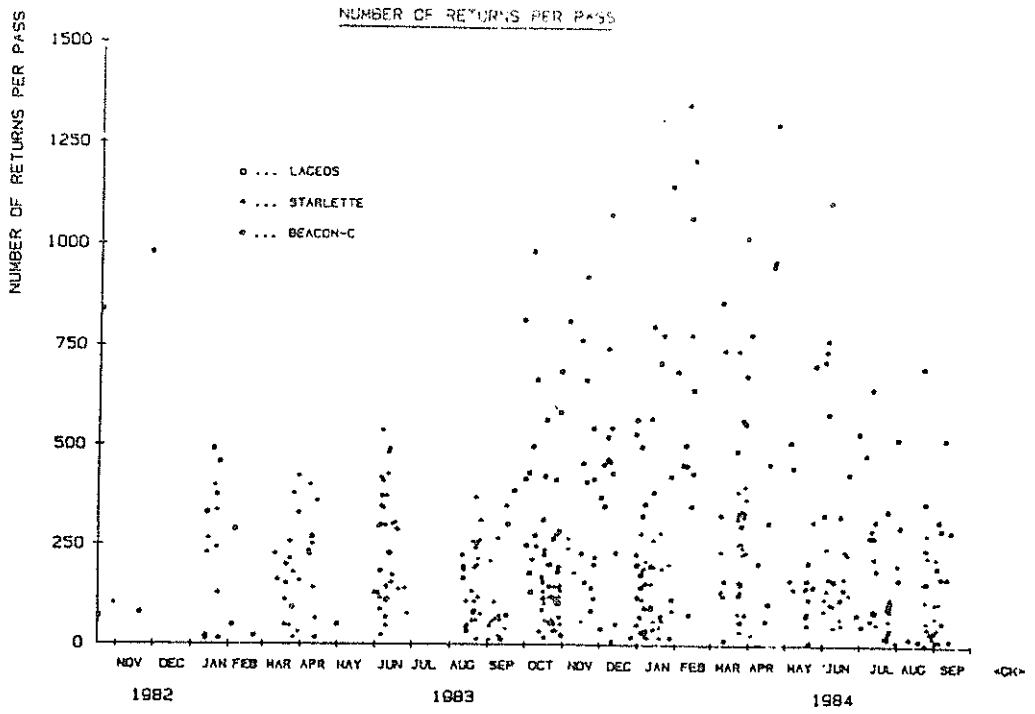

Fig. 1: Number of returns per pass

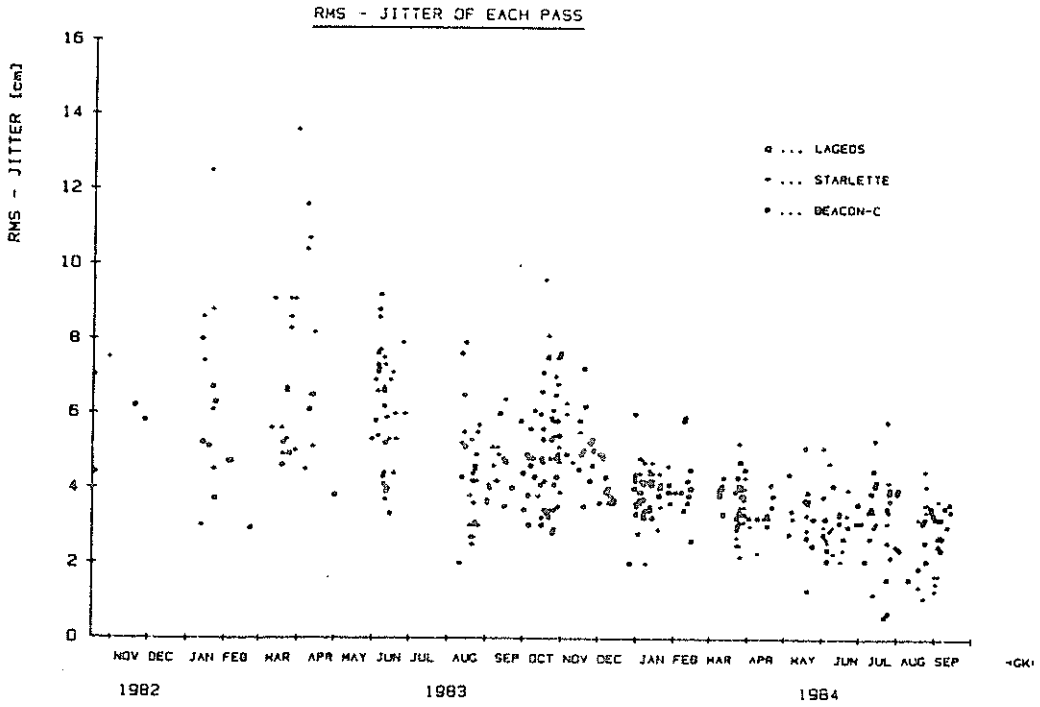

Fig. 2: RMS jitter of each pass

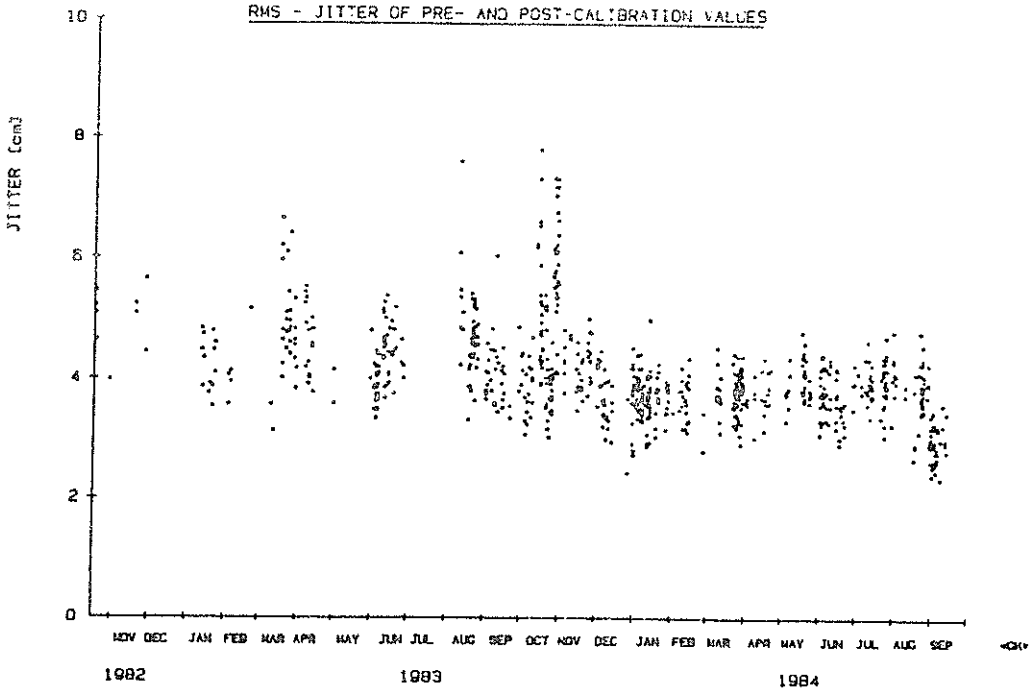

Fig. 3: RMS jitter of pre- and postcalibration values

FIRST RESULTS FROM SATELLITE LASER RANGING ACTIVITY AT MATERA

F. Palutan, M. Boccadoro, S. Casotto, A. Cenci, A de Agostini
Telespazio S.P.A., Roma

Telephone 64 987 254
Telex 611596

A. Caporali
Physics Department,
University of Padova

Telephone 49 661 1499
Telex 430176

ABSTRACT

Since September 1983 the Matera Laser Ranging Station has been tracking passes of LAGEOS, Starlette, Beacon-C, six days a week, on the basis of schedules provides by SAO and, more recently, by GLTN. In twelve months, more than 300 passes of LAGEOS have been observed. In many cases we had between 500 and 800 returns per LAGEOS pass, working at a pulse repetition frequency of 0.5 Hz. The range data for most of LAGEOS passes have a r.m.s. precision between 10 and 15 cm (1 sigma), as is indicated by the comparison of r.m.s. of polynomial fit of range data and the results of detailed calibrations. In this paper we review the system performance and report on preliminary results from the data analysis, in particular on the determination of the station coordinates within a network of laser stations, and preliminary baselines estimates.

FIRST RESULTS FROM SATELLITE LASER RANGING ACTIVITY AT MATERA

1. INTRODUCTION

The Matera Laser ranging station operates since September 1983 under an agreement between the National Aeronautics and Space Administration (NASA) and the Consiglio Nazionale delle Ricerche - Piano Spaziale Nazionale (CNR/PSN). Most of the equipment is an upgraded version of the Smithsonian Astrophysical Observatory (SAO) laser ranging system which has been operational at Natal, Brazil. The site near Matera was selected for several reasons, particularly because of its position in the Mediterranean area, its known seismicity, local geology (bed-rock) and weather conditions. The active support provided by the local Government of Regione Basilicata proved to be very important at every stage of the project. Telespazio provided technical support for the construction of the station and the installation of the equipment, and presently operates the station under a contract with CNR/PSN.

The construction of the station started in late 1982. In the same period, Telespazio engineers spent two months at the SAO station near Arequipa (Peru) and at SAO Headquarters in Cambridge, Mass., becoming familiar with the equipment and maintenance procedures.

In Spring 1983 SAO and Telespazio engineers jointly took care of the installation of the ranging system in the station, as well as of the final tests. Since January 1984 the station operates solely with Telespazio personnel.

In this paper we review the system performance and discuss an estimate of the overall level of repeatibility of the range measurements. Our analysis of calibration measurements indicates a precision between 10 and 15 cm for LAGEOS and

between 4 and 8 cm for Starlette.
Preliminary results are presented on the scientific work centered on the use of the data from the international laser network for the estimation of geodetic parameters, as Matera coordinates, and european baselines.

2. SYSTEM PERFORMANCE

2.1. GENERAL

A summary of the main technical data is given in Table 2.1. The characteristics of the upgraded SAO system are well known and we refer to the paper by Pearlman, Lanham, Wohn and Thorp (1) for their discussion.
With the exception of time synchronization system, some technical difficulties have been encountered, mostly due to aging of the equipment mainly at the beginning of operation. One of the most remarkable problems, during the first months (late September, October and early November 1983), has been the bad performance of the pulse chopping system which caused up to 10% of the pulse amplitude to be leaked in a leading edge extending as much as one half the length of the unchopped oscillator pulse (20 ns FWHM). As a consequence it often happened that, upon reception of the pulse, the stop-channel was anomalously triggered, especially when working at low return areas.
After some weeks of work and testing, the problem was fixed. The overall performance of the chopping system resulted considerably improved (leakage below 4%) even in comparison to the nominal level of performance.
No major problem was encountered in the start-stop system.

2.2. TIMING STABILITY

The time system in Matera is based on two rubidium frequency standards. Since the beginning of October we anticipate the

replacement of the primary standard with a HP 5061 cesium standard, procured by NASA.

Due to the vicinity of the LORAN-C station in Sellia Marina (about 200 km due South), synchronization to UTC (USNO) can be controlled to within 1 microsec by means of an Austron 2100 receiver of LORAN-C signals.

"A posteriori" check is done by means of an independent technique called TV SYNC. The method, proposed by prof. S. Leschiutta (2) (3), consists in comparing the second provided by the local clock with the epoch of the first vertical sync-pulse broadcasted by the national TV network. When two stations simultaneously compare their local second with the common TV sync-pulse, they can determine their relative time offset.

This method assumes a pre-synchronization of the clocks to within 10 msec, to avoid ambiguity with adiacent pulses which in fact are 20 msec long, according to Italian standards.

The precision of the time synchronization can be as high as 1 microsec, provided that the differential time of propagation of the TV signal between the two stations is known to the same accuracy (e.g. clock trip).

The advantages of TV sync are low cost and simple instrumentation, possibility of making measurements during each TV transmission and of monitoring the local time with respect to the national time scale which is maintained by Istituto Elettrotecnico Nazionale (IEN) in Torino. A somewhat cumbersome feature of the method is that a procedure of data exchange must be set up between the stations.

The behaviour of the Station Primary Standard with respect to UTC is shown in fig. 2.1. The initial synchronization to UTC was made on July 29, 1983 using the portable Cesium clock of IEN. This synchronization will be repeated in the occasion of the installation of the new cesium standard.

Although - as mentioned earlier - the synchronization to UTC could be precise to within 1 microsec, the local station time is permitted to drift from UTC (USNO) up to $\pm$ 20 microsec, in order to limit the number of resettings of the cycle-counter or of the frequency of the master oscillator. The epoch of

the observations are corrected to within 1 microsec during the data preprocessing phase.

So far, the average stability of the Primary Standard has been about 2×10^{-12} (occasionally 5×10^{-13}), so that the resetting of the cycle counter is necessary every 3-4 months. Only three resettings of the frequency of the master oscillator were up to now (August 1984) necessary.

Every time-jump is recorded on paper tape and noted in the log-book. We have noted that the time-jumps can sometimes be caused by electrostatic discharges or fluctuations in the power supply from the regional network. For this reason an autonomous power supply system is being considered to guarantee the necessary stability and continuity.

2.3. CALIBRATION STABILITY

All calibrations are made by ranging to a target board placed at a distance from the station of about 1.17 km. The separation between the center of the target and the Az-El axes intersection of the laser mount has been accurately surveyed by the Istituto Geografico Militare Italiano (IGMI) and is reported on Tab. 2.1.

Differences between the surveyed value and the values obtained by laser ranging are caused in part by gradients of the air refraction index along the line of sight, in part by internal system drift.

The first type of change in path length is correctable by means of local meteo data and a standard formula. Our main concern has been to use the calibration data to monitor the system drifts and to have an estimate of the achievable level of repeatibility in ranging to the target.

We distinguish between detailed target calibrations and prepass-postpass calibrations.

Detailed target calibration consists in ranging to the target and examining the response of the detection system to return pulses of various level of strength. We fire a number of pulses (25 to 100) and attenuate the returning light by means

of a neutral density filter at the receiving telescope. In this way we simulate the response of the detection system to pulse strengths typical of LAGEOS (0.3 to 3 photoelectrons) and of Starlette (3 to 100 photoelectrons).
Fig. 2.2 summarizes the results of the detailed target calibrations done so far. The "leakage" problem mentioned in subsect. 2.1 is evident in the first period of operation. For the remaining data we see that the level of system stability is between 0.7 and 1 nsec (10 to 15 cm) for low areas of the return pulses (up to 3 photoelectrons) and about 0.3 nsec (5 cm) for areas of the return pulses greater than 3 photoelectrons.
Pre-pass and post-pass calibrations are made with different neutral density filters, depending on the satellite.
Fig. 2.3 plots the difference between pre-pass and post-pass calibrations for the Lageos passes since beginning of operations: in most cases, these differences are below 0.2 nsec.

3. SATELLITE TRACKING

At Matera satellites are tracked on the basis of six nights per week, following schedules provided by the Goddard Laser Tracking Network (GLTN). LAGEOS is given top priority during the night. Starlette and - on a lower priority - Beacon-C are tracked also on daytime.
As part of the offline operations at the station, the computer generates schedules of observation. These are memorized on magnetic tape (Linc - Tape) and are used during the online operations (prepass calibration, satellite tracking, postpass calibration).
During each pass, the tracking system is monitored by the operators who intervene to maintain optimal tracking conditions by:

- operating "early-late" corrections on the timing of pulse emission, in order to keep the satellite under conditions

of optimal illumination, thus minimizing the effects of non linearities in the photomultiplier;
- attenuating the receiving signal whenever the electronics of the detection system is going to respond non linearly;
- varying the range gate, e.g. to lower background noise or minimize the risk of missing the satellite;
- changing the field of view of the telescope;
- changing the voltage of the flash-lamps, to have the required energy;
- modifying the trigger threshold of the chopping system, to maintain the chopping pulse near or slightly before the maximum of the oscillator pulse, to maximize the energy of the output pulse and keep leakage within tolerance.

In fig. 3.1 a "tracking budget" is summarized since the beginning of operations. "Successful passes" have at least 20 returns.
A pass is acquirable when maximum elevation is above 20 degrees. For LAGEOS the pass must take place during the night. For Starlette, nightly passes cannot conflict with LAGEOS.
In fig. 3.1. one recognizes that bad weather still is the main reason for unsuccessful tracking.
In order to improve the planning of the shifts, a METEOSAT receiver was installed on December 1983.
Its data have proven most useful in local weather forecasting and other operational activities.

4. ANALYSIS OF THE PASSES

Since the beginning of the operational activity of the station, our group is also performing data analysis, as shown in fig. 4.1.
The "full rate" data produced at Matera are saved on linc-tapes and regularly shipped to GLTN. In order to have these data available in a short time for pass-analysis, a procedure was developed to transfer the data on 9-track

magnetic tapes.
The data are then systematically processed by the pass-analysis program with the VAX at Telespazio. In this way we could keep a record of some interesting information for each pass, such as duration, total number of returns, r.m.s. of "best-fitting" (in the weighted least squares sense) polynomials, number of "good" returns (i.e. residual less than 2.5 r.m.s.), the difference between pre and post-pass calibration.
Fig. 4.2 gives an example of "historical record": the r.m.s. of post-fit residuals of the raw data of each pass to the "best-fitting" polynomials is plotted as a function of time. Initially we had the leakage problem mentioned in subsection 2.1, so that large r.m.s.'s are not surprising in passes from late September to early November.
Apart from that, on average the r.m.s.'s are between 10 and 15 cm for LAGEOS and 4 to 8 cm for STARLETTE.
We consider this result very interesting, because it is fully consistent with the system precision independently measured during the detailed target calibrations (see subsection 2.3). Moreover, this level of intrinsic repeability of the ranging system at Matera is also in agreement with the values provided by SAO on its latest upgraded equipment (4).
Finally, we have worked on several orbital solutions with GEODYN, using LAGEOS full rate data from 1 to 15 October 1983 (about 12000 observations from 13 stations) and from 10 to 25 November 1983 (about 11000 observations from 13 stations).
The statistical analysis of the passes over Matera (the coordinates of which were estimated) show that the Matera weighted residuals have a r.m.s. value of 23 cm for the october data and of 19 cm for the november data; the total r.m.s. of residuals for all the stations are respectively 18 cm and 17 cm. These values are slightly larger than the estimates obtained through target calibrations. This increase in r.m.s. values can be interpreted in terms of uncertainties of the force model of the order of 15 cm (1 sigma).

5. PRELIMINARY RESULTS OF SCIENTIFIC WORK

Our data analysis work is part of a scientific project of investigation of Crustal Dynamics in the Mediterranean Basin endorsed by PSN-CNR and approved by NASA within the Geodynamics Program.
The three main goals of our work are:

- to monitor the Matera coordinates and compare the laser estimates with those obtained by means of Doppler and conventional ground-based surveying;
- to obtain polar motion estimates with increasing time resolution, possibly one-day or better;
- to compute baselines joining Matera to other laser stations, particularly the European ones.

Estimates of Matera coordinates with several techniques and obtained by differed Institutions are given in Tab. 5.1. The estimates with GEODYN appear to be significantly repeatable independently of the analyst and of the set of data.
Table 5.2 contains preliminary estimates of european baselines. We remark that these estimates, obtained by means of a multiparameter dynamical solution with GEODYN, await for comparison with a similar solution using other sets of full rate data or normal points, and with solutions obtained with the translocation method.
We have verified that adjusting the coordinates of the polar axis and UT1-UTC at a frequency higher than the usual five days decreases the r.m.s. of the post-fit residuals of a few centimetres.
It is possible that polar motion has structure with nearly diurnal period, in the reference system we use. We are working on solutions with diurnal or even semi-diurnal adjustments of the pole coordinates, and the results will be published soon.

6. CONCLUSION

In 1981 one of us attended at the 4° edition of this Symposium at Austin, Texas. In that occasion the idea of placing a laser station in Southern Italy was first conceived, particularly because of the interest and support of the late prof. G. Colombo.

Three years later, the Matera station is a reality, thanks to the support provided by Piano Spaziale Nazionale and Regione Basilicata, the collaboration from Colleagues of Italian and Foreign Institutions, particularly NASA-GSFC, EG&G and SAO, and the dedicated work of the Station Team, led by Mr. W. Sacchini.

The work done permits to report at this Symposium on preliminary technical evaluations and scientific results.

Still considerable work remains to be done. We feel that the data analysis can probably be continued systematically, since adequate software is available. For the future, most of the effort will have to be put in the replacement of the actual equipment with a third generation laser system in Matera, and in the construction of a transportable system, for the systematic surveying of some reference baselines in Italy.

R E F E R E N C E

1. M.R. Pearlman, N. Lanham, J. Wohn, J. Thorp:
Current Status and Upgrading of the SAO Laser Ranging Systems.
Proc. of the 4° International Workshop on Laser Ranging Instrumentation, Univ. of Texas at Austin, Ed. by P. Wilson, Bonn 1982, Vol. 1, pg 43

2. D.W. Allan, S. Leschiutta, G. Rovera:
TV Frame Pulses Used for Precision Time Synchronization and Their Noise Distribution
Alta Frequenza, Vol. 39, pg 452, 1970

3. S. Leschiutta:
Long Term Accuracy and Time Comparisons Via TV Signal Along Radio Relay Links.
Trans. IEEE, Vol. IM-22, pg 84, 1973

4. Smithsonian Astrophysical Observatory, Experimental Geophysics Group:
Modified Laser Data System Manual
Vol. 1 pg 1-11, Change 4-2-83

LASER SYSTEM	
- wavelength	6943 A°
- energy/pulse	0.5 joule
- pulse width	3 ns
- firing frequency	30 ppm max
OPTICS	
- transmitting telescope	galilean, 12.7 cm lens
- beam divergence	2 arc min
- receiving telescope	Cassegrain, 50.8 cm mirror
- mount type	Az-El, computer controlled
- pointing accuracy	$\pm$ 30 arcsec, with thermal control of backlash
- slew rate	2°/sec
- pass-band filter	3 A°
PHOTOMULTIPLIER	
- type	Amperex XP2233P
- quantum efficiency	4%
- gain	$3-4 \times 10^{7}$
- rise time	2 ns
TIME AND FREQUENCY SYSTEM	
- frequency standard	Rubidium
- estimated stability	2×10^{-12}
- synchronization	Loran C/TV Sync
- resolution of interval counter	0.1 ns
CALIBRATION	
- external target	1172.190 m
- standard deviation of the detection system	$\pm$ 1 nsec at 1 p.e.
- short term drift (prepass - postpass)	0.1 - 0.5 nsec
METEO SYSTEM	
- Meteosat receiver	24 h coverage
- digital pressure sensor	resol. 1 mB
- digital temperature sensor	resol. 0.1 C
- digital humidity sensor	resol. 1%
COMPUTER	
- Data General NOVA 1200 (16 bit)	32 k core memory

TABLE 2.1.
TECHNICAL CHARACTERISTICS OF THE
SAO LASER STATION AT MATERA

SOURCE	LATITUDE (deg)	LONGITUDE (deg)	HEIGHT (m)	X (m)	Y (m)	Z (m)	SIGMA (m)
IGM (ED79) (FEB 83)	40°38'59".2245	16°42'19".6437	490.22				
DOPPLER (SEPT 83)	40°38'55".546	16°42'16".097	505.2	4641973.9	1393053.8	4133257.2	
GTDS (24.3.84) (1-15 SEPT 83)	40°38'55".004	16°42'17".824	516.281	4641945.5	1393087.6	4133258.9	2.8
GEODYN (15.3.84) (1-15 JAN 84)	40°38'55".7783	16°42'16".6955	529.242	4641966.9	1393066.4	4133262.1	0.3
UNIV. OF TEXAS (SL5.1)	40°38'55".7484	16°42'16".6608	528.385	4641967.7	1393065.8	4133261.4	
GEODYN (20.8.84) (1-15 OCT 83)	40°38'55".7969	16°42'16".6761	528.970	4641966.46	1393065.76	4133262.34	0.21
GEODYN (30.8.84) (10-25 NOV 83)	40°38'55".7834	16°42'16".6821	528.751	4641966.52	1393065.93	4133261.89	0.20
GEODYN * (OCT 83)	40°38'55".79	16°42'16".69	528.9				

ELLIPSOID			
	GTDS	: R = 6378.144	1/F = 298.255
	GEODYN	: R = 6378.144	1/F = 298.255
	TEXAS	: R = 6378.145	1/F = 298.255
	DOPPLER	: R = 6378.388	1/F = 298.0

* Private communication of P. DUNN, August 1984

TABLE 5.1

ESTIMATES OF MATERA COORDINATES

	WETTZELL	RGO	GRAZ
MATERA	990118.51 ± 0.80	1694490.71 ± 0.31	719404.63 ± 0.32
GRAZ	302138.21 ± 0.99	1183242.71 ± 0.38	
RGO	917334.43 ± 1.15		

a) Quick look data 1-15 january 1984

	WETTZELL	GRAZ
MATERA	990118.92 ± 0.17	719405.15 ± 0.15
GRAZ	302138.22 ± 0.21	

b) Full rate data 1-15 october 1983

	WETTZELL	GRAZ
MATERA	990119.14 ± 0.15	719405.07 ± 0.16
GRAZ	302138.64 ± 0.13	

c) Full rate data 10-25 november 1983

TABLE 5.2.

SOME EUROPEAN BASELINES IN METERS ESTIMATED WITH GEODYN
(FORMAL ERROR 1 SIGMA)

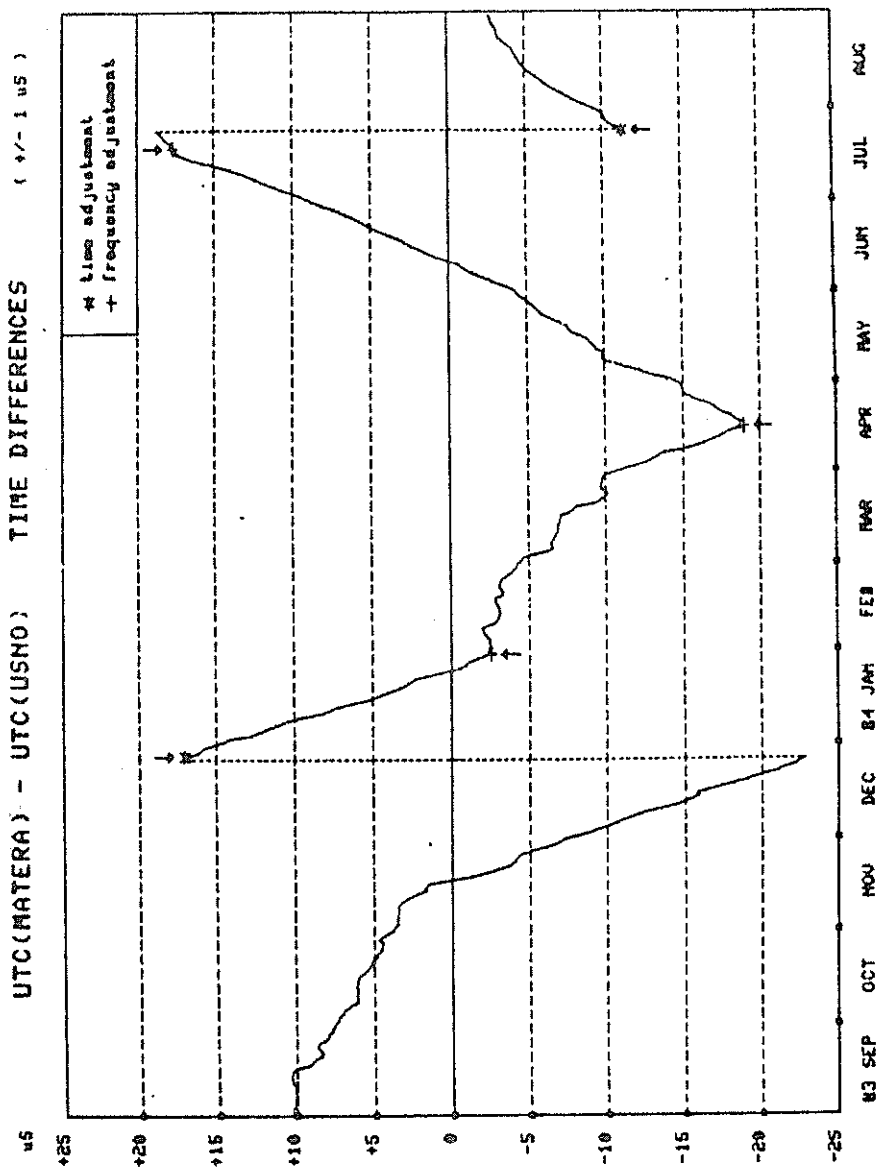

Fig. 2.1 - Behaviour of the Matera master clock with respect to UTC

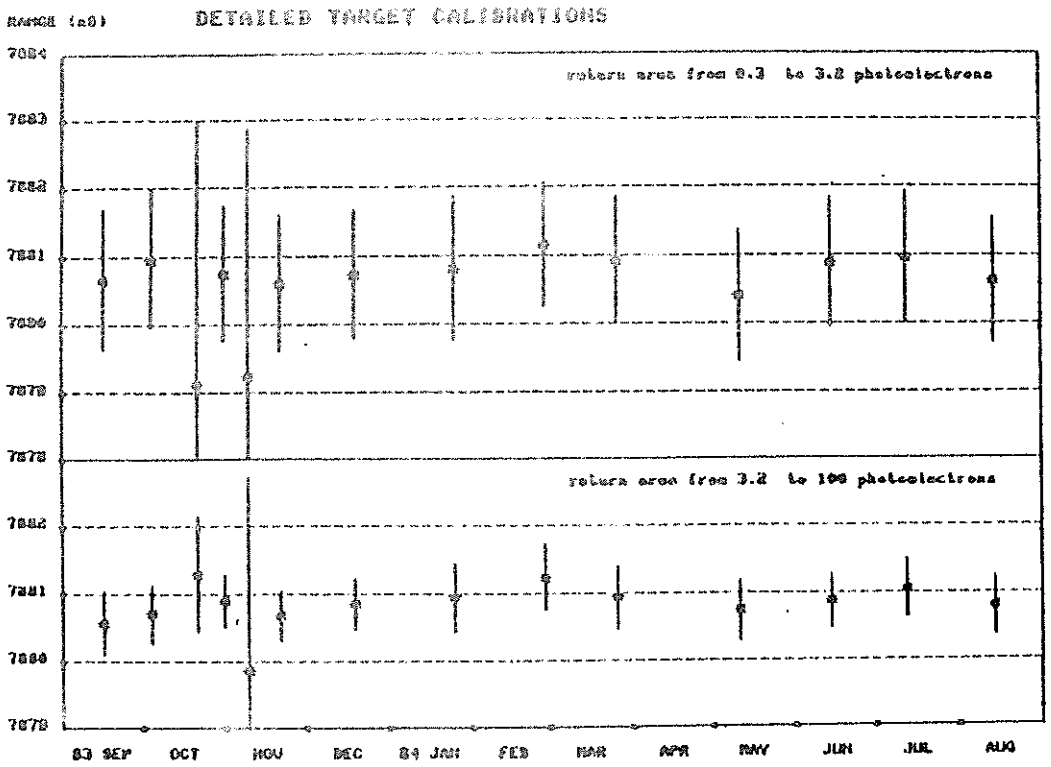

Fig. 2.2 - Results of the detailed target calibrations for different return areas

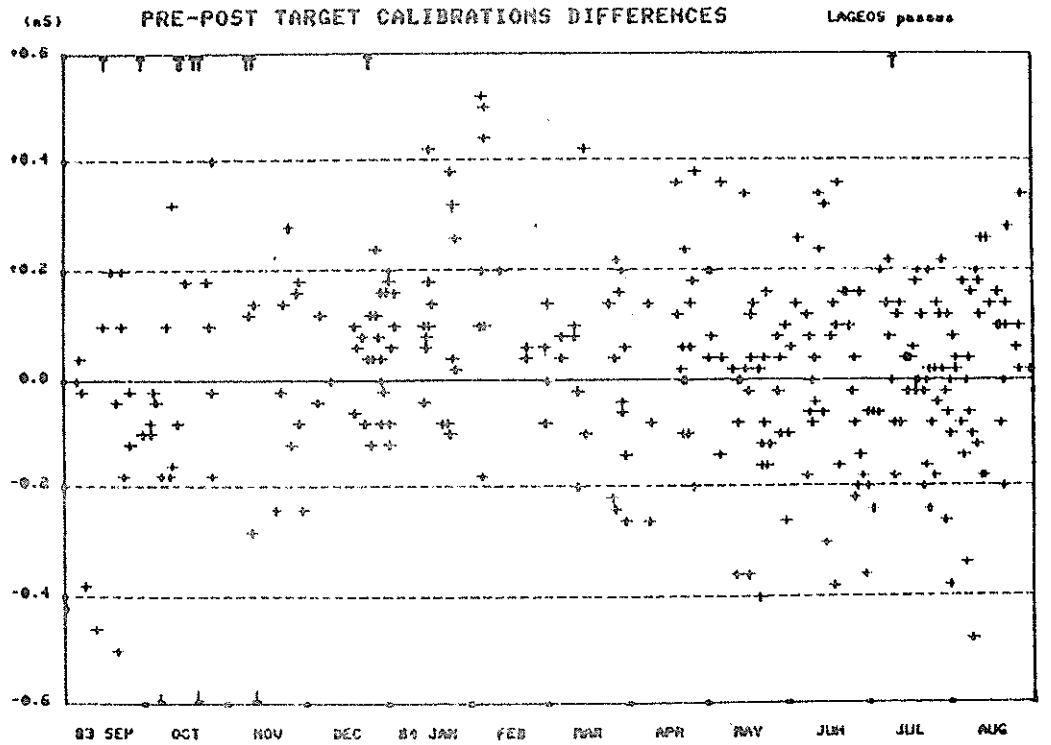

Fig. 2.3.

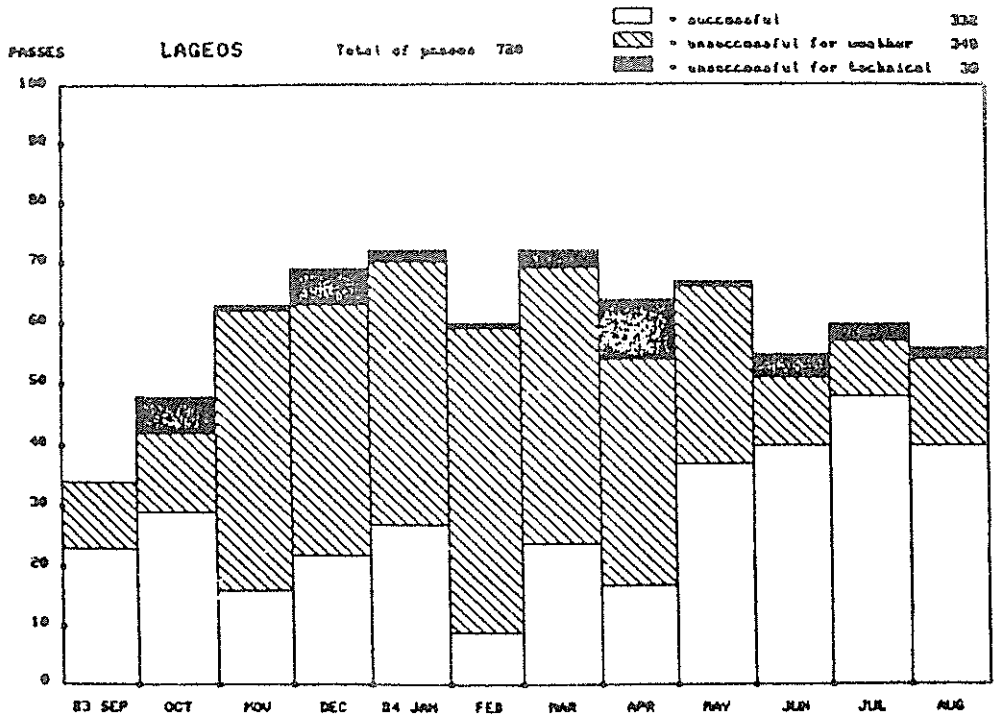

Fig. 3.1.a - Influence of weather and technical problems in the tracking of LAGEOS

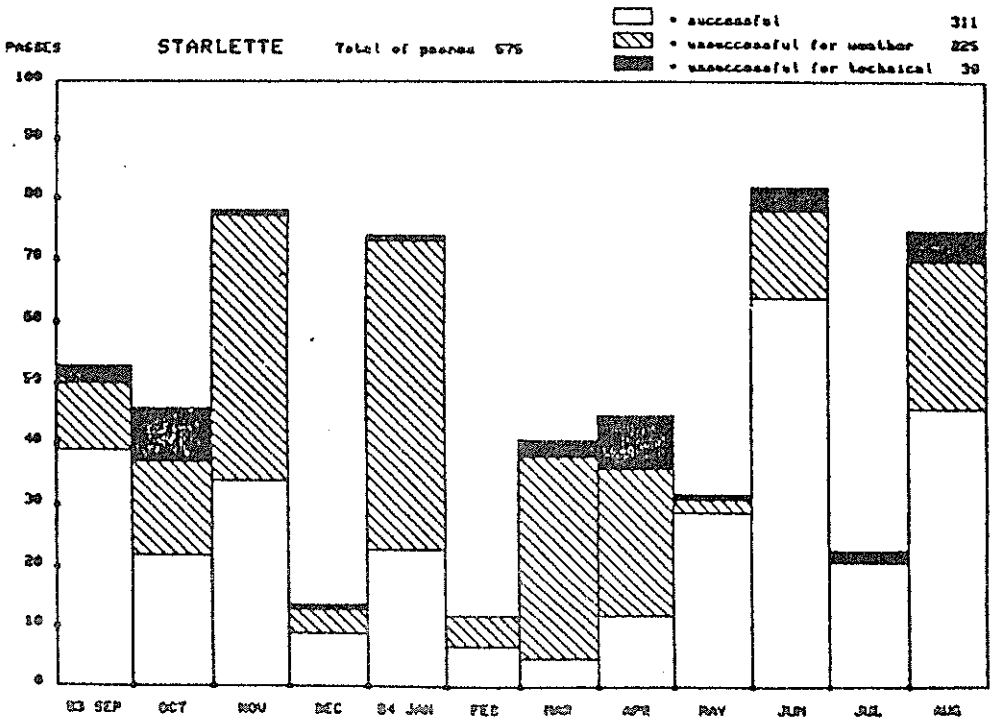

Fig. 3.1.b - Influence of weather and technical problems in the tracking of STARLETTE

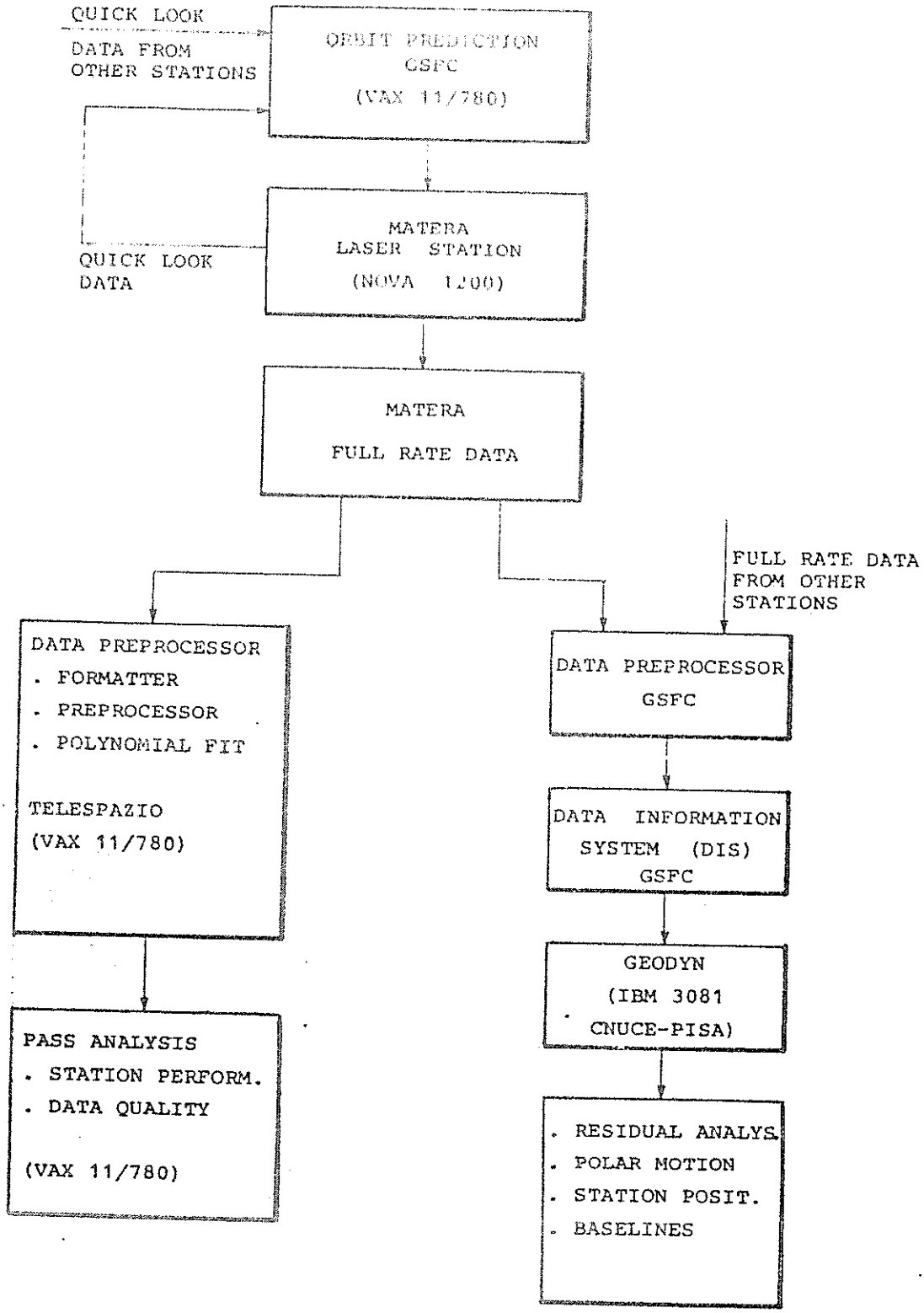

FIG. 4.1. - BLOCK DIAGRAM OF MATERA LASER DATA HANDLING AND SCIENTIFIC ANALYSIS

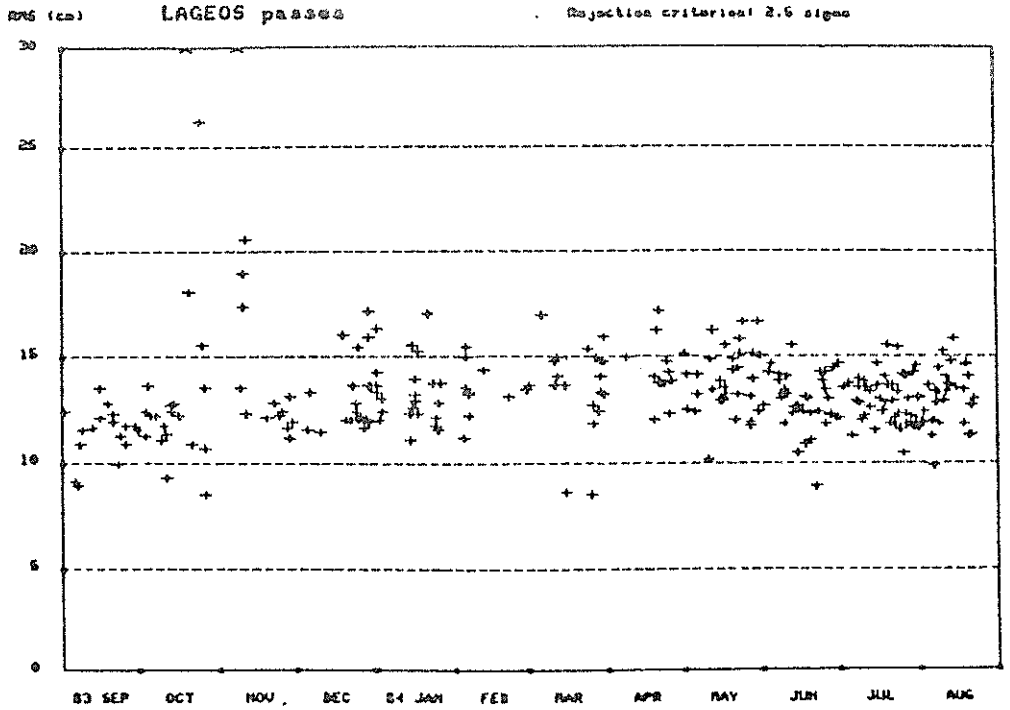

Fig. 4.2.a - Time-behaviour of the r.m.s. of best fitting polynomials to LAGEOS DATA

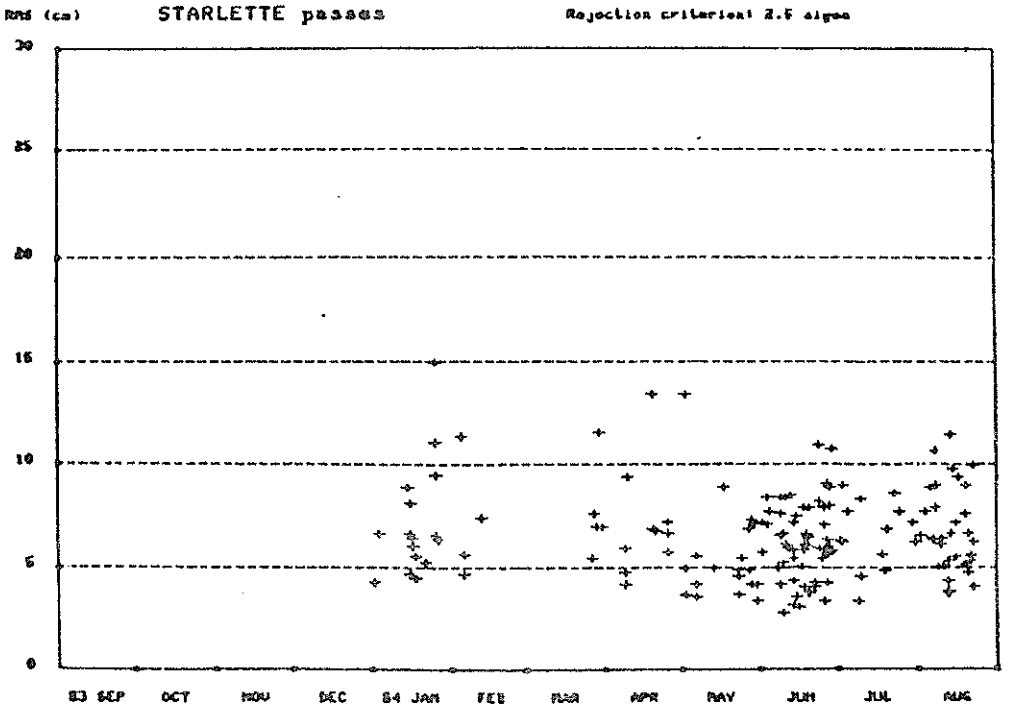

Fig. 4.2.b - Time-behaviour of the r.m.s. of best fitting polynomials to STARLETTE DATA

PROGRESS REPORT 1984

I. Bauersima, P. Kloeckler, W. Gurtner,
Astronomisches Institut
Sidlerstrasse 5
CH - 3012 Bern Suisse

Telephone 31 65 85 91
Telex 32320

1. INTRODUCTION

Purpose of this report

The report presented in this brochure covers the progress achieved at Zimmerwald Laser Observation Station during the years 1979-1984. It also outlines some plans for further development of the Sation. Form and contents of the report have been chosen to serve the following two purposes:

- Exchange of experience with stations both already existing or under construction.
- Progress report to the organisations which provide funds for our research. These organisations are:

  The Swiss National Science Foundation
  The Canton of Berne
  The Geodetic Commission of the Swiss Academy of Science and
  The Swiss Federal Department of Defense .

1.1. Historical Remarks

The experiences with the original ruby laser (Klöckler et al., 1978) during SHORT MERIT (August/September 1980) have shown that any further efforts with this system would be inefficient and could no longer be justified. With the aim of joining the main MERIT campaign 1983/84, the acquisition of a third generation laser system was immediately initiated (Bauersima, 1981, paragraph 4.3.5). The scientific importance of this development had already been laid down in (Bauersima, 1979, Table 2).

The building of the new LRS was delayed by financial problems until spring 1983. The construction itself was taking a relatively slow pace because many obstacles had to be overcome. (Optical and mechanical properties of components were not consistent with the vendor's specifications.) A diagram of the LRS is presented in Fig. 1.
The first successful ranges to LAGEOS were finally obtained on May 15, 1984. From there on, an increasing amount of ranging data could be acquired and sent to the computing centres.

1.2. Direction Observations

The original dye laser for illumination/purposes is no more contained in the present system. It should have permitted photographic direction observation to geodynamic satellites as STARLETTE and LAGEOS. The importance of such observations had often been noted (e.g. Klöckler et al., 1978 or Bauersima, 1981). Since then we have evaluated the possibility of optoelectronic observation of certain celestial fields along the satellite's orbits. The concept of illumation lasers appears for many reasons to be outdated.

The development of an appropriate digital image processing system could not be started yet because of scarcity of funds. Yet we hope to tackle this challenge in the frame of our CQSSP*) project (Bauersima, 1984) which has won support of the Swiss National Science Foundation.

1.3. Outlook

The digital optoelectronic image processing system that will comprise the cornerstone of project CQSSP*) will also be linked with the tracking TV-camera of our LRS. This will allow simultaneous ranging and direction observations of geodetic satellites.

The accuracy of relative station positions determined by laser ranging observations increases with the number of such observations. To each number of observations, an average time interval can be related in which these observations have been made. There exists a characteristic time interval such that the local anomaly of corresponding position shift due to crustal dynamics significantly becomes greater than the mean error of the station's positions gained during this interval. This characteristic interval is generally not known in advance; therefore it is suggested that periodical surveying links between the LRS and a large network of triangulation markers be made (e.g. once per year). The latter should be resting in a common and geologically stable formation. This task is equally important as the laser observations themselves are. Not long ago, the surveying expense for this goal would have been enormous. In the near future, this high precision local survey will be made possible thanks to radio-interferometric observations of GPS satellites (Bauersima, 1983a),b) and Beutler et al., 1984). Here we want to stress the point that if a network of more than three points has to be surveyed, a minimum of four receivers (e.g. MACROMETER-stations) is necessary for high precision surveying. This for the reason that the influence of ephemeris errors practically cancel if during each quasi-simultaneous observation set at least three receivers are placed at sites which have been previously surveyed in a quasi-simultaneous mode (Bauersima, 1983b), p. 41).
In order to undertake autonomously radio-interferometric GPS observations in a country like Switzerland, at least four receiving sets will have to be either acquired, loaned or rented.

---

*) The aim of CQSSP is, briefly spoken, to provide a reliable link between a star catalog (as the one being generated by project HIPPARCOS) and a quasar fixed reference frame. One segment, called CSSP, will link catalog stars and satellites of the Global Positiong System by optical observations. The other, CQSP, will provide a link between quasars and GPS-satellites by radio-interferometry.

The result of such periodic surveying ties between the LRS and the surveying markers mentioned above would be equivalent to the fictive foundation of that LRS in the local primitive rocks. Besides the importance of this fact for global geodynamics, also questions about local or regional geodynamics can be tackled in the same radio interferometric survey. With regard to the organisation of such local GPS campaigns we hope to gain support from organisations which have supported the activities of Zimmerwald Laser Observation Station so far, as well as from such organisations that have an interest in these campaigns for other reasons.

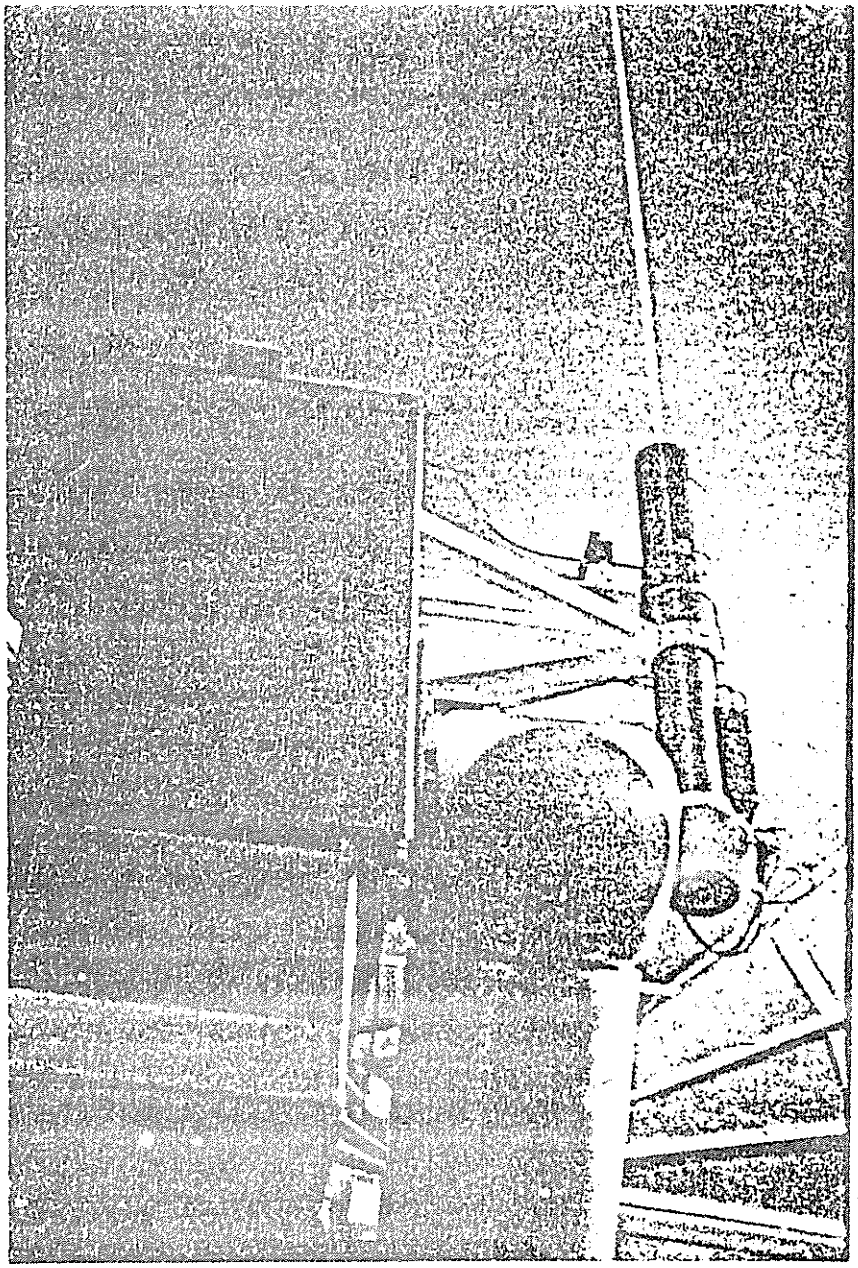

NIGHT EXPOSURE OF THE UPGRADED ZIMMERWALD LASER RANGING TELESCOPE

2. HARDWARE

2.1. Laser Transmitter

The new Nd-YAG laser has the characteristics of a QUANTEL YG 402 DP model, although it has been built from components on the existing stone bench without the performance warranty which usually is part of the deal. The mechanical and optical quality of components supplied by QUANTEL (France) was not always satisfactory, heavy radio interference had to be coped with, and the pulse selector crystal had to be replaced because of electrode disintegration.

Since early 1984, the laser operates satisfactorily, though at a reduced output level. A pyroelectric energy meter (LASER PRECISION RJ7100) was utilized to monitor the output. Its readings appear doubtful, but calibration is under way. Lifetime problems exist with KD*P crystals of the second harmonic generator.

Further improvements of the laser should include spatial filtering and possibly active/passive mode locking to improve beam quality and reduce energy fluctuations.

2.2. Receiver, Timing

The receiver subsystem and the associated electronics are depicted in Fig. 2. It is shown as used in MERIT 1984 and is commented on in the following paragraphs.

Photomultiplier

Various types can be housed in the refrigerated cabinet by PRODUCTS FOR RESEARCH Inc. Presently used is the linear focused, 13 dynode device D341B by EMI-GENCOM, yielding a gain of $5 \cdot 10^7$ @ 2400 V. The timing resolution was found to be approx. 500 ps at 1 photoelectron and 100 ps at 10 photoelectrons.*)
A second detector tube utilizing two microchannel plates was experimentally being used. The results indicate that a timing resolution below 200 ps can be achieved in single photoelectron regime.*)

The P.M. tube is preceded by the laser line filter, where two band widths can be selected. A BALZERS Inc. 60 Å filter was utilized throughout MERIT 1984, because only night time tracking was performed. The second one, a DAYSTAR 3 Å filter, will be employed as soon as daytime operations commence. Its transmission is approx. 20 - 30 %, if temperature is optimized.

The chopper wheel was not in use as to this date in order to keep receiver complexity as low as possible. Backscatter from the laser is a problem if the microchannel device is used (lifetime problem). It also blocks the pulse amplitude reading when in-pass calibration is made (viz. 4.1.).

*) viz. the paper "First Experiences with Microchannel Photomultiplier" at this workshop

Time-of-Flight Electronics

An ORTEC 934 model constant fraction discriminator, preceded by a LECROY 133B amplifier (risetime 1 ns , gain 10x), discriminates all pulses above 100 mV. The residual time walk is substantial (viz. Figs. 3 and 4), so leading edge discrimination is still considered, particularly with the 380 ps risetime pulse of the microchannel device. In this case, the amplifier used will be the model AC 3000 by B&H (risetime 130 ps).
The pulse charge (number of photoelectrons x gain) is monitored by a LECROY 2249 mod. charge-to-digital converter.

Time-of-flight is measured with a LECROY 4202 model extended time-to-digital-converter (T.D.C.). Resolution is 156 ps, with a differential nonlinearity of ± 2 LSB. This could only be achieved after an external 100 MHz clock pulse was used instead of an internal crystal oscillator, which had too much phase noise. The external standard is derived from the 5 MHz station oscillator by harmonic multiplication, so its time bias is monitored and controlled to be smaller than $10^{-10} \hat{=}$ 1,5 mm/15000 km.

The range gate delay and width, and the epoch are generated in 3 separate real time clock modules, the resolution being 100 ns with an uncertainty of ± 50 ns. Minimum gate width is chosen to be 200 ns. Gating is performed within the T.D.C.

The range gate is controlled by a real time filter algorithm*) in the computer which adapts gate delay and width to the return pulse offsets. Once the filter is in "lock"-mode, very few false return are noticed (night operation).

Epoch timing

The epoch is compared with the LORAN-C second (a total timing delay of 33.074 ms being applied) for a quick look timing accuracy of ± 5 µs. Daily TV comparisons with UTC (OFM) allow an "a posteriori" adjustment to within ± 1 µs.

Station frequency standard is basically a model B1326 oven-controlled crystal oscillator by OSCILLOQUARTZ SA. Its phase vs. LORAN-C is registered and steered to be < 10 µs/day.

*) viz. the paper "Real Time Filtering of Laser Range Observations" at this workshop

Mount and Associated Electronics

The mount is driven by two DC servo motors and computer controlled via CAMAC. Position feedback comes from two incremental angle encoding systems (resolution 16 microradians). An angular readout processor corrects the optical encoder outputs for bias variations. The encoder disks are mounted directly in the instrument's axes in order to avoid gear errors.

The errors in the mount axes could be well determined by star tracking. Still lacking is a model of the transmit/receive noncollimation which would be necessary for daylight tracking.

The transmit optics have been fitted with a divergence control (.1 through 1 mrad).

On the receiving side, the calibration paths (light fibre and direct) with variable attenuator and the light collection optics have been added. A variable speed/laser synchronous chopper and a safety shutter are part of the receiver package, as well as the refrigerated photomultiplier cabinet and the associated HV supply.

A digital remote control unit monitors the above devices from the operator's console which also comprises a joystick to allow for tracking corrections by joystick.

The most valuable asset for this purpose is still the Intensified-Silicon-Intensified-Target TV-camera seated on top of the receiving telescope (limiting magnitude m ∿ 14).

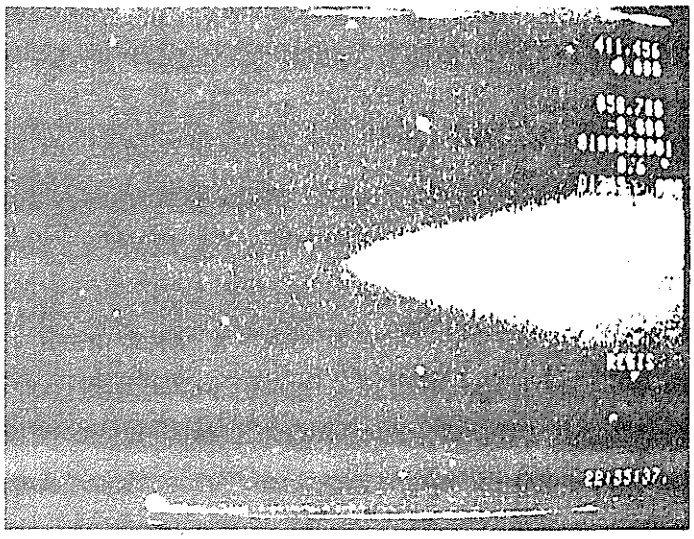

IMAGE PRESENTED TO THE OBSERVER DURING TRACKING SESSION. LAGEOS IS BARELY VISIBLE AT THE APEX OF THE LASER BEAM. SOME OF THE DISPLAYED INFORMATION IS NOT LEGIBLE BECAUSE OF LASER FIRING.

3. COMPUTER FACILITIES

3.1. Hardware

Station computer is a PDP-11/40 under RT-11 operating system. Core memory is 64 K bytes. Peripherals comprise a graphic display (VT 11 graphic processor), a second data terminal, two RKØ5 disk drives, a 9-track magtape (800/1600 bpi), a CAMAC interface system and 5 channel paper tape reader and punch.

Off-line data processing can be done on the University's IBM 3083/ 3033 mainframe computer. Data communication between mainframe and mini is by magtape or via telephone modem.

This modem also will facilitate access to G.E. Mk. III data network, which possibility is presently considered.

3.2. Software

General software for telescope handling allows positioning, initializing and testing of angle encoders and determination of the telescope's axes by evaluation of encoder readings to catalog stars.

Preparatory programs perfom the following tasks:

- input and error detection of SAO mean elements telex message.
- listing of possible satellite passes and ephemeris computation thereof AIMLASER (adapted to IBM mainframe by Delft University) and University of Texas IRVINT have been adapted to run on the University's mainframe computer.
- computation of coefficients and parameters used for the on-line filter algorithm.*)

The tracking software controls the laser and collects time-of-flight, angle encoder readings, epoch, return pulse strenght and various relevant system parameters. It also performs on-line filtering of data, range gate control and in-pass range calibration.**) This data can be monitored by the operator on the TV screen, along with the tracking camera's image.

Further off-line data screening of range measurements affords graphic display of residuals against ranges computed with AIMLASER or IRVINT reference orbit. Subsequent orbit improvement is made by least squares parameter estimation using numerical orbit integration. R.m.s. values of ranges are displayed and false returns eliminated. In-pass calibration values**) are first screened and then curve fitted and interpolated for each range measurement.

---

*) viz. paper "On-line Filter Control of the Range Gate" at this workshop

**) viz. paper on "In-Pass Calibration during Laser Ranging Operation" at this workshop

Final data handling procedures are:

- storing of range data and system parameters in an internal format on backup disk or tape.
- extraction of a portion of observations for quick look data and generation of a telex paper tape in SAO format.
- copying of range data onto magtape in the SEASAT format for distribution to computing centers.
- display of residuals (raw and respective to best fit orbit). Also being displayed are range residuals vs. return strenght to visualize residual discriminator systematics.

4. RESULTS

4.1. Calibration

A prerequisite for precise ranging results is certainly a good and consistent range calibration. During MERIT 1983/1984, this calibration value was subject to change because of delay line adjustment of the constant fraction discriminator. The temporal variations of the calibration "constant" are presented elsewhere *).

The noise contributions of the various timing components have been partly isolated. It was demonstrated that the main contributor to timing noise (jitter) is still the photomultiplier. What accuracy concerns, there have been rangings made to an external target at about 1.4 km. This distance has been verified by an independent survey of the Federal Office of Topography to within ± 1 cm, as compared with the laser results using "in-pass" (internal) calibration.

4.2. Ranging Data

A list of data submitted to the computing centers in a "quick-look" selection is presented in the appendix. The given r.m.s. noise of the data is estimated after passing our off-line screening where 4 (Starlette) or 5 (Lageos) orbital parameters are fitted. This being an absolute minimum of coefficents to be estimated, we believe these values to be a conservative estimate.
A set of plots is presented in Figures 3 - 6 , where the present capabilities of our data screening and displaying software are demonstrated.

---

*) viz. the separate paper on "In Pass Calibration during Laser Ranging Operation" at this workshop

CONTRIBUTORS

The following persons have contributed to this project for the reported period:

Dr. Ivo Bauersima (group leader geodynamics); Dr. Gerhard Beutler (celestial mechanics, digital filtering, numerical analysis); Dr. Werner Gurtner (geodesy, hard- and software design, operations); Paul Klöckler (electronics and hardware design, operations); Eugen Pop (laser physics, operations); Markus Rothacher (software); Samuel Röthlisberger (mechanical engineering); Thomas Schildknecht (electronics, operations); Prof. Max Schürer (optical design); Christine Strickler (secretary).

REFERENCES

Bauersima, 1979	Memorandum über die Aufgaben und den heutigen Stand der Satellitengeodäsie in der Schweiz
Bauersima, 1981	Konzept der Satelliten-Beobachtungsstation Zimmerwald (Bericht an den Schweizerischen Arbeitskreis Geodäsie/Geophysik), Mitteilungen der Satellitenbeobachtungsstation Zimmerwald, Nr. 6
Bauersima, 1983 a)	Navstar/Global Positioning System (GPS) (II), Radiointerferometrische Satellitenbeobachtungen, Mitteilungen der Satellitenbeobachtungsstation Zimmerwald, Nr. 10
Bauersima, 1983 b)	Navstar/Global Positioning System (GPS) (III), Erdvermesssung durch radiointerferometrische Satellitenbeobachtungen, Mitteilungen der Satellitenbeobachtungsstation Zimmerwald, Nr. 12
Beutler et al., 1984	Some Theoretical and Practical Aspects of Geodetic Positioning Using Carrier Phase Difference Observations of GPS Satellites, Mitteilungen der Satellitenbeobachtungsstation Zimmerwald, Nr. 14
Klöckler et al., 1978	Progress Report 1978 of the Zimmerwald Satellite Observation Station, Mitteilungen der Satellitenbeobachtungsstation Zimmerwald, Nr. 3
Bauersima, 1984	Coupled Quasar, Satellite and Star Positioning (CQSSP), Mitteilungen der Satellitenbeobachtungsstation Zimmerwald, Nr. 13

TECHNICAL SPECIFICATION OF ZIMMERWALD LASER RANGING STATION
(1984, SEPTEMBER)

1. Telescope

	Tracking:	Receiving:
mirror size	525 mm	
focal length	1 m	
field of view	33' × 44'	6' diameter
spectral bandwidth	400-500/550-650 nm	532 ± .15 nm

Transmitting

type	coudé refractor
front lens diameter	.1 m
beam expantion factor	5 ×

Mount

type	biaxial horizontal
drive	DC servo disc motors
angular readout accuracy	5"
gear ratio	4800 : 1
max. speed	4°/sec
min. speed	5"/sec

2. Tracking

methods	closed-loop by computer with mount flexure model or visual using ISIT camera
pointing accuracy (visual)	± 30" (objects m < 15)
pointing accuracy (computer)	± 10"

3. Laser

type	mode-locked, frequency doubled Nd-YAG laser
emitted energy	450 mj IR, 125 mj green
puls width	100 ps
beam divergence	laser: .6 mrad, telescope: variable from .1 to 1 mrad
pulse frequency	5 Hz or less

4. Echo detection

line filter	DAYSTAR 3 Å / BALZERS 60 Å
photomultipliers	a) HAMAMATSU R1244 TANDEM MICROCHANNEL PLATE b) EMI GENCOM D341B
quantum efficiency	10/12 % at 532 nm
pulse rise time	.35/1.3 ns
timing system	Le Croy 4202 TDC
timing resolution	156 ps
calibration method	internal, pre & post pass plus one cal. shot in n (n=2,3...)

5. Epoch Timing

system	Quartz time base controlled by LORAN-C
time base accuracy	± 10 µs (quick look); ± 1 µs (final data)
time base verification	travelling clock plus daily TV comparison with UTC(OFM)

6. Overall Performance

ranging accuracy	± 10 cm or better single shot
range	to LAGEOS

7. Operatability

manned	5 nights a week / 8 months per year

Table A

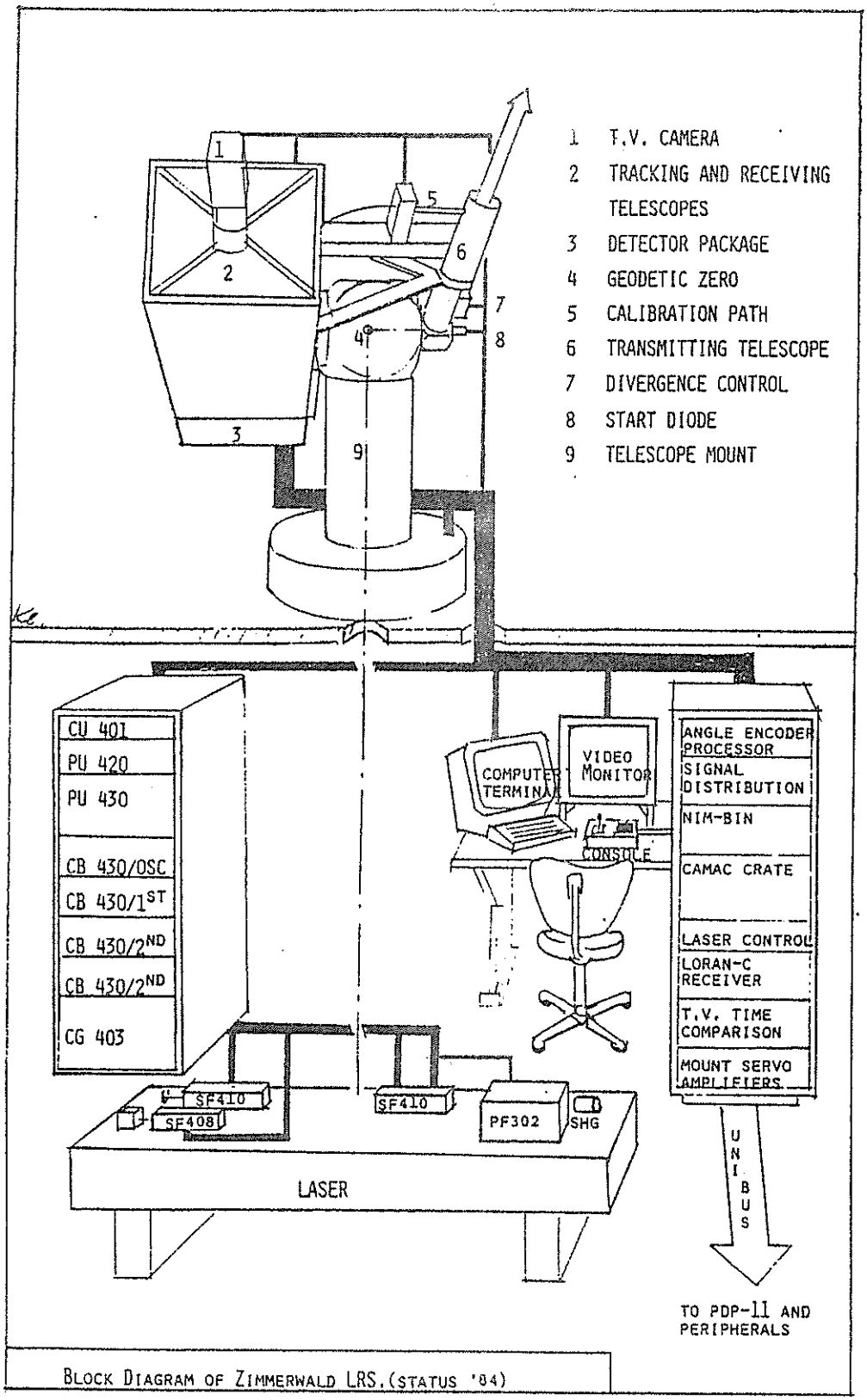

BLOCK DIAGRAM OF ZIMMERWALD LRS. (STATUS '84)

Figure 1

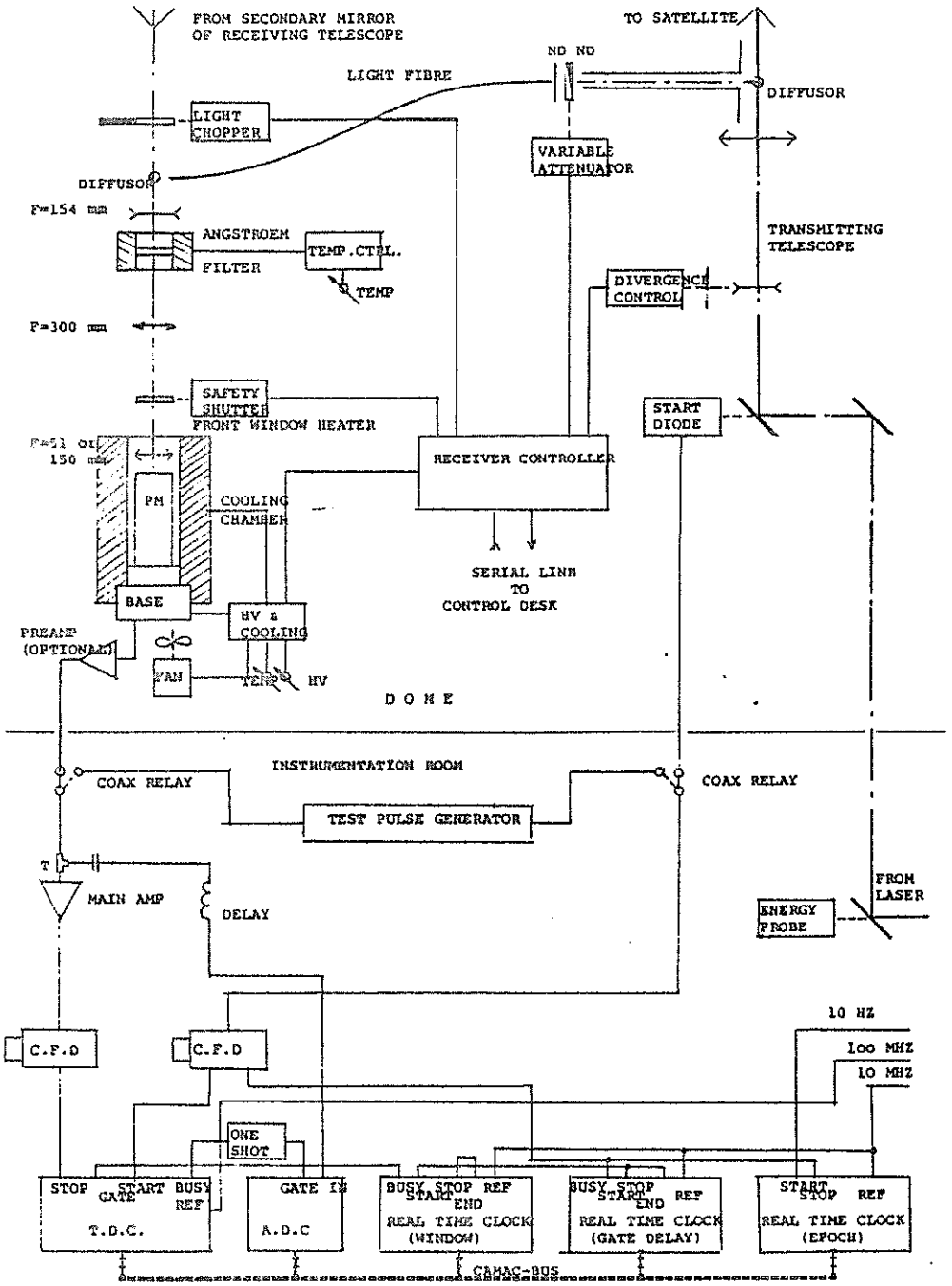

FIGURE 2 THE ZIMMERWALD LRS RECEIVER

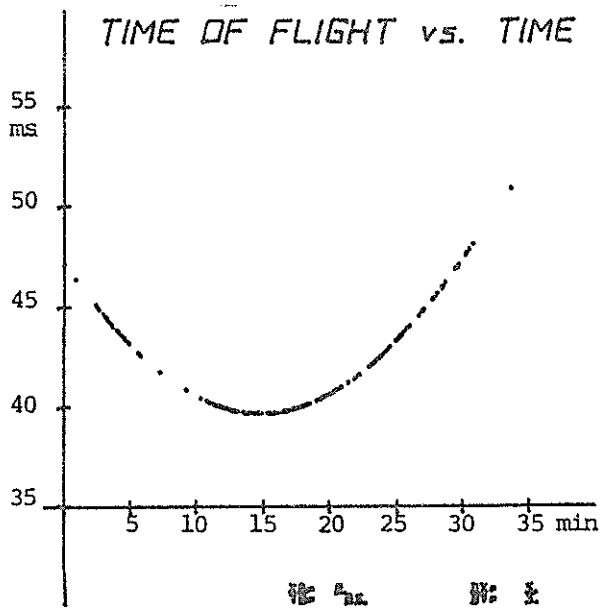

Fig.3 Raw results of one LAGEOS-pass

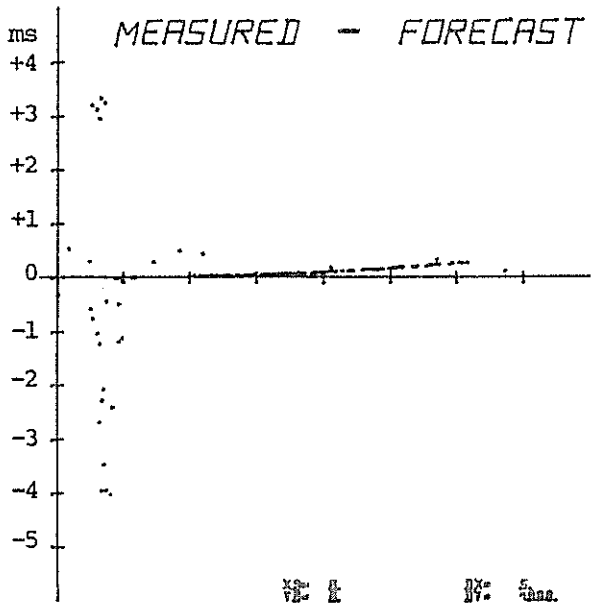

Fig.4 Same pass, forecast subtracted

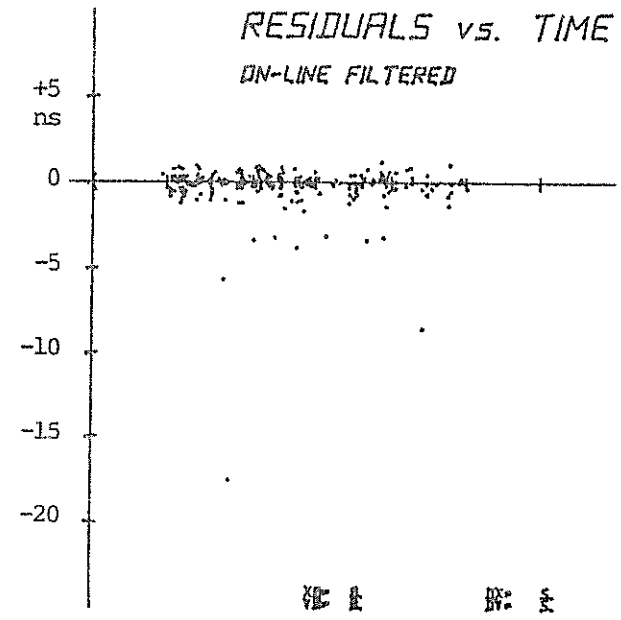

Fig.5 Result of on-line filtering

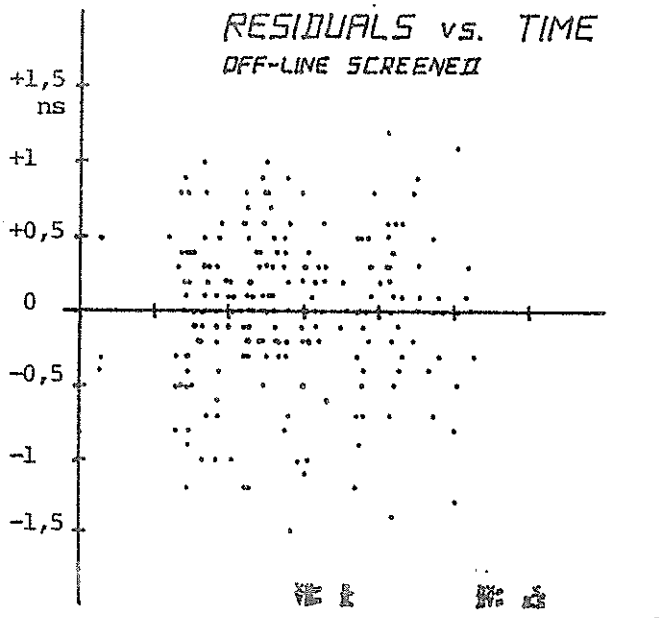

Fig.6 Final residuals after off-line screening. Vertical scale is equal to 7.5 cm per division.

SATELLITE		DATE	TIME	RET	RMS NS
7603901	LAGEOS	15- 5-1984	1:22: 0	131	0.6
7603901	LAGEOS	16- 6-1984	22:44: 0	43	0.8
7603901	LAGEOS	17- 6-1984	21:27: 0	184	0.6
7501001	STARLETTE	17- 6-1984	0:16: 0	81	0.5
7501001	STARLETTE	17- 6-1984	20:57: 0	223	0.7
7501001	STARLETTE	18- 6-1984	0:37: 0	111	0.5
7603901	LAGEOS	18- 6-1984	0:50: 0	164	0.6
7501001	STARLETTE	17- 6-1984	22:47: 0	256	0.7
7501001	STARLETTE	18- 6-1984	21:16: 0	140	0.6
7501001	STARLETTE	19- 6-1984	0:56: 0	45	0.5
7501001	STARLETTE	19- 6-1984	21:36: 0	20	0.5
7603901	LAGEOS	19- 6-1984	22:12: 0	343	0.6
7501001	STARLETTE	19- 6-1984	23:24: 0	250	0.8
7603901	LAGEOS	20- 6-1984	1:37: 0	436	2.7
7501001	STARLETTE	20- 6-1984	23:46: 0	32	0.5
7603901	LAGEOS	25- 6-1984	21: 8: 0	33	0.5
7501001	STARLETTE	25- 6-1984	21:44: 0	151	0.9
7501001	STARLETTE	26- 6-1984	22: 4: 0	66	0.5
7603901	LAGEOS	26- 6-1984	23: 9: 0	240	0.8
7603901	LAGEOS	27- 6-1984	21:52: 0	93	0.5
7501001	STARLETTE	27- 6-1984	22:25: 0	30	0.5
7603901	LAGEOS	29- 6-1984	22:37:18	189	0.6
7603901	LAGEOS	17- 7-1984	0: 6:10	42	0.5
7603901	LAGEOS	17- 7-1984	22:43:36	345	0.6
7603901	LAGEOS	18- 7-1984	2:16: 2	395	0.5
7603901	LAGEOS	19- 7-1984	23:28: 1	316	1.0
7603901	LAGEOS	20- 7-1984	22: 9:28	308	1.9
6503201	BEACON-C	21- 7-1984	1:18: 6	124	0.7
7603901	LAGEOS	21- 7-1984	1:39:57	885	0.5
7603901	LAGEOS	22- 7-1984	22:54:58	318	0.8
6503201	BEACON-C	22- 7-1984	23:55:33	173	0.6
7603901	LAGEOS	23- 7-1984	2:33:18	29	0.7
7603901	LAGEOS	27- 7-1984	23: 7:51	504	2.1
7603901	LAGEOS	29- 7-1984	20:32:36	235	2.5
6503201	BEACON-C	29- 7-1984	22:49:54	183	0.5
7603901	LAGEOS	29- 7-1984	23:59:20	215	0.8
7603901	LAGEOS	30- 7-1984	22:34:58	95	1.5
6503201	BEACON-C	30- 7-1984	22: 8:13	108	0.7
7603901	LAGEOS	31- 7-1984	2:13:24	230	0.5
7603901	LAGEOS	2- 8-1984	22: 1:54	329	0.5
7603901	LAGEOS	3- 8-1984	1:36:16	286	0.6
7603901	LAGEOS	5- 8-1984	21:29:26	460	0.5
6503201	BEACON-C	3- 8-1984	21:17:17	76	0.8
7603901	LAGEOS	14- 8-1984	23:16:15	219	0.6
7603901	LAGEOS	15- 8-1984	21:55: 1	205	0.5
7501001	STARLETTE	15- 8-1984	1:53:55	295	0.8
7501001	STARLETTE	16- 8-1984	0:26:28	71	0.4
7603901	LAGEOS	16- 8-1984	1:33:29	87	0.5
7501001	STARLETTE	16- 8-1984	2:13:26	197	0.8
7603901	LAGEOS	16- 8-1984	20:36:58	203	0.5
7603901	LAGEOS	17- 8-1984	0: 5:25	493	0.5
7501001	STARLETTE	17- 8-1984	0:46:18	113	0.5
7501001	STARLETTE	17- 8-1984	2:33: 9	110	0.5
7603901	LAGEOS	17- 8-1984	22:41:45	408	0.6
7501001	STARLETTE	18- 8-1984	1: 3:45	242	0.6
7603901	LAGEOS	19- 8-1984	23:36: 2	606	0.5
7501001	STARLETTE	20- 8-1984	3:31:48	119	0.4
7603901	LAGEOS	20- 8-1984	22: 8:10	142	0.5
7603901	LAGEOS	21- 8-1984	1:52:11	141	0.5
7501001	STARLETTE	21- 8-1984	0:13: 6	132	0.5
7501001	STARLETTE	20- 8-1984	1:42:36	332	0.7
7603901	LAGEOS	21- 8-1984	20:49:29	423	0.5
7603901	LAGEOS	22- 8-1984	0:21:28	356	0.5
7501001	STARLETTE	22- 8-1984	2:21:36	157	0.6
7501001	STARLETTE	27- 8-1984	21: 2:25	100	0.5
7603901	LAGEOS	27- 8-1984	23:10: 5	230	0.6
7501001	STARLETTE	28- 8-1984	19:33:31	124	0.5
7501001	STARLETTE	28- 8-1984	21:21:31	246	0.8
7603901	LAGEOS	28- 8-1984	21:48:12	358	0.5
7501001	STARLETTE	29- 8-1984	19:52:11	140	0.5
7603901	LAGEOS	29- 8-1984	20:29:27	261	0.5
7501001	STARLETTE	29- 8-1984	21:42:39	212	0.5
7603901	LAGEOS	30- 8-1984	0: 5:25	249	0.5
7603901	LAGEOS	30- 8-1984	22:35:49	178	0.5
7501001	STARLETTE	31- 8-1984	20:30:56	390	0.7
7603901	LAGEOS	31- 8-1984	21:14:57	504	0.6
7501001	STARLETTE	31- 8-1984	22:20:21	152	0.5
7501001	STARLETTE	1- 9-1984	0:14: 8	18	0.6
7603901	LAGEOS	1- 9-1984	0:53:45	308	0.5
7603901	LAGEOS	1- 9-1984	19:58:23	592	0.5
7603901	LAGEOS	1- 9-1984	23:24:50	494	0.5
7501001	STARLETTE	2- 9-1984	19:22: 1	37	0.6
7501001	STARLETTE	2- 9-1984	21:10:17	259	0.6
7501001	STARLETTE	2- 9-1984	22:59:22	106	0.5
7603901	LAGEOS	2- 9-1984	22: 3:40	376	0.6
7603901	LAGEOS	3- 9-1984	20:43:38	37	0.6
7501001	STARLETTE	3- 9-1984	21:30: 6	173	0.5

Table B: List of Passes as per September,3

PROPOSED ONE MILLION KILOMETER LASER GRAVITATIONAL WAVE ANTENNA IN SPACE

P.L. Bender, J.E. Faller, J.L. Hall, D. Hils, M.A. Vincent
Joint Institute for Laboratory Astrophysics
National Bureau of Standards and University of Colorado
Boulder, Colorado 80309, USA

Telephone (303) 492 6952
Telex 910 940 3441

ABSTRACT

We are investigating the possible use of laser heterodyne measurements between free test masses in three separate spacecraft to observe gravitational waves with periods of roughly 0.1 to 10^6 seconds. The geometry is the same as for a Michelson interferometer with nearly equal arms. The beam splitter is mounted in the test mass in the central spacecraft. A laser in each end spacecraft is phase-locked to the received light, and the output power is sent back to the central spacecraft. The returned beams from the two arms are beat against the laser in the central spacecraft, and the phases of the two resulting Doppler signals are reccorded as a function of time. With 1 mW of visible light from a helium-neon laser and 50 cm diameter transmit-receive optics, the shot noise limit on measuring the fractional difference in length of the two arms is about $10^{-19}/\sqrt{\text{Hz}}$, independent of the arm length. The use of other types of lasers with better efficiency and higher power output may be possible, provided sufficient stability and reliability can be achieved.

One case we have considered involves 10^6 km spacecraft separation, with all three spacecraft located roughly 15° behind the earth in nearly circular orbits about the sun. By choosing the starting conditions correctly, the lengths of the two arms will stay equal to about 1 part in 10^3 over several years. A major goal of the spacecraft design would be to keep the spurious accelerations of the test masses small enough so that the gravitational wave measurements are mainly shot noise limited for periods up to at least 10^4 sec. Unmodeled planetary perturbations will be extremely small out to periods longer than 10^5 sec, so observations on one arm can be used to determine fluctuations in the laser wavelength. The corrected laser wavelength then is used to measure the difference in length of the two arms. With this approach, the stability of helium-neon lasers carefully locked to Fabry-Perot cavities appears to be adequate.

For periodic sources and a 10^6 sec measurement time, the strain sensitivity would be about 10^{-22} over the period range from 10 to 10^4 sec. This range includes the following expected observable sources : a few known rotating binaries ; perhaps 100 close double white dwarf binaries with periods of roughly 100 sec and longer ; and a large number of unknown W UMa binaries with periods near 10^4 sec. For impulsive sources, the sensitivity would be sufficient to see pulses from the formation of black holes of 10^4 to 10^8 solar mass at large redshifts, if such events occured in most galaxies. Some useful information on a possible stochastic back-ground also could be obtained, despite having only one antenna, provided that the spectrum is quite different from that expected for spurious accelerations of the test masses and other disturbances in the system.

Two other possible antenna geometries for extending the observable period range also have been considered. One uses spacecraft at the L1, L4 and L5 points of the earth-sun system, and therefore a 1.5×10^8 km separation. This would make possible much better performance for periods longer than 10^4 sec, but with worse performance below 10^3 sec period. Additional care would be needed in the optical design because of the 2×10^4 times weaker laser power that would be received. However, it would not be necessary to measure to as small a fraction of a wavelength. Therefore, thermal distortion in the optical system, laser beam direction variations, and mirror irregularity effects would be less severe. The other geometry consists of three spacecraft 90° apart in geosynchronous earth orbits, giving 60 000 km arm lengths. In this case the performance for periods of 0.1 to 10 sec would be improved. However, performance for periods longer than about 3 000 sec would be considerably worse. Thermal disturbances and certain other perturbations also would be worse.

TREAK CAMERA-BASED LASER RANGING RECEIVER DEVELOPMENT

J.B. Abshire, J.F. McGarry, H.E. Rowe, J.J. Degnan
Instrument Electro-Optics Branch
NASA Goddard Space Flight Center
Greenbelt, MD 20771 USA

Telephone (301) 344 7000
TWX 710 828 9716

ABSTRACT

A laser ranging (LR) system which uses a 2 psec resolution streak camera (SC) receiver has been designed and constructed. The system features a 48 nsec imaging optical delay path to compensate for the trigger delay of the SC and utilizes an amplified photomultiplier (PMT) as the SC trigger detector. The system transmitter is a modelocked Nd:YAG laser which emits 30 psec pulses at 1064, 532 and 355 nm. Pulsed two-color ranging tests with this system show differential ranging accuracies of +-0.5 mm after the 355 and 532 nm pulse traverse a 921 m round trip horizontal path.

Initial SC sweep speed calibration has utilized an etalon, and the results show SC sweep nonlinearities of 8 percent. Sensitivity measurements show a minimum detectable signal of ~ 125 photoelectrons (PE) at 532 nm. This can be enhanced to the single PE level by adding an image intensifier to the system.

INTRODUCTION:

Present laser ranging (LR) systems which use modelocked laser transmitters, MCP-based PMT's, high speed preamplifiers, and low time-walk discriminators, can achieve 1 cm range accuracy (Ref. 1). For much higher accuracies, substantial improvements in receiver bandwidth must be made. Such an improvement is readily available in streak cameras which have psec time resolution. For such devices to achieve mm-level accuracies in LR systems, they must be carefully calibrated and interfaced to the ranging system. This paper reviews recent work to achieve these goals at NASA-Goddard.

The operation of a typical linear scan SC is shown in Fig. 1. The incident optical pulse illuminates the photocathode and frees photoelectrons from its rear surface. These are accelerated rapidly by a mesh electrode and then are deflected vertically by a fast electrical sweep. This results in a time-to-space mapping of the electron stream. The resulting electron distribution impinges on the microchannel plate, which preserves the spatial distribution and amplifies it. The amplified electron bundle exits the rear of the plate, and is accelerated into a phosphor screen. This produces a weak optical image whose spatial intensity distribution is proportional to the temporal intensity distribution of the illuminating optical pulse. In most streak cameras, an intensified video camera reads out this image and a OMA system converts it back to an intensity versus time profile. The phosphor image from a exponentially decaying set of optical pulses is shown at the bottom of the figure, along with the intensity versus time profile.

Circular scan SC's also have been developed for LR applications (Ref. 2). However dual channel linear-scan SC are presently favored at Goddard since they will record extended optical signals in both channels. This capability is important for sea state, altimetry, and pressure measuring applications (Ref. 3-5).

CURRENT DEVELOPMENTS:

The optical configuration of our present laboratory system is shown in Fig. 2, and its parameters are summarized in Table 1. This system operates in the following manner. The 30 psec pulses from the dye-modelocked ND:YAG laser first enter the transmit beam aligner system, which matches the divergence angles and center points of the 355 and 532 nm beams. The original offset is caused by the angle tuned KD*P doubler and tripler inside the laser. The aligned beams then are reflected up into the periscope system, and are directed to the target cube-corner (CC) by the roof periscope mirror. The optical return from the CC is reflected by the roof mirror and is collected by the receiver telescope. It is reimaged by an eyepiece, which relays the focal point to the start of the optical delay system. Just before this point, a beamsplitter reflects ∿8 percent of the optical signal into a PMT, whose output is then amplified and triggers the SC. The remainder of the energy enters the imaging delay line, which operates in the same manner as a White cell. The signal from this system then enters a light-tight enclosure, where the 355 nm pulses are reflected from a dichroic beam splitter, while the 532 pulses pass through it. The pulses in each path then pass through a bandpass filter for background light rejection. They are then recombined by a second dichroic and are focussed onto the SC photocathode.

The characteristics of the horizontal path which is currently used for 2-color ranging tests are summarized in Table 2. The 1 inch CC is mounted on a water tower, and the path passes over parking lots and buildings. Owens' 1967 refractivity formula is used to predict the refractive delay difference between the 532 and 355 nm pulses. The wavelength dependence of the refractive delay under standard atmospheric conditions is shown in Fig. 3. The meteorological data for this formula is taken from P, T, & Rh sensors mounted at the periscope mirror. Sensor accuracy is sufficient to allow less than 1 psec uncertainty in differential delay over this short path.

Laser pulse shapes recorded by the system are shown in Fig. 4. The left hand pulses were recorded from the reference path, while the right hand pulses were recorded after a second pulse pair traversed the horizontal path. The pulses are correctly aligned in time for both figures. The shift of the 355 nm pulse in the right hand pair is caused by the additional refractive delay it encounters in the path. The small scale structure within the pulses shows the psec temporal resolution capability of the SC system.

A typical output of the computer program which processes the SC data for dispersion measurements is shown in Fig. 5. Recorded waveforms at 532 & 355 nm are shown on the left hand side, while the convolution of the two is shown at the top right. For every laser firing, the program selects the peak of the convolution as its best estimate of the differential delay. The bottom figure right shows the histogram of the differential delay values. The mean and standard deviation of the differential delay are calculated from this histogram. Here, one channel corresponds to 2.2 psec.

To achieve accurate timing, the streak camera time base must be accurately calibrated. This is done by inserting a lossy etalon into the reference path, as is shown in Fig. 6. A single pulse input into the etalon results in a train of pulses with exponentially decaying intensities. These pulses are separated by the etalon round trip time. Since this time is accurately known by the setting of the translation stage, the pulses can be used as calibration markers.

A typical output from the calibration computer program is shown in Fig. 7. The upper left waveform shows the raw 532 nm data from a single laser firing as recorded by the SC. For this data, the etalon was aligned to emit only two pulses into the system. The upper right waveform shows the raw data after being convolved with a 25 channel-wide raised cosine impulse response.

The peak x-values from each pulse is then recorded. After multiple laser firings, the computer calculates the average value of the first peak x-value and the x-separation. The sweep speed profile can be measured by repeating this procedure after changing the x-value of the first peak.

The results of this procedure are shown in Fig. 8. Each point plotted here is the average of approximately 25 measurements, and the error bars are the standard deviation of the sample mean values. The data show that the sweep speed is fastest at the start of the sweep, and slows by ∿8 percent over the region shown.

To calculate the atmospheric delay, the fixed offsets within the LR system also must be removed. This is done by first measuring the differential delay over the horizontal path. Then the laser output is blocked from traversing the path and the reference shutter is opened. The same procedure is then repeated while the laser pulses traverse only the reference path. Since all fixed offsets within the system are common to both paths, subtracting the reference values from the path values leaves only differential delay caused by the atmosphere. Both the sweep speed and offset corrections are very similar to those developed for a waveform digitizer-based two color LR system (Ref. 6).

Results from repetitively measuring the atmospheric dispersive delay after using these procedures are shown in Fig. 9. Each plotted point is the mean value of 25 measurements while the error bars show +- one standard deviation. The average bias of the first set of 4 points is -3 psec, while the average bias of the second set of 9 points is ∿2 psec. The shifts in the average values are thought to be caused by small errors in spatially aligning the reference to the tower path. Even with these errors, the differential ranging accuracy is within +-0.5 mm for this measurement set. This data shows the very high LR accuracy which is available with SC-based receivers.

FUTURE DEVELOPMENTS:

SC technology also can be used in an "optical time-interval-unit" (OTIU). This devices utilizes the high time resolution of the SC for its optical interpolator. A "coarse" 500 MHz electronic counter is used to measure the integer number of clock pulses between the incoming optical start and stop pulses. Such an approach based upon our existing SC technology is shown in Fig. 10. This approach is somewhat similar to our earlier one for circular-scan SC's (Ref. 2), but uses optical clock pulses. In the present design, both the start and stop laser pulses are detected by the PMT, which triggers both the electronic TIU and the SC. Most of the optical pulse energy is directed into the optical delay line for recording by the SC. Short optical pulses which are coincident with the TIU clock are generated by a several GHz bandwidth laser diode within the optical clock module. These are optically summed with the laser pulses into the SC optical input. Both the SC and TIU output digitized data into the computer for each start/stop laser pair.

The principle of a two-color OTIU operation is shown in Fig. 11. In the left column, both the SC image and the optical waveforms are shown for the start pulse. In this representation, both laser colors are shown to be coincident in time. Therefore only the time interval between the first clock pulse and the laser pulse must be recorded. The right column shows the same data for the stop pulse. For this return, the two-color pulses have been temporally separated by the atmosphere. Therefore the computer must calculate the differential arrival time between pulses as well as the single color delay at wavelength 1. Given this data, it is straitforward to calculate the single color delay and the atmospheric correction by using the formulas shown. Such a system is presently being constructed by the authors.

SUMMARY:

SC-based laser ranging receivers are currently being developed at NASA-Goddard. Test results show that when systematic errors are properly controlled, differential range accuracies of +-0.5mm are readily achievable. Higher accuracies should be possible with more work. The accuracies already achieved exceed those typical of state-of-the-art PMT-based receivers by an order of magnitude. Such SC-based systems can be used to measure single color atmospheric delays to 5mm using two-color ranging. They also can be used to construct complete ranging receivers with accuracies of a mm or better.

ACKNOWLEDGEMENT:

We would like to thank Kent D. Christian for his technical assistance in operating the SC system.

REFERENCES:

1. J. J. Degnan, T. W. Zagwodzki, H. E. Rowe, "Satellite Laser Ranging Experiments With an Upgraded Moblas Station," this proceedings.
2. C. B. Johnson, S. Kevin, J. Bebris, and J. B. Abshire, Applied Optics, Volume 19, 3491 (1980).
3. C. S. Gardner, B. M. Tsai, and K. E. Irw, Applied Optics, Volume 22, 2571 (1983).
4. J. B. Abshire and J. E. Kalshoven, Jr., Applied Optics, Volume 22, 2578 (1983).
5. J. B. Abshire, J. F. McGarry, B. M. Tsai, and C. S. Gardner, Conference on Lasers and Electro-Optics, Paper WL2, Anaheim CA, June 1984.
6. J. B. Abshire, "Pulsed Multiwavelength Laser Ranging System," NASA Technical Memo 83917, March 1982

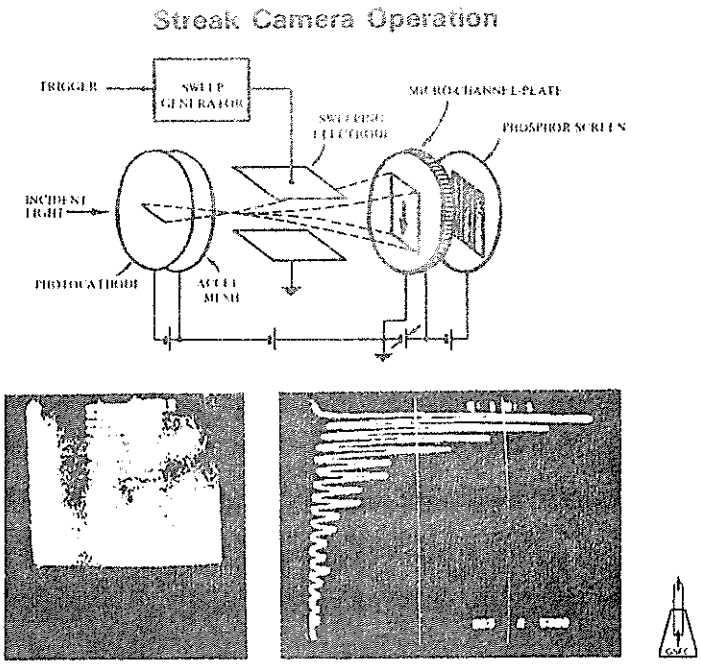

Figure 1 - Streak Camera Operation

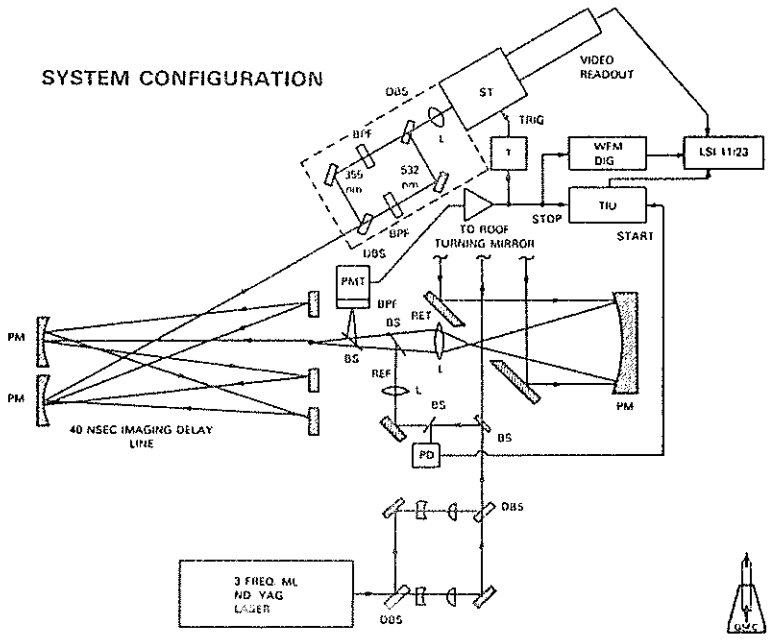

Figure 2 - Present Streak Camera-Based Ranging System

STREAK CAMERA-BASED RANGING SYSTEM PARAMETERS

LASER	QUANTEL YG 40 dye ml, 30 psec FWHM 5 mJ @ 1064 nm, 2 mJ @ 532 nm, 1 mJ @ 355 nm DIV 0.3 TO 1.0 mrad, align: <10% DIV
MIRRORS	Double dielectric, MAX R @ 355 & 532 nm
T_{sys}	Typ 45% AT 532 & 355 nm, (excluding telescope & periscope)
TELESCOPE	460 cm^2 AREA, 91 cm FL
PMT	HAM R1294, MCP type, QE ~ 4%, G ≈ 10^5
WAVEFORM DIGITIZER	TEKTRONIX R7912
TIU	HP5370, 100 psec accuracy
STREAK CAMERA	HAM 1370, 2 psec resol., 550 psec window, 2.2 psec/chan
MINICOMPUTER	DEC LSI 11/23, SKYMNK array proc., dual floppy disks

Table 1 - Streak Camera System Parameters

TWO COLOR RANGING TEST PATH

LENGTH	:	921.2 m (round-trip)
ELEVATION ANGLE	:	+3.5 deg
REFLECTOR	:	2.54 cm CC
END POINT SENSORS	:	T — aspirated thermometer P — setra 270 Rh — hair hygrometer
ALGORITHM	:	$\Delta T_{32} = \frac{L}{c} \Delta r_{g32} (P_m, T, Rh)$ $L = cT_2 [1 - r_{g2} (P_m, T, Rh)]$ $r_{g\lambda} (P_m, T, Rh) \equiv$ group refractivity at λ (OWENS, APP. OPT., 1967) P_m — midpoint pressure T_2 — TIU reading at λ_2

Table 2 - Horizontal Path Used for Ranging Tests

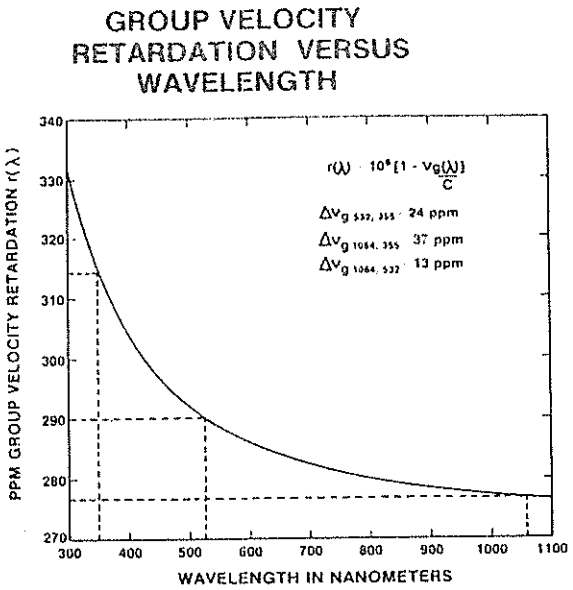

Figure 3 - Group Velocity Dispersion of Air Under Standard Conditions

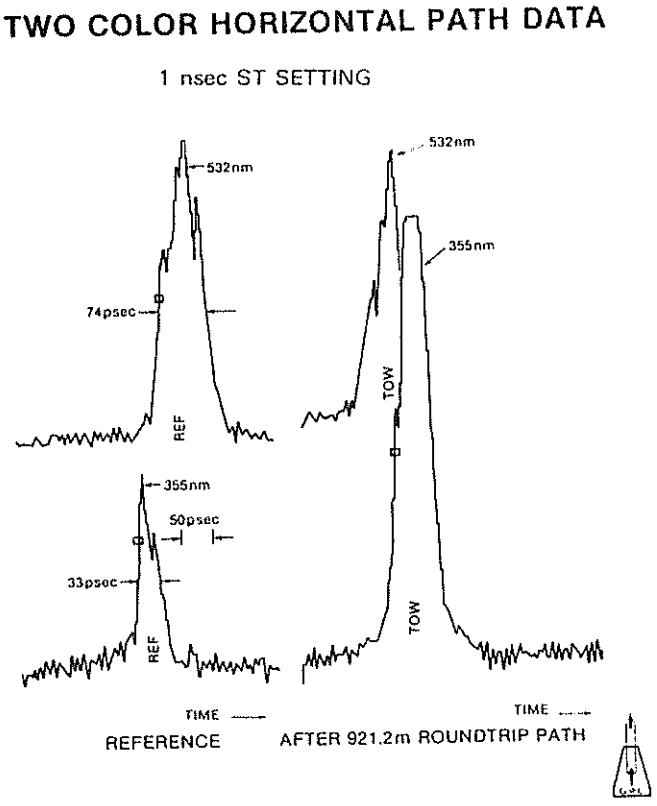

Figure 4 - Optical Pulse Shapes Recorded by Streak Camera Receiver System

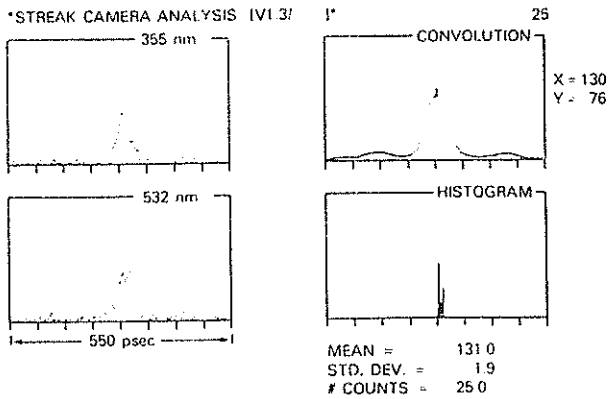

Figure 5 - Typical SC Computer Analysis

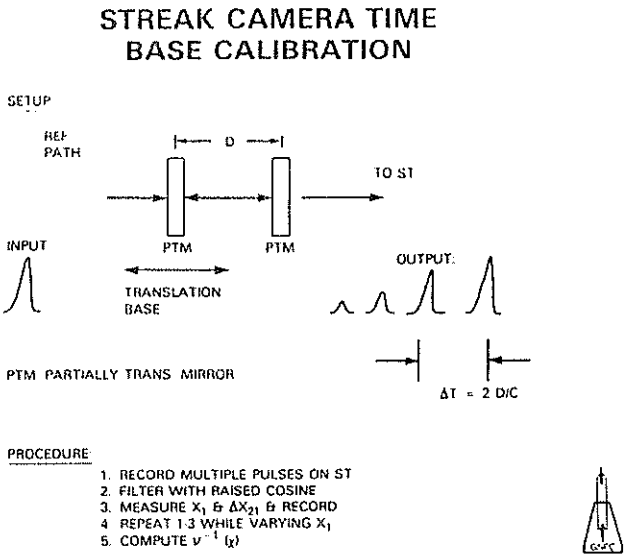

Figure 6 - Calibration Procedure for the SC Time Base

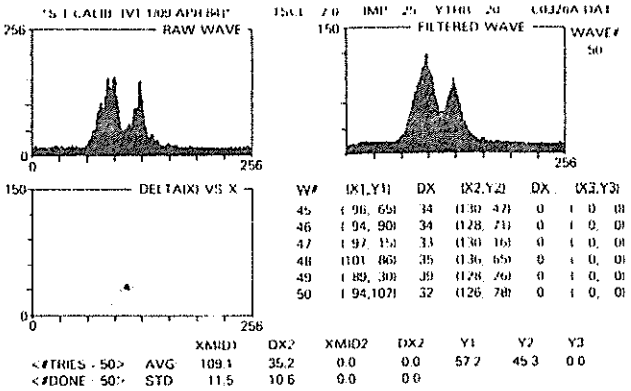

Figure 7 - Typical Output of SC Time Base Calibration Program

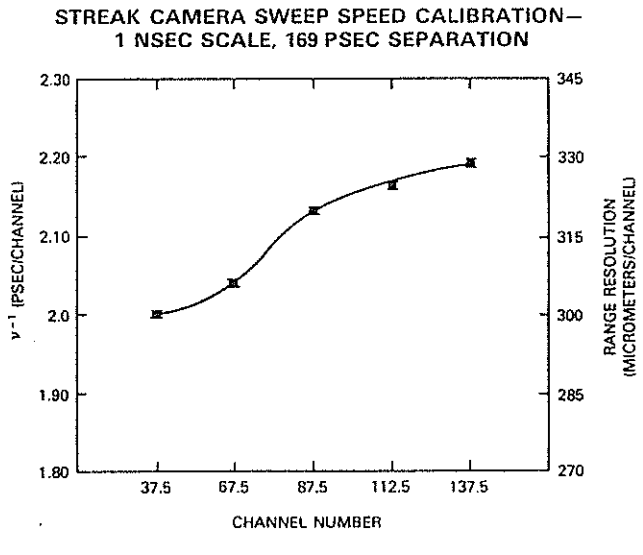

Figure 8 - SC Sweep Speed Profile

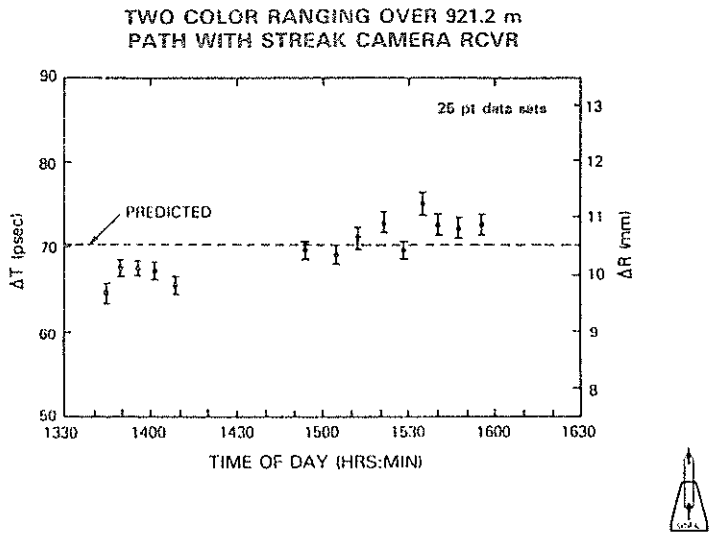

Figure 9 - Two Color Ranging Results Using SC Based Receiver

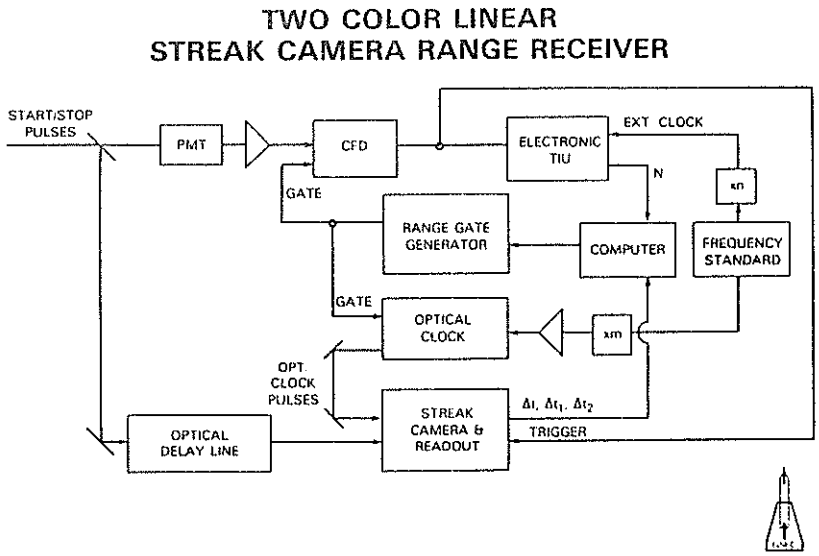

Figure 10 - SC Based Optical Time Interval Unit

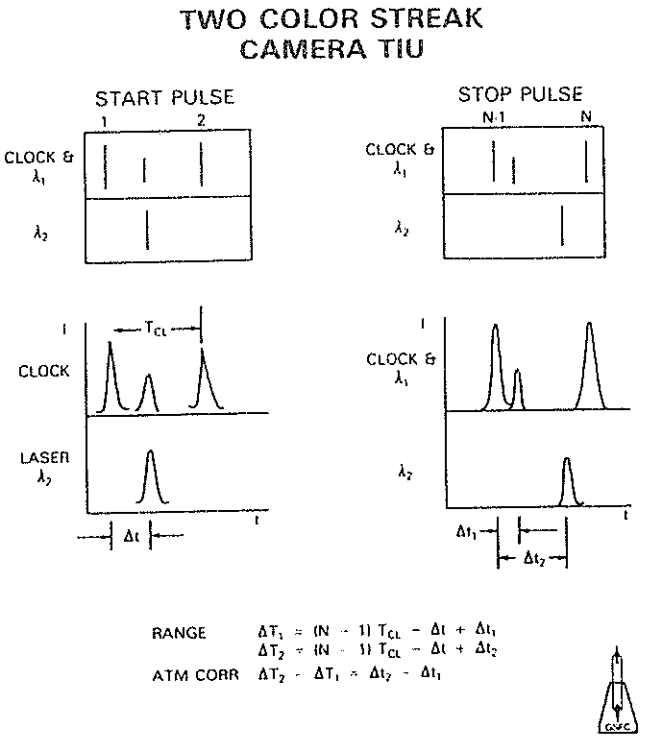

Figure 11 - Start and Stop Sweeps of Optical Time Interval Unit

NEW LASER DEVELOPMENTS TOWARD A CENTIMETER ACCURACY LUNAR RANGING SYSTEM

S.R. Bowman, C.O. Alley, J.J. Degnan*
W.L. Cao**, M.Z. Zhang**, N.H. Wang**
Dept. of Physics and Astronomy
University of Maryland
College Park, Maryland 20742 USA

Telephone (301) 454 3405
Telex 908787

*Now at Goddard Space Flight Center of the National Aeronautics and Space Administration

**Visiting Scholars from the Shangahai Institute of Optics and Fine Mechanics Academica Sinica, P.R.C.

ABSTRACT

The design considerations and performance characteristics of the currently operating laser are briefly described. The laser was designed and constructed for the specific purpose of lunar ranging.

Our goal is the establishment of a high accuracy lunar ranging station at the 48-inch Precision Tracking Telescope located on the Goddard Optical Research Facility in Greenbelt, Maryland. This paper describes the laser system designed and built to be the transmitter for this station.

Losses in the atmosphere and telescope were a major concern in the ranging system design. To overcome these losses we pressed the laser design for high average power. Of course, short pulse length, low output divergence, and reliability could not be compromised. Eventually, a mode-locked Neodymium YAG laser configuration emerged which we feel should give acceptable signal strength. The optical layout and output parameters are given in Fig.1.

The heart of a laser system is the oscillator. Our oscillator design emphasizes maximum output energy in a single, gaussian spatial mode pulse. This reduces the number of amplifiers needed thereby simplifying the overall system. A polarization switch cavity dump gives a factor of at least three improvement in energy compared to external pulse selectors. A combination of active mode-locking with an acousto-optic modulator and passive Q-switching with a nanosecond recovery dye (Kodak 14617 dye in dichloro-ethane) produced the 100 picosecond pulse length we wanted.[1,2] Simple passive mode-locking and etalon pulse stretching techniques did not allow stable Q-switching at higher energies.

Damage in the flowing Q-switch dye cell was the most difficult problem we encountered. We now believe it was due to absorptive heating near the dye cell windows. The problem was overcome by using a large transmission dye cell near the cavity center which slowly translates perpendicular to the beam.

The oscillator now delivers 800 to 1000 microjoules in a single, "S" polarized pulse. The transverse mode is TEM_{oo} and the energy stability is 5 to 10 percent. The half power pulse duration is 107 picoseconds as measured by a picosecond resolution Hadland Photonics streak camera.

After the oscillator, we have two high gain laser amplifiers. Two amplifiers are required to get the energy up near the damage threshold, because of the onset of amplified spontaneous emission when the gain becomes too high.

Fig. 1 Goddard/Maryland Lunar Ranging System
Laser Transmitter

Output Parameters:

- Single pulses at 10 Hertz
- Pulse duration 107 picoseconds
- Pulse energy 0.52 Joules @ 1064nm
  0.31 Joules @ 532nm
- Beam divergence less than 200 microradians
- Polarization 98% "P" @ 1064nm

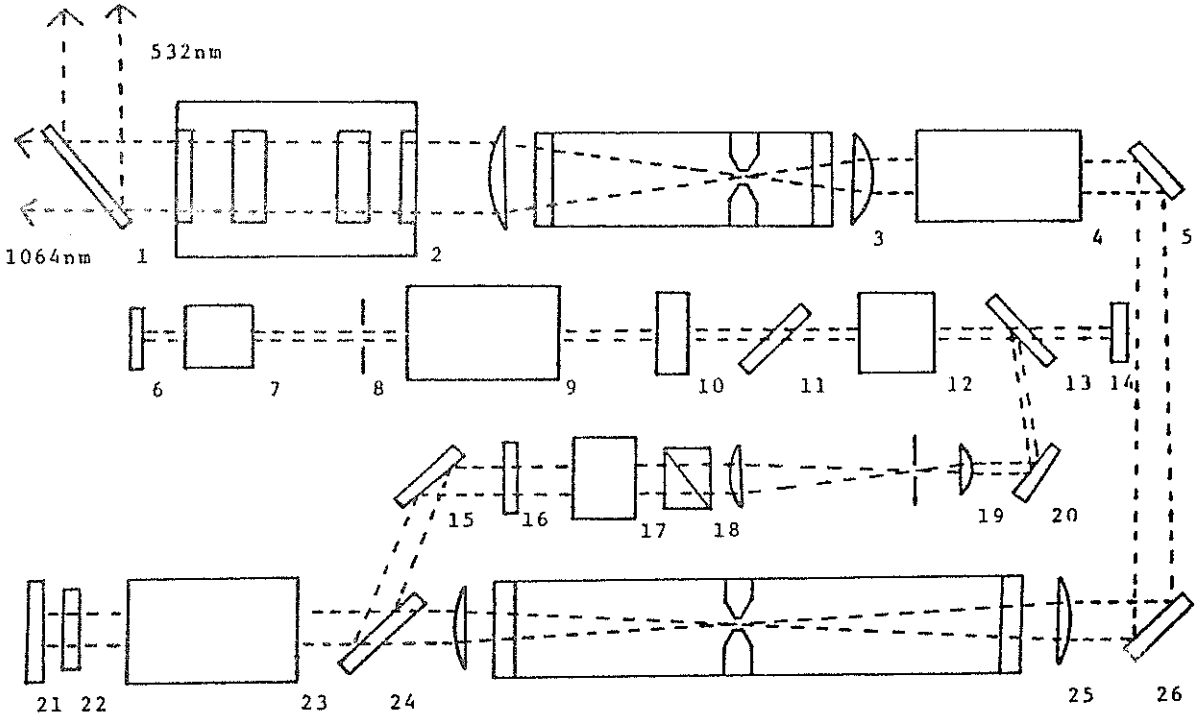

1 - 45° dichroic beamsplitter
2 - Two crystal harmonic generator
3 - F/20 vacuum spatial filter
4 - Nd:YAG amplifier (9 mm diameter)
5,26 - 45° HR mirrors
6 - Normal incidence HR mirror (10m curvature)
7 - Acoustooptic modulator
8 - Mode selection aperature
9 - Nd:YAG oscillator head (3mm diameter)
10 - Flowing saturable dye cell
11,13,15,24 - Multi-layer dielectric polarizers
12,17 - Pockels cells
14,21 - Normal incidence HR mirrors (flat)
16 - Half wave plate
18 - Glan-Thompson polarizer
19 - F/50 spatial filter
20 - 33° HR mirror
22 - Quarter wave plate
23 - Nd:YAG amplifier (7mm diameter)
25 - F/50 vacuum spatial filter

Separating components in the amplifier chain, there are three spatial filters. These increase the system's average power in a number of ways:[3,4]

i) reduced damage caused by the growth of high spatial frequency intensity components;
ii) reduced damage from diffraction ripple by image relaying;
iii) increased energy from amplifiers by efficient filling of laser rods;
iv) increased firing rate by correcting for thermal lensing of laser rods;
v) increased isolation between amplifiers allows higher gain.

Infrared output of the laser system is 520 millijoules per pulse with pre-pulse energy of less than one millijoule. At 10 Hertz firing rate the output beam is 98 percent "P" polarized with less than two times diffraction limited divergence.

The 532 nanometer second harmonic is generated with a KD*P type II, angle tuned crystal. The crystal is 15 millimeter long and immersed in a temperature stabilized, index matching fluid. The last spatial filter expands the beam so that the intensity on the doubler is 2×10^9 watts/cm^2. Present doubling efficiency is a somewhat disappointing 45 percent. Single crystal doubling efficiencies as high as 74 percent have been reported in the literature and we are still working to improve our number.

In addition to the single crystal second harmonic work, we have tested one of several two crystal doubling techniques.[5,6] Two KDP type II crystals have been used in a quadrature scheme to generate 60 percent conversion efficiency. Some practical problems remain to be solved and we are continuing this work.

The Maryland/Goddard Lunar Ranging Station was activated briefly in the fall of 1984. Ranging results from LAGEOS at that time uncovered some minor problems in the system. At the time of this writing (January, 1985), those problems have been solved and the station is about to resume operation.

An additional amplifier with slab geometry is being designed to increase the output energy further. It utilizes recently available large size neodymium doped YAG material and will probably utilize an active mirror configuration.

References

1. W. Seka and J. Bunkenburg, J. Appl. Phys. 49, 2277 (1978).
2. G. A. Reynolds and K. H. Drexhage, J. Appl. Phys. 46, 4852 (1975).
3. J. T. Hunt, J. A. Glaze, W. W.Simmons, and P. A. Renard, Appl. Opt. 13, 2053 (1978).
4. J. Holzrichter, "High-power pulsed lasers," Lawrence Livermore Laboratory Internal Report UCRL-52868 (April 1980).
5. V. D. Volosov, A. G. Kalintsev, and V. N. Krylov, Sov. J. Quantum Electronics 6, 1163 (1976).
6. G. J. Linford et al., Appl. Opt. 21, 3633 (1982).

PROGRAMMING FOR INTERLEAVED LASER RANGING

J.D. Rayner
Dept. of Physics and Astronomy
University of Maryland
College Park, Maryland 20742 USA

Telephone (301) 454 3405
Telex 908787

ABSTRACT

The use of epoch timing and multi-tasking in the University of Maryland Lunar Ranging System is described with emphasis on the problems created by interleaved starts and stops.

The only significant difference between programming for lunar and for satellite ranging is that in the lunar case, the time between laser shots is considerably less than the round trip time to the target. This complicates the timing since we now have many interleaved start pulses between corresponding start and stop pulses. In this situation a single time interval meter is no longer sufficient. One way to deal with this problem is to measure independently the epoch of the outgoing and returned pulses. The round trip time can then be derived by simple subtraction.

Although this is the chief reason to go to epoch timing there are several other advantages to be gained by incorporating an epoch timer in a ranging system. Among these are:

1) The epoch timer serves as the station time of day clock,

2) It can directly measure the station epoch,

3) It can generate a return gate for the received pulse,

4) The laser firing epoch is automatically measured to high accuracy.

Although use of a multi-tasking operating system is desirable for any ranging system, it is particularly valuable for one based on epoch timing and almost indispensable for one with interleaved starts and stops. The key feature of a multi-tasking operating system is its ability to run many programs at the same time. This is accomplished by switching control of the computer between the various competing programs. Use of a multi-tasking system allows the ranging program to be separated into pieces without regard to the details of timing. These pieces or tasks are then synchronized by exchanging messages between themselves. For example, a data collection task can send a message to a data output task saying "I have some data for you to write to disk". The output task then starts up and writes the data out.

The partitioning of a multi-tasking program into its various tasks is one of the key decisions in the design process. The partitioning of the Maryland ranging program is shown in Figure 1. As the figure shows, the program consists of four tasks. The range task calculates the range to the moon once a second. It is synchronized to the real world by a message sent once a second by the epoch timer control task. On receiving the message it makes the range and range rate available to the event timer control task in a buffer. The display task runs at the lowest priority using whatever time is not used by more important tasks to plot a histogram of as many range residuals as possible. It sets a flag when it is ready to process a point, then the data from the next

return is sent as a message by the epoch timer control task. As range data is acquired it is sent to the output task. Then when a buffer fills up, the output task writes it to disk.

This leaves the epoch timer control task which is the heart of the system. This is really a collection of tasks all executing the same code. Three different structures were considered. We could have had one task devoted to the epoch timer which then decides whether the next measurement is a stop or start. An alternative to this is to have two tasks one for starts and one for stops. You then need a scheduler to decide which task to activate next. Our system uses a third approach, with each shot handled by a separate task which measures the start epoch then goes dormant until it is time to take care of the stop. The actual code for the three different approaches is quite similar, in that they all need to schedule the epoch timer. The third method was chosen because arranging the code sequentially for one shot seemed conceptually simpler. At a 10 pps repetition rate we have about 25 invocations of the epoch timer control task running. Of course all but one are dormant, waiting for their turn at the epoch timer program. Each task uses the same copy of the Event Timer Program, but each has its own data block in which it keeps its own local data.

The key to the program is the scheduling of the epoch timer which is handled by the scheduler sub-routine. The scheduler maintains two lists or queues of data blocks, one for starts and one for stops. The epoch timer control program gives the scheduler a data block and a pointer to the appropriate queue. The block is then linked to the end of the indicated queue and the calling task is suspended. When the epoch timer finishes measuring the time of a start or stop it is necessary to determine the next task to use the epoch timer. Each data block contains the expected time for its associated start or stop. Therefore, it is just a matter of comparing the times contained in the data blocks heading the two queues and scheduling the one with the earliest time. If the the times are within 1 millisecond of each other, the stop task is aborted and the start task scheduled, since the laser firing would wipe out any return.

By using an epoch timer and a standard multi-tasking operating system we were able to generalize our non-interleaved satellite ranging progam to the interleaved lunar ranging case with a minimial amount of trouble using many pieces of the satellite program.

TASK STRUCTURE

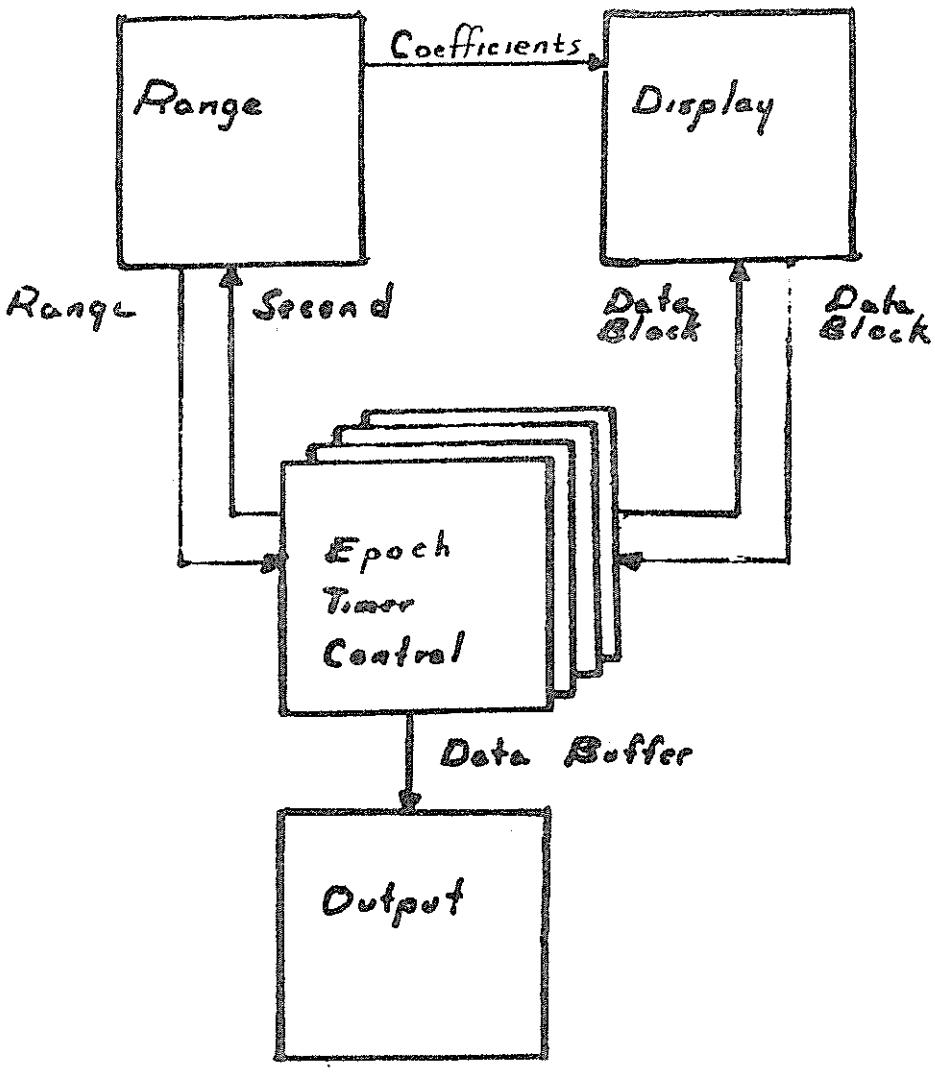

FIGURE 1

PERFORMANCE OF SATELLITE LASER RANGING DURING MERIT

B.E. Schutz, B.D. Tapley, R.J. Eanes
Center for Space Research
The University of Texas at Austin
Austin, TX 78712 USA

Telephone (512) 471 5573
Telex 7044265

ABSTRACT

Over 30 stations contributed data to the MERIT Project, with some stations operating at the 1-2 cm single range measurement level of precision. Thes stations tracked over 5000 LAGEOS Passes and over 2500 STARLETTE passes during the 14 month campaing, an average of over 10 passes per day for LAGEOS. Rapid service earth rotation solutions were possible because of the timely availability of the data. Improvements in the models used for the analysis of the data have enabled identification of instrumental anomalies at the 20 cm level in range bias and 150 microsecond level in time bias.

PERFORMANCE OF SATELLITE LASER RANGING DURING MERIT

Introduction

Since the Fourth Laser Ranging Workshop in October 1981, numerous developments in applications to artificial satellites have occurred. These developments include the introduction of new mobile satellite laser ranging (SLR) systems, the introduction of improved hardware in existing systems, and the addition of new stationary systems. Although some aspects of the developments can be regarded as the result of the SLR evolutionary process, most of the developments have been motivated by the NASA Crustal Dynamics Project and the IAU/IUGG project to monitor earth rotation and intercompare the techniques (MERIT).

This paper summarizes the performance of SLR systems in the MERIT period (September 1, 1983, to October 31, 1984) and contrasts the performance to the pre-MERIT period. The performance is characterized in terms of tracked passes, estimated instrument precision and number of participating sites. Because of improvements that have been possible as the result of improved instrument performance, concommitant improvements have been possible in the satellite force models, measurement models and kinematic models. These latter improvements have produced analysis techniques that enable identification of instrumental errors in near real-time at levels of 20 cm in range bias and 150 microseconds in time bias.

Data Sets

The results have been obtained using full-rate (FR) and quick-look (QL) data. The QL data are sampled at approximately 50 points per pass and are transmitted within a few hours after acquistiion via telex, GE Mark 3, computer modem or other means of data communication. The FR data, on the other hand, encompass the complete set of data and are usually transmitted from the respective station via magnetic tape to a Data Collection Facility (DCC). During the MERIT period, the DCC for QL and FR data has been located at the Goddard Space Flight Center (GSFC).

The pulse repetition rate now used with new laser systems is sufficiently high that some passes exceed 10,000 full-rate LAGEOS range measurements at a single station. To reduce the computer time required for data analysis while retaining the information content of the individual measurements, a data compression technique has been used to create normal points (NP). The LAGEOS normal points used in this paper were created from bins of raw data spanning three minutes. The technique used is essentially "Recommendation 84A: SLR Normal Point Generation and Exchange," differing only by the compression window (three minutes versus the recommended two minutes). STARLETTE normal points have been formed using 30-second bins.

Analysis Procedures

The analysis of laser range data is performed on a regular basis at the Center for Space Research. Quick-look data are received in a PDP 11/60 computer via a computer modem, and the received files are merged and preprocessed. The data are translated into the Modified Seasat Decimal format and transferred electronically via a dedicated circuit to The University of Texas academic computing facility for further processing on the dual CDC Cyber 170/750 computers. The accumulated data are processed each Tuesday for the earth rotation solutions which are then placed on the GE Mark 3 system. Since May 1984, the earth rotation solutions have been performed using normal points formed from the QL data. The formation of the normal points provides an initial level of data editing through computation of a preliminary earth rotation solution based on the raw QL data. The range residuals resulting from this solution are further analyzed and edited to create QL normal points. The resulting normal points are used in the final earth rotation solutions reported on Mark 3 as ERP (CSR) 84 L 02. The reported solutions include both "final" and "preliminary" solutions, where the latter case represents an incomplete five-day interval or that additional data are expected. In addition, unreported solutions are made based on all available data, however, these solutions may span only one or two days. Both the preliminary and the unreported solutions provide a near real-time opportunity to assess the current data quality and to aid in the identification of anomalous station performance. These basic procedures have been in use since the short MERIT Campaign in 1980.

In addition to the weekly assessment, a somewhat more formal process is performed on a monthly basis for LAGEOS. This analysis is distributed in a monthly report of the Center for Space Research, "Analysis of LAGEOS Laser Range Data," prepared with the support of NASA. The monthly report provides detailed information on the stations used in the earth rotation solutions and provides additional information on individual station performance. The station performance is summarized through the use of a single, continuous orbital arc spanning at least one month. This arc is fit to the unedited QL data for the purpose of providing detailed analysis of station performance, computing final QL normal points and incorporating data into the data base that was received too late for the weekly earth rotation solutions. The force and kinematic model used for the long-arc orbit computations in UTOPIA (Schutz, et al., 1982) is essentially consistent with the MERIT Standards (Melbourne, et al., 1983). Because of small errors in these models, the least squares estimation process is unable to fit the data to the measurement noise. Nevertheless, these model errors normally have unique signatures when compared with the instrumental error sources discussed by Pearlman (1984). Further information on the analysis procedures is given by Tapley, et al. (1981).

Performance

International tracking campaigns such as MERIT have made significant contributions to the performance of laser systems. Such campaigns have encouraged the development of improved systems, promoted the

development of new systems and fostered international cooperation. The growth in laser ranging activities from operational systems capable of tracking LAGEOS is reflected in the number of full-rate passes tracked in each five-day interval since May 8, 1976, until September 30, 1984. This feature is shown in Figure 1. The steady increase during the Main MERIT Campaign is readily apparent, in part because of the participation during the Intense Campaign during April-June, 1984. It is also apparent that more passes of LAGEOS were obtained during MERIT than during any other comparable period.

Before the MERIT Campaign was completed, 20 stations had provided data during a single 5-day period (earth rotation epoch 26 October 1984), a remarkable change from the number of stations contributing in 1981 (typically, 4 to 6). The individual pass contributions of each station during MERIT are shown in Table 1 for LAGEOS and STARLETTE. Additional information on the individual station hardware characteristics are given by Schutz (1983).

The monthly assessment of station performance using the previously described procedures generally results in range residuals with an overall RMS of 10-12 cm. In this assessment, all range measurements are equally weighted except for those stations with known systematic problems or new stations with significantly uncertain station coordinates. As a consequence, the resulting RMS is indicative of remaining force and kinematic model errors as well as possible instrumental problems. Through the process described by Tapley, et al. (1982), the range residuals in a pass can be resolved into "range bias" and "time bias." After removal of the range bias and time bias, the remaining systematic trends in the residuals can be removed by appropriate polynomials, and an estimate of the instrument precision can be made from the resulting residuals. As an indication of current performance in quick-look (QL) and full-rate (FR) data, Tables 2 and 3 illustrate the precision estimates for August 1984. It is evident from these tables that the precision of raw QL and FR data is comparable and ranges from 1-2 cm for some stations to tens of centimeters for others. Because the edit criteria generally used is about 30 cm, the data are significantly edited from stations which operate with precision greater than 20 cm.

It is the general guideline that about 50 points of QL data be transmitted per LAGEOS pass; however, as noted previously, some stations obtain more than 10,000 FR points in a pass. As a consequence, the normal points created from the QL and FR data have somewhat different levels of precision due to the significant difference in the number of measurements that are compressed into a single normal point. Although the selected QL points are somewhat randomly spread over the pass, judicious selection of QL points has consistently resulted in smaller QL precision than FR precision for at least one station (Simosato).

The STARLETTE station performance is summarized in Table 4. Comparison of the precision estimates in this table with the LAGEOS values in Table 2 show comparable performance.

For various reasons, the editing criteria used in the analysis of QL data generally results in an editing of 5-20 percent of the data. Further analysis of the edited data provides an indication of anomalous performance or other problems. Based on the current force and kinematic model accuracies, it is possible to resolve instrumental problems with the previously described procedures at the level of 20 cm in range bias and 150 microseconds in time bias. As a consequence, time tag errors at the millisecond or more level have been readily observed, and information has been provided to the stations regarding such an anomaly.

Because of the rapid availability of QL data, it has been possible to provide timely results of earth rotation parameters (ERP). As noted previously, the ERP from SLR have been produced weekly and made available on the GE Mark 3 System. Because of the inherent delays in making FR data available, the comparable ERP solutions have lagged the QL solutions by several months. However, comparisons between ERP results obtained from QL and FR data for the first three months of the MERIT Campaign showed differences in the x and y pole position of less than one milliarcsecond. Experience has shown that the QL data not only provide a significant data resource for the identification of anomalous instrument performance and orbit maintenance, but it is also a very useful scientific resource. To enhance the scientific usefulness, the transmittal of QL normal points, rather than selected raw ranges, is a matter that should be encouraged.

Analyses for earth rotation parameters obtained during MERIT has illustrated the high performance of the stations. Comparisons with other techniques, such as VLBI, have demonstrated consistent agreement at the 2 milliarcsecond level (Robertson, et al., 1985). Such comparisons have generally been based on the QL results of SLR data, thereby emphasizing the significant scientific importance of QL data.

Conclusions

The satellite laser ranging community put forth a very strong effort during the MERIT project. Over 30 stations contributed data to the project, with some stations operating at the 1-2 cm single range measurement level of precision. Rapid service earth rotation solutions were possible because of the timely availability of data. Improvements in the models used for the analysis of the data have enabled identification of instrumental anomalies at the 20 cm level in range bias and 150 microsecond level in time bias.

Acknowledgments

The contributions of John Ries and M. K. Cheng are gratefully acknowledged. This research was supported by NASA Contract No. NAS5-27344.

References

Melbourne, W. G., R. J. Anderle, M. Feissel, R. King, D. D. McCarthy, D. E. Smith, B. D. Tapley and R. O. Vicente, Project MERIT Standards, USNO Circular No. 167, Washington, D. C., 1983.

Pearlman, M. R., "Laser System Characterization," Presented at the Fifth International Workshop on Laser Ranging," Herstmonceux, 1984.

Robertson, D. S., W. E. Carter, B. D. Tapley, B. E. Schutz and R. J. Eanes, "Polar Motion Measurements: Sub-Decimeter Accuracy Verified by Intercomparison," Science, To Appear, 1985.

Schutz, B. E. and B. D. Tapley, "UTOPIA: University of Texas Orbit Processor," Center for Space Research, The University of Texas at Austin, 1984.

Schutz, B. E., "Participants During Project MERIT," CSR-83-3, Center for Space Research, The University of Texas at Austin, 1983.

Tapley, B. D., B. E. Schutz and R. J. Eanes, "A Critical Analysis of Satellite Laser Ranging Data," Proceedings of the Fourth International Workshop on Laser Ranging, pp. 523-567, Geodetic Institute, Bonn University, 1982.

TABLE 1. MERIT QUICK-LOOK SUMMARY

Passes reported September 1, 1983, to October 31, 1984, as quick-look data (unedited)

		LAGEOS PASSES	STARLETTE PASSES
1072	Zvenigorod	21	7
1148	Ondrejov	4	53
1181	Potsdam	127	67
1873	Simeiz	33	23
1893	Crimea	7	0
7086	Ft. Davis	147	0
7090	Yaragadee	291	129
7105	Greenbelt	248	152
7109	Quincy	452	248
7110	Monument Peak	473	256
7112	Platteville	165	155
7121	Huahine	158	55
7122	Mazatlan	186	70
7210	Haleakala	389	23
7805	Metsahovi	31	2
7810	Zimmerwald	57	39
7824	San Fernando	5	3
7831	Helwan	3	3
7833	Kootwijk	72	32
7834	Wettzell	330	55
7835	Grasse	93	9
7837	Shanghai	58	0
7838	Simosato	243	141
7839	Graz	177	117
7840	Herstmonceux	339	59
7843	Orroral	42	0
7886	Quincy/TLRS-1	49	0
7907	Arequipa	432	627
7935	Dodair	13	5
7939	Matera	383	363
7940	Dionysos	3	2
8833	Kootwijk/MTLRS-1	13	1
Total		5044	2696

TABLE 2. AUGUST 1984 LAGEOS QUICK-LOOK (QL) DATA AND THREE-MINUTE NORMAL POINTS (NP)

Station	Passes	Number of QL Ranges	QL Precision (cm)	Number of NP Ranges	NP Precision (cm)
1181 Potsdam	16	417	19.8	87	8.6
7086 Ft. Davis	14	694	6.8	121	2.5
7090 Yaragadee	15	684	1.5	175	0.7
7105 Greenbelt	23	1050	2.7	228	1.2
7109 Quincy	54	2631	2.6	733	1.2
7110 Monument Peak	50	2403	2.7	544	1.2
7112 Platteville	13	332	14.9	96	7.3
7121 Huahine	6	256	8.8	53	4.0
7122 Mazatlan	14	632	6.9	126	2.3
7210 Haleakala	27	1237	3.7	209	1.2
7805 Metsahovi	5	62	21.7	34	15.1
7810 Zimmerwald	17	836	9.8	171	4.2
7833 Kootwijk	6	191	17.0	56	9.0
7834 Wettzell	30	1147	6.4	227	2.3
7835 Grasse	4	56	5.5	18	2.7
7837 Shanghai	3	18	11.0	11	11.0
7838 Simosato	24	842	3.9	138	1.2
7839 Graz	6	261	3.6	46	1.5
7840 Herstmonceux	31	1231	4.7	295	2.1
7886 Quincy/TLRS-1	3	248	6.8	32	2.4
7907 Arequipa	50	2146	14.2	375	5.7
7939 Matera	39	1818	13.8	419	6.3
Totals	450	19192	8.6	4194	1.5

TABLE 3. AUGUST 1984 LAGEOS FULL-RATE (FR) DATA AND THREE-MINUTE NORMAL POINTS (NP)

	Station	Passes	Number of FR Ranges	FR Precision (cm)	Number of NP Ranges	NP Precision (cm)	FR UTC
1181	Potsdam	17	382	17.6	86	8.3	BIH
7086	Ft. Davis	14	8210	6.9	138	0.8	USNO
7090	Yaragadee	14	74246	1.5	180	0.1	USNO
7105	Greenbelt	23	102386	2.5	239	0.1	USNO
7109	Quincy	54	382862	2.4	740	0.1	USNO
7110	Monument Peak	50	268043	2.4	553	0.1	USNO
7112	Platteville	13	1690	12.2	111	2.9	USNO
7121	Huahine	5	2781	8.2	40	0.9	USNO
7122	Mazatlan	14	34171	5.3	137	0.3	USNO
7210	Haleakala	25	64344	3.1	225	0.2	USNO
7805	Metsahovi	7	82	19.9	47	16.4	BIH
7810	Zimmerwald	13	4602	7.5	148	1.3	BIH
7833	Kootwijk	6	428	13.0	57	7.3	BIH
7834	Wettzell	30	19426	6.2	265	0.7	USNO
7835	Grasse	3	1832	7.1	27	0.7	BIH
7837	Shanghai	5	39	17.0	16	12.0	BIH
7838	Simosato	27	13656	9.1	166	1.0	USNO
7839	Graz	9	1616	3.6	59	0.7	TUG
7840	Herstmonceux	31	8001	4.5	299	0.8	BIH
7886	Quincy/TLRS-1	38	70596	6.4	434	0.5	USNO
7907	Arequipa	50	13578	14.4	550	2.8	USNO
7939	Matera	40	10378	13.7	495	2.8	USNO
Totals		488	1082882	4.0	5012	0.2	

TABLE 4. ESTIMATES OF STARLETTE QUICK-LOOK PRECISION DURING MERIT

		Precision Estimate (cm)
1148	Ondrejov	18.7
1181	Potsdam	19.1
1873	Simeiz	21.0
7090	Yaragadee	2.2
7105	Greenbelt	4.7
7109	Quincy	3.1
7110	Monument Peak	2.9
7112	Platteville	8.9
7121	Huahine	6.8
7122	Mazatlan	9.6
7210	Haleakala	3.6
7810	Zimmerwald	16.1
7833	Kootwijk	16.7
7834	Wettzell	7.5
7835	Grasse	4.2
7838	Simosato	7.6
7839	Graz	3.5
7840	Herstmonceux	5.3
7907	Arequipa	10.6
7935	Dodair	16.1
7939	Matera	9.1
7940	Dionysos	17.5

Edit criteria: 30 cm

Analysis of other stations is incomplete.

FIGURE 1

LAGEOS TRACKING FROM 8 MAY 1976 TO 31 SEPTEMBER 1984
PASSES IN 5 DAY BINS

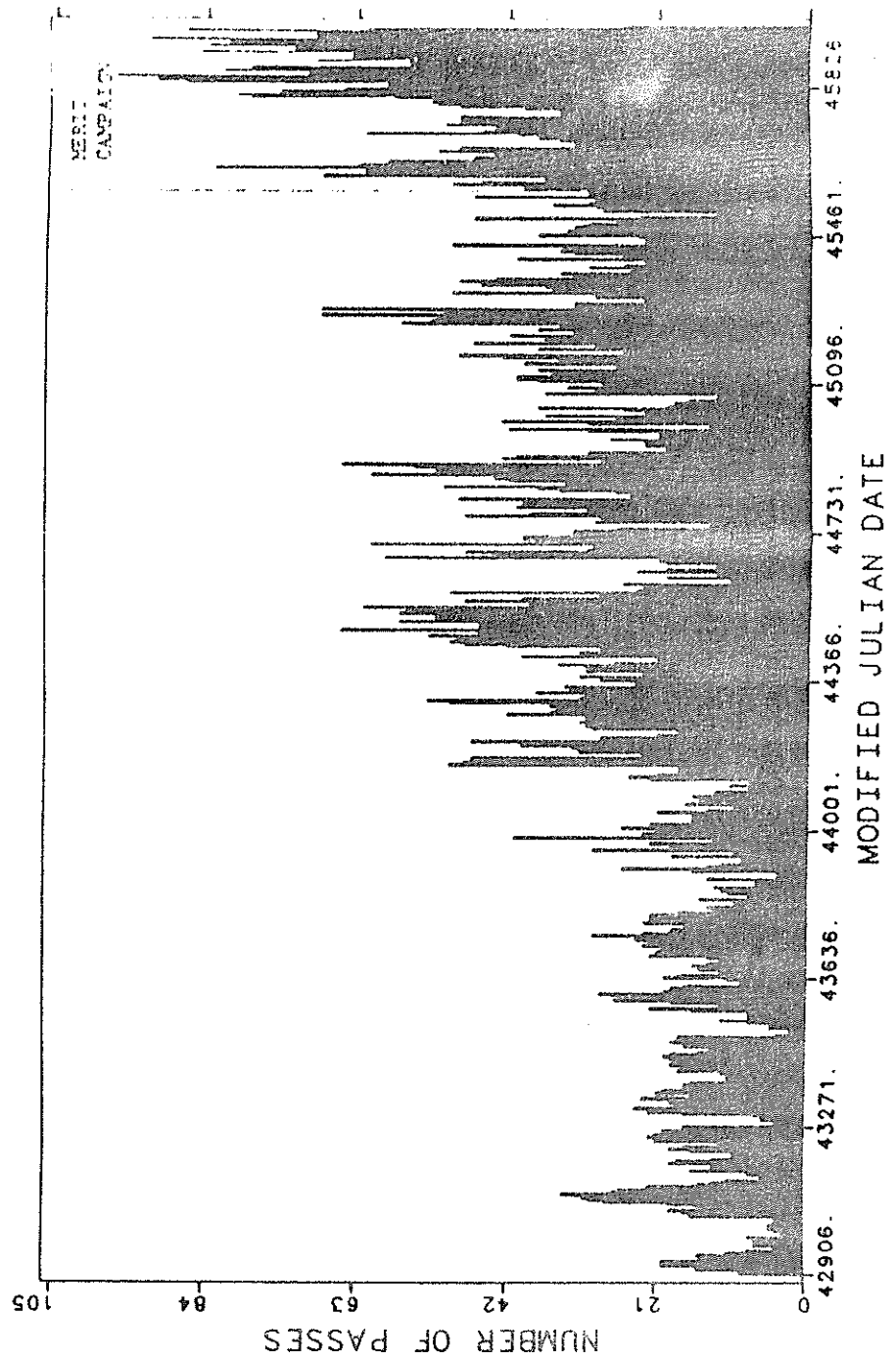

CURRENT DEVELOPMENTS IN EVENT TIMERS AT THE UNIVERSITY OF MARYLAND

C.A. Steggerda
Dept. of Physics and Astronomy
University of Maryland
College Park, Maryland 20742 USA

Telephone (301) 454 3405
Telex 908787

ABSTRACT

The Maryland dual slope Event Timer resolution has been improved to 50 ps. A dual frequency one stop Event Timer with resolution of 20 ps is under development.

The dual slope Event Timer originally developed in 1973 [1] has been updated and improved to have a 50 ps resolution. Specifically, the charging resistors affecting the dual slope sweep were changed so that the ratio of the slopes of the two sweeps is 250 to 1 instead of 125 to 1. This change causes the vernier to divide the basic 10 MHz clock rate into 2000 parts instead of 1000 parts. One of the MECL II integrated circuits was updated to its MECL 10K equivalent. The start amplifier has been replaced with a Tennelec model 455 Quad. constant fraction discriminator and LEMO connectors have been installed on all input ports for ease in maintenance and operation. The Event Timer can be run in the conventional single input mode which will allow detection of four events each about 6 nsec apart, or, with a small modification, the system can be made into four independent single event Event Timers.

A dual frequency Event Timer using the vernier principle of the Hewlett Packard 5370A[2] interpolator is currently under development. The Event Timer has a resolution of 20 ps and should be able to make two measurements 2 μs apart using one vernier. The Event Timer is connected to a microprocessor to form a time of day clock, range gate and Event Timer system. The micro processor puts the data in an IEEE format and interprets the IEEE format for the range gate. The Event Timer may be synchronized to either a 5 or 10 MHz standard or may operate alone with reduced accuracy.

A block diagram of the present form of the new Event Timer is shown in Figure 1. A 5 or 10 MHz external frequency standard is applied to one of the input ports of a phase detector while the 200 MHz signal generated by a voltage controlled crystal oscillator is divided by 40 or 20 and applied to the other input. The D.C. output of the phase detector controls the voltage controlled crystal oscillator which generates F_o = 200 MHz. This is one of the dual frequencies.

In the absence of an input pulse, a delay line oscillator, made by Hewlett Packard, generates a second frequency, F_1= 199.2217899 MHz, which will be referred to as F_1 or 199* MHz. The two frequencies F_o and F_1 are applied to the "D" and "clock" inputs of a "D type" flip flop which is used as a mixer. The output of the mixer is a square wave with a period of 1.285 μs and a frequency (F_o - F_1) of .778210 MHz. The beat frequency (F_o - F_1) is further synchronized to F_1 by the Sync. F.F., and applied to one of the inputs of a phase comparator while the second input of the comparator is supplied by (F_1 ÷ 256).

(1) 1973 A Precision Event Timer for Lunar Ranging, University of Maryland Department of Physics and Astronomy Tech Report 74-038.
(2) Manual for Hewlett Packard 5370A Universal Time Interval Counter.

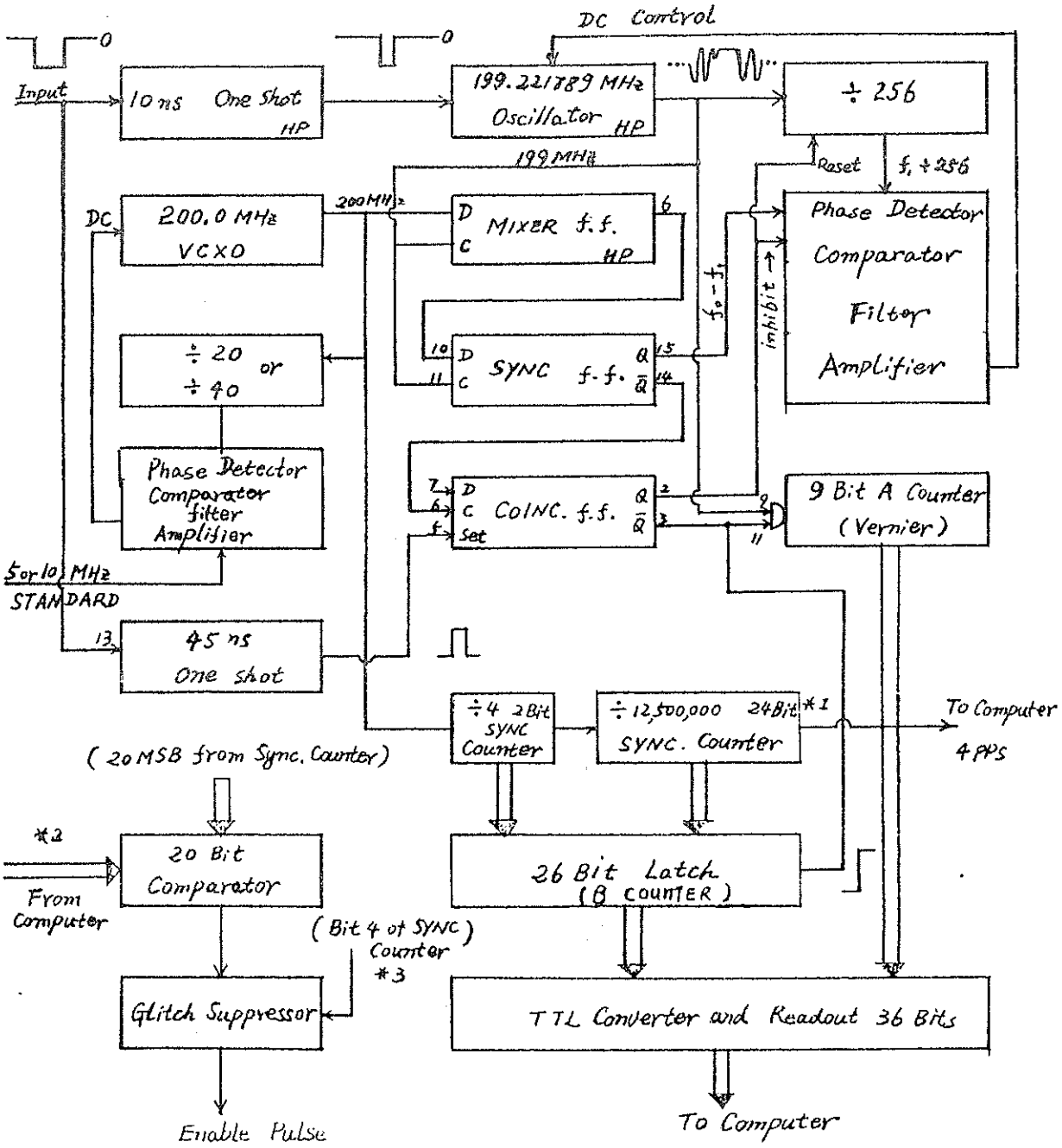

*1: THE 24 BIT COUNTER HAS $16,777,216_{(10)}$ STATES TO DIVIDE BY 12,500,000 THERE MUST BE 12,500,000 STATES SO
LAST COUNT = $16,777,215_{(10)} = 77,777,777_{(8)}$
FIRST COUNT = $4,277,216_{(10)} = 20,241,740_{(8)}$

*2: THE COMPUTER SENDS THE 20 MSB'S OF THE SYNC. COUNTER CODE $77,777,760_{(8)} \geq N \geq 20,241,740$

*3: BIT 4 (FROM LSB) RESOLUTION OF 320 ns

EVENT TIMER BLOCK DIAGRAM

figure 1

The comparator output is a D.C. voltage used to control the 199* MHz oscillator and to establish the equation:

$$(F_o - F_1) = F_1/256$$

which establishes the frequency F_1.

F_o is applied to the clock line of a 26 bit synchronous counter which consists of a two bit pre-scaler and a 24 bit synchronous counter which is adjusted to count exactly 12,500,000 states. The counter drive signals are adjusted so that in combination the two counters appear as one 26 bit synchronous counter with 50,000,000 states. The output of the synchronous counter is a pulse 4 times per second which is counted by the computer to form the time of day.

The rising edge, going from -.70 to 0 volts, of the input pulse, starts the Event Timer. In the test circuit the trailing edge of a negative going 30 ns pulse both edges of which are very precisely synchronized to F_o, activates the Event Timer. When a PMT is used, the input quiescent state will be -.70 volts and the leading edge of a positive going pulse is the starting event. This rising edge triggers a very precise 10 ns phase disconnect one shot.

The phase disconnect one shot stops the 199* MHz oscillator for about two cycles. When the oscillator restarts, hopefully, the frequency remains constant but the phase of the oscillation is synchronized to the input pulse rising edge. The rising edge of the input pulse also triggers a 45 ns anti-coincidence one shot which forces the coincidence F.F. to the set state. When the coincidence F.F. is set, the divide by 256 counter is held in the reset position, the phase detector is inhibited so that the D.C. control does not change, and a 9 bit "A counter" is enabled to count pulses from the 199* MHz oscillator occuring after the input pulse. After 45 ns, the set signal is removed and the coincidence F.F. is allowed to reset on the next synchronizer pulse which occurs when F_o and F_1 have the proper over-lap to cause the mixer to change state. When the co-incidence F.F. is reset, the divide by 256 counter is allowed to count from zero, the phase detector is reactivated, the "A counter" is stopped with the total number of counts proportional to the time from T, the time of the event, to the time of coincidence; and, a 26 bit latch or "B counter" stores the state of the synchronous counter when coincidence occurred.

Referring to Figure 2, at the end of the cycle of events, the "A counter" contains the number of 199* MHz (or 5.0195 ns) pulses from the event being timed to coincidence, the "B counter" contains the state of the 26 bit synchronous counter which is a measure of the number of 200 MHz (or 5.00 ns) pulses from the last 1/4 second to coincidence, and the phase locked loop is again closed with very little perturbations of F_1 due to the way that the divide by 256 counter is restarted at the time of coincidence.

THE EVENT TIMER HAS TWO OUTPUT REGISTERS, THE 9 BIT A REGISTER RECORDS THE NUMBER OF 199 * MHZ CYCLES FROM THE EVENT MEASURED TO THE TIME OF CO-INCIDENCE. THE 26 BIT B REGISTER RECORDS THE NUMBER OF 200 MHZ CYCLES FROM THE LAST 1/4 SECOND TIME MARK TO THE TIME OF CO-INCIDENCE.

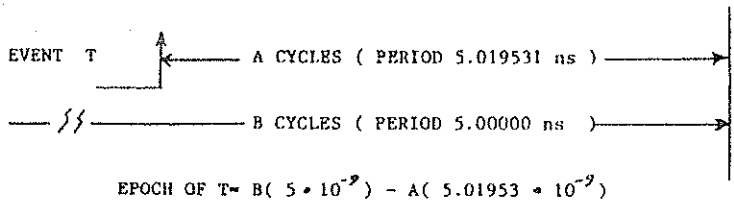

EPOCH OF T= B($5 * 10^{-9}$) - A($5.01953 * 10^{-9}$)

T= (B - A) * 10^{-9} - A($19.53 * 10^{-12}$)

DIAGRAM SHOWING HOW AN EPOCH MEASUREMET IS MADE

figure 2

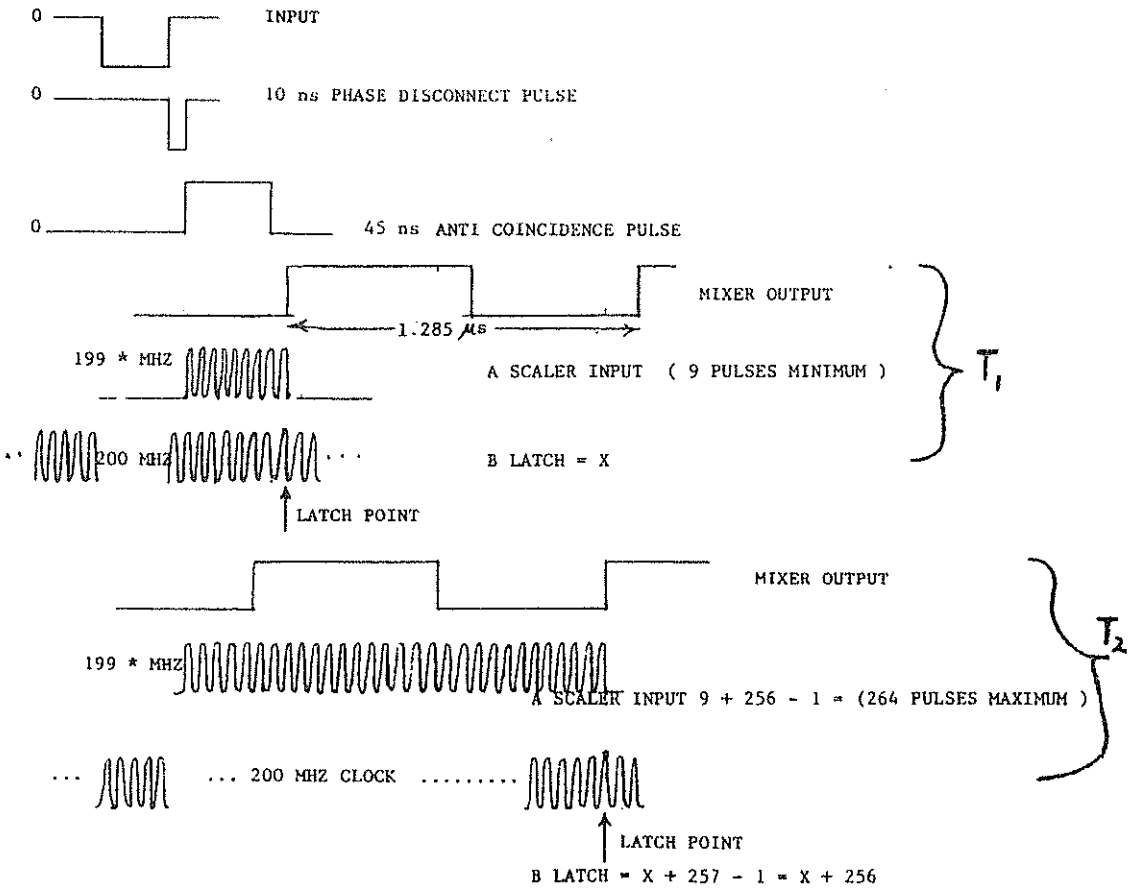

TIMING DIAGRAM SHOWING THE MEASUREMENT OF TWO PULSES T_1 AND T_2

(WHEN $T_2 = T_1 + .2500$ S. + 19.53 μS.)

figure 3

During measurements of the Event Timer, an input pulse was generated every 1/4 second and was synchronized very precisely with F_o. The phase of the input pulse with respect to F_o was adjusted with a "trombone" adjustable delay line. The adjustable delay line system made it possible to sweep over one entire 5 ns time period. Figure 3 shows what happens at the fold point when the A and B counters jump 256 and 257 counts respectively.

As the "trombone" delay line is adjusted, the point of coincidence as seen by the mixer output rising edge, comes progessively closer to the trailing edge of the anti-coincidence pulse. Further adjustment of the delay line moves the mixer rising edge inside the anti-coincidence pulse which blocks the coincidence F.F. from resetting. The result is that the "A counter" jumps 255 of the 5.01953 ns counts and the "B counter" jumps 256 of the 5.000 ns counts. Any deviation from this procedure results in an error when the epoch is calculated.

Figure 4 shows one of the prototype Event Timers and Figure 5 shows an interface card and an 8-bit microprocessor system used with the Event Timer. A great deal of effort has gone into making the fold-over point accurate. One of the problems that occurs is that when the 199* MHz oscillator is restarted during the measurement time, the oscillator is free running and its frequency will be slightly raised due to coupling to the 200 MHz. As soon as the phase locked loop is reclosed, F_1 returns to 199* MHz, but the fold-over point has too many counts. A further problem occurs if the "A counter" couples into F_1. This coupling appears to cause the odd states of the "A counter" to be favored over the even states. It is anticipated that these problems can be overcome however and that a 20 ps resolution Event Timer ca be built requiring no adjustments.

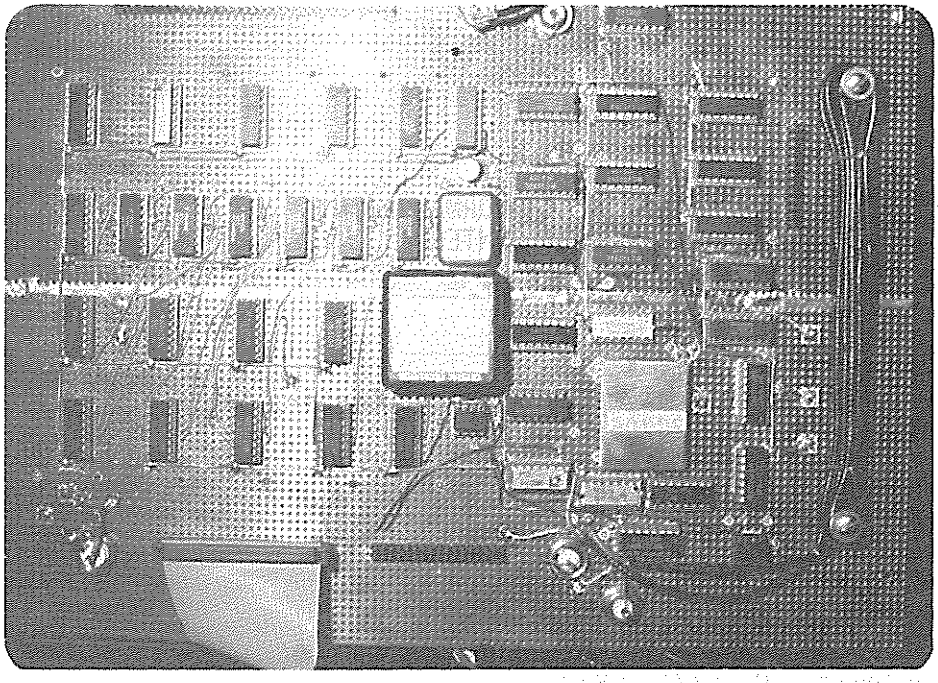

Figure 4 Prototype of Event Timer.

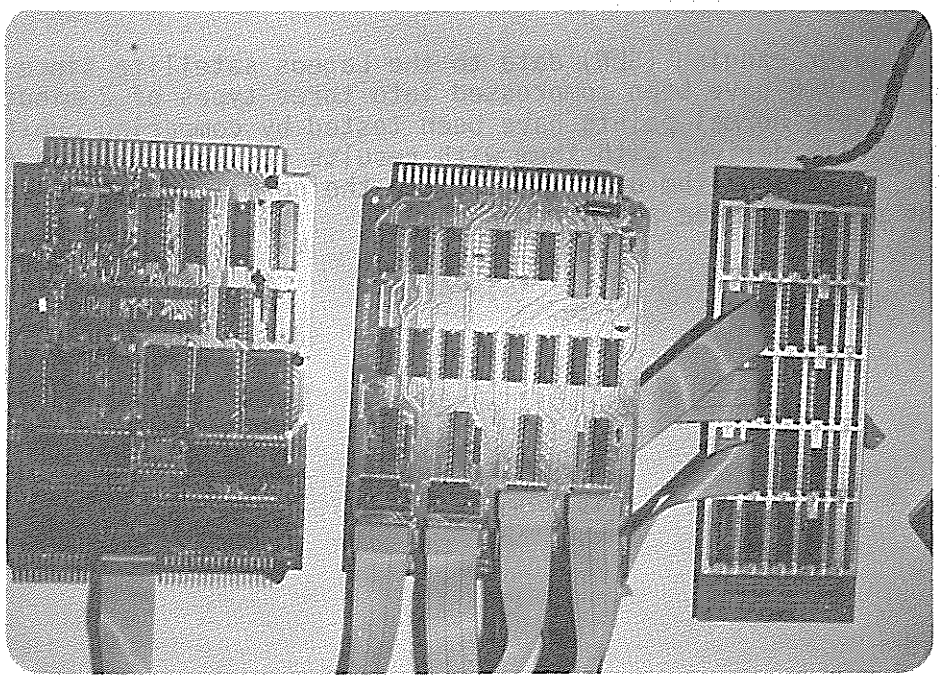

Figure 5 Interface and Microprocessor.

THE CONSTRUCTION AND TESTING OF NORMAL POINTS AT GODDARD SPACE FLIGHT CENTER

M.H. Torrence, S.M. Klosko
EG&G Washington Analytical Services Center, Inc.
Lanham, Maryland 20706, USA

Telephone (301) 731 2044
Telex 590613

D.C. Christodoulidis
Geodynamics Branch,
NASA Goddard Space Flight Center
Greenbelt, MD 20771 USA

Telephone (301) 344 7000
TWX 710 828 9716

ABSTRACT

Satellite laser ranging (SLR) data to the Lageos satellite since its launch in May of 1976 have been compressed into three types of 2 minutes normal points. These normal points have been tested by comparing orbital and geodetic results derived with them with results derived with the full rate SLR data. The alogorithm udes to generate the normal points is very similar to the proposal made at this workshop.

THE CONSTRUCTION AND TESTING OF NORMAL POINTS AT GODDARD SPACE FLIGHT CENTER

INTRODUCTION

At the National Aeronautics and Space Administration's Goddard Space Flight Center (GSFC), satellite laser ranging (SLR) data to the Lageos satellite has been compressed into normal points. Recently the SLR data has become so numerous, with current data rates of 1 to 5 points per second and almost thirty systems tracking worldwide, that some aggregation method has become necessary to avoid very costly analysis of the data. For a satellite such as Lageos, which is orbiting at nearly an earth's radius in altitude, utilization of data of this temporal density yields a redundancy of information which is approximately two orders of magnitude greater than that which is needed to fully monitor the perturbed motion of this satellite. While large data sets of independent observations reduce the influence of data noise on the calculated orbit, experience has shown that data noise is not a dominant error source for most applications of these data, and can be reduced through statistical methods which use the full data density to filter out the noise. The SLR data is compressed using temporal sampling based upon the presence of some minimum number of data points in the sampling interval. Other groups, Hauck and Lelgemann (1982) and Masters et al. (1983), have adopted methods to both thin the data while at the same time reducing noise in that data set. Masters et al. used successive differences in the second time derivative of the

range to edit the data and Chebyshev polynomial fits to short spans (150 sec) of the editted data to produce so called "laser normal points". This procedure accomplished three objectives: (1) outlying differences were used to edit anomalistic points, (2) the noise over these short spans was reduced by being averaged over the empirical function, and (3) filtered data, absent this noise, were produced. We have adopted similar procedures to accomplish these same objectives. Our approach was adopted to address not only the formation of normal points but also to assist with the assesment of the systematic stability of the laser systems, and their relative perfomance with respect to the other laser systems.

DEFINITIONS

Measurements inherently contain random error of observation. Ideally, the normal points associated with a given set of observations would be those same observations without the noise, i.e., the observations which would have been made if the process were noise free.

Consider laser ranging observations. The observed range at time t is

$$R_o(t) = R(t) + \varepsilon(t)$$

where $R(t)$ is the true range and

$\varepsilon(t)$ is the observational noise.

Mathematically, we can remove the error by averaging sufficient observations at time t so that the expected contribution of the random error to the average is insignificant. (for example, .1mm). In the real world there is only one measurement at each time t, and we rely on having observations at a rapid rate over a short period of time Δt. There must be sufficient observations during Δt so that the expected noise contribution is insignificant. The unmodelled change in the observation during this Δt must also have an insignificant contribution.

Because the noise removal must be performed over a non-zero time span, we have been required to introduce the concept of an observation model and a noise model.

We know that the true range at time t is given by

$$R(t) = f(O,S,A,t)$$

where f is a function of

- O the parameters defining the geocentric position of the instrument,

S the parameters describing the position of the satellite,

A the parameters describing the atmospheric effects.

That is to say, the range to the satellite at any time is the result of known modelable physical processes. These models are capable of predicting range at all times within a pass, not just at the times of the observations, to the same general level of accuracy: it is deterministic. (A pass is a set of tracking data which is acquired as the satellite goes from horizon to horizon.) There are errors in our modeling of the "true" range, $R_c(t)$. $R_c(t)$ is accurate to the decimeter level; our model of the evolution of the range in time is correct for the first seven or so significant figures. This error in $R_c(t)$ is the residual $\delta R(t)$ given by:

$$\delta R(t) = R(t) + \varepsilon(t) - R_c(t)$$

where $R(t)$ is the true noiseless range or the "normal" point range which is to be obtained.

Given a process, we would have normal points at each observation time. This is a very dense set, far more often than is required to demonstrate physical phenomena. Therefore, along with normal point creation (or noise removal) we also thin out the data. Typical practical solutions to this are decimation, interpolating the observation model to specified times, or just selecting the observation closest in time to the $\frac{\Delta t}{2}$ point - the bin midpoint.

Several considerations are necessary in order to construct normal points. First, we need to characterize the expected range as a function of time. Through knowledge of the spectral characteristics of the O, S, A above we can find a "sampling" interval (bin) which permits the reconstruction of all known "true" physical signals in the observed ranges from the thinned normal points.

Second, it is necessary to understand the behavior of δR within each bin. The spectra of δR and ε should be identical at short periods, i.e., the bin width, with some difference at longer periods due to unmodeled orbit errors. Harmonic analyses of the force model error perturbations on Lageos show no perturbation greater that a centimeter for periods of less than five minutes. Thus normal points formed from normally distributed data could safely be made at periods of less than 2.5 minutes. A numerical analysis of the order of the orbit integrator and the integration step size available for use in the computer program GEODYN (Putney, 1977) reveals that a good combination is a twelvth order integrator coupled with a 150 second step size. Both the error spectra of orbit

perturbations and the consideration of numerical accuracy has led us to choose two minutes for the bin to be used for forming normal points. On the basis of these analyses, we can state that the errors are modeled adequately by a low degree polynomial over a pass of residuals and may vary linearly within a properly selected bin width. This is a result of using an accurate R_c.

Therefore, we can state

$$R_N(t) \equiv R(t) = f(\delta R(t)) + R_c(t)$$

where $f(\delta R(t))$ is some functional representation over both the pass and the individual bin width which merely filters out, ε, the noise, and corrects our calculated range for the error in our models through the resulting signal in the range residuals.

We make three types of compressed range observations, or normal points, only one of which is a true normal point.

To do so, we follow these steps:

1. GEODYN, based on our best knowledge of the forces, etc. produces a set of residuals from 15 days worth of global range data

   $$\delta R(t) = R_o(t) - R_c(t)$$

2. A polynomial is fitted to the residuals to a pass of data

   $$\delta R(t) = g(t) + \xi(t)$$

   so each residual is then characterized in terms of signal and noise.

3. The remaining residuals are then:

   $$\delta r(t) = \delta R(t) - g(t)$$

4. δr is characterized by the mean residual in the bin

   $$\overline{\delta r}_b = \langle \delta r(t) \rangle + \langle \xi(t) \rangle$$

5. Form "poly-points" as:

   $$R_p(T) = g(T) + R_c(T)$$

   where T is time in the pass measured in two minute intervals from 0 hours UTC.

6. Form "bin corrected poly-points" as:

$$R_B(T) = g(T) + R_c(T) + \overline{\delta r}_b$$

where T is defined as in 5 above.

7. Form "true normal points" as:

$$R_N(t') = R_C(t') + g(t') + \overline{\delta r}_b$$

alternatively:

$$R_N(t') = R_o(t') - (\delta r(t) - \overline{\delta r}_b)$$

where t' is the time of an observation closest to the mean observation time within the bin.

See Figure 1 for a graphical representation of these data types.

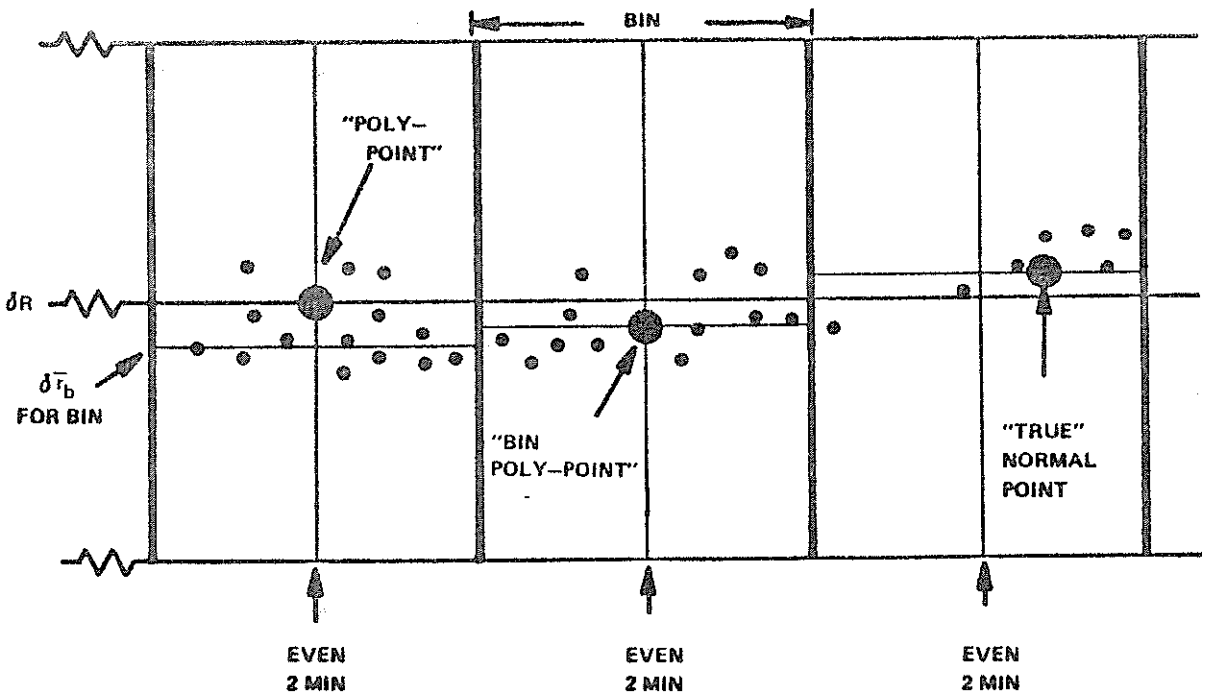

Figure 1.

Thus the "true" normal point noise at a specific point is estimated by the "signal" over the bin width. The noise error for a single point is then estimated and subtracted off the original range which is simply the true range (or normal point range) plus noise. Note also, our "true" normal point is at the time of a real observation. We have merely removed noise

from this observation to form a "normal point" at the mean observation time within each bin. This algorithm for "true" normal points conforms to the concept being put forth by this workshop.

VERIFICATION OF THE GSFC NORMAL POINT PROCEDURE

The Lageos range data is being taken to yield a data set to build an accurate model for the satellite's orbital motion to the accuracy of the data. The establishment of a reference frame defined by the orbit permits the accurate estimation of station positions and earth orientation parameters to help improve the understanding of the dynamics of the earth. In addition, improvements to and understanding of the force model is also accomplished. Thus, our testing philosophy was simple: do the normal points preserve the information content of the full rate data for calculating the Lageos orbit and for the recovery of station positions.

Three types of tests have been done to assess the performance of our normal points. For the first test, an orbit calculated with the full rate tracking data is fixed and station positions are adjusted. This is done with each of the three types of normal points and with the full rate data. The resulting sets of station positions are compared. The second test is the converse of the first; an orbit is converged with a fixed set of station positons. As before, this is done using the full rate data and each of the normal points data types individually. Then the four orbits are compared. The third test involves the convolution of the first two tests; the full rate data is used to converge an orbit and to solve for station positions, and the three types of normal points are used to converge the same orbit and solve for the same set of stations. The resulting orbits and station position are compared. The significance of these tests are evaluated by comparing the changes in the solved for quantities from the different data types with the formal errors.

TESTS FOR ORBIT RECOVERY: FIXING STATION POSITIONS

This test is to determine which, if any of the normal points can reproduce the orbit determined from the full rate data given the identical force model and station positions. Each normal point data type and the full rate data are used individually with the GEODYN program to solve for an epoch state vector for Lageos from the same time span of data. (For the purpose of this paper "state vector" refers to not only the position and velocity of Lageos but also includes the coefficients of along track acceleration and solar radiation pressure.) For this test each orbit determination is done with the same set of tracking stations which are not adjusted. When the true normal points were weighted at $1/\sqrt{n}$ m., where n is the number of fullrate points in the two minute bin, the state vector derived in the orbit determination reproduces the state vector determined from the full rate data when

that data is weighted at 1 m. If the true normal points were weighted at 1 m. the difference in the state vectors is significant, as is the case for uniformly weighted bin poly-points and poly-points. The true normal points, weighted at $1/\sqrt{n}$ m., reproduce the orbit recovered from the full rate data to a satisfactory level, but uniform weighting of the three normal point types is not equivalent to weighting the data by $1/\sqrt{n}$. Table 1 shows the difference of the x position and velocity component, along track acceleration, and coefficient of solar radiation from the corresponding quantity determined from the full rate data.

Table 1. Test of Orbit Adjustment: four fixed stations, 3 day arc

data type	weight (meters)	difference from apriori epoch full rate determination			
		ΔX (m)	$\Delta \dot{X}$ (m/s)	Accel $\times 10^{-11}$ m/sec^2	Cr
true normal point	$1/\sqrt{n}$	0.004	-0.004	0.001	0.0000
true normal point	1	0.793	-0.049	-0.049	0.0069
bin poly-point	1	0.847	-0.050	-0.044	0.0063
poly-point	1	0.793	-0.053	-0.041	0.0069

Tables 2 and 3 show the adjustments and their noise sigma of the epoch position and velocity from the same initial conditions for each of the normal point data types. These orbit determinations were done with four tracking stations and fifteen days of tracking data weighted at 0.10 m. Each of the four tracking stations had 0.10 m. quality full rate data and at least eight robust passes of data in the fifteen day span. The differences between adjustments from each normal point data type are small and not statistically significant. Thus orbits determined with any of the three normal point data types from robust, low noise data are equivalent.

Table 2. Test of Orbit Adjustment: four stations, 15 day arc, 0.1 m. weight

data type	adjustment from aprori position (meters)					
	ΔX	σX	ΔY	σY	ΔZ	σZ
true normal point	-0.430	0.024	-0.081	0.021	1.016	0.020
bin poly point	-0.439	0.026	-0.130	0.023	1.124	0.021
poly-point	-0.469	0.025	-0.104	0.023	1.121	0.021

Table 3. Test of Orbit Adjustment: four stations, 15 day arc, 0.1 m. weight

data type	adjustment from aprori velocity (meters/sec) ΔX	σX	ΔY	σY	ΔZ	σZ
true normal point	-0.019	0.042	-0.037	0.100	-0.014	0.042
bin poly-point	-0.023	0.042	-0.041	0.104	-0.015	0.042
poly-point	-0.022	0.041	-0.040	0.104	-0.015	0.042

TESTS FOR STATION RECOVERY: FIXING THE ORBIT

These tests are performed by comparing station positions determined from fifteen days of data in the presence of a fixed orbit. The data from each of the normal point types is weighted at 0.1 m. or $0.1/\sqrt{n}$ m. Table 4 shows the amount of adjustment and the noise sigmas of the adjustment in meters for the three data types.

Table 4. Test of Station Position Adjustment: 15 day arc, epoch state fixed

data type	weight (meters)	Earth Centered Component Adjustment (meters) ΔX	σX	ΔY	σY	ΔZ	σZ
true normal point	0.1	-0.137	0.021	-0.145	0.019	0.007	0.018
bin poly-point	0.1	-0.126	0.023	-0.142	0.020	0.002	0.019
poly-point	0.1	-0.121	0.023	-0.122	0.020	0.018	0.019
true normal point	$0.1/\sqrt{n}$	-0.114	0.017	-0.090	0.016	0.023	0.013
bin poly-point	$0.1/\sqrt{n}$	-0.104	0.017	-0.079	0.016	0.023	0.014

When the data are equally weighted, the differences between normal point types for each component adjustment of the station position are within the noise sigma of the adjustments. The RSS difference between the 0.1 m. weighted solutions are 0.012 m. for the true normal point minus the bin poly-point, and 0.036 m. for the true normal point minus the poly-point, and 0.026 m. for the bin poly-point minus the poly-point. These small numbers indicate that there is no significant difference between station positions determined from any of the uniformly weighted normal point types. This is also the case for a comparison between the uniformly weighted determination and the determination with the data weighted at $0.1/\sqrt{n}$ m. But, in this instance the RSS differences are larger than those above being 0.062 m for the true normal points and 0.070 for the bin poly-point.

TESTS FOR ORBIT AND STATION RECOVERY

This test is done by combining station position adjustment with state vector adjustment. For this test, a 15 day arc is determined with data from stations which had at least 10 passes of 3 cm precision data. Each type of normal points are weighted at 0.1 m in each of the least squares adjustment of the state vector and station position. Table 5 shows the resulting adjustment of a station position for each of the normal point types. There is no significant difference between these determinations.

Table 5. Station Position Adjustment: orbit adjusted, 5 day arc, 0.1 m. weights

data type	Earth Centered Component Adjustment (meters)					
	ΔX	σX	ΔY	σY	ΔZ	σZ
true normal points	-0.328	0.024	0.027	0.021	0.079	0.020
bin poly-points	-0.329	0.026	0.010	0.023	0.053	0.021
poly-points	-0.327	0.025	0.027	0.023	0.065	0.021

It is important to note, however, that station positions determined with sparse or noisy data weighted at 0.1 m. will show larger but still statistically insignificant differences between solutions done with the three types of data.

CONCLUSIONS

At GSFC, our analyses have shown that SLR data compression for the Lageos satellite is best done with two minute spans (bins) of full rate data. The algorthim we use to construct true normal points is virtually the same as recommended by this workshop, and we construct two other types of compressed data at the same time. From the analyses briefly reported above, we conclude that the true normal point constructed at GSFC can reproduce the results of the full rate data for state vector and station position determination when the true normal points are weighted at $1/\sqrt{n}$ m., where n is the number of points in the two minute bin. In addition, use of any of the normal point types, when equally weighted, to determine a state vector and/or station positions will produce results which differ insignificantly from each other.

ACKNOWLEDGMENTS

These investigations have profitted greatly from the participation of David Smith, Peter Dunn, Ron Kolenkiewicz, and Ron Williamson.

REFERENCES

Hauck, H., Lelgemann, D., "Die Bildung der Datenmittelwerte (normalpoints) aus Laserentfernungsmessungen. Arbeiten des Sonderforschungsbereiches 78 Satellitengeodäsie der TU München, Veröff.d.Bayer.Komm.f.d. Intern. Erdm., Astron.-Geod.Arb., Nr. 42, S.137-141 (1982).

Masters, E.G., Stoltz, A., Hirsch, 3., "On Filtering and Compressing Lageos Laser Range Data," Bull. Geod. 57, 121-130, 1983.

Putney, B.H., "General Theory for Dynamic Satellite Geodesy," National Geodetic Satellite Program, NASA SP365, 1977.

FIRST LEUT MEETING

ROYAL GREENWICH OBSERVATORY, 12 SEPTEMBER 1984

List of participants :

B. SERENE	ESA/Toulouse
S. LESCHIUTTA	Politecnico di Torino
J. DOW	ESA/ESOC
F. PALUTAN	TELESPAZIO
B. BERTOTTI	Uni. di Pavia
M. LISTER	Naval Research Laboratory
M. PAUNONEN	Finnish Geodetic Institute
G. VEIS	National Tech. Univ. of Athens
E. VERMAAT	Observatory Kootwijk
W. BEEK	Observatory Kootwijk
R. DASSING	Satellitenbeobachtungsstation Wettzel
R. HOPFL	Satellitenbeobachtungsstation Wettzel
JF. MANGIN	C.E.R.G.A.
F. PIERRON	S.L.R. G.R.G.S., C.E.R.G.A.
G. KIRCHNER	Lustbühel Observatory
D. KIRCHNER	Graz Tech. University
G. De JONG	Van Swinden lab. (VSL)
J. PILKINGTON	Royal Greenwich Observatory
J. GAIGNEBET	G.R.G.S., C.E.R.G.A.
C. ALLEY	University of Maryland
P. KLOCKLER	University of Berne
M. BOLOIX	Observatorio de Marina San Fernado

A G E N D A

1. Adoption of the Agenda.
2. LEUT Organisation.
3. Status of LASSO on board METEOSAT-P2.
4. Status of participating Laser Stations (including technical aspects).
5. Communication Network.
6. Calibration.
7. A. O. B.
8. Date and place of next meeting.

The meeting was held on 12 September 1984 at Herstmonceux Castle during the Fifth International Workshop on Laser Ranging Instrumentation.

As this LEUT meeting was the first to be held since the revival of LASSO, Dr. SERENE presented the goals :

- restart the organisation and work of the group;
- establish good relationships between the participants.

1. ADOPTION OF THE AGENDA

The agenda was amended to include a proposal of USNO to implement its bulletin in IRS DDS (Annex 1).

2. LEUT ORGANISATION

The LEUT Group was chaired by two Co-Chairmen :

- Dr. B. SERENE (representing the European Space Agency),
- Prof. S. LEISCHIUTTA, Politecnico di Torino (representing the Users).

Mr. GAIGNEBET acted as Session Secretary.

The minutes of the meeting will be typed and distributed by ESA.

3. STATUS OF LASSO ONBOARD METEOSAT-P2

The package designed for SIRIO-2 is going to be implemented on the METEOSAT-P2 satellite, after refurbishment. Like SIRIO-2, the satellite is spun but at 100 rpm. Its main mission implies a high stability of the spin rate and the synchronisation signal for image-taking must be very accurate.

Now the retro-reflectors and the detection unit are located side by side.

The nominal position of the satellite after launch is 0^{o} in longitude for a duration of about one year. It should be moved over the Atlantic Ocean as soon as a METEOSAT Operational satellite is in operation at the same site. This will allow the USA to participte in the programme.

ESA has to provide the group members with more precise specifications of the spacecraft, in particular its structure, frequency of the manoeuvres. A history of the manoeuvres of the existing meteorological satellites is thought to be very useful by the off-line members (Messrs. BERTOTTI, DOW, LESCHIUTTA).

4. STATUS OF THE STATIONS

Stations at Grasse (2), Kootwijk, San Fernando and Graz will participate as from commissioning.

The station of the University of Maryland, GSFC, will participate as soon as the position of the satellite permits.

The station of the Finnish Geodetic Institute is ready but its northern position limits the possibilities of ranging.

Stations at Wetzell (FRG), Dyonisos (GR), Matera, Zimmerwall (CH) and Cagliari (I) are willing to participate but are not certain to be ready in time.

The Herstmonceux station (UK) is neither not able to nor interested in participation.

Off-line members are interested by the ranging data and hope that the satellite will be kept without manoeuvres for long periods.

BIH will participate, in collaboration with CERGA, in pre-processing the data (Stations Synchronisations), the results being implemented on IRS/DDS as well as being included in the BIH Bulletin.

Participation of Intercosmos network stations :

Potsdam is still willing to participate. They are willing to switch to a YAG picosecond laser.

Mrs. TATEVIAN is interested in participating and would like more documentation.

The laser station representatives are requested to fill in the questionnaire (Annex 3) and to return it to ESA.

5. COMMUNICATION NETWORK

ESA is willing to keep the arrangement set up for SIRIO-2, i.e. use of the ESA network IRS/DDS. Many users feel that as they are already connected to MK III this could be the best means. The compatibility with the procedure defined for SIRIO-2 has to be confirmed by ESRIN. In any case, participating members hope that the network will operate very early to restart the knowledge and habits.

The Users ask ESA to study the possibility of taking charge of the network. This problem was opened by Dr. SERENE who reminded the participants that the budget is fixed and every over-cost will be taken off the exploitation time (predicted for 3 years).

The members ask ESA to provide cost figures for the use of IRS/DDS (Annex 2).

- implementation of USNO Bulletin on IRS/DDS :

  The stations have unanimously expressed their interest in this implementation.

6. CALIBRATION

Mr. GAIGNEBET has to provide cost figures for calibration round trips to all participating stations.

7. NEXT MEETING

TBD.

RESOLUTIONS ADOPTED AT THE FIFTH (1984) INTERNATIONAL WORKSHOP ON LASER RANGING INSTRUMENTATION

==========

RESOLUTION 1 : On the dedication of the proceedings

The participants in the fifth (1984) International Workshop on Laser Ranging Instrumentation consider that the proceedings of the Workshop should be dedicated to Frank Zeeman, late engineer at the Observatory for Satellite Geodesy at Kootwijk, Netherlands, who made major contributions to the development of the techniques of satellite laser ranging.

RESOLUTION 2 : On the need for the continuation of Loran-C emissions

The participants in the fifth (1984) International Workshop on Laser Ranging Instrumentation :

considering that the closure of the Mediterranean Loran-C chain is now foreseen for the year 1985 instead of 1992 as previously planned, that other clossures can be foreseen, and that the Loran-C signals constitute the main time synchronisation system for the laser stations operating in the northern hemisphere ;

and recognizing the needs of the Agency responsible for the Loran-C chains to terminate this service, and the adequacy of the interval until the year 1992 to introduce other synchronisation means for the laser ranging stations ;

urge the Agency responsible for the Loran-C system to review the proposed closure and to delay it at least until alternative means for time synchronisation are available to the laser ranging community.

RESOLUTION 3 : On the generation of normal points and the exchange of SLR data

The participants in the Fifth (1984) International Workshop on Laser Ranging Instrumentation recommend that :

1) The technique identified as Recommendation 84A for SLR normal-point generation and data exchange be adopted as an approved technique for the aggragation of SLR data ;

2) Details of the formats to accomodate normal points should be formulated by IAG SSG-2.81 and the final formats should be published in the proceedings of this workshop ; the formats should (a) provide for information that will cover the highest available quick-look normal-point accuracy, including time connections, (b) enable the identification of the normal-point generation technique, and (c) be suitable for the efficient exchange of SLR data ;

3) All stations or their agencies should make every effort to provide quick-look normal points in accordance with Recommendation 84A as soon as possible after the formats are finalized.

Recommendation 84A : On SLR normal-point generation and data exchange

The procedures for engineering anlysis and data screening that take place before quick-look data are transmitted should include a data compression step to provide high-quality quick-look data for scientific applications and to provide for the further avaluation of the data by the individual station or operating agency. The aggregation of raw data into a satellite-dependent fixed-time interval by an appropriate technique will produce a "normal-point range" and associated statistical properties. The resulting normal points should be transmitted as quick-look observations and should include the transmission of the associated statistics as well as information to enable the reconstruction of a raw measurement within the fixed interval. The following general procedure is recommended :

(1) Use high-accuracy predictions to generate prediction-residuals PR. (PR = Observation - prediction : include best available estimate for a time-bias and possible UT1-correction ; predicted range must include refraction).

(2) Use a suitable range (and time) window to remove large outliers.

(3) Solve for a set of parameters (orbital parameters are preferable) to remove the systematic trends of the prediction residuals, not introducing spurious high-frequency signals into the trend-function f(p).

(4) Compute fit-residuals FR = PR - f(p), and identify remaining gross errors using a 3 criterion.

(5) Iterate the two previous steps until no more can be identified ; previously rejected observations should always be reconsidered.

(6) Subdivide the edited fit residuals into fixed intervals (bins) starting from 0^h UTC ; the bin size should be the following :

Lageos : 2 minutes
Starlette : 30 seconds
Others : to be decided

(7) Compute the mean value $\overline{FR}_1$ and the mean epoch of the fit residuals for each bin.

(8) Locate the particular observation O_i, with its fit residual FR_1, whose observation time t_i is nearest the mean epoch of the bin i.

(9) Compute the normal-point range NP_i for each bin i using

$$NP_i = O_i - (FR_i - \overline{FR}_i)$$

(10) Compute the root-mean-square deviation m_i of the fit residuals for bin i from their mean, using

$$m_i = \sqrt{((\sum (FR - \overline{FR_i}))/(n-i))} \quad \text{or} \quad m_i = \sigma \text{ if } n = 1.$$

(11) Report for each bin i :

t_i observation time

NP_i normal-point range

n_i number of observations in the bin i

$\overline{FR_i}$ mean value of FR in the bin i

m_i bin standard error of single observations

Also report : σ pass standard error of single observations

(12) Use the format that is specified by SSG 2.82 for normal-point quick-look data.

(13) Report both old and new messages for at least ten passes for each station at the beginning of the distribution of quick-look data as normal-point ranges.

(14) Continue to report screened full-rate data in the standard format to the established data centres.

RESOLUTION 4 : On the need for lunar laser ranging observations

The participants in the Fifth (1984) International Workshop on Laser Ranging Instrumentation :

recognising the need for lunar laser ranging (LLR) data for use in current comparative studies of earth rotation and references systems, the value of LLR data in many scientific investigations, and that for the first time three LLR stations (CERGA, McDonald 107 and MLRS) are simultaneously operational ;

commend these stations for their successful efforts ;

urge other stations (e.g. Orroral, MAUI, Wetzell and the Crimea) to become operational as soon as possible ;

and strongly encourage all stations to obtain high-quality LLR data during the second MERIT-COTES intensive campaign in 1985 (May 23-31 ; June 6-14, 21-24 ; July 6-14, 20-28).